THE ANALYSIS OF CHIMERIC RIBOZYMES IN PLANTS

Rhonda Jean Perriman

March 1995

A thesis submitted for the degree of Doctor of Philosophy of The Australian National University

Table of Contents

Statement of originality i
Acknowledgments ii
Abstract iii

CHAPTER 1
INTRODUCTION

1.1 Enzymes 1
1.2 Ribozymes 1
  1.2.1. Group I introns 1
  1.2.2. RNase P 2
  1.2.3. Other catalytic RNAs 3
  1.2.4. The hairpin ribozyme 4
1.3. Hammerhead ribozymes: an introduction 5
1.4. Satellites and viroids 6
1.5. The hammerhead domain 7
1.6. *In vitro* mutagenesis of the catalytic core 9
  1.6.1. Ribonucleotide substitutions 9
    1.6.1.1. The unpaired core and helix II 9
    1.6.1.2. Helices I and III and the target site 10
  1.6.2. Deoxyribonucleotide substitutions 12
  1.6.3. Chemically modified nucleotide substitutions 14
    1.6.3.1. The base 15
    1.6.3.2. The phosphodiester linkage 15
    1.6.3.3. The ribose 17
  1.6.4. Role of divalent metal ions in cleavage 19
  1.6.5. The optimal conditions for *in vitro* hammerhead cleavage 20
1.7. RNA binding proteins and cleavage 21
1.8. A structural model for the hammerhead ribozyme domain 23
1.9. Designing hammerhead ribozymes for *in vivo* applications 24
  1.9.1. Optimising *in vivo* cleavage 25
    1.9.1.1. Intracellular localisation 26
    1.9.1.2. Stability of the ribozyme *in vivo* 27
      (i) 5' capped and 3' polyadenylated ribozymes 27
      (ii) ribozymes transcribed by RNA polymerase III 30

1.9.1.3. Enhancing expression levels by delivery 32
1.10. Conclusions and aims of this thesis 35

CHAPTER 2
MATERIALS & METHODS

Plasmid Constructions 36
2.1. pApoly 36
2.2. CaMV-35S CAT & pACAT, long ribozyme & antisense 37
(i) pJ35SCATN 37
(ii) pACAT 37
(iii) pAAsCAT/RzCAT 37
2.3. tRNAs 38
(i) pGtRNA^{Tyr} 38
(ii) pGtRNAp 38
(iii) Rz12 ribozyme 38
(iv) As24 antisense 39
(v) RzCA ribozyme 39
(vi) AsGUC antisense 39
(vii) intron-minus tRNAs 39
2.4. Mutant CAT target - CM2 39
2.5. Modified pApoly vector 40
2.6. pApolyM expressing tRNA & non-embedded ribozyme/antisense sequences 40
2.7. Mutant RNA polymerase II and III pAtRNARz12 40
***In vitro* analysis** 41
2.8. *In vitro* RNA transcription 41
2.9. *In vitro* cleavage reactions 42
2.10. Wheatgerm S100 extraction 42
2.11. tRNA^{Tyr} processing in S100 wheatgerm extracts 43
***In vivo* expression** 43
2.12. (i) Protoplast isolation 43
(ii) Transfection 44
(iii) CAT assays on transiently expressing cells 45
(iv) DNA isolation from transiently expressing cells 45
(v) Southern blotting 46
(vi) RNA isolation from transiently expressing cells 46
(vii) Ribonuclease protection assays 47
(viii) Reverse-transcriptase (RT-PCR) of *in vivo* CAT

mRNA 47

Transgenic Plant Analysis 48

- **2.13** (i) Crossing CAT & tRNAAs24 or tRNARz12 transgenic tobacco lines 49
  - (ii) Seed germination 49
  - (iii) Histochemical GUS assays 49
  - (iv) CAT assays 50
  - (v) DNA extraction 50
  - (vi) PCR analysis 51
  - (vii) RNA extraction 51
  - (viii) RT-PCR analysis of transgenic CAT mRNA 52
  - (ix) RT-PCR analysis of transgenic tRNAAs24 & tRNARz12 RNAs 52

CHAPTER 3

ENHANCED *IN VIVO* EXPRESSION OF LONG RIBOZYME, ANTISENSE & CAT TARGET SEQUENCE USING A SELF-REPLICATING VIRAL-BASED VECTOR.

INTRODUCTION 53

RESULTS 55

- **3.1. Comparison of CAT activities from pJ35SCATN & pACAT vectors** 55
- **3.2. Co-transfection of ACMVAsCAT/RzCAT with ACMVCAT constructs** 56
- **3.3. Altering the ratio of pARzCAT/pAASCAT to pACAT** 57
- **3.4. Replication of pARzCAT & pAAsCAT** 57

DISCUSSION 58

CHAPTER 4

IN VITRO ANALYSIS OF tRNA EMBEDDED RIBOZYME AND ANTISENSE RNAs

INTRODUCTION 61

RESULTS 63

- **4.1. Maturation of recombinant & wildtype tRNA^{Tyr} transcripts in wheatgerm extracts** 63
- **4.2. Analysis of steps I and II - 5' & 3' processing & the addition of the 5'CCA 3' triplet to the mature 3' end** 63
- **4.3. Analysis of step III - splicing the endogenous**

13 base intron 63
4.4. Processing rates of intron & intronless recombinant tRNAs 64
4.5. Analysis of *in vitro* cleavage efficiencies by tRNA^{Tyr}-embedded & non-embedded Rz12 & RzCA ribozymes 64
4.6. *In vitro* cleavage efficiencies of processed & unprocessed tRNARz12 & tRNARzCA ribozymes 65
DISCUSSION 65

CHAPTER 5
EXPRESSION OF tRNA^{Tyr}-EMBEDDED & NON-EMBEDDED RIBOZYME & ANTISENSE SEQUENCES IN PLANT CELLS

INTRODUCTION 70
RESULTS 71
5.1. CAT activities from the mutant & normal CAT targets 71
5.2. Analysis of replication of ACMV constructs *in vivo* 72
5.3. *In vivo* efficiencies of non-embedded & tRNA-embedded ribozymes 72
5.4. Analysis of tRNA-embedded ribozyme & antisense transcripts 73
5.5. Effect of mutagenising coat protein and/or tRNA promoter sequences on tRNA-embedded ribozyme 73
5.6. Analysis of accumulation of CAT mRNA and ribozyme cleavage products *in vivo.* 74
DISCUSSION 75

CHAPTER 6
ANALYSIS OF tRNARz12 & tRNAAs24 CONSTRUCTS IN TRANSGENIC TOBACCO

INTRODUCTION 78
RESULTS 79
6.1. The tRNA-ribozyme or tRNA-antisense co-segregates with GUS activity 79
6.2. Analysis of CAT expression in transgenic plants 79
6.3. CAT mRNA levels in transgenic plants: a comparison with pACAT transfected plant cells 79

6.4. tRNARz12 expression in transgenic plants: a comparison with pAtRNARz12 transfected plant cells 80

DISCUSSION 81

CHAPTER 7

THE APPLICATION OF HAMMERHEAD RIBOZYMES FOR TARGETED *IN VIVO* GENE INACTIVATION

7.1. Conclusions of this study 86

7.2. The *in vivo* requirement for high molar concentrations of ribozymes 88

7.3. The delivery of tRNA-ribozymes 89

7.4. The ACMV-tRNA system as an *in vivo* screen 90

7.5. Prospects for *in vivo* gene inactivation using hammerhead ribozymes 91

REFERENCES 93

List of Figures following page

1.1a. Hammerhead chemical cleavage reaction 5
1.1b. Hammerhead self-cleaving domain 5
1.2. Rolling circle model for replication 6
1.3a. *Cis* hammerhead cleavage domain (Forster & Symons, 1987a) 8
1.3b. *Trans* hammerhead cleavage domain (Uhlenbeck, 1987) 8
1.3c. *Trans* hammerhead cleavage domain (Haseloff & Gerlach, 1988) 8
1.4. Conserved ribonucleotides in unpaired core 9
1.5. Conserved ribonucleotides in helix II and the tetraloop 9
1.6. Conserved ribonucleotides in target site triplet 11
1.7. Critical 2'OH groups 12
1.8a. Critical guanosine amino groups 15
1.8b. Critical adenosine N7 15
1.9a. Phosphorothioates 16
1.9b. Critical phosphate linkages 16
1.10a. 3'endo & 2' endo ribose moieties 17
1.10b. Critical ribose moieties 17
1.11. Summary of base substitutions 21
1.12a. 3D-folded structure of hammerhead ribozyme 24
1.12b. Base-pairing in the 3D structure 24
1.13. Summary of successful *in vivo* applications 25
1.14. Intracellular considerations for hammerhead ribozymes 26
2.1a. Map of ACMV "pApoly" vector 36
2.1b. CAT expressed from pJ35SN and pApoly vectors 37
2.1c. CAT antisense and long ribozyme in pApoly vector 37
2.2a. tyrosine-tRNA in pGEM3zf- 38
2.2b. Clover leaf motif of tyrosine-tRNA 38
2.2c. Sequence of Rz12 ribozyme 39
2.2d. Sequence of RzCA ribozyme 39
2.3. Site directed mutagenesis of "GUC" on CAT 40
2.4. modified pApoly vector 40
2.5a. Site directed mutagenesis of coat protein promoter 41
2.5b. Site directed mutagenesis of tRNA promoter 41
2.6. Method for PCR analysis of *in vivo* CAT mRNA 48
2.7a. Primer positions for PCR analysis of tRNAAs24 51
2.7b. Primer positions for PCR analysis of tRNARz12 51
2.8. Sequence of primers used for CAT and tRNA analysis 52
3.1. Time course of pJ35SCATN & pACAT CAT activities 55
3.2. Replication of ACMVCAT 55

3.3. Summary of pACAT CAT activity in presence of pAAsCAT or pARzCAT (1:3) 56
3.4. As for 3.3 but ratio of 1: 2 or 1:1 57
3.5. Replication of pAAsCAT and pARzCAT 57
4.1. Clover leaf motif of tyrosine-tRNA 62
4.2. Steps involved in processing tyrosine-tRNA 62
4.3. *In vitro* maturation of recombinant and wildtype tRNA 63
4.4. *In vitro* maturation to step II 63
4.5. *In vitro* maturation of intron-plus and intron-minus recombinant tRNAs 64
4.6. Average *in vitro* processing rates 64
4.7. *In vitro* cleavage of CAT or CM2 targets by tRNA and non-tRNA ribozymes 65
4.8. Summary of *in vitro* cleavage of CAT target 65
4.9. Summary of *in vitro* cleavage by processed & non-processed tRNA-ribozymes 65
5.1. *In vivo* CAT activities for CAT & CM2 targets 71
5.2. Replication of ACMVCAT 72
5.3. Replication of ACMV ribozyme & antisense constructs 72
5.4a. Summary of CAT activities in presence of ACMV expressing ribozyme or antisense constructs 72
5.4b. As for 5.4a but except CM2 target 72
5.5a. Map of pAtRNARz12 & pAtRNAAs24 constructs 73
5.5b. RNase protection assay of tRNARz12 & tRNAAs24 RNAs 73
5.6. RNase protection assay of tRNA, tRNAAs24 & tRNARz12 73
5.7a. Site directed mutagenesis of pAtRNARz12 construct 74
5.7b. RNase protection assay of pAtRNARz12 mutant promoter constructs 74
5.7c. Summary of CAT activities in presence of mutant tRNARz12 promoter constructs 74
5.8. RNase protection of CAT mRNA 74
5.9. RT-PCR of CAT mRNA 74
6.1. Co-segregation of GUS and tRNAAs24 or tRNARz12 transgenes 79
6.2. Summary of CAT activities in tRNARz12 x 35SCAT or tRNAAs24 x 35SCAT transgenic tobacco 79
6.3. RT-PCR analysis of CAT mRNA in tRNARz12 x 35SCAT or tRNAAs24 x 35SCAT transgenic tobacco 80
6.4. Comparison of CAT mRNA from pACAT transfected plant cells and 35SCAT transgenic plants 81
6.5. Comparison of tRNARz12 RNA levels from pAtRNARz12MA transfected plant cells and tRNARz12 transgenic plants 81

This thesis contains no material which has been accepted for the award of any other degree or diploma in any university. To the best of my knowledge, this thesis contains no material previously published, or the result of any work by another person, except where due reference is made in the text.

The research described in this thesis is my own original work, with the following exceptions.

The pACMV vector was partially constructed by Paul Feldstein and Cathy Chay as detailed in Chapter 2 (Chapter 3 & 5). Rob de Feyter and Judy Gaudron performed the agrobacterium-mediated transformation of the tRNARz12 and tRNAAs24 sequences into Ti68 *N.tabacum* (Chapter 6). Danny Llewellyn produced the Ti68 *N.tabacum* line expressing CAT (Chapter 6).

R. Perriman.

ACKNOWLEDGMENTS

I would like to thank several people who have encouraged and advised me during my PhD. Firstly, my original supervisors, Wayne Gerlach and Angela Delves. Also to George Bruening and many colleagues and friends at the University of California, Davis where approximately 1/3 of this research was undertaken. Finally to my current supervisors Carol Behm and Jim Peacock, firstly thank-you for taking me on, and secondly for all your encouragement. At this point I should also acknowledge my "surrogate" supervisor, Liz Dennis. A special note of gratitude also to Paul Keese, who has advised, edited and encouraged beyond the call of duty.

In addition there are many people in the lab and throughout Plant Industry who have helped me at some stage during my PhD.

Finally I thank my mother and sister and partner Peter all of whom have encouraged and supported me throughout. I would like to dedicate this thesis to the memory of my father, Alan Perriman, whose unerring enthusiasm and fascination for everything, provided me with a childhood filled with queries and quandaries and awakened in me the desire to question and understand.

This research was conducted in the Division of Plant Industry, CSIRO. I acknowledge the financial support of Gene Shears Pty. Ltd. who provided a post-graduate research award for this research.

ABSTRACT

Ribozymes are RNA sequences capable of carrying out catalytic functions. This thesis has investigated the application of hammerhead ribozymes for the specific inactivation of a target gene in plants.

Results were obtained for 2 types of RNA transcripts containing hammerhead ribozyme sequences designed to inactivate the CAT target gene. Initial *in vivo* screening of the hammerhead ribozymes was done using transient expression in *N.tabacum* plant cells. To increase ribozyme and CAT expression in the plant cells, both sequences were expressed from a self-replicating viral vector, pACMV. Expression from this vector, as judged by CAT enzyme activity, was 19 times greater than from a non-replicating vector in which CAT was expressed from the 35S promoter.

The first ribozyme construction analysed (Chapter 3) was a long ribozyme in which four hammerhead domains were incorporated within the complete CAT-antisense sequence. Previous analyses, in which expression of this ribozyme and corresponding antisense was obtained from the 35S promoter, had suggested that the long ribozyme could enhance antisense-mediated inhibition of the CAT target by 30% (Perriman *et al*, 1993). In contrast to these data, the results presented in chapter 3 show that co-transfection of pACMV expressing CAT and either antisense or ribozyme-antisense, gave significant but equivalent reductions in CAT enzyme activity.

The second ribozyme constructions were two short molecules, Rz12 and RzCA, which were embedded within a tobacco tyrosine tRNA ($tRNA^{Tyr}$) sequence (Chapter 4). These ribozymes, and the corresponding control antisense sequences, were assayed both *in vitro* and *in vivo*. The *in vitro* analyses included monitoring the steps of $tRNA^{Tyr}$ maturation, and ribozyme-cleavage rates induced by the $tRNA^{Tyr}$-embedded and analogous non-embedded ribozymes. The maturation assays showed that the chimeric tRNAs were not processed to completion; a 13 base intron contained within the

molecule was not spliced out during processing of these tRNA sequences. The cleavage assays showed that the Rz12 ribozyme, in the non-tRNA^{Tyr}-embedded form, was the most efficient at cleaving the CAT target. The tRNA^{Tyr}-embedded Rz12 was approximately 50% less efficient, although rates of cleavage were significantly increased when the tRNARz12 ribozyme was processed prior to cleavage.

Co-transfection of pACMV expressing CAT target, Rz12 ribozymes or control antisense constructs into plant cells, and the subsequent analysis of CAT enzyme activities, showed that CAT activity was 85% reduced in the presence of the tRNARz12 ribozyme construct (Chapter 5). This was significantly more than the reduction in the presence of non-embedded Rz12 ribozyme, or tRNA^{Tyr}-embedded and non-embedded antisense. A mutant CAT sequence, CM2, which contained a non-cleavable target site, gave CAT activity which was reduced to the same level in the presence of all antisense and Rz12 ribozyme constructs. This suggested that the greater reduction observed for the wildtype CAT target and tRNARz12 ribozyme, was due to ribozyme-mediated cleavage. CAT mRNA analysis supported this view by showing, in the presence of the tRNA^{Tyr}-ribozyme, a reduction in full length message and a significant accumulation of RNA representing the 3' cleavage product.

The tRNA^{Tyr}-ribozyme constructs contained active RNA polymerase II and III promoters. Mutagenesis of these promoter sequences revealed that the active and predominant ribozyme transcript was derived from the RNA polymerase III promoter of the tRNA^{Tyr} sequence. This transcript was present in a 620 molar excess over the CAT mRNA in the plant cells.

Following the transient studies, the tRNA^{Tyr}-ribozyme and tRNA^{Tyr}-antisense were transformed into *N tabacum* Ti68 plants (Chapter 6). The CAT target was expressed as a single homozygous insertion in a separate Ti68 plant. CAT x tRNA^{Tyr}-ribozyme or tRNA^{Tyr}-antisense crosses were carried out and the progeny assayed for relative CAT activties. No reduction in CAT enzyme activity or CAT mRNA levels were observed in the presence of the tRNA^{Tyr}-ribozyme or tRNA^{Tyr}-antisense transgenes. The analysis of tRNA^{Tyr}-ribozyme expression showed significantly reduced levels relative to the transient expression obtained from the replicating vectors in plant cells. This resulted in a molar ratio of 0-0.7 ribozyme : 1 CAT substrate. This reduction in the ribozyme: substrate ratio was probably responsible for the lack of effect on CAT mRNA observed in this study.

INTRODUCTION

1.1 Enzymes

Most chemical reactions that take place within biological systems are catalysed by proteinaceous enzymes. These enzymes accelerate the rate of a reaction by providing an alternate reaction pathway which has a lower activation energy. They are highly specific with regard to the substrates they act upon and the products they generate, and are not consumed within the reaction (Alberts *et al.*, 1989). Recently several RNA molecules, found in a wide range of systems have been shown to catalyse the cleavage and ligation of phosphodiester bonds within specific nucleic acid sequences. These RNA molecules have been collectively called "ribozymes" (Kruger *et al.*, 1982). Ribozymes exhibit many catalytic activities including cleavage, replication and ligation of nucleic acid substrates (for review see Pyle, 1993).

In many cases ribozymes, and their site of cleavage, are intramolecular. Such ribozymes can only catalyse a single reaction and are often modified during this process. These ribozymes have been termed "quasi-catalytic" (Cech and Bass, 1986). Other ribozymes can act in *trans* , and take part in multiple reactions without being modified themselves. These ribozymes act in a truly catalytic manner and can therefore be classified as enzymes. The study of one such ribozyme, the hammerhead ribozyme, forms the basis of this thesis. However, before I describe the hammerhead ribozyme in detail, it is important to introduce and summarise some of the other catalytic RNAs and also to provide an historical perspective to the origins of the discovery of these novel RNA molecules.

1.2. Ribozymes

1.2.1 Group I introns

The first ribozyme to be described was a 413 nucleotide intron found in the nuclear rRNA precursor of the protozoan *Tetrahymena thermophila* (Kruger *et al.*, 1982). This intron is one of almost 100 which have been classified as group I introns. Group 1 introns are characterised by conserved sequence homologies and secondary structures which mediate self-splicing. To date, at least twelve group I introns have exhibited self-splicing. The self-splicing process involves the covalent bonding of a guanosine nucleotide to the 5' end of the intron which acts as a nucleophile in producing the first excision step. An internal guide sequence (IGS) "CUCUCU", forms base-pairing with sequences adjacent to, and including the 5' splice site. Base-pairing of this region must occur for the nucleophilic attack by the guanosine nucleotide. Excision at the 3' end of the intron is catalysed by ligation of the 3'-hydroxyl on the 5' exon to the 5'-phosphate on the 3' exon, thus excluding the intron. After excision, the intron forms a circular RNA, covalently closed by a 5'-3' phosphodiester bond (Cech, 1987). This whole process can occur in the complete absence of any protein interaction.

1.2.2 RNase P

At around the same time as the *Tetrahymena* self-splicing intron was discovered, Altman and colleagues demonstrated the first *trans* acting ribozyme (Guerrier-Takada *et al.*, 1983). The RNase P enzyme is responsible for the maturation of pre-tRNA molecules. This enzyme is made up of two subunits, an RNA and a protein. In bacteria, the 400 nucleotide RNA component of the RNase P enzyme was found to cleave the precursor tRNA in the absence of the protein subunit (Guerrier-Takada *et al.*, 1983). The RNase P RNA exhibited multiple turnover and remained unmodified during the reaction. This difference, along with the fact that this is a *trans* reaction (as distinct from the *cis* acting *Tetrahymena* self-splicing intron) made the RNase P RNA the first truly catalytic RNA enzyme to be described.

Soon after this discovery, Cech and co-workers showed that by separating the 5' and 3' exons from the intron, the *Tetrahymena* self-splicing intron could also catalyse a number of novel *trans* reactions. The novel RNA substrates required only complementary sequence with which to "base-pair" to the IGS sequence (see Cech, 1990 for review). This discovery demonstrated that the *Tetrahymena* self-splicing intron was also capable of behaving in a catalytic fashion.

In their native state, both of these ribozymes, are relatively large (approximately 400 nucleotides) and require specific "guide" sequences on their target RNA. In the case of the *Tetrahymena* intron, the six base sequence "CUCUCU" acts as a recognition site for the initial guanosine bonding (Cech, 1987). However, mutagenic analysis has established that as few as two bases ("CU") are sufficient for cleavage to occur (Murphy and Cech, 1989). For the RNase P RNA, the acceptor stem at the 3' end of the tRNA acts as an "external guide sequence" (EGS). The nucleotide sequence of the EGS is not conserved but identifies the site of cleavage by forming base-pairs with the segment that is cleaved (Forster and Altman, 1990). Additionally, the conserved triplet "CCA" at the 3' end of the acceptor stem of the tRNA is essential for the cleavage reaction.

Since both ribozymes are able to act in *trans,* application of these to novel RNA substrates could provide a powerful tool for targeting, cleaving and inactivating specific RNAs. Application of the *Tetrahymena* self-splicing process has been limited, due mainly to the lack of target specificity (Zaug and Cech, 1986; Sullenger and Cech, 1994). In contrast, the RNase P protein-RNA moiety from both *E.coli* and human cells have been successfully used to cleave new mRNA targets (Li *et al.*, 1992; Yuan *et al.*, 1992; Yuan and Altman, 1994, 1995). By delivering specifically designed EGS guide sequences, which can anneal to the target mRNA, the endogenous RNase P recognises the engineered target-EGS hybrid as a site of cleavage and cleaves the mRNA.

1.2.3 Other catalytic RNAs

Since the discovery of the *Tetrahymena* and RNAse P ribozymes, several other catalytic RNA sequences have been described (for reviews see Cech and Bass, 1986; Symons, 1992, 1994). In addition to the group I introns, to which the *Tetrahymena* sequence belongs, a second class of self-splicing introns called group II have been described (Michel and Dujon, 1983). Group II introns contain conserved structures which are different from those found in group I introns. In addition, group II intron excision does not require a guanosine nucleotide and the excised intron is held together by a 2'-5' phosphodiester bond (i.e. unlike the 3'-5' bond found in the circularised group I introns).

Along with these self-splicing introns, several small circular RNAs have been found to contain sequences capable of undergoing autocatalytic cleavage (see Bruening, 1990 for review). These include two mitochondrial sequences from *Neurospora* , the genomic(+) and antigenomic(-) sequences from hepatitis delta virus (HDV) and several small parasitic RNAs sometimes found associated with plant viruses (i.e. satellite or viroid RNAs). In addition, similar sequences have been found in transcripts of a nuclear satellite DNA from newt.

Like the *Tetrahymena* self-splicing intron, the naturally occurring cleavage process in these small circular RNAs acts in *cis*. Mutagenic analysis has identified the sequences within these RNAs that are responsible for the self-cleaving process. This has led to their successful separation into *trans* ribozyme-mediated cleavage reactions (e.g. Haseloff and Gerlach, 1988; Feldstein *et al.*, 1989; Branch and Robertson, 1991; Guo and Collins, 1995). Of these reactions, the isolation and manipulation of two distinct ribozyme sequences has attracted much attention for their use as potential gene therapy agents. The respective two-dimensional folded conformations of these two ribozymes has led to their naming as hairpin (or paperclip; Buzayan *et al.*, 1986; Hampel and Tritz, 1989; Feldstein *et al.*, 1989; Haseloff and Gerlach, 1989) and hammerhead ribozymes (Forster and Symons, 1987a).

1.2.4 The hairpin ribozyme

Unlike the hammerhead motif , which is present in several naturally occurring self-cleaving RNAs, the only hairpin ribozyme so far identified derives from the satellite RNA associated with tobacco ringspot virus (sTobRV). The replication of sTobRV involves the autolytic cleavage of positive and negative strand RNA (see also section 1.4). The positive strand RNA is cleaved by a hammerhead ribozyme, and the negative strand by a hairpin ribozyme (Buzayan *et al.*, 1986; Hampel and Tritz, 1989; Feldstein *et al.*, 1989; Haseloff and Gerlach, 1989).

Site specific cleavage, by the hairpin ribozyme, is 5' of a "GUC" triplet and the reaction is readily reversible (i.e. ligation). Like the hammerhead, the adaptation of the hairpin from a *cis* to a *trans* reaction has led to the development of hairpin ribozymes designed to target and cleave new RNA substrates (e.g. Yu *et al.*, 1993). As this thesis involves the use of the hammerhead ribozyme, and the literature involving this ribozyme is extensive, the hairpin ribozyme will not be further discussed.

This thesis details investigations toward optimising the stability, expression and intracellular location of hammerhead ribozymes for *in vivo* applications. The remainder of this review will focus on hammerhead ribozymes, and include a detailed analysis of the literature concerning the *in vitro* optimisation of the hammerhead ribozyme reaction, followed by the data available for the *in vivo* activity. The research carried out in this thesis is put into the context of the current literature.

1.3. Hammerhead ribozymes: an introduction

Hammerhead ribozymes are characterised by the presence of self-cleaving sequences which, in neutral or higher pH, autolytically cleave RNA to generate a 5' hydroxyl group on the 3' fragment and a 2', 3' cyclic phosphate on the 5' fragment (Fig. 1.1a; Prody *et al.*, 1986; Forster and Symons, 1987a & b; Buzayan *et al.*, 1986;). The overall number of phosphodiester bonds does not change during the reaction, nor is there the addition or removal of a nucleotide at the cleavage site. As might be expected from an enzymic reaction, the reverse reaction (i.e. ligation) has been shown to occur *in vitro*, but at a low efficiency(Prody *et al.*, 1986). The only exogenous requirement for the reaction is a divalent cation such as magnesium. The exact function of this cation in the cleavage reaction is unknown. In most instances, this self-cleaving

Figure 1.1

a: The self-cleavage reaction of RNA catalysed by the presence of a hammerhead ribozyme and divalent cations (Mg^{2+}). The susceptible phosphodiester bond in the substrate RNA is cleaved to produce products with a 2'3' cyclic phosphate at the 3' terminus and a 5' hydroxyl at the 5' terminus.

b: The hammerhead cleavage domain. It consists of three helices (I, II and III) which radiate from the central core. The arrow indicates the susceptible phosphodiester bond which is cleaved as described in **(a)**. Watson-Crick base pairing in helices I, II and III is shown. Non-conserved nucleotides are designated "N".

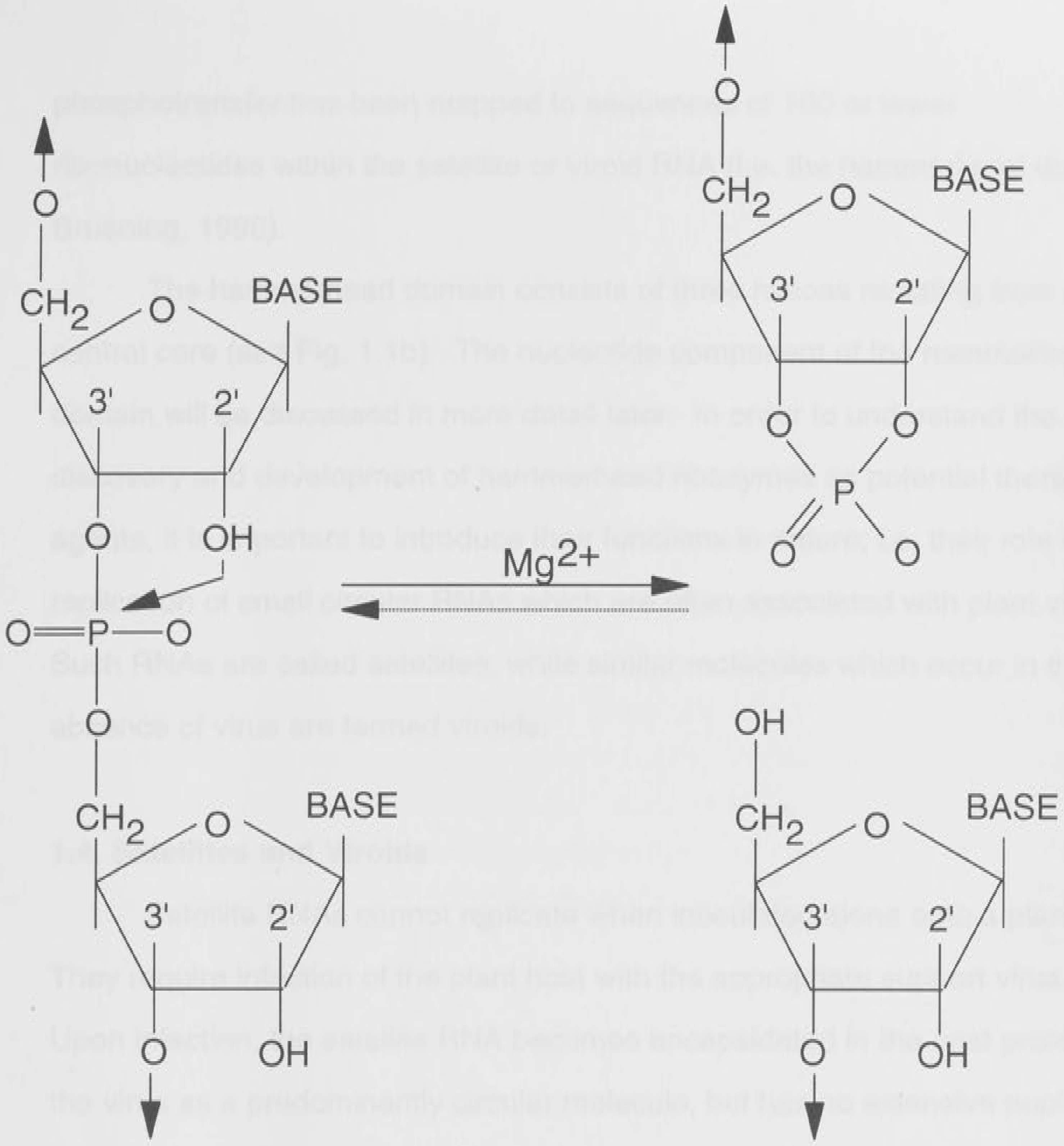

BASE
CH2
O
3'
2'
OH
Mg2+
O=P—O
BASE
CH2
O
3'
2'
O
P
O
O
OH

Figure 1.1a

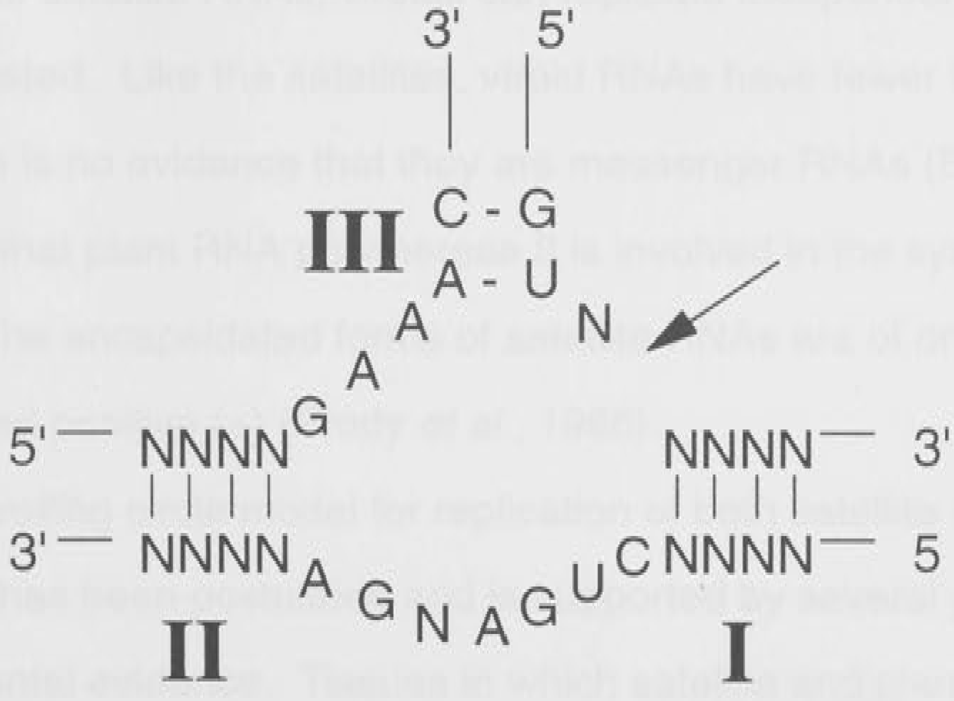

3'
5'
C - G
A - U
III
A
A
G
N
5'
NNNN
NNNN
3'
3'
NNNN
A
G
N
A
G
U
C
NNNN
5
II
I

Figure 1.1b

phosphotransfer has been mapped to sequences of 100 or fewer ribonucleotides within the satellite or viroid RNA (i.e. the hammerhead domain; Bruening, 1990).

The hammerhead domain consists of three helices radiating from a central core (see Fig. 1.1b). The nucleotide component of the hammerhead domain will be discussed in more detail later. In order to understand the discovery and development of hammerhead ribozymes as potential therapeutic agents, it is important to introduce their functions in nature; i.e. their role in the replication of small circular RNAs which are often associated with plant viruses. Such RNAs are called satellites, while similar molecules which occur in the absence of virus are termed viroids.

1.4. Satellites and Viroids

Satellite RNAs cannot replicate when inoculated alone onto a plant. They require infection of the plant host with the appropriate support virus. Upon infection, the satellite RNA becomes encapsidated in the coat protein of the virus as a predominantly circular molecule, but has no extensive nucleotide homology with the plant virus. Despite this, the satellite has an absolute dependence upon that virus for replication. Satellites are less than 400 ribonucleotides in length and do not appear to encode for any protein. In contrast to satellite RNAs, viroids can replicate independently and are not encapsidated. Like the satellites, viroid RNAs have fewer than 400 nucleotides and there is no evidence that they are messenger RNAs (Bruening, 1990). It is believed that plant RNA polymerase II is involved in the synthesis of most viroid RNAs. The encapsidated forms of satellite RNAs are of one polarity, designated positive (+) (Prody *et al.,* 1986).

A rolling circle model for replication of both satellite and viroid RNAs (see Fig. 1.2) has been postulated and is supported by several pieces of experimental evidence. Tissues in which satellite and plant virus are replicating, or viroid alone, have been found to contain RNA of both polarities.

Figure 1.2: Rolling circle model for replication by which satellite and viroid RNAs are thought to replicate. The steps are: **1**, the circular plus (+ - green) strand is copied to form tandemly repeated multimeric minus (-) RNA; **2**, Site specific cleavage of this strand produces - strand monomers: in sTobRV, this process is catalysed by the hairpin ribozyme; **3**, circularisation of - strand monomer; **4**, circular - strand is copied to produce multimeric + strand; **5**, Site specific cleavage produces monomeric + strand: this process is catalysed by the hammerhead ribozyme; **6**, circularisation of the + strand monomers: this is the dominant form found *in vivo.*

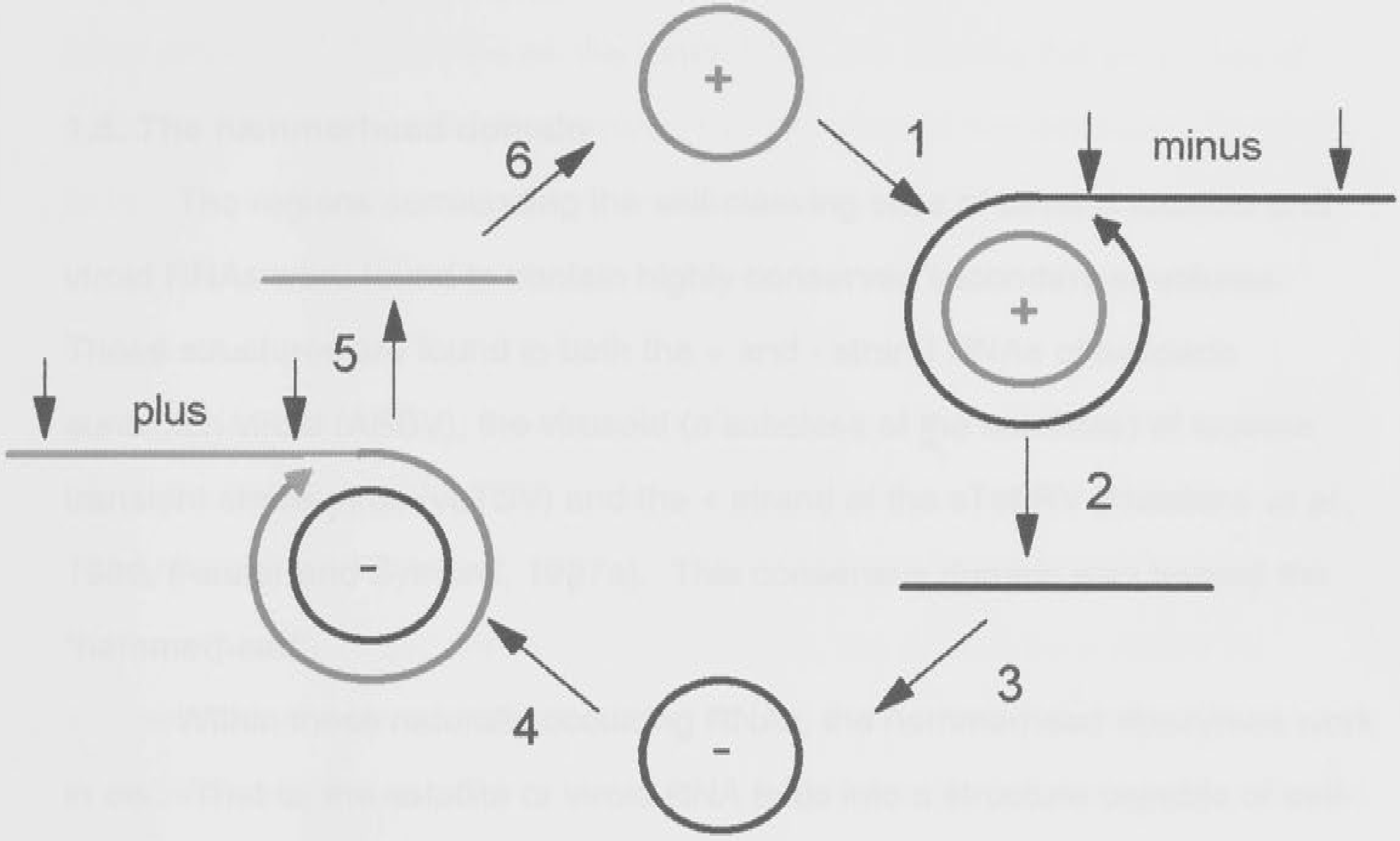
+
6
1
minus
+
5
plus
2
-
3
4
-

Figure 1.2

This RNA is found not only as the unit length sequence but also as tandemly repeated multimeric sequences. The positive polarity multimers contain conserved hammerhead sequences and are the precursors of the monomeric RNA (Buzayan *et al.,* 1986; Hutchins *et al.*, 1986; Forster and Symons, 1987a). The formation of monomeric RNAs is the consequence of the self-cleaving hammerhead ribozyme reaction.

1.5. The hammerhead domain

The regions surrounding the self-cleaving sites of several satellite and viroid RNAs were found to contain highly conserved secondary structures. These structures are found in both the + and - strand RNAs of avocado sunblotch viroid (ASBV), the virusoid (a subclass of the satellites) of lucerne transient streak virus (vLTSV) and the + strand of the sTobRV (Hutchins *et al.*, 1986, Forster and Symons, 1987a). This consensus domain was termed the "hammerhead".

Within these naturally occurring RNAs, the hammerhead ribozymes work in *cis* . That is, the satellite or viroid RNA folds into a structure capable of self-cleavage. Several important studies carried out in the late 1980's led to the manipulation of this *cis* reaction. Forster and Symons (1987a) delimited the minimum sequence requirements for self-cleavage of the + strand of the virusoid lucerne transient streak (vLTSV) to 52 nucleotides (Fig. 1.3a). As well, they proposed that the "hammerhead" structure was sufficient and necessary for self-cleavage (Forster and Symons, 1987b). Following this, Uhlenbeck transcribed two RNA molecules *in vitro* from synthetic deoxyoligonucleotides, and showed that a 19 nucleotide RNA fragment could rapidly and specifically induce cleavage of a 24 nucleotide fragment (Fig. 1.3b.; Uhlenbeck, 1987). Although this work showed that the reaction could occur in *trans* as well as *cis,* the active structure, as depicted by Uhlenbeck, required that the "substrate" RNA contain several conserved nucleotides and a stem-loop. These requirements significantly reduced the applicability of this ribozyme sequence to new RNA targets. Haseloff and Gerlach (1988) while carrying out structure-function analysis of the sTobRV sequences, identified a non-essential loop of the hammerhead structure. The removal of this loop allowed them to separate target and catalytic domains of the self-cleaving sequence, thereby creating the hammerhead ribozyme as depicted in figure 1.3c. Unlike the Uhlenbeck design, the Haseloff and Gerlach hammerhead ribozyme required only a three base recognition sequence on the target RNA. By altering the sequence of helix I and III on the catalytic domain, they designed a hammerhead ribozyme to target and cleave a completely unrelated RNA *in vitro.* This work was successful and the first synthetic hammerhead ribozyme had been used to cleave an unrelated RNA *in vitro.*

This *trans*-acting hammerhead ribozyme had a number of advantages over other catalytic RNA molecules. It was much smaller than both the *Tetrahymena* and RNaseP ribozymes and required only a three base target sequence on the substrate RNA. Additionally, the added requirement for sequence complementarity of helices I and III meant that highly specific synthetic hammerhead ribozymes could be designed to hybridise and cleave at a number of sites on any given RNA. The work of Haseloff and Gerlach (1988) led to the establishment of simple rules for the design of short hammerhead ribozymes sequences. Adherence to these rules can theoretically allow for the specific targeting, cleaving and inactivating of any designated RNA sequence, potentially making the hammerhead ribozyme a powerful tool. These rules are:

1. the presence of the highly conserved "catalytic domain" in the ribozyme RNA
2. a cleavage site on the substrate RNA, generally a GUC triplet, although other triplets have also been shown to cleave *in vitro* (Koizumi *et al.*, 1989; Sheldon *et al.*, 1989; Ruffner *et al.*, 1990; Perriman *et al.*, 1992).
3. complementary sequences between the substrate RNA and the hammerhead ribozyme in "hybridising arms" flanking the active site.

Figure 1.3

a: Minimal sequence requirements for obtaining *cis* cleavage of the virusoid, lucerne transient streak (Forster and Symons, 1987a). The three helices are indicated, and the arrow shows the site of cleavage. This structure led to self-cleavage reactions of this type being designated "hammerhead ribozymes".

b: Manipulation of the hammerhead ribozyme from a *cis* to a *trans* reaction (Uhlenbeck, 1987). The loops connecting helices I and II have been removed and replaced by a connecting loop at helix III. Cleavage site and designation of helices are as in (**a**). Using this design, the "substrate" RNA is required to contain several conserved nucleotides and a stem-loop 5' of the site of cleavage.

c: Further modification of the *trans* hammerhead cleavage reaction (Haseloff and Gerlach, 1988). In this design, helices I and III are unconnected and helix II contains a connecting loop. Using this design, the two RNA sequences can be separated as "substrate" and "enzyme" (i.e. ribozyme) and the substrate is required to contain only three conserved nucleotides for cleavage (i.e. nucleotides 16.1, 16.2 and 17 depicted in green). Annealing of the ribozyme to the substrate is via Watson-Crick base-pairing of helices I and III. Apart from the two base-pairs at the cleavage site (i.e. nucleotides 15.1 and 15.2 depicted in green), the nucleotide component of helices I and III is not conserved. The unpaired core and helix II make up the "catalytic domain" of the ribozyme and contains several conserved nucleotides. These are discussed in detail in the text and figures 1.4-1.11. The numbering of this catalytic domain conforms with Hertel *et al.*, 1992 and is used throughout this review.

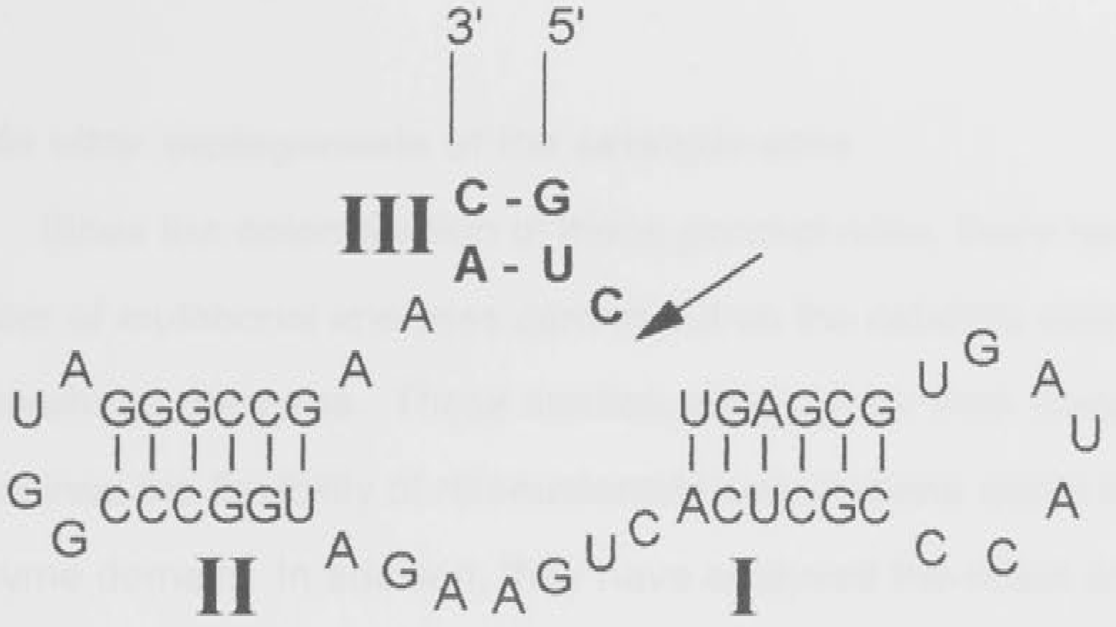
3'
5'
III
C - G
A - U
A
C
A
U A GGGCCG
G CCCGGU
G
II
A G A A G U C
UGAGCG
ACUCGC
U G A U A C C
I

Figure 1.3a

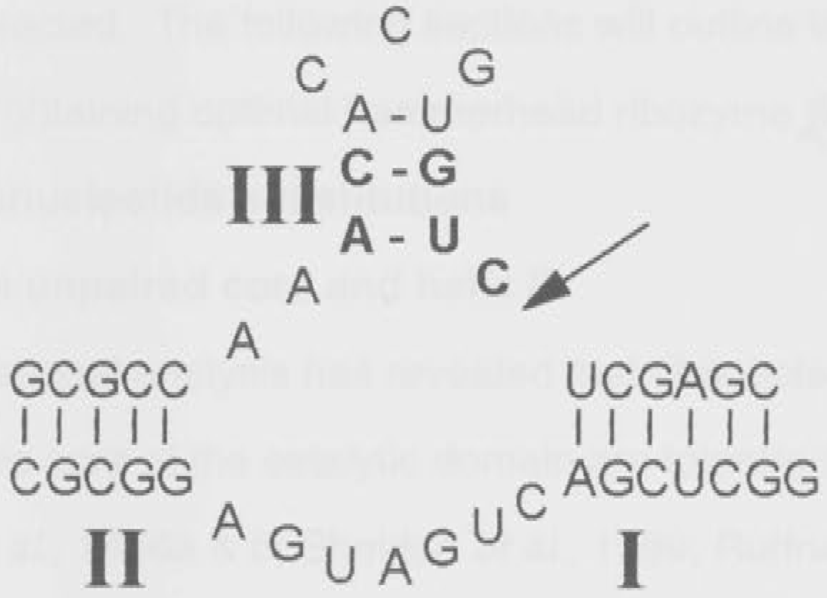
C
C G
A - U
III
C - G
A - U
A
C
A
GCGCC
CGCGG
II
A G U A G U C
UCGAGC
AGCUCGG
I

Figure 1.3b

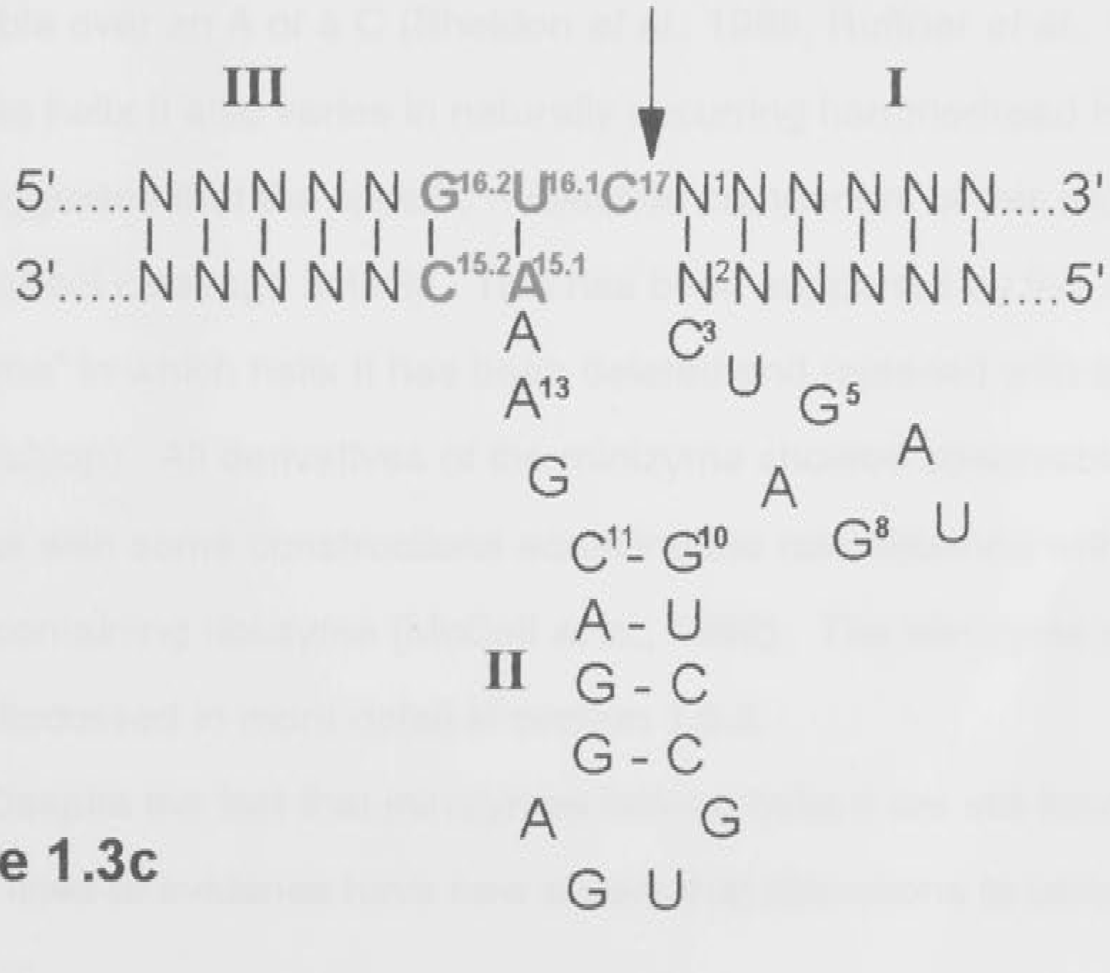
III
I
5'.....N N N N N G16.2 U16.1 C17 N1 N N N N N....3'
3'.....N N N N N C15.2 A15.1 N2 N N N N N....5'
A
C3
A13
U
G5
A
G
A
U
C11 - G10
G8
A - U
II
G - C
G - C
A
G
G U

Figure 1.3c

1.6. *In vitro* mutagenesis of the catalytic core

Since the determination of these general rules, there has been a large number of mutational analyses carried out on the catalytic core of the hammerhead ribozyme. These studies, although far from complete, have determined the flexibility of ribonucleotide substitutions within the hammerhead ribozyme domain. In addition, they have analysed the effect of substituting deoxynucleotides or chemically modified nucleotides in place of the standard ribonucleotides of the hammerhead domain. In this way the requirements for specific components of the ribonucleotides within the hammerhead structure can be dissected. The following sections will outline what is known from *in vitro* studies for obtaining optimal hammerhead ribozyme derived cleavage.

1.6.1. Ribonucleotide substitutions

1.6.1.1 The unpaired core and helix II

Mutational analysis has revealed that ribonucleotide substitutions within the unpaired core of the catalytic domain are tolerated poorly, if at all (Fig. 1.4- Koizumi *et al.*, 1988a & b; Sheldon *et al.*, 1989; Ruffner *et al.*, 1990). An exception is nucleotide 7, which varies in naturally occurring hammerhead sequences, and can be altered with minimal affect, although a G or a U appear favourable over an A or a C (Sheldon *et al.*, 1989; Ruffner *et al.*, 1990).

As helix II also varies in naturally occurring hammerhead RNAs, reports have suggested that the specific nucleotide component of this region may not greatly affect cleavage activity. This has been supported by the creation of a "minizyme" in which helix II has been deleted and replaced with a 4 base loop (i.e. tetraloop). All derivatives of the minizyme showed observable rates of cleavage with some constructions equalling the rate obtained with the original helix II containing ribozyme (McCall *et al.,* 1992). The minizyme constructions will be discussed in more detail in section 1.6.2.

Despite the fact that minizymes lacking helix II are still functional, several lines of evidence have now shown that alterations to certain base-pairs

Figure 1.4: Conserved nucleotides (red) in the unpaired core of the catalytic domain which are required for *in vitro* hammerhead ribozyme cleavage. The single variable nucleotide, U7 (shown boxed) can be substituted with minimal effect.

Figure 1.5: Analysis of the requirements of helix II and the tetraloop of the catalytic domain of the hammerhead ribozyme. G10 - C11 (shown in blue) must be conserved for efficient *in vitro* cleavage. The remaining three base-pairs in helix II can be altered in sequence as well as the number of base-pairs (see section 1.6.1.1 for details). The four base tetraloop joining helix II can also be altered although most efficient cleavage has been obtained with 5'GNRA 3' loops (i.e. N = A, C, G or U; R = G or A; see boxed blue nucleotides) as detailed in the text.

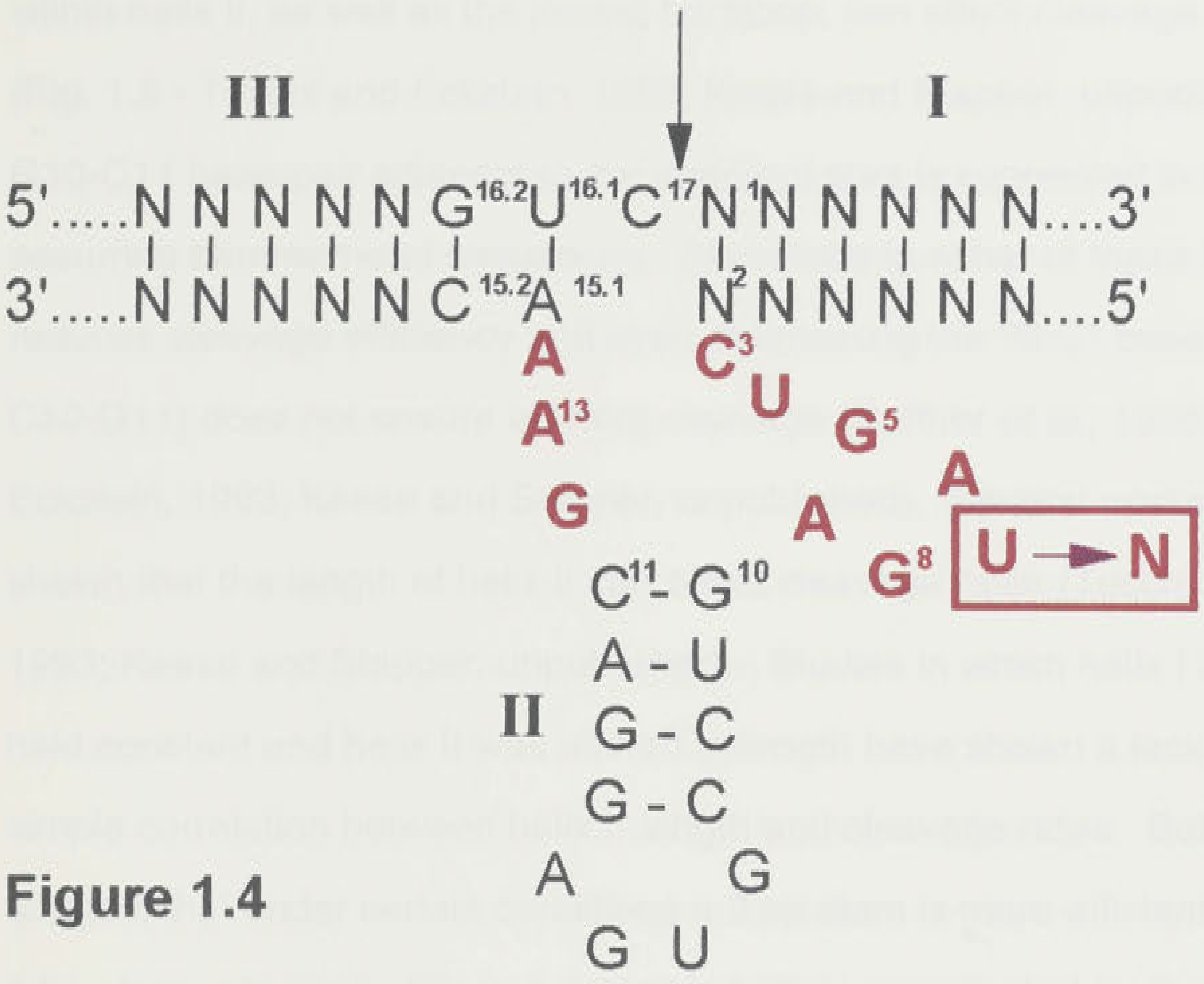
III
I
5'.....N N N N N G16.2 U16.1 C17 N1 N N N N N....3'
3'.....N N N N N C15.2 A15.1 N2 N N N N N....5'
A
C3
A13
U
G5
A
G
A
G8
U → N
C11 - G10
A - U
II
G - C
G - C
A
G
G U

Figure 1.4

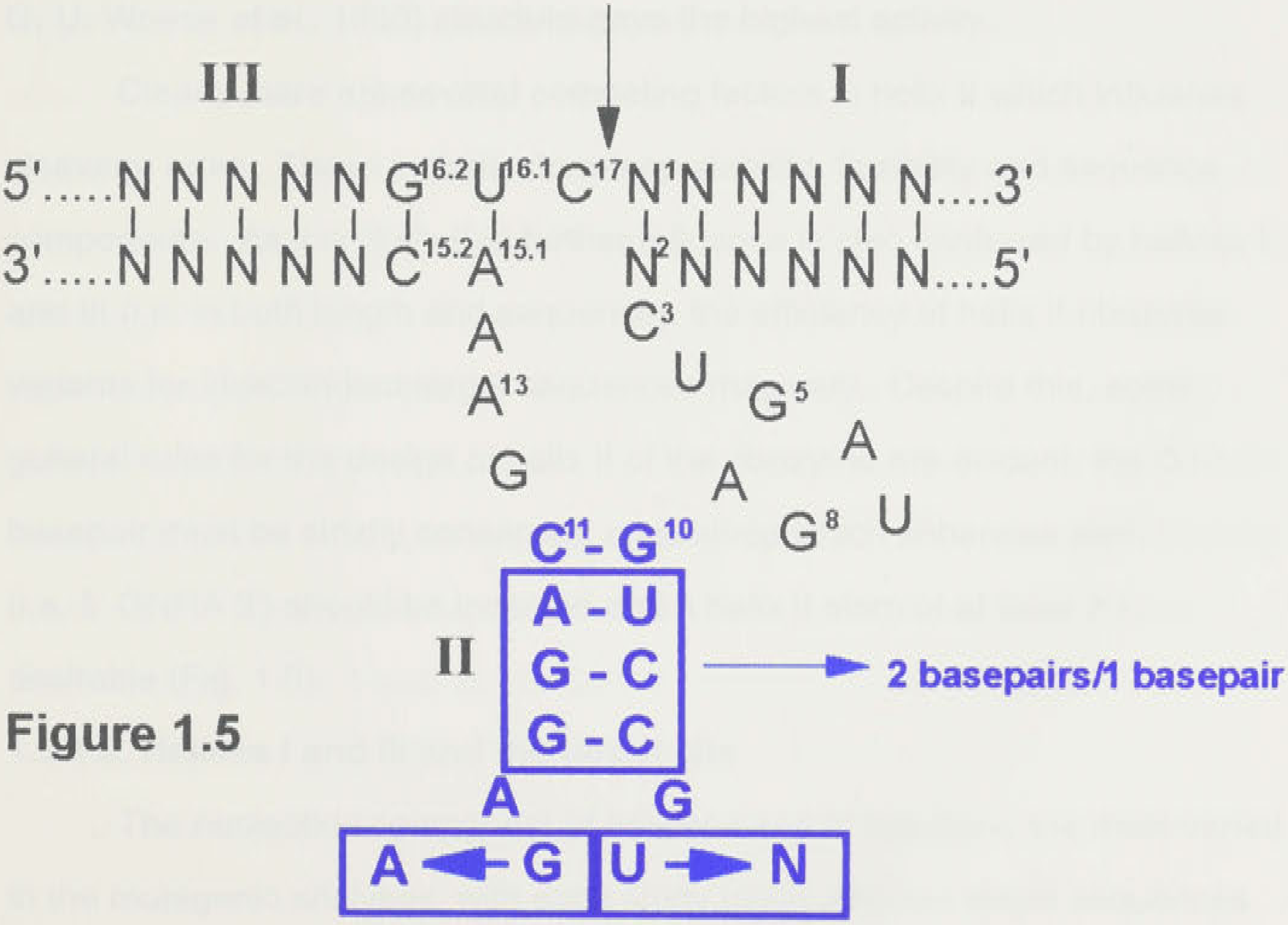
III
I
5'.....N N N N N G16.2 U16.1 C17 N1 N N N N N....3'
3'.....N N N N N C15.2 A15.1 N2 N N N N N....5'
A
C3
A13
U
G5
A
G
A
G8
U
C11 - G10
A - U
II
G - C
G - C
2 basepairs/1 basepair
A
G
A ← G
U → N

Figure 1.5

within helix II, as well as the joining tetraloop, can affect cleavage rates *in vitro* (Fig. 1.5 - Tuschl and Eckstein, 1993; Keese and Stapper, unpublished). The G10-C11 base-pair adjacent to the unpaired core is conserved in naturally occurring hammerhead sequences. Alterations to either of these two bases reduces cleavage efficiency and even maintaining the "G-C" base pair (i.e. as C10-G11) does not ensure efficient cleavage (Ruffner *et al.*, 1990; Tuschl and Eckstein, 1993; Keese and Stapper, unpublished). Several workers have also shown that the length of helix II can affect cleavage rates (Tuschl and Eckstein, 1993; Keese and Stapper, unpublished). Studies in which helix I and III are held constant and helix II was altered in length have shown a lack of any simple correlation between helix II length and cleavage rates. Both studies suggest that under certain conditions a 2 bp stem is more efficient than control 4 bp stem. However, this conclusion is further complicated by the effect induced by the nucleotides comprising the tetraloop at the base of helix II. Tuschl and Eckstein (1993) found that ribozymes with the same 2 bp helix II stems, but with variable tetraloop sequence showed very different rates of cleavage. Tetraloops which conformed to the 5'GNRA3' (R = A, G; N = A, C, G, U; Woese *et al.*, 1990) structure gave the highest activity.

Clearly there are several competing factors in helix II which influence cleavage rates. These include stem-loop stability, flexibility and sequence components. As it is likely that further influence is also conferred by helices I and III (i.e. in both length and sequence), the efficiency of helix II ribozyme variants for independent target sequences may vary. Despite this, some general rules for the design of helix II of the ribozyme are evident: the G10-C11 basepair must be strictly conserved, a tetraloop which enhances stem stability (i.e. 5' GNRA 3') should be included and a helix II stem of at least 2 bp is desirable (Fig. 1.5).

1.6.1.2. Helices I and III and the target site

The nucleotide component of helices I and III has been the most varied in the mutagenic analyses, with each study using different target sequences and lengths. This has led to some confusion as to the effect these sequences may have on cleavage rates. Clearly, secondary structure within either the substrate or the ribozyme can play a role in cleavage efficiency. Fedor and Uhlenbeck (1990) found that certain substrate RNA sequences can form aggregates that are virtually non-reactive. van der Vlugt *et al.* (1993) found that ribozymes against the viral target potato virus Y showed no detectable cleavage products. Analysis of the ribozyme/substrate interaction in this study indicated that incorrect base-pairing of helices I and III were responsible for the lack of cleavage observed. This situation was reversed when the same cleavage site was targeted with a ribozyme providing much longer hybridisation of helices I and III. Similarly an A or a C residue at position 16.2 have shown differential rates of cleavage in different systems varying from equivalent to a G (Koizumi *et al.*, 1988b; Ruffner *et al.,* 1990) to no cleavage at all (Perriman *et al.*, 1992). This strongly suggests that sequences in helices I and III are having a profound effect on cleavage rates.

There has been extensive mutational analysis of the three nucleotides which make up the target site triplet. Independent laboratories have analysed single and double ribonucleotide substitutions and determined a number of effective target site triplets (Fig. 1.6). Nucleotide 17 can be substituted with an A or a U, although the U residue does show reduced cleavage rates (Koizumi *et al.*, 1989; Ruffner *et al.*, 1990; Perriman *et al.*, 1992). There is also evidence to suggest that a G can be placed at this position, however this appears to be dependent upon the nucleotide sequence or context of helix II (Sheldon *et al.*, 1989; Perriman *et al.*, 1992). Reductions in cleavage rates due to alterations at nucleotide 17 have been attributed to the formation of alternate and/or inactive conformations between or within the substrate and ribozyme sequences (Ruffner *et al.*, 1990; Heus *et al.*, 1990; Fedor and Uhlenbeck, 1990; Perriman *et al.*, 1992). For example, a G or U at position 17 can pair with C3 or A14 respectively, thereby disrupting the critical catalytic core structure.

Figure 1.6: Summary of the nucleotide requirements at the cleavage site of the hammerhead ribozyme reaction (shown in green). The unpaired C17 can be substituted for an A or a U and G16.2 - C15.2 can be altered to C16.2 - G15.2 or A 16.2 - U15.2. U16.1 and A15.1 must be conserved for efficient cleavage.

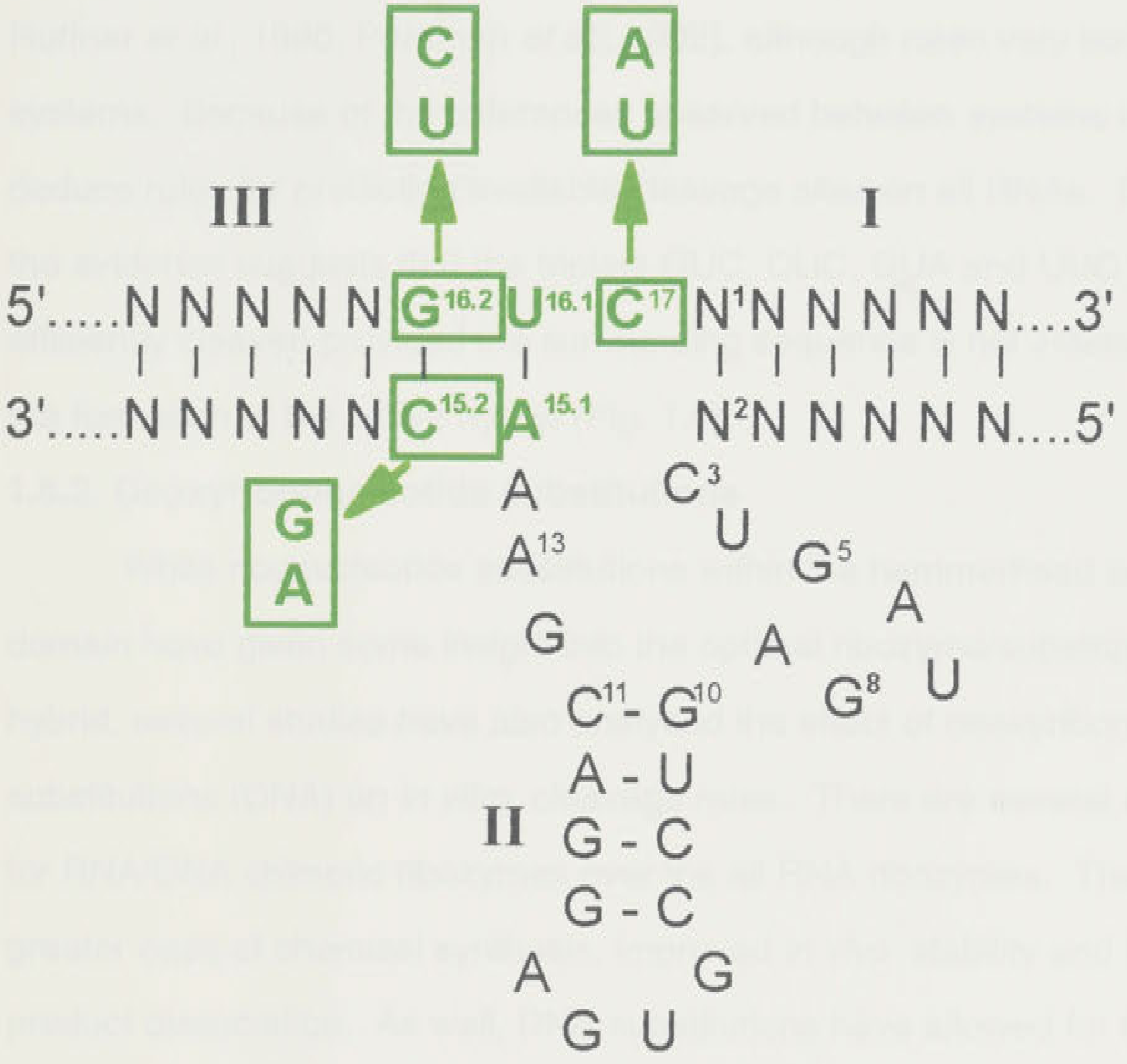
C
U
A
U
III
I
5'.....N N N N N G16.2 U16.1 C17 N1N N N N N....3'
3'.....N N N N N C15.2 A15.1 N2N N N N N....5'
G
A
A
C3
A13
U
G5
A
G
A
C11- G10
G8
U
A - U
II
G - C
G - C
A
G
G U

Figure 1.6

The central residue of the target site, nucleotide 16.1 (and 15.1 on the ribozyme) is the most inflexible nucleotide. It must be a U residue (with base-pairing A at 15.1) in order to obtain good rates of cleavage (Koizumi *et al.*, 1988b; Ruffner *et al.*, 1990; Perriman *et al.*, 1992). An A or a C at this position do show cleavage *in vitro* however rates are drastically reduced (Perriman *et al.*, 1992). Position 16.2 is a G in all naturally occurring hammerhead ribozyme sequences. *In vitro* data has shown that a C or U at this position can also cleave (provided base-pairing is maintained with 15.2 - Koizumi *et al.*, 1989; Ruffner *et al.*, 1990; Perriman *et al.*, 1992), although rates vary between systems. Because of the differences observed between systems it is difficult to deduce rules for predicting available cleavage sites on all RNAs. Despite this, the evidence suggests that the triplets GUC, CUC, GUA and UUC can be efficiently cleaved provided the surrounding sequence is not incompatible with the formation of the active hybrid (Fig. 1.6).

1.6.2. Deoxyribonucleotide substitutions

While ribonucleotide substitutions within the hammerhead self-cleaving domain have given some insight into the optimal ribozyme/substrate reaction hybrid, several studies have also analysed the effect of deoxyribonucleotide substitutions (DNA) on *in vitro* cleavage rates. There are several advantages for RNA/DNA chimeric ribozymes over the all RNA ribozymes. These include greater ease of chemical synthesis, improved *in vivo* stability and faster product dissociation. As well, DNA substitutions have allowed for the analysis of the importance of the 2'-hydroxyl on the ribose sugar of ribonucleotides within the ribozyme domain.

DNA substitutions are tolerated to some degree in all positions, except the conserved core and nucleotide 17 (Dahm and Uhlenbeck, 1990; Perrault *et al.*, 1990, 1991; Yang *et al.*, 1990; Paolella *et al.*, 1992). 2'-hydroxyl groups which have been identified as particularly important for full catalytic activity are those at positions 5, 9, 15.1, 16.1 and 17 (Fig. 1.7). The absence of the 2'-hydroxyl at position 17 completely abolishes cleavage activity thus confirming

Figure 1.7: Nucleotides within the hammerhead ribozyme reaction which must maintain a 2'-hydroxyl (i.e. as established by deoyribonucleotide substitutions) for efficient cleavage. Nucleotides are boxed and indicated in red.

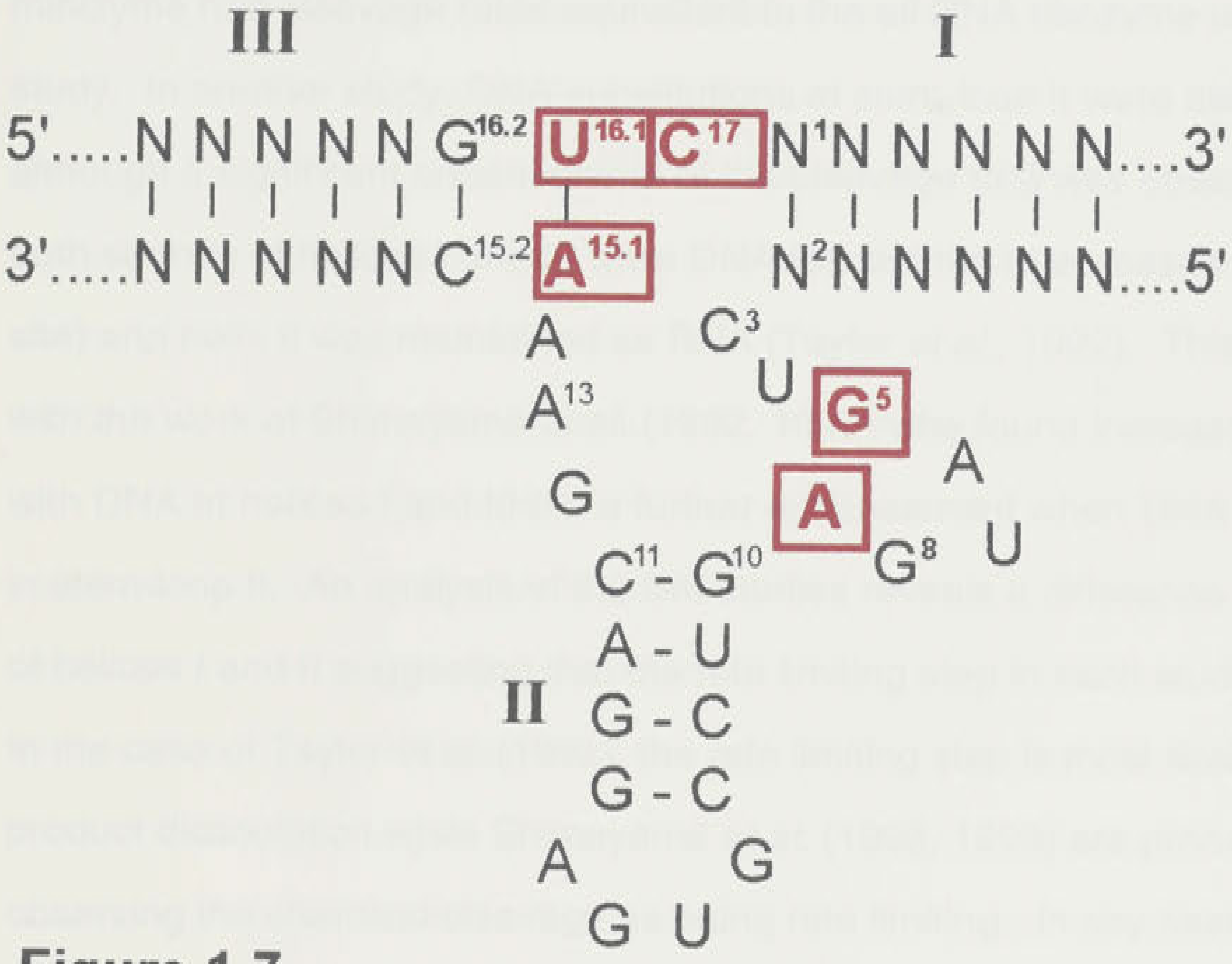
III
I
5'.....N N N N N G16.2 U16.1 C17 N1 N N N N N....3'
3'.....N N N N N C15.2 A15.1 N2 N N N N N....5'
A
C3
A13
U
G5
A
G
A
C11 - G10
G8
U
A - U
II
G - C
G - C
A
G
G U

Figure 1.7

the importance of this group in the nucleophilic attack on the phosphate at the cleavage site. Yang *et al.* (1990) have determined that the minimum 2'-hydroxyl content required to sustain some activity of the ribozyme is five ribose residues at positions 5, 8, 9, 15.1 and 17. In fact, several laboratories have now shown that ribozyme/substrate hybrids containing DNA residues can have equivalent or enhanced *in vitro* catalytic efficiencies over their ribonucleotide (RNA) counterparts (Hendry *et al.*, 1992; McCall *et al.*, 1992; Shimayama *et al.*, 1992, 1993; Taylor *et al.*, 1992).

McCall *et al.* (1992) found the most active minizyme in their study was one which had DNA in helices I and III as well as a DNA tetraloop. This minizyme had cleavage rates equivalent to the all RNA ribozyme used in their study. In another study, DNA substitutions at stem-loop II were also tolerated although a significant enhancement of the cleavage rate was observed when both strands of helices I and III were DNA (except the three bases at the target site) and helix II was maintained as RNA (Taylor *et al.*, 1992). This contrasts with the work of Shimayama *et al.* (1992, 1993) who found increased cleavage with DNA at helices I and III but a further enhancement when DNA was present in stem-loop II. An analysis of the two studies reveals a difference in the length of helices I and II suggesting that the rate limiting step in each study may differ. In the case of Taylor *et al.* (1992), the rate limiting step is most likely to be product dissociation while Shimayama *et al.* (1992, 1993) are probably observing the chemical cleavage as being rate limiting. In any case, it seems that provided nucleotide 17 remains a ribonucleotide, these DNA substitutions can enhance the cleavage efficiency over that observed for the RNA ribozyme (Hendry *et al.*, 1992; Shimayama *et al.*, 1992, 1993; Taylor *et al.*, 1992). In general, the increase in cleavage observed by a DNA substituted ribozyme can be attributed to a faster rate of dissociation of the cleavage products. As well as providing faster rates of cleavage the chimeric DNA/RNA ribozymes also exhibit enhanced levels of stability when transfected into human T-lymphocytes (Taylor *et al.*, 1992).

Despite the inherent advantages of the chimeric DNA/RNA ribozyme, the requirement for continual chemical synthesis and topical application makes its use unsuitable in some circumstances. In human therapeutics, where exogenous delivery is the likely mode of introduction, the enhanced stability provided by these chimeric ribozymes makes them desirable alternatives. The first example of this was recently published by Snyder *et al.* (1993) who designed and tested a chimeric DNA/RNA ribozyme against the *BCRABL* oncogene. The ribozyme contained DNA in helices I, II and III and was able to reduce *bcr-abl* mRNA by 49% while control antisense was able to inhibit by 25%. Unfortunately, no *in vivo* comparison was carried out between the DNA-RNA construct and the analogous all-RNA ribozyme so the direct advantage of the DNA-RNA chimera cannot be assessed. In contrast, in most plant applications, foreign genes are delivered as stably integrated sequences which are endogenously expressed. Thus in this situation, chimeric sequences such as the DNA-RNA ribozyme cannot be employed.

1.6.3. Chemically modified nucleotide substitutions

With the development of chemical synthesis of nucleic acids, it is now possible to introduce chemically modified analogues of nucleotides into RNA and DNA strands. These types of substitutions have an added advantage over the traditional forms of deoxy and ribo-nucleotide sequences listed above, as they allow for the analysis of the effect of each of the three constituents of the ribonucleotide (i.e. the base, the sugar and the phosphate bond). As with ribozymes containing deoxyribonucleotide substitutions, ribozymes containing certain modified nucleotides can have equivalent rates of cleavage and enhanced stability compared to standard RNA ribozymes (e.g. Pieken *et al.*, 1991; Paolella *et al.*, 1992; Heidenreich and Eckstein, 1992; Heidenreich*et al.*, 1994).

1.6.3.1 The base

The importance of various functional groups on the bases has been assessed by incorporating nucleotide analogues. The 2-amino group on guanosine (see Fig. 1.8a) was analysed by replacing all guanosines with inosine which differs only by lacking this 2-amino group (Odai *et al.*, 1990; Fu and McLaughlin, 1992a; Slim and Gait, 1992). These substitutions showed that the 2-amino group on guanosine residues at positions 5 and 12 are critical for catalytic activity. The G at position 5 (the 2'-OH of which is also required) is extremely important for obtaining cleavage activity by the hammerhead ribozyme. Along with the requirement for a 2-amino base at this position, this base has also been implicated in cation "binding". This will be discussed in more detail in section 1.6.4.

Substitution of adenosine with nebularine (an adenosine analogue) which lacks the 6-amino group did not affect cleavage activity (Fu and McLaughlin, 1992a; Slim and Gait, 1992). Further studies have shown that the N7 group of adenosine is important at A6 within the unpaired core where its elimination causes a 35-fold reduction in cleavage (Fig. 1.8b - Fu and McLaughlin, 1992b).

1.6.3.2 The phosphodiester linkage

The role of the phosphate backbone in ribozyme cleavage has been studied by using phosphorothioate-containing nucleotide derivatives (Eckstein, 1985). The phosphorothioate (which replaces the phosphate) contains sulphur in place of oxygen at either or both internucleotide linkages (i.e. the Rp or the Sp configuration - see Fig. 1.9a). They are ideally suited for determining the importance of particular phosphate groups within the hammerhead ribozyme since they introduce minimal structural change. The difference between the phosphate and phosphorothioate lies in their contrasting ability to co-ordinate "hard" and "soft" metal ions. Hard metal ions, such as magnesium (Mg^{2+}), co-ordinate to oxygen and not sulphur, whereas soft metal ions such as manganese (Mn^{2+}) can co-ordinate to either oxygen or sulphur (Jaffe and Cohn, 1979; Pecoraro *et al.*, 1984). Cleavage rates of ribozyme/substrate complexes containing phosphorothioate insertions can be compared in the presence of either divalent metal ion. In this way, the role of each

Figure 1.8

a: Determination of the importance of the 2-amino group on the guanosine nucleotides within the catalytic domain of the hammerhead ribozyme. Inosine substitutions have shown that the 2-amino groups at G5 and G12 (boxed in blue) are essential for efficient cleavage.

b: Analysis of the importance of N7 on the adenosine nucleotides within the unpaired region of the catalytic domain of the hammerhead ribozyme. The N7 on nucleotide A6 is required for efficient cleavage (boxed in green).

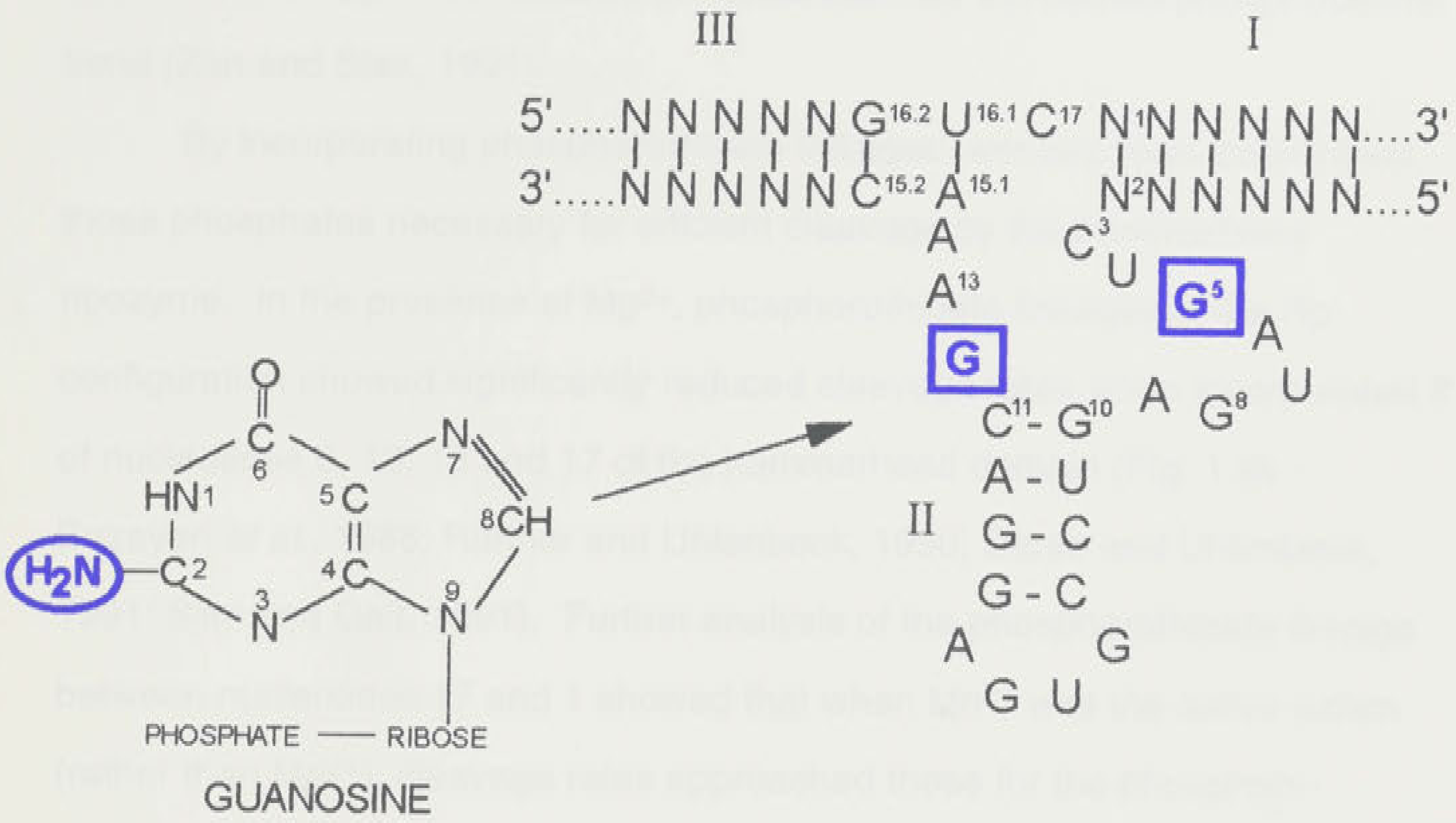
III
I
5'.....N N N N N G16.2 U16.1 C17 N1N N N N N....3'
3'.....N N N N N C15.2 A15.1 N2N N N N N....5'
A
C3
U
A13
G5
A
G
U
A
G8
C11- G10
A - U
II
G - C
G - C
A
G
G U
O
C
6
HN1
5C
N
7
8CH
H2N
C2
4C
3
N
9
N
PHOSPHATE
RIBOSE
GUANOSINE

Figure 1.8a

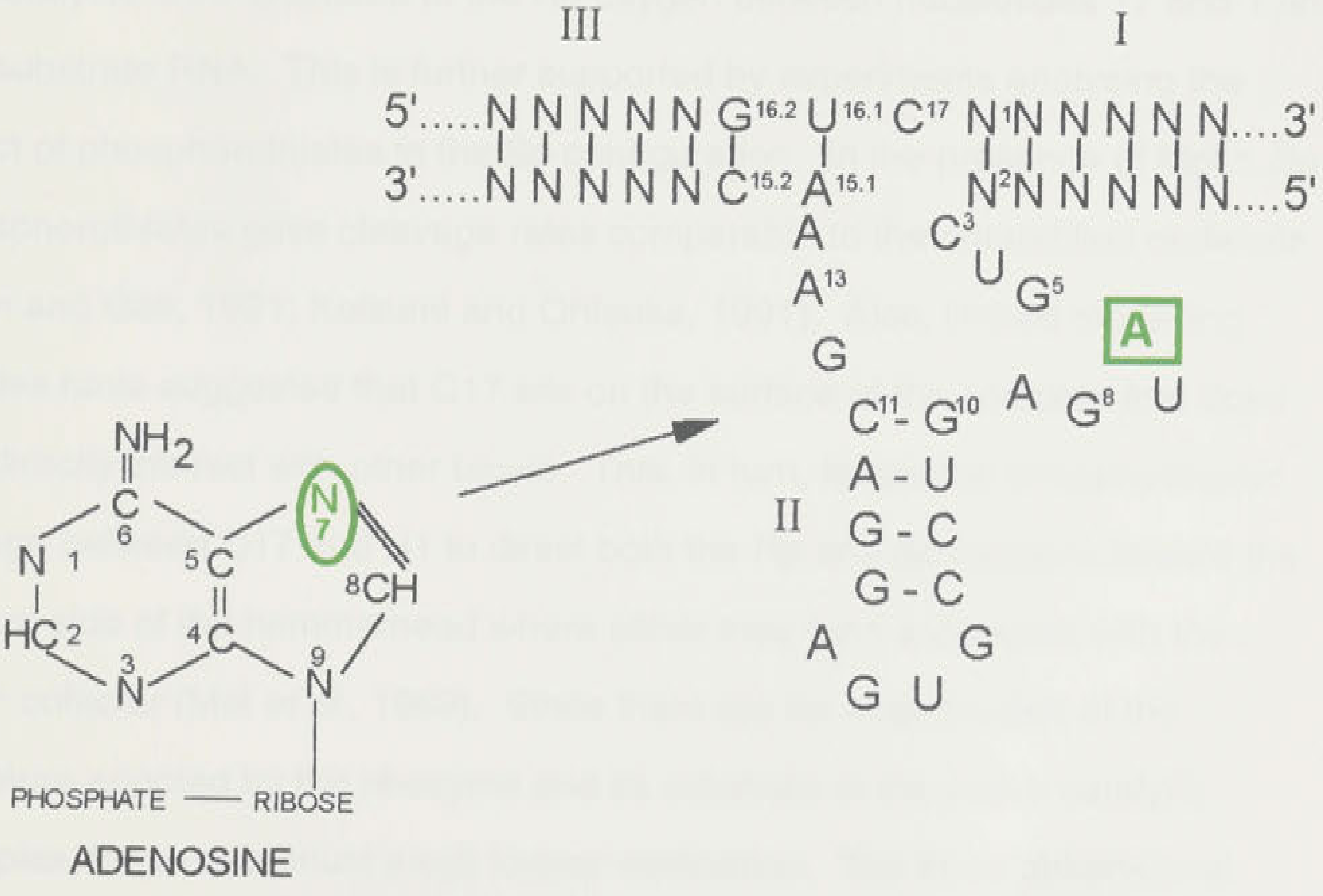
III
I
5'.....N N N N N G16.2 U16.1 C17 N1N N N N N....3'
3'.....N N N N N C15.2 A15.1 N2N N N N N....5'
A
C3
A13
U
G5
A
G
C11- G10
A
G8
U
A - U
II
G - C
G - C
A
G
G U
NH2
C
6
N 1
5C
N
7
8CH
HC2
4C
3
N
9
N
PHOSPHATE
RIBOSE
ADENOSINE

Figure 1.8b

phosphodiester linkage in cation co-ordination of the hammerhead ribozyme cleavage reaction can be analysed. Additionally, phosphorothioate bonds have been shown to be more resistant to nucleases than the normal phosphodiester bond (Zon and Stec, 1991).

By incorporating phosphorothioate linkages, workers have determined those phosphates necessary for efficient cleavage by the hammerhead ribozyme. In the presence of Mg^{2+}, phosphorothioate linkages in the Rp configuration showed significantly reduced cleavage rates when incorporated 3' of nucleotides 8, 12, 13 and 17 of the hammerhead domain (Fig. 1.9b - Buzayan *et al.*, 1988; Ruffner and Uhlenbeck, 1990; Dahm and Uhlenbeck, 1991; Slim and Gait, 1991). Further analysis of the phosphorothioate linkage between nucleotides 17 and 1 showed that when Mn^{2+} was the active cation (rather than Mg^{2+}), cleavage rates approached those for the phosphate-containing substrate (Dahm and Uhlenbeck, 1990; Slim and Gait, 1991). Since we know that Mg^{2+} and Mn^{2+} co-ordinate preferentially to oxygen or sulphur and oxygen respectively, these results suggest that the metal ion responsible for catalysis is co-ordinated to the Rp oxygen between nucleotides 17 and 1 on the substrate RNA. This is further supported by experiments analysing the effect of phosphorothiates in the Sp configuration. In the presence of Mg^{2+}, Sp phosphorothiates gave cleavage rates comparable to the unmodified molecule (Slim and Gait, 1991; Koizumi and Ohtsuka, 1991). Also, limited modelling studies have suggested that C17 sits on the surface of the complex and does not directly interact with other bases. This, in turn, forces the phosphodiester linkage between C17 and N1 to direct both the Rp and Sp oxygens toward the inward side of the hammerhead where either may form a complex with the Mg^{2+} cofactor (Mei *et al.*, 1989). Since there are no x-ray studies of the structure adopted by the ribozyme and its substrate in the active catalytic complex, these data must await further verification. The three dimensional structure of the hammerhead domain will be discussed in more detail in section 1.8.

Figure 1.9

a: The structure of the phosphorothioate - containing nucleotides (Eckstein, 1985) used to probe the importance of specific phosphate groups within the hammerhead domain. Oxygen is replaced by sulphur in either the Sp or Rp configuration as shown.

b: Phosphate linkages determined to be important for efficient *in vitro* hammerhead cleavage by phosphorothioate (Rp) substitutions. Phosphate groups (designated as green circles) between nucleotides G8/A9, G12/A13/A14 and C17/N1 have been shown to be required for hammerhead cleavage.

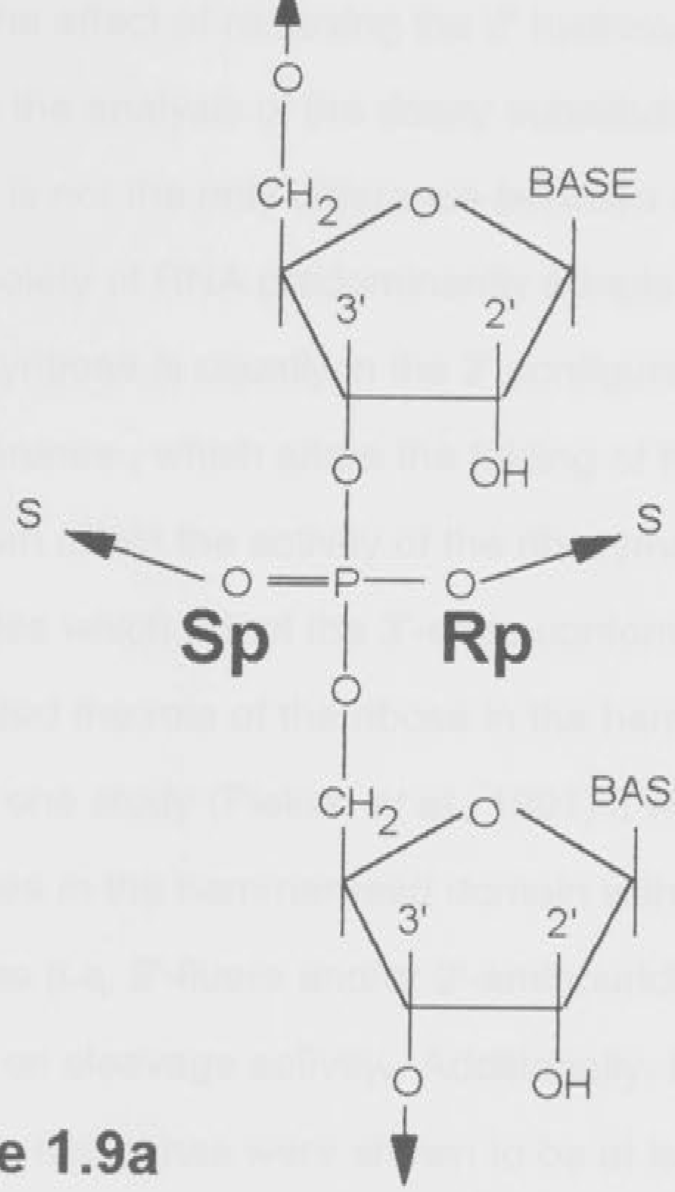
O
CH2
O
BASE
3'
2'
O
OH
S
S
O
P
O
Sp
Rp
O
CH2
O
BASE
3'
2'
O
OH

Figure 1.9a

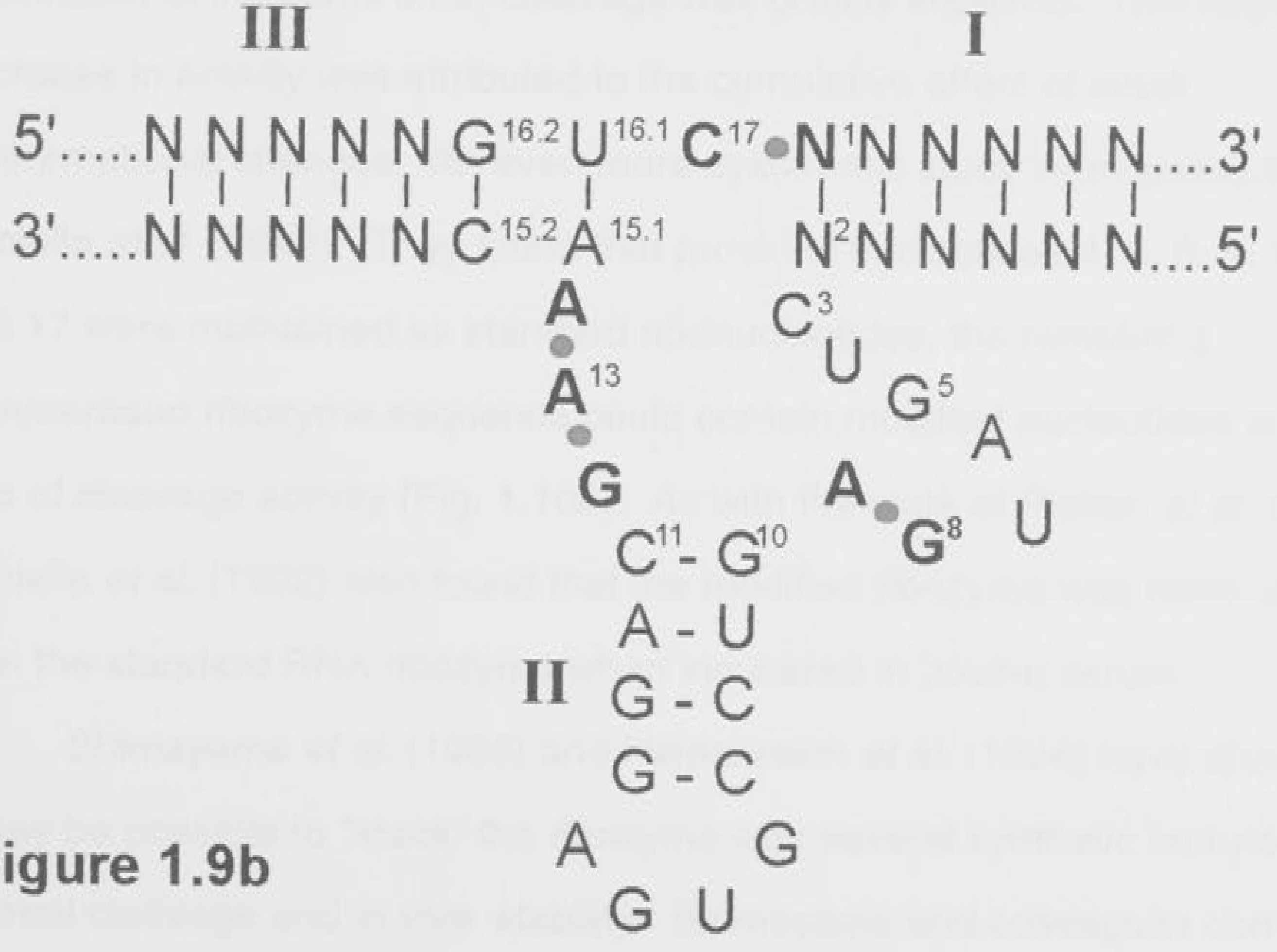
III
I
5'.....N N N N N G16.2 U16.1 C17 N1 N N N N N....3'
3'.....N N N N N C15.2 A15.1 N2 N N N N N....5'
A
A13
G
C3
U
G5
A
A
G8
U
C11 - G10
A - U
G - C
G - C
II
A
G
G
U

Figure 1.9b

1.6.3.3. The ribose

The effect of removing the 2' hydroxyl of the ribose has been discussed above in the analysis of the deoxy substitutions. However, the lack of a 2'-hydroxyl is not the only difference between deoxy and ribo-nucleotides. The ribose moiety of RNA predominantly adopts the 3'-endo configuration whereas the deoxyribose is usually in the 2' configuration (Fig. 1.10a - Saenger, 1984). This difference , which alters the folding of the sugar-phosphate backbone, may in turn affect the activity of the ribozyme. By using chemical analogues of nucleotides which adopt the 3'-endo conformation, several laboratories have investigated the role of the ribose in the hammerhead cleavage reaction.

In one study (Pieken *et al.*, 1991) it was found that substitutions of all pyrimidines in the hammerhead domain with the appropriate nucleotide derivatives (i.e. 2'-fluoro and/or 2'-aminouridines and 2'-fluorocytidines) showed no effect on cleavage activity. Additionally, both the 2'-fluoro and 2'-amino containing ribozymes were shown to be at least 1000 times more stable than the standard RNA ribozyme in rabbit serum. Olsen *et al.* (1991) systematically substituted each adenosine with 2'-fluoroadenosine nucleotide analogues and also found no loss of catalytic activity. However, when all the adenosines were substituted at the same time, cleavage was greatly impaired. This large decrease in activity was attributed to the cumulative effect of small conformational changes. An even more systematic study was carried out by Paolella *et al.* (1992). They found that provided nucleotides 4, 5, 6, 8, 12,15.1 and 17 were maintained as standard ribonucleotides, the remaining hammerhead ribozyme sequence could contain modified nucleotides without loss of cleavage activity (Fig. 1.10b). As with the work of Pieken *et al.* (1991), Paolella *et al.* (1992) also found that the modified ribozyme was more stable than the standard RNA ribozyme when incubated in bovine serum.

Shimayama *et al.* (1993) and Heidenreich *et al.* (1994) have shown that it may be possible to "stack" the ribozyme with several synthetic features for optimal cleavage and *in vivo* stability. Shimayama and colleagues combined

Figure 1.10

a: The configuration of the ribose moiety in deoxy and ribo-nucleotides. The ribose moiety of RNA predominantly forms the 3'-endo configuration while the deoxyribose usually has the 2'-endo configuration. This difference alters the folding of the sugar-phosphate backbone, which may in turn affect cleavage. The use of nucleotides containing chemical analogues of the ribose moiety that conform to the 3'-endo structure means that these substitutions can be incorporated without altering backbone folding (see section 1.6.3.3 for further details).

b: Nucleotides (shown in yellow) within the hammerhead cleavage reaction required to contain standard ribose moieties for efficient cleavage.

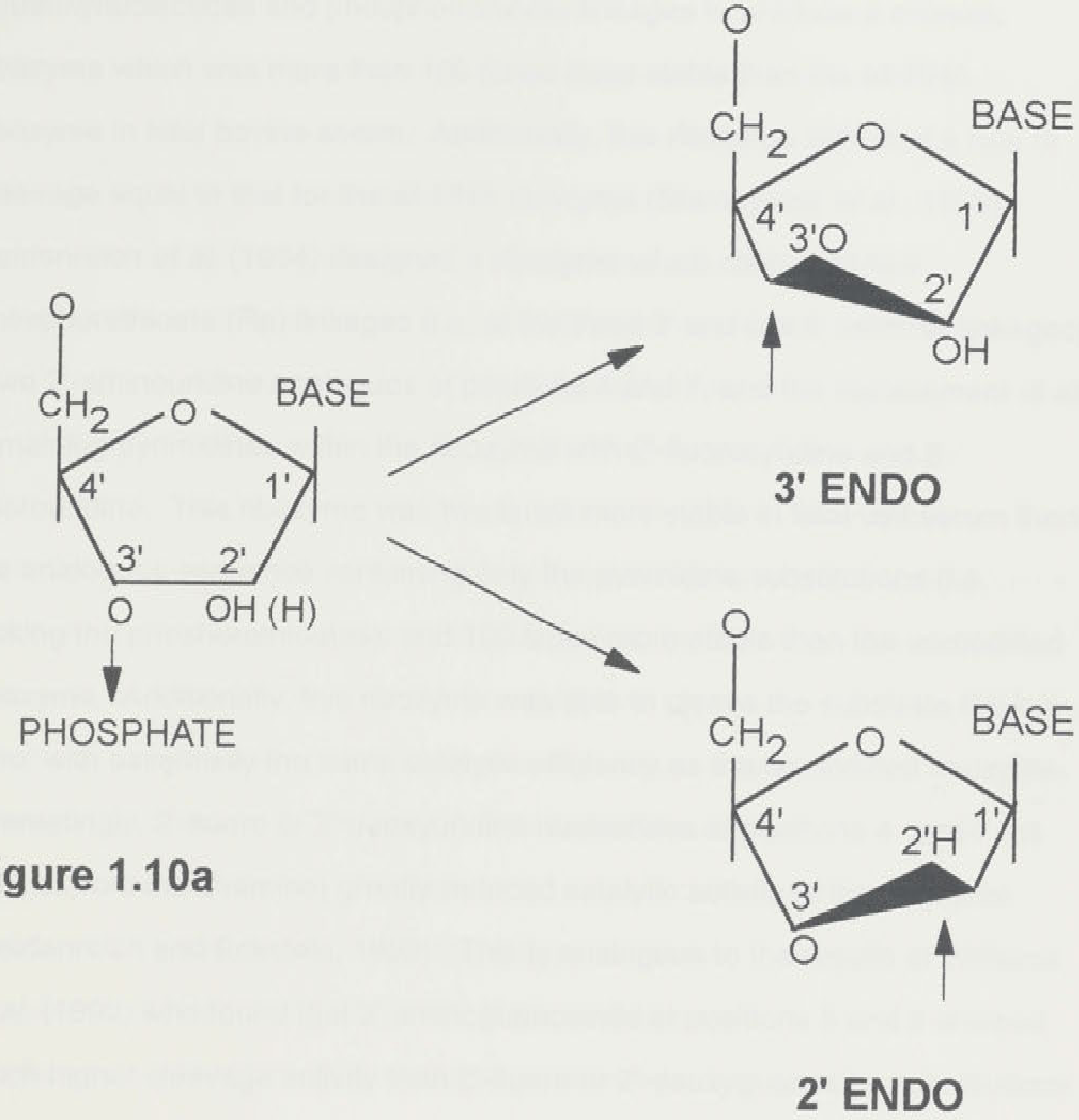
O
CH2
O
BASE
4'
1'
3'
2'
O
OH (H)
PHOSPHATE
O
CH2
O
BASE
4'
3'O
1'
2'
OH
3' ENDO
O
CH2
O
BASE
4'
2'H
1'
3'
O
2' ENDO

Figure 1.10a

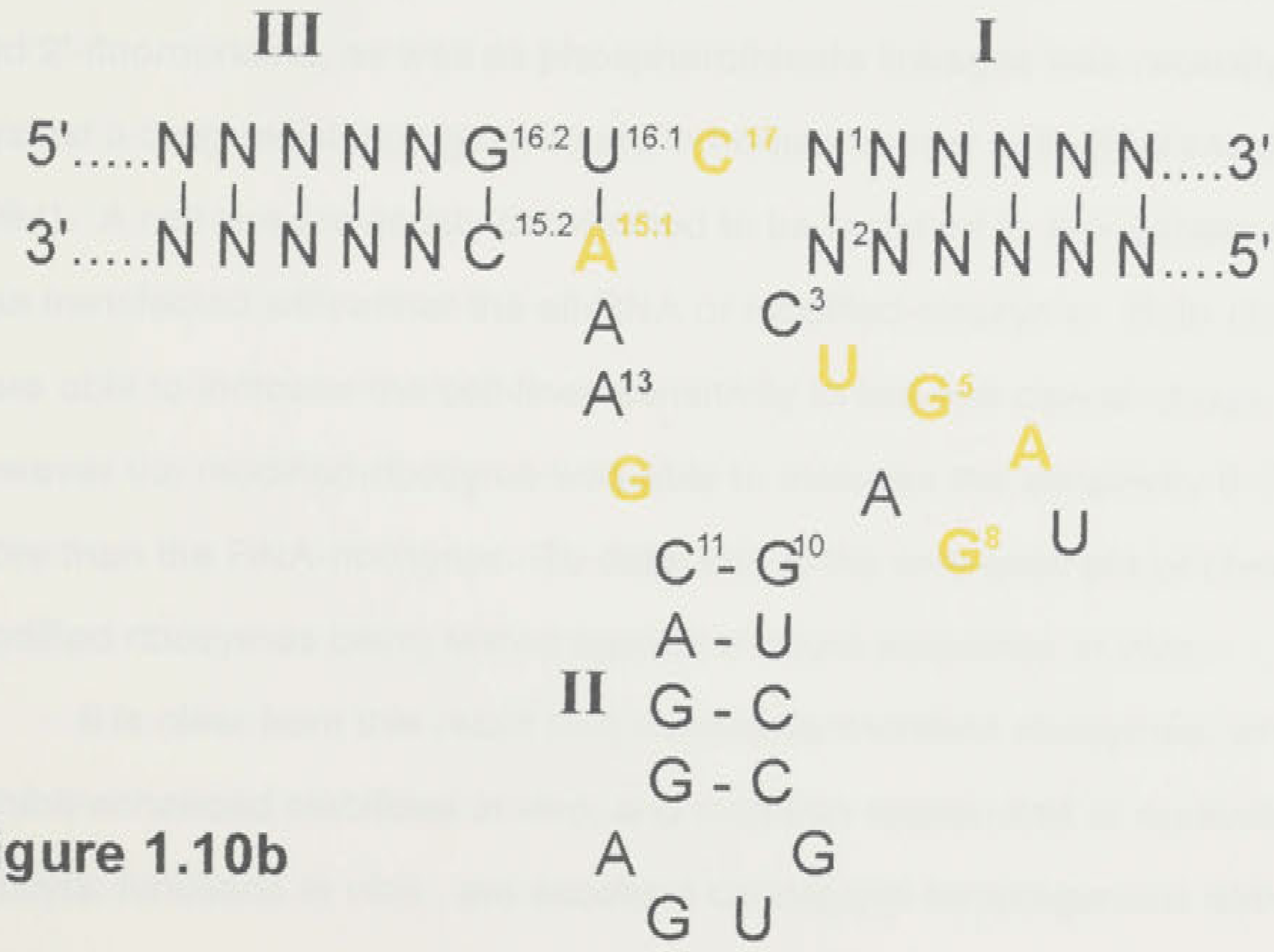
III
I
5'.....N N N N N G16.2 U16.1 C17 N1 N N N N N....3'
3'.....N N N N N C15.2 A15.1 N2 N N N N N....5'
A
C3
A13
U
G5
A
G
A
G8
U
C11 - G10
A - U
II
G - C
G - C
A
G
G U

Figure 1.10b

2'-deoxynucleotides and phosphorothioate linkages to produce a chimeric ribozyme which was more than 100 times more stable than the all-RNA ribozyme in fetal bovine serum. Additionally, this ribozyme exhibited a rate of cleavage equal to that for the all-RNA ribozyme (Shimayama *et al.*, 1993). Heidenreich *et al.* (1994) designed a ribozyme which contained four phosphorothioate (Rp) linkages (i.e. at the three 3' and last 5' terminal linkages) , two 2'-aminouridine analogues at positions 4 and 7, and the replacement of all remaining pyrimidines within the ribozyme with 2'-fluorocytidine and 2'-fluorouridine. This ribozyme was two times more stable in fetal calf serum than the analogous sequence containing only the pyrimidine substitutions (i.e. lacking the phoshorothioates), and 100 times more stable than the unmodified ribozyme. Additionally, this ribozyme was able to cleave the substrate RNA *in vitro* with essentially the same catalytic efficiency as the unmodified ribozyme. Interestingly, 2'-fluoro or 2'-deoxyuridine nucleotides at positions 4 and 7 (as distinct from the 2'-amino) greatly reduced catalytic activity of the ribozyme (Heidenreich and Eckstein, 1992). This is analogous to the results of Williams *et al.* (1992) who found that 2'-aminoguanosines at positions 5 and 8 showed much higher cleavage activity than 2'-fluoro or 2'-deoxyguanosine substitutions.

A synthetic ribozyme containing deoxyribonucleotides, 2'-fluorocytidine and 2'-fluorouridine, as well as phosphorothioate linkages was recently tested against a drug resistance gene found in human cancer cells (Kiehntopf *et al.*, 1994). A cell-line previously determined to be resistant to anti-cancer drugs was transfected with either the all-RNA or modified-ribozyme. Both ribozymes were able to increase the cell-lines sensitivity to two anti-cancer drugs, however the modified-ribozyme was able to increase the sensitivity 6-7 fold more than the RNA-ribozyme. To date, this is the only example of chemically modified ribozymes being tested against a target sequence *in vivo.*

It is clear from this result that chemically-modified ribozymes, which exhibit enhanced stabilities *in vivo*, and maintain reasonable or equivalent catalytic functions *in vitro* , are excellent candidates for exogenous delivery of hammerhead ribozymes to cells. Future work, where exogenous delivery of ribozymes is applicable, will determine whether these sequences are truly viable alternatives to all-RNA ribozymes.

1.6.4. Role of divalent metal ions in cleavage

Although cleavage by the hammerhead ribozyme is generally carried out in the presence of magnesium ions, several other cations can also support the reaction (Dahm and Uhlenbeck, 1991). I have already discussed cleavage in the presence of manganese (Mn^{2+}) but other active cations include cobalt (Co^{2+}), zinc (Zn^{2+}), cadmium (Cd^{2+}) and strontium (Sr^{2+}). This work has provided some clues as to the exact function the divalent metal ion may play in the cleavage process. Correct folding of the hammerhead ribozyme in the presence of Zn^{2+} or Cd^{2+} required the addition of the primary amine, spermine. Spermine also increased the rate of cleavage induced by Sr^{2+} although low levels of cleavage were also observed in the absence of spermine. This suggests that while these three metal ions were not able to promote correct folding of the hammerhead very efficiently, once folded, they were able to stimulate cleavage. Co^{2+}, Mn^{2+} and Mg^{2+} exhibited rapid cleavage in the presence or absence of spermine. Larger ions tested such as lead (Pb^{2+}) and barium (Ba^{2+}) induced very slow or no cleavage rates, even in the presence of spermine. The conclusions of this study were that all ions with an ionic radius of less than 1Å were able to induce cleavage while those greater than 1Å were not . This suggests that the divalent binding site(s) within the hammerhead domain must have very specific size requirements.

Several lines of evidence are now accumulating concerning ribozyme cleavage catalysis and cation binding. The phosphorothioate substitutions outlined in section 1.6.3.2 strongly suggest that one important binding site is closely associated with the Rp-oxygen of the phosphodiester linkage between nucleotides 17 and 1. Some of the DNA substitutions have also provided valuable information. Based on a series of DNA-containing ribozymes and varying Mg^{2+} concentrations, Perreault *et al.* (1991) suggest that the 2'-

hydroxyls on residues 5, 9 and 16.1 are involved in the low-affinity binding of Mg^{2+}. It could be envisaged that, during the cleavage process, the magnesium enters a pre-existing "cavity" in the ribozyme/substrate complex and is rapidly directed toward the phosphodiester linkage between nucleotides 17 and 1 by specific and highly conserved residues in the ribozyme domain. Three dimensional studies of the mechanism of catalysis will be required to verify this hypothesis.

1.6.5. The optimal conditions for *in vitro* hammerhead cleavage

Although there is a large volume of literature regarding the effect of substitutions within the hammerhead ribozyme complex, many aspects of the cleavage process are still poorly understood. All but nucleotides 7 and 17 within the conserved core of the hammerhead domain must be conserved for cleavage. Analysis of some of these conserved residues has revealed the absolute requirement for the 2'-hydroxyl of the ribose component on the ribonucleotide. Further studies have shown that the Rp-oxygen on the phosphodiester linkage between several nucleotides is required. Other work has suggested that the composition of the base moiety of at least 4 sites is crucial for obtaining cleavage. While the stringency of these requirements for the conserved core is essential, analysis of the remaining regions of the hammerhead ribozyme complex has revealed a large degree of flexibility. Helix II and the tetraloop can be altered in both length and complexity, although certain general rules for this region should be adhered to. Helices I and III can also tolerate what appears to be infinite base combinations varying in both length and sequence. However, despite this apparent flexibility in the design of these regions, variation in cleavage efficiencies does occur. This variation is due, in part, to intra and intermolecular aggregations which can severely affect accessibility of the target site triplet. Extracting general rules from these data is complex, as many of the studies contain variables which make direct comparison difficult. Nevertheless, several common features are prevalent and should be observed when attempting to design a hammerhead ribozyme for optimal target RNA destruction. The combined results of all these studies are shown in figure 1.11.

1.7. RNA binding proteins and cleavage

One important difference between the *in vitro* cleavage assays described above, and ribozyme-catalysed cleavage within living cells is that most RNAs within a cell exist as tightly folded RNA-protein complexes, not as free molecules. Such RNA-protein complexes have been shown to affect annealing, unwinding and strand exchange of the nucleic acids (Rozen *et al.*, 1990; Wassarman and Steitz, 1991; Casas-Finet *et al.*, 1993; Kumar and Wilson, 1990; Pontius and Berg, 1990; Lee *et al.*, 1993; Portman and Dreyfuss, 1994; Pontius and Berg, 1992). Clearly cellular proteins binding to a target RNA or to an introduced ribozyme could have an effect on the cleavage rate. Preliminary studies have indicated that certain proteins can enhance the efficiency of ribozyme action (Tsuchihashi *et al.*, 1993; Herschlag *et al.*, 1994; Bertrand and Rossi, 1994; Coatzee *et al.*, 1994, Sioud, 1994).

Several laboratories are beginning to investigate the effect some of these proteins have on cleavage rates. Although this work is being carried out *in vitro* with purified proteins, the results are providing valuable information for the future design of hammerhead ribozymes for *in vivo* application. Tsuchihashi *et al.* (1993) have shown that the nucleocapsid protein from human immune deficiency virus (HIV, p7) is able to enhance cleavage by a hammerhead ribozyme 10-20 fold. The p7 protein had been implicated in increasing the rates of helix association and dissociation and therefore was a good candidate for enhancing the catalytic efficiency of the hammerhead ribozyme. In the absence of p7, the rate limiting step in this reaction was binding of the substrate and ribozyme and subsequent dissociation of products. When p7 was added to *in vitro* cleavage reactions, association of the two molecules was increased at least 10 fold and dissociation of products improved 20-30 fold (Herschlag *et al.*, 1994). Later work has shown that increased

Figure 1.11: The combined results of available data derived from deoxy, ribo and chemically modified nucleotide substitutions for efficient *in vitro* cleavage of a hammerhead ribozyme cleavage reaction. This figure provides a guide toward the design of an efficient hammerhead ribozyme cleavage reaction. The key to colored and/or boxed nucleotides, as well as circle linkages is shown beneath the substrate/ribozyme hybrid. Further details of the studies from which this data is derived can be found in section 1.6. Note that all nucleotides, except C17, which require an unmodified ribose moiety (shown in yellow) are also invariant.

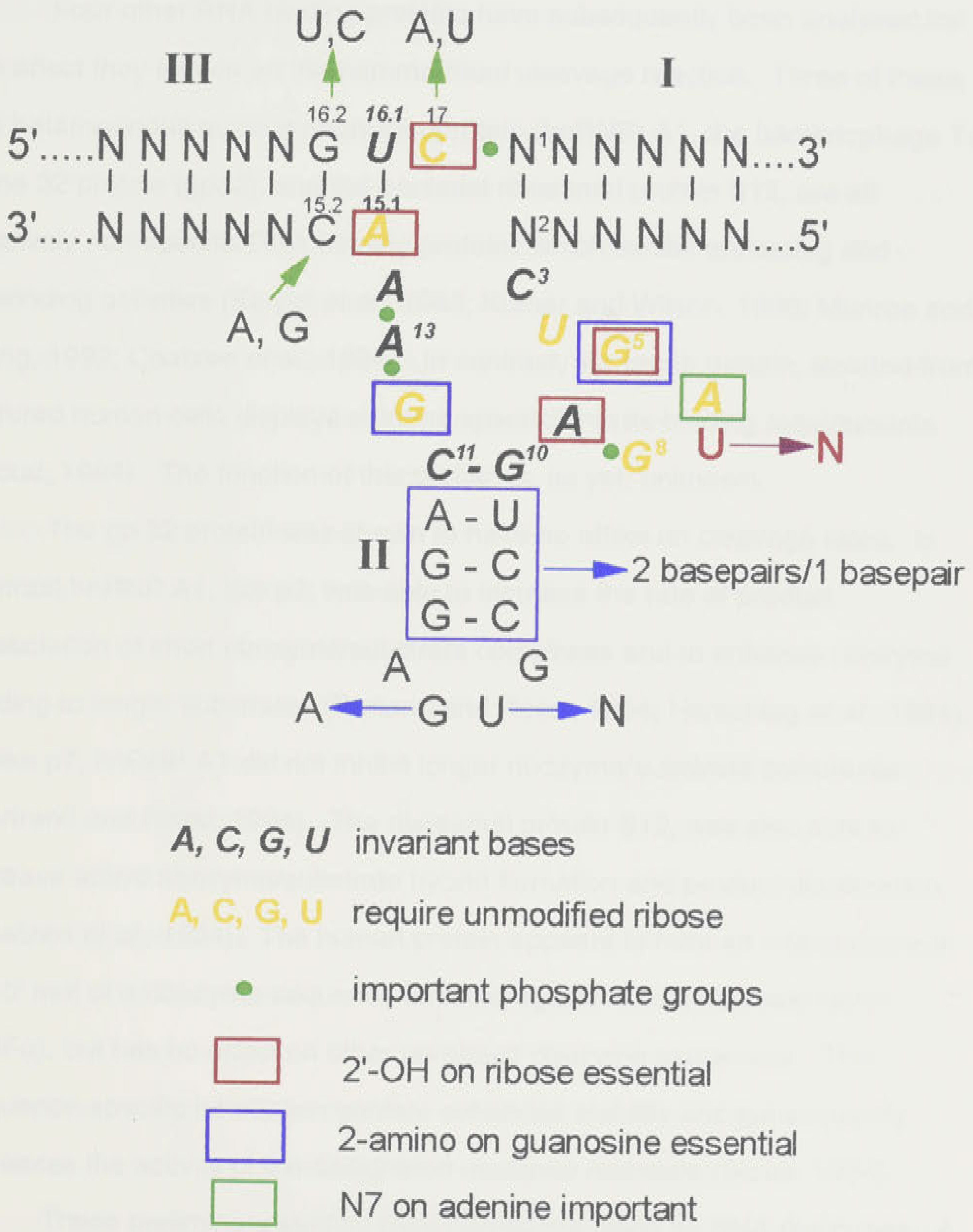
U,C
A,U
III
I
16.2
16.1
17
5'.....N N N N N G U C • N¹N N N N N....3'
15.2
15.1
3'.....N N N N N C A
N²N N N N N....5'
A, G
A
C³
A¹³
U
G⁵
G
A
A
C¹¹- G¹⁰
•G⁸
U
N
II
A - U
G - C
G - C
2 basepairs/1 basepair
A
G
A
G
U
N
A, C, G, U invariant bases
A, C, G, U require unmodified ribose
important phosphate groups
2'-OH on ribose essential
2-amino on guanosine essential
N7 on adenine important

Figure 1.11

product dissociation in the presence of p7, is greatly decreased when the complex is greater than 14 bp in length. Interestingly, substrate/ribozyme complexes greater than 16 bp were actually inhibited in the presence of p7. Short ribozyme binding to longer substrates, such as mRNAs which contain internal structures that inhibit binding, was also shown to be enhanced in the presence of p7 (Bertrand and Rossi, 1994).

Four other RNA binding proteins have subsequently been analysed for the effect they induce on the hammerhead cleavage reaction. Three of these, the heterogenous nuclear ribonucleoprotein (hnRNP) A1, the bacteriophage T4 gene 32 protein (gp32), and the bacterial ribosomal protein S12, are all relatively non-specific RNA binding proteins which exhibit annealing and unwinding activities (Karpel *et al.*, 1982; Kumar and Wilson, 1990; Munroe and Dong, 1992; Coatzee *et al.*, 1994). In contrast, the fourth protein, isolated from cultured human cells displays extreme specificity in its binding requirements (Sioud, 1994). The function of this protein is, as yet, unknown.

The gp 32 protein was shown to have no effect on cleavage rates. In contrast hnRNP A1, like p7, was able to increase the rate of product dissociation of short ribozyme/substrate complexes and to enhance ribozyme binding to longer substrates (Bertand and Rossi, 1994; Herschlag *et al.*, 1994). Unlike p7, hnRNP A1 did not inhibit longer ribozyme/substrate complexes (Bertrand and Rossi, 1994). The ribosomal protein S12, was also able to increase active ribozyme/substrate hybrid formation and product dissociation (Coatzee *et al.,* 1994). The human protein appears to form an interaction with the 5' half of a ribozyme sequence directed against tumor necrosis factor (TNFα), but has no effect on other unrelated ribozyme sequences. This sequence-specific interaction confers enhanced stability and subsequently increases the activity of the designated ribozyme molecule (Sioud, 1994).

These preliminary studies were carried out using all-RNA ribozymes. A recent study, however, has also suggested that the p7 protein can enhance the *in vitro* cleavage rates induced by ribozymes containing several ribonucleotides with a chemically modified ribose moiety. In the absence of p7, this ribozyme produced almost no cleavage products. However, when p7 was present, catalytic activity of the ribozyme was significantly increased (Muller *et al.*, 1994). This suggests that the chemically modified ribozymes which show enhanced *in vivo* stability, such as those outlined in section 1.6.3, could also display enhanced cleavage in the presence of p7. In addition to this, results have shown that the hnRNP A1 protein can promote base-pairing of DNA and RNA, suggesting that it may also be effective in enhancing the cleavage rates induced by DNA/RNA chimeric ribozymes (Pontius and Berg, 1990).

The results of these studies suggest that manipulation of proteins such as p7, S12 and hnRNP A1 could enhance ribozyme activity *in vivo*. Since hnRNP A1 is one of the most abundant proteins involved in nuclear RNA processing, one could envisage targeting the ribozyme to the nucleus, thus increasing the likelihood of interactions. Additionally, linking the ribozyme to a binding site for hnRNP A1 may further increase the chances of the two molecules interacting. Furthermore, since there is evidence to suggest that hnRNP A1 binds preferentially to sequences at the intron/exon splice junction (Swanson and Dreyfuss, 1988; Buvoli *et al.*, 1990), selecting a target site close to this region could further enhance the chances of co-localisation. In this way, it may act like a chaperone by binding to the ribozyme and substrate forcing co-localisation of the two molecules and enhancing cleavage of the substrate RNA. Finally, by providing ribozymes which have exhibited enhanced *in vivo* stability (such as those containing chemically modified nucleotides) it may be possible to further increase *in vivo* cleavage of the substrate RNA.

1.8. A structural model for the hammerhead ribozyme domain

Until very recently, the hammerhead ribozyme was depicted in a two dimensional manner in which the three helices radiated out from the unpaired core. Clearly, however, the molecule adopts a far more elaborate structure in which several changing secondary and tertiary interactions are involved in the formation of the active complex. The work of Pley *et al.* (1994) is the first example of the three dimensional structure of the hammerhead ribozyme as derived from studies involving x-ray crystallography. In this structure, the ribozyme-substrate interaction resembles a wishbone (Fig. 1.12a) in which helices I and II diverge from the core at an acute angle while helix III points in the opposite direction. Unlike earlier hammerhead ribozyme depictions, the "unpaired" core is actually made up of several non Watson-Crick base-pairing interactions (Fig. 1.12b). Despite these advances in the understanding of the three dimensional structure of the hammerhead ribozyme, it has not been possible to elucidate the mechanism of catalysis from this work. Most puzzling is the fact that clear biochemical evidence exists showing a critical divalent metal ion bound to the Rp oxygen between nucleotides 17 and 1 (see also section 1.6.4; Dahm and Uhlenbeck, 1991); however, such an interaction cannot be observed in the crystal structure. This discrepancy could be due to the fact that the substrate used for the crystallisation was a DNA analogue, hence lacking the critical 2'-hydroxyl for cleavage. Clearly, further work is required before we are able to fully understand the mechanism of cleavage by the hammerhead ribozyme.

1.9. Designing hammerhead ribozymes for *in vivo* application

Along with the large number of *in vitro* analyses carried out using the hammerhead ribozyme, many laboratories have also investigated the applicability of hammerhead ribozymes against specific RNA targets *in vivo.* The success of such endeavours would be very exciting as the ability to control target RNAs such as oncogenic and/or viral sequences could reverse the terminal nature of such ailments. Additionally, in plants, pests and disease currently destroy a significant proportion of the worlds food crops. Crop plants expressing ribozymes specifically designed to cleave and inactivate the essential transcripts of these organisms could mean efficient pathogen control

Figure 1.12

a: 3-dimensional structure of the hammerhead ribozyme reaction as determined by x-ray crystallography (Pley *et al.*, 1994). The substrate RNA is shown in green; the ribozyme is in blue. Non Watson-Crick base-pairs are indicated in red while standard base-pairing is shown in black. The site of cleavage on the substrate RNA is arrowed and helices I, II and III are labelled.

b: base-pairing within the catalytic domain of the hammerhead ribozyme as determined by x-ray crystallography (Pley *et al.*, 1994). Color coding for substrate and ribozyme, as well as helix designation are as in **(a)**. The arrow depicts the site of cleavage.

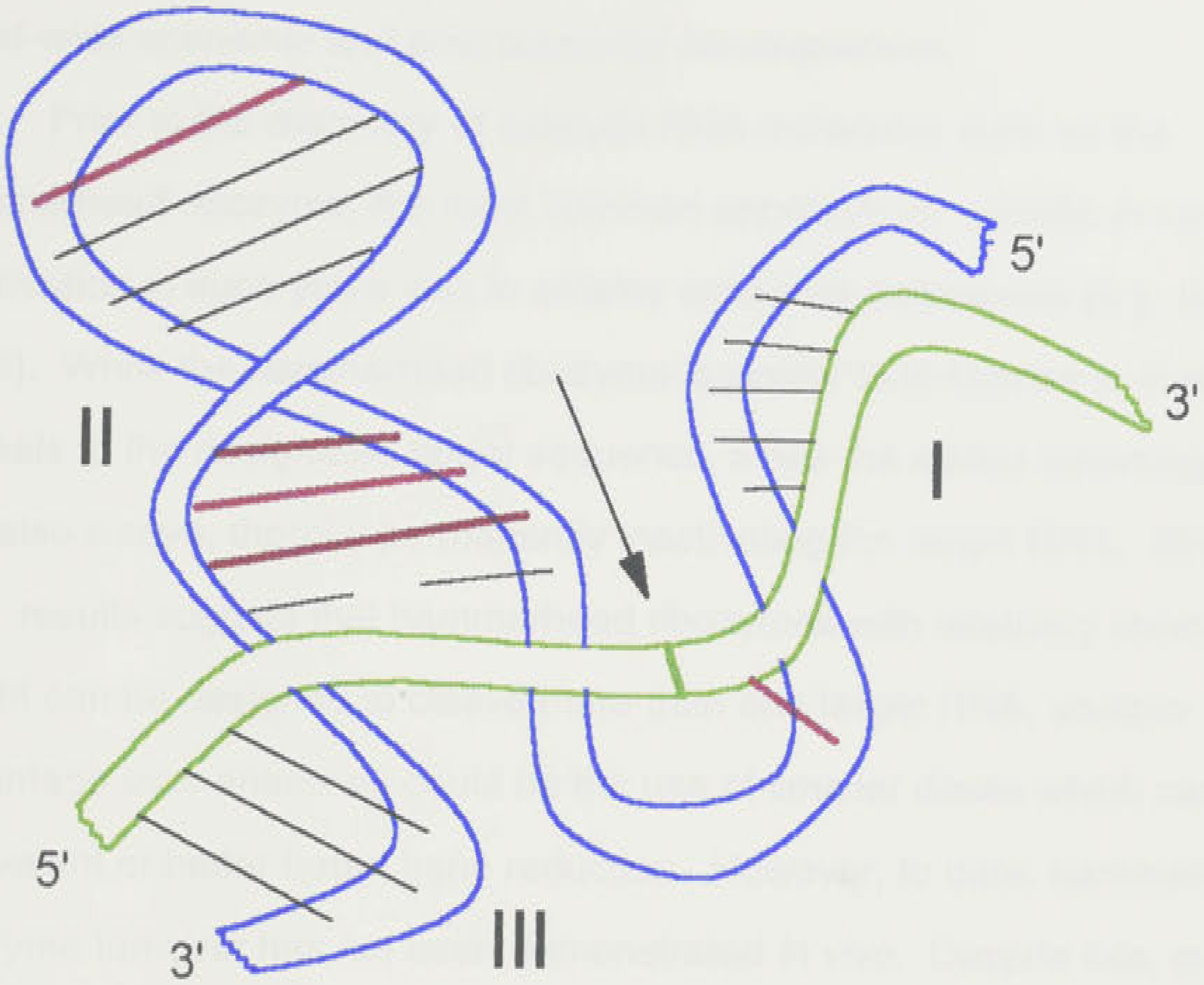
II
5'
3'
I
5'
3'
III

Figure 1.12a

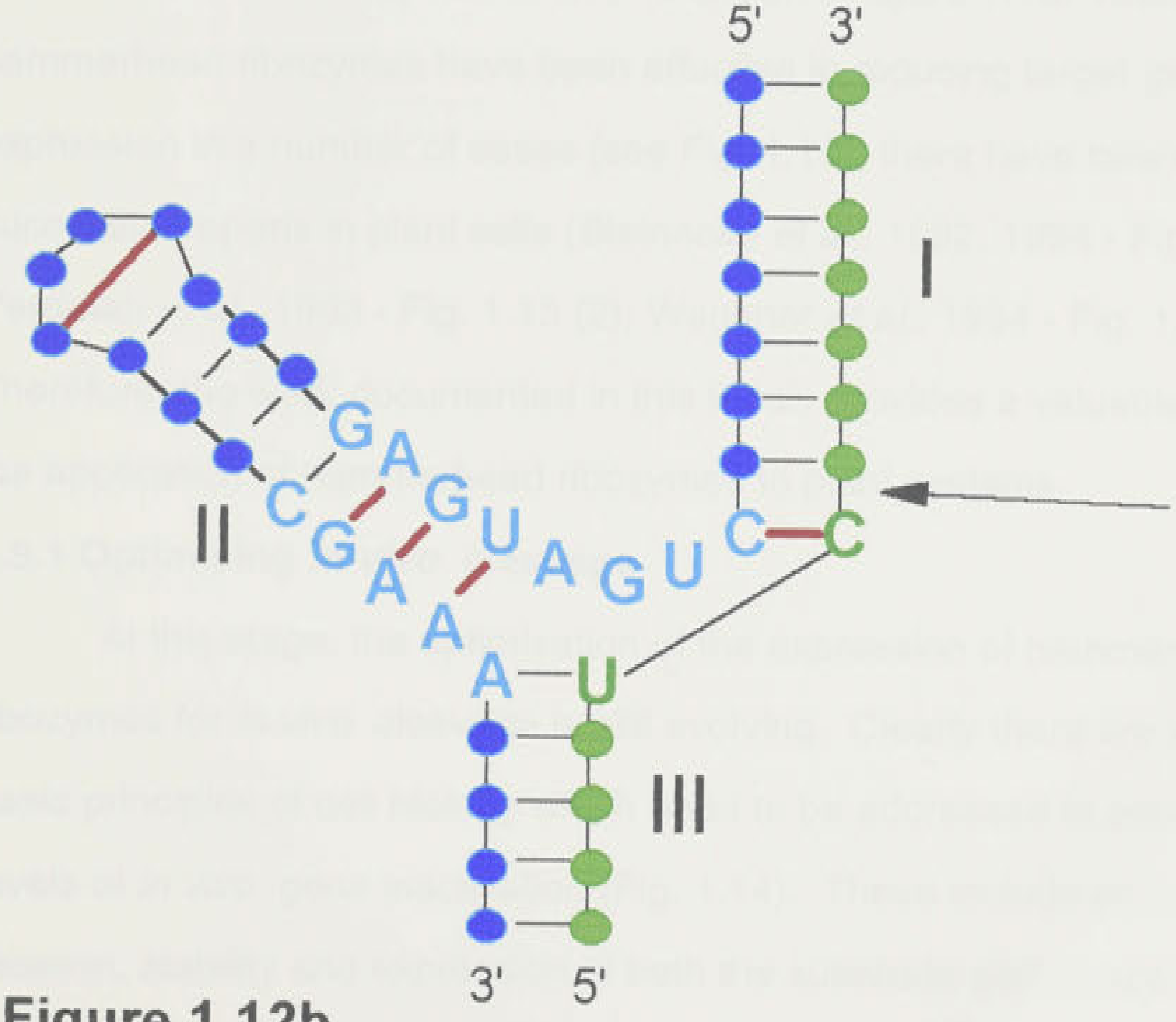
5'
3'
I
G
A
G
U
A
G
U
C
C
C
G
A
A
A
U
II
III
3'
5'

Figure 1.12b

without the requirement for large scale chemical sprays. This would have world-wide economic and environmental consequences.

Prior to the discovery of catalytic RNA molecules such as the hammerhead ribozyme, the most common approach for specific *in vivo* gene inactivation in eucaryotes was to employ antisense sequences (e.g. Izant *et al.*, 1992). While the hammerhead ribozyme is similar to antisense in that it anneals to the designated target sequence, it has the added advantage that it can also cleave, thereby permanently inactivating the target RNA. Since *in vitro* results suggest that hammerhead ribozymes with relatively short helices I and III can be designed to cleave more than one target RNA, another advantage over antisense could be the use of smaller doses which can achieve equivalent or better target gene reduction. However, to date, hammerhead ribozyme turnover has not been demonstrated *in vivo.* Despite this, many studies have shown an enhanced effect over that obtained for antisense controls. A summary of the large number of experiments involving the use of the hammerhead ribozymes *in vivo* is shown in figure 1.13. Although hammerhead ribozymes have been effective in reducing target gene expression in a number of cases (see Fig. 1.13), there have been few successful reports in plant cells (Steinecke *et al.*, 1992, 1994 - Fig. 1.13 (1); Perriman *et al.*, 1993 - Fig. 1.13 (2); Wegener *et al.*, 1994 - Fig. 1.13 (27)). Therefore, the work documented in this thesis provides a valuable addition to the application of hammerhead ribozymes to plant systems.

1.9.1 Optimising *in vivo* cleavage

At this stage, the optimisation of the expression of hammerhead ribozymes for *in vivo* cleavage is still evolving. Clearly there are a number of basic principles of cell biology which need to be addressed to obtain optimal levels of *in vivo* gene inactivation (Fig. 1.14). These include intracellular location, stability and expression of both the substrate and ribozyme molecules. This section will describe the attempts and future directions toward optimising these aspects of the *in vivo* hammerhead ribozyme cleavage reaction. The

Figure 1.13: Summary of the application of hammerhead ribozymes to target and inactivate specific mRNAs *in vivo.* The key to column 3, "Cleavage product analysis" is shown at the end of the table. Where targets have been referred to in the text, a bold bracketed number is present at the end of the target title. This number is also present in the text.

Figure 1.13 (1 of 3)

Target	Expression system	Cleaved product analysis	Results	Reference
BCRABL **(18)** (chronic myelogenous leukemia)	tRNA^{Met} in retroviral vector	ND	elimination of *BCRABL* expression	Shore *et al.*, 1993
BCRABL	*in vitro* derived ribozyme, liposome delivery to human cancer cells	4	~50% reduction in *BCRABL* mRNA; elimination of *BCRABL* protein	Snyder *et al.*, 1993
BCRABL	*in vitro* transcribed, lipofection delivery to human cancer cells	3, 4	5-fold reduction in *BCRABL* mRNA per cell.	Lange *et al.*, 1993a & b
H4 histone	*cis*-acting in monkey COS cells	1, 3	*cis*-acting Rz mediates 3' end formation of histone H4	Eckner *et al.*, 1991
H1 histone **(19)**	tRNA^{Tyr} in *Xenopus* oocytes	ND	4-5 fold reduction in accumulated H1 histone	Bouvet *et al.*, 1994
H1 histone **(25)**	tRNA^{Tyr} in *Xenopus* oocytes	ND	~90% reduction in accumulated H1A histone	Kandolf, 1994
HIV-1 *gag* (human immunideficiency virus) **(4)**	β-actin promoter, human cells	2	~100 fold reduction in HIV-1 pro-viral sequence	Sarver *et al.*, 1990
HIV-1 leader **(22)**	MoMLV *tat* inducible promoter in human cells	ND	no HIV-1 production up to 22 days post infection	Weerasinghe *et al.*, 1991
HIV-1 *int* **(9)**	T7 in *E.coli*	1, 4	elimination of *int* protein synthesis	Sioud & Drlica, 1991
HIV-1 U5	MuLV, human cells	2, 4	moderate suppression of HIV-1 infection	Dropulic *et al.*, 1992
HIV-1 *env* **(11)**	SV40 in human cells	ND	elimination of *env* transcript	Chen *et al.*, 1992
HIV-1 *gag* **(15)**	*in vitro* transcribed, CaPO$_4$ tranfected human cells	3,4	96% reduction in HIV-1 replication	Homann *et al.*, 1993
HIV-1 *tat* **(23)**	retroviral vector in human cells	3, 4	approximately 86% reduction in HIV-1 replication up to 14 days post infection	Crisell *et al.*, 1993
HIV-1 *tat*	retroviral LTR in human cancer cells	3	delay of HIV-1 replication for up to 20 days post transfection	Zhou *et al.*, 1994
HIV-ψ (packaging signal)	SV40 promoter, human cells	ND	~5 fold reduction in HIV replication	Sun *et al.*, 1994
HIV-1 LTR-CAT **(26)**	Va (pol III) promoter in human cells	4	up to 50% reduction in CAT activity expressed from HIV-1 LTR region	Ventura *et al.*, 1994

2/..

Figure 1.13 (2 of 3)

Target	**Expression system**	**Cleaved product analysis**	**Results**	**Reference**
MDR-1	human expression vector in mammalian cancer cells	3	up to 96% restoration of drug sensitivity	Kobayashi *et al.*, 1994
MDR-1	β-actin promoter in human cancer cells	ND	~ 99% restoration of drug sensitivity for up to 3 months	Scanlon *et al.*, 1994; Holm *et al.*, 1994
CAT **(12)**	SV40 in monkey COS cells	4	~60% reduction in CAT gene expression	Cameron & Jennings, 1989
CAT **(2)**	CaMV 35S promoter in plant cells	4	44% reduction in CAT gene expression	Perriman *et al.*, 1993
CAT	PGK promoter in *S.cerevisiae*	4	no reduction in CAT mRNA or gene expression	Atkins & Gerlach, 1994
CAT **(16)**	SV40 in monkey COS cells	4	60% reduction in CAT gene expression	Cameron and Jennings, 1994
GUS	CaMV35S promoter, plant cells	4	No reduction in GUS activity	Mazzolini *et al.*, 1992
GUS	*in vitro* transcribed, PEG delivery to plant protoplasts	ND	no reduction in GUS expression	Evans *et al.*, 1992
H-*ras* (oncogene)	SV40 promoter, human cancer cells	3	2-fold increase in survival of transfected mice	Kashani-Sabet *et al.*, 1992, 1994; Tone *et al.*, 1993
c-Ha-*ras*	RSV LTR promoter in human cancer cells	5	~ 50% reduction in activation of c-Ha-*ras* gene	Koizumi *et al.*, 1992, 1993
c-*fos* (oncogene) **(5)**	MMaTV, human cancer cells	2, 3	2-10 fold reduction in *fos* protein synthesis & restored drug sensitivity.	Scanlon *et al.*, 1991, 1994
U7snRNA **(13)**	$tRNA^{Met}$ in *Xenopus* oocytes	ND	elimination of U7snRNA	Cotten & Birnstiel, 1989
acetyl-CoA carboxylase	CMV promoter, mammalian cells	3	30-70% reduction in fatty acid synthesis	Ha & Kim, 1994
glucokinase (involved in mature onset diabetes) **(8)**	rat insulin II promoter, transgenic mice	ND	up to 70% reduction in glucokinase expression	Efrat *et al.*, 1994
β2M (β-2-microglobulin -involved in immune system) **(21)**	CMV promoter in mouse cells & transgenic mice	ND	80% reduction in β2M mRNA in cells; up to 90% (in lungs) in mice	Larsson *et al.*, 1994
BLV- *rex/tax* (bovine leukemia virus) **(7)**	Rous sarcoma virus promoter, bat cells	2, 3	BLV replication suppressed by 92%	Cantor *et al.*, 1993
lacZ **(3)**	MoMLV packaging vector, mouse cells	3	90% reduction in MoMLV containing *lacZ*	Sullenger & Cech, 1993

3/..

Figure 1.13 (3 of 3)

Target	Expression system	Cleaved product analysis	Results	Reference
NPTII **(1)**	CaMV35S promoter, plant cells	1, 3	100% reduction in NPTII activity	Steinecke *et al.*, 1992, 1994
NPTII **(27)**	CaMV35S promoter, transgenic tobacco	ND	~ 80% reduction in NPTII activity	Wegener *et al.*, 1994
ANF -Atrial natriuretic factor-hypertension **(17)**	U1snRNA or T7 RNA polymerase in monkey COS cells	3	~90% reduction in ANF mRNA for U1snRNA & ~80% for T7	DeYoung *et al.*, 1994
Influenza A (segment 5)	SV40 promoter, monkey COS cells	4	70-80% reduction in plaque formation	Tang *et al.*, 1994
α-lactalbumin **(6)**	T7-vaccinia virus, mouse cells	3	60-80% reduction in α-*lac* mRNA	L'Hullier *et al.*, 1992
TNFα (tumour necrosis factor) **(10)**	*in vitro* transcribed, liposome delivery in human cancer cells	4	90% reduction in TNFα mRNA and 85% reduction in protein	Sioud *et al.*, 1992
β-gal	M13 phage	ND	suppression of β-gal expression in *cis* but not in *trans*	Chuat & Galibert, 1989
α-sarcin	*in vitro* transcribed, injection in *Xenopus* oocytes	1, 3	*in vivo* cleavage of α-sarcin demonstrated but no difference in phenotype between active and mutant ribozyme	Saxena & Ackerman, 1990
lck & *fyn* protein kinases **(24)** (involved in T-cell activation)	tRNA^{Met} in retroviral vector in human leukemia cells	ND	61% (*fyn*) or 81% (*lck*) reduction in mRNA levels but no reduction in target proteins	Baier *et al.*, 1994
A2 RNA coliphage SP	*lac/lpp* promoters in *E.coli*	3,4	55% reduction in phage proliferation	Inokuchi *et al.*, 1994
MGMT (methyl tranferase involved in loss of drug cytotoxicity)	RSV LTR promoter in human cancer cells	2	no MGMT mRNA or protein detected	Potter *et al.*, 1993

Key to Cleaved Product Analysis

1 direct detection of cleavage products by RNase protection assays or Northern hybridisation.
2 RT-PCR analysis of cleavage products
3 mutant ribozyme; control in which the ribozyme contains a base-substitution rendering it inactive
4 antisense; same length of hybridisation as the ribozyme but lacking the catalytic domain
5 mutant target; target site triplet contains base-substitutions producing a non-cleavable target RNA
ND no analysis of cleavage products or control sequences reported

work carried out for this thesis has addressed the aspects of stability and expression of the hammerhead ribozyme in plant cells.

1.9.1.1. Intracellular localisation

While many people have recognised that a critical component of the hammerhead ribozyme reaction is that the ribozyme and substrate should be sequestered in the same compartment of the cell, the application of this notion is difficult. Although there are increasing data available concerning the timing, maturation and transport of transcripts from the nucleus to the cytoplasm, several aspects of the process are yet to be determined (Carter *et al.*, 1991, 1993; Xing *et al.*, 1993). Most importantly, although we are able to construct a sequence that is transported from the nucleus to the cytoplasm, we have only limited knowledge on how to manipulate a sequence so that it can be expressed and maintained in the nucleus. Additionally, since the *in vivo* application of ribozymes is still young, there are few clues as to which part of the cell would be best for cleavage to occur. However, since there is data suggesting ribozyme mediated gene reduction for both intra and extranuclear targets, it may be that both compartments are suitable for obtaining *in vivo* cleavage (see Fig. 1.13).

Sullenger and Cech (1993 - Fig. 1.13 (3)) have exemplified the notion that delivery of a ribozyme to the same cellular location as its target can substantially increase the effectiveness of the ribozyme. Their work involved the co-expression of two retroviral vectors, one encoding the hammerhead ribozyme and the second encoding the target mRNA (*lacZ*), inside retroviral packaging cells. These packaging cells were engineered to constitutively express the viral proteins gag, pol and env which allow co-packaging of the retroviral vector derived transcripts into viral particles. This means, co-expression of the two retroviral vectors encoding the target mRNA and the hammerhead ribozyme results in packaging of the two transcripts into the same viral particle, thus ensuring their co-localisation. Using this system, Sullenger and Cech obtained 90% reduction of the target mRNA. A control sequence

Figure 1.14: Some of the aspects of hammerhead ribozyme design which should be considered when designing a ribozyme for *in vivo* applications. The stylised cell depicts ribozyme (Rz) and substrate expressed from separate chromosomes. The levels of ribozyme and/or substrate **transcripts** produced, the **stability** of these RNAs, and their subsequent intracellular **localisation**, are all crucial aspects which should be addressed when designing a hammerhead ribozyme for *in vivo* applications.

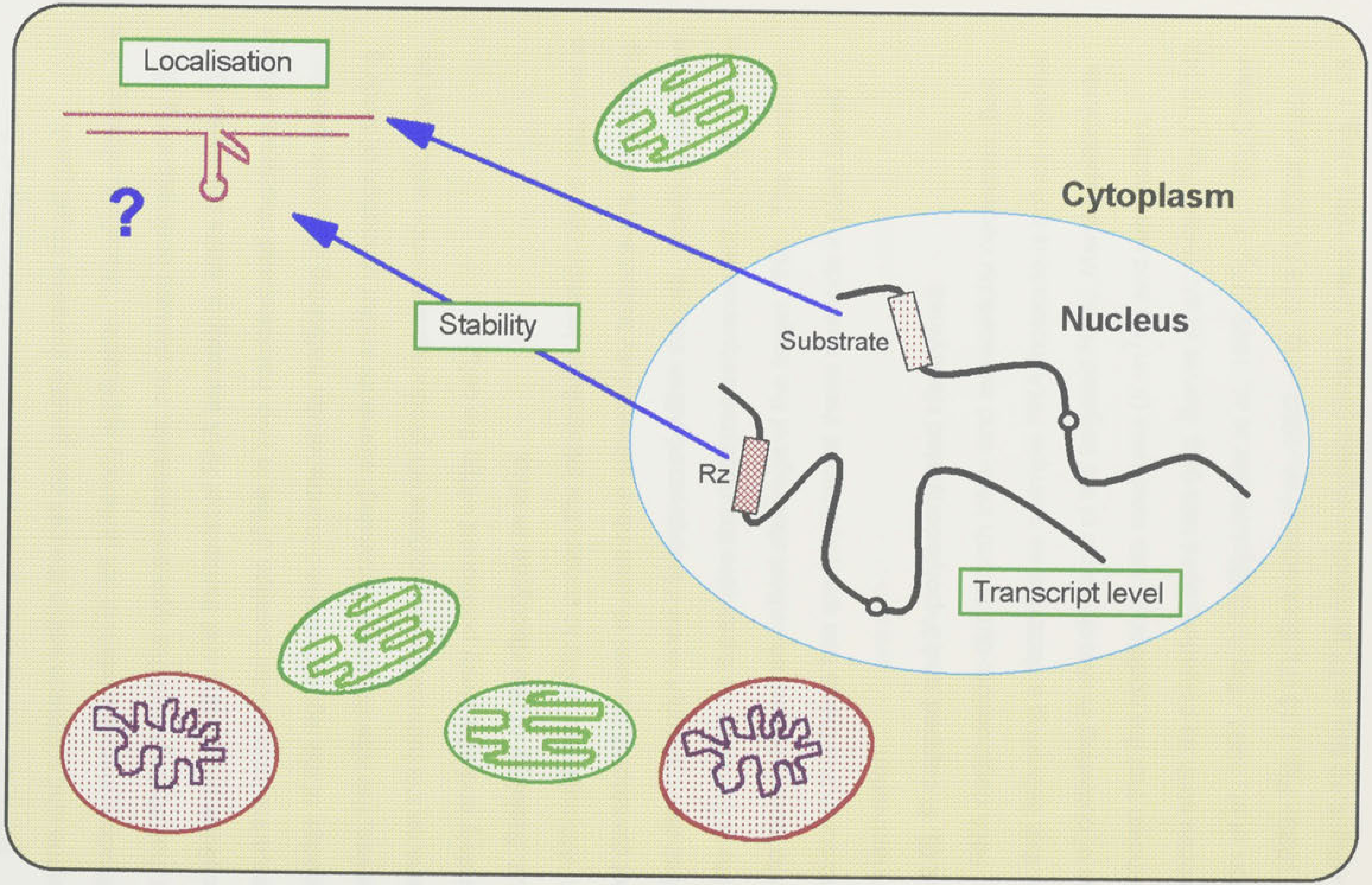
Localisation
?
Cytoplasm
Stability
Nucleus
Substrate
Rz
Transcript level

Figure 1.14

encoding an inactivated ribozyme provided evidence that the effect observed was ribozyme mediated.

While the results of this study prove that the co-localisation of the ribozyme and substrate within the cell can greatly increase target gene inactivation, such a system is not generally applicable. Therefore, although it is clear that strategies of this type are desirable, our present understanding of intracellular processing and transport of RNA transcripts, limits our ability to enhance the intracellular location of the *in vivo* hammerhead ribozyme. As our knowledge of the signals involved in intracellular trafficking of nucleic acids increases, the attachment of "localising" elements and/or utilisation of binding proteins on the hammerhead ribozyme will produce a sequence which can be accurately and effectively positioned within the cell.

1.9.1.2. Stability of the ribozyme *in vivo*.

Although our ability to control the intracellular location of the ribozyme is not yet developed, several studies have successfully tested ways of stabilising the ribozyme transcript, once it is expressed within the cell. Obviously such an attribute is desirable as it provides the ribozyme sequence with a longer time in which to locate, anneal and affect cleavage of the target RNA. The research carried out in this thesis has analysed two of these methods in plant based gene inactivation.

1.9.1.2 (i). 5'-capped and 3'-polyadenylated ribozymes

RNA degradation, due to both intra- and extracellular nucleases, has meant that delivering a ribozyme as a simple RNA molecule is not an effective means of obtaining *in vivo* cleavage of the targeted RNA. Many experiments have shown that the addition of cap structures (5'-m^{7}G) and termination sequences such as polyadenylated tails (e.g. Sarver *et al.*, 1990 - Fig. 1.13 (4); Scanlon *et al.*, 1991 - Fig. 1.13 (5); L'Hullier *et al.*, 1992 - Fig. 1.13 (6); Cantor *et al.*, 1993 - Fig. 1.13 (7); Steinecke *et al.*, 1992 - Fig. 1.13 (1); Efrat *et al.*, 1994 - Fig. 1.13 (8)) or T7 termination signals (Sioud & Drlica 1991 - Fig. 1.13 (9), Sioud *et al.*, 1992 - Fig. 1.13 (10); DeYoung *et al.*, 1994 - Fig.1.13 (17)) to

single hammerhead ribozymes are sufficient to obtain gene inactivation *in vivo*. Other experiments have incorporated multiple ribozyme domains within 5' and 3' stabilised transcripts, so as to increase the number of cleavage sites on the substrate RNA (Chen *et al.*, 1992 - Fig. 1.13 (11); Ohkawa *et al.*, 1993). Other studies have suggested that, as well as 5'-m7G cap and 3'-polyadenylation, the ribozyme requires additional sequences which, upon entry into the cell, provide a further stabilising effect (e.g. Cameron and Jennings, 1989 - Fig.1.13 (12); Cotten and Birnsteil, 1989 - Fig.1.13 (13); DeYoung *et al.*, 1994 - Fig.1.13 (17)). This apparent inconsistency between studies probably reflects a number of fundamental differences within each system. One obvious factor is the target accessibility of different substrate RNAs.

Cameron and Jennings (1989 - Fig. 1.13 (12)) reasoned that a ribozyme embedded within the 3' end of an actively transcribed mRNA, could confer stability to that ribozyme sequence. They incorporated a ribozyme into the 3' untranslated end of the gene for firefly luciferase and showed that, while the non-embedded ribozyme was ineffective , the luciferase embedded ribozyme could specifically suppress target gene expression by up to 60%. In this system, the ribozyme was estimated to be present in >1000-fold molar excess over the target RNA.

Other methods have constructed ribozymes which utilise both an antisense and a catalytic approach to gene inactivation by incorporating ribozyme domains into long stretches of antisense sequence (Heinrich *et al.*, 1993 - Fig.1.13 (14); Homann *et al.*, 1993 - Fig.1.13 (15); Perriman *et al.*, 1993- Fig.1.13 (2); Cameron and Jennings, 1994 -Fig.1.13 (16)). Homann *et al.* (1993 - Fig.1.13 (15)) incorporated a single hammerhead domain into a 413 base antisense targeted against the 5' leader/gag region of HIV-1. They found that the presence of the hammerhead domain in the antisense increased the ability of the molecule to reduce HIV-1 replication 4-7 fold over that obtained for the unmodified antisense. A hammerhead domain rendered inactive by deletion of U7 from the conserved core was even less effective than the unmodified antisense. These results suggest that the major mechanism of gene inactivation in this system was cleavage of the target RNA.

Similarly, we have previously shown that an 800 base antisense containing four hammerhead domains can enhance target gene reduction in plant cells by up to 30% over that obtained for the non-modified antisense (Perriman *et al.,* 1993 - Fig.1.13 (2)). Using the same ribozyme-antisense construction in animal cells, Cameron and Jennings (1994 - Fig.1.13 (16)) have also shown a 25-30% enhancement in target gene reduction over the antisense control. In an attempt to further enhance the effect of this antisense-ribozyme construct, the initial research for this thesis involved the development of a modified vector construction designed to increase the expression of this sequence. This construction will be outlined briefly in section 1.9.1.3. and in more detail in chapter 3.

An additional study by Heinrich and colleagues involved inserting a hammerhead domain into a 290 base antisense targeting the *white* gene in *Drosophila melanogaster*. Although a specific reduction in *white* gene phenotype was observed (Heinrich *et al.*, 1993 - Fig.1.13 (14)) this study did not include an antisense control so the effect of the antisense sequence alone cannot be accounted for.

As an alternative approach to the *in vivo* stabilisation of the ribozyme, DeYoung *et al.* (1994 - Fig.1.13 (17)) developed a small nuclear RNA (snRNA), U1, to express ribozymes against a peptide hormone (ANF) thought to be involved in hypertension. U1 genes are ubiquitously expressed under the control of a strong RNA polymerase II promoter but are not polyadenylated. A stem-loop structure and conserved 3' sequence determine correct 3' end formation and provide protection from 3' exonucleases (Ciliberto *et al.*, 1986). Therefore, one potential advantage over polyadenylated RNA polymerase II RNAs, is the lack of extensive 3' sequences which may interfere with correct substrate-ribozyme hybrid formation. Using this approach DeYoung *et al.* (1994) demonstrated a 90% reduction in ANF mRNA levels when compared with control levels. The use of catalytically inactive control ribozymes established that the observed effect was ribozyme mediated.

1.9.1.2 (ii). Ribozymes transcribed by RNA polymerase III

All of the systems discussed so far have taken advantage of RNA polymerase II based promoters (pol II) to obtain intracellular transcription of hammerhead ribozymes. However, several studies have now successfully embedded the ribozyme within an actively transcribing sequence derived from RNA polymerase III (pol III). At the commencement of the research for this thesis, one laboratory had published data in which a hammerhead ribozyme was expressed using a methionine tRNA-sequence in *Xenopus* oocytes (Cotten and Birnsteil, 1989 - Fig.1.13 (13)). Since this time, several reports have demonstrated the efficacy of using a tRNA-ribozyme (Yuyama *et al.*, 1992; Shore *et al.*, 1993 - Fig.1.13 (18); Bouvet *et al.*, 1994 - Fig.1.13 (19); Baier *et al.*, 1994 - Fig.1.13 (24); Kandolf, 1994 - Fig.1.13 (25)) or related RNA polymerase III transcribed sequences (Ventura *et al.*, 1994 - Fig.1.13 (26)). The work carried out in this thesis is based on the work of Cotten and Birnsteil (1989 - Fig.1.13 (13)) and has also involved the development of a plant tRNA transcription system for delivery of ribozymes to plant cells.

tRNAs have several advantages as delivery systems for ribozymes. They are abundantly expressed (Darnell, 1986) and extremely stable molecules (Karnail and Wasterneck, 1992) therefore meeting two of the requirements for *in vivo* optimisation of ribozymes. Additionally, unlike RNA polymerase II transcripts, they are small and do not contain long transcription leaders or polyadenylation sequences. These sequences, which stabilise the RNA polymerase II transcript *in vivo*, may also reduce the ribozymes efficiency by folding into inactive conformations (Rossi *et al.*, 1991). Since the structure of the tRNA is known, ribozyme insertion sites can be situated to minimise any reduction in cleavage due to interactions with the surrounding tRNA sequence.

Three sites within tRNA molecules have been successfully used to express hammerhead ribozymes in both *Xenopus* oocytes and a human cell line. Cotten and Birnsteil (1989 - Fig.1.13 (13)) incorporated a hammerhead ribozyme into the anticodon loop of a methionine tRNA. Using this construction they were able to demonstrate transcription of the tRNA-embedded ribozyme and specific reduction of a cytoplasmic target RNA in *Xenopus* oocytes. This was despite the fact that the tRNA-ribozyme remained predominantly in the nucleus. The ribozyme: substrate ratio in this system was found to be at least 1000 : 1. Additionally, the tRNA-ribozyme showed enhanced stability over the non tRNA-embedded ribozyme when assayed in nuclear extracts. The enhanced stability of a similar tRNA-ribozyme construction has also been shown by Yuyama *et al.* (1992). They found that the tRNA-ribozyme was approximately 10-fold more stable in fetal bovine serum than the analogous non-embedded ribozyme.

Another region of the tRNA was used by both Bouvet *et al.* (1994 - Fig.1.13 (19)) and Kandolf (1994 - Fig. 1.13 (25)) who introduced a ribozyme into the intron of a tyrosine tRNA and successfully reduced accumulation of the H1 histone protein in *Xenopus* oocytes. Microinjection of 10ng of the tRNA-ribozyme led to a four-five fold reduction of H1 protein synthesis. Shore *et al.* (1993 - Fig.1.13 (18)) have expressed a ribozyme at the 3' end of a human methionine tRNA ($tRNA^{Met}$) targeting the *BCRABL* oncogene associated with human chronic myelogenous leukemia. *In vivo* expression of the tRNA-ribozyme resulted in the elimination of *BCRABL* gene activity. An identical approach to this was also used by Baier *et al.* (1994) in targeting two protein kinases involved in T-cell activation. Expression of the $tRNA^{Met}$-ribozyme constructs resulted in 61-80% reduction in target mRNA.

Another RNA polymerase III transcribed ribozyme sequence has been used recently against a human immunodeficiency virus-CAT construction. The *Va* gene from human adenovirus 2 provides RNA polymerase III based transcription from internal A and B box promoter elements in the same way as tRNA genes are transcribed. A ribozyme, inserted at the 3' end of *Va* was able to reduce HIV-CAT activity by up to 50% over control levels (Ventura *et al.*, 1994).

The research in this thesis has developed a plant tyrosine-tRNA to act as a hammerhead ribozyme delivery system to plant cells. We have used the approach of Cotten and Birnsteil (1989 - Fig.1.13 (13)) and incorporated our ribozyme into the anticodon loop of the tRNA sequence. As well as analysing tRNA-ribozymes *in vitro* and *in vivo*, this thesis has compared a tRNA-antisense and the analogous non-embedded ribozyme and antisense sequences.

1.9.1.3. Enhancing expression levels by delivery

While it is important to equip the ribozyme with sequences which can enhance its *in vivo* stability, maximising the levels of expression (i.e. transcription) are also important. I have already discussed the tRNA vector system which can enhance both the expression and stability of the hammerhead ribozyme. However, systems such as the tRNA or any of the RNA polymerase II constructions can be further enhanced by maximising the number of DNA templates from which ribozyme transcription, pol II or pol III, can occur.

Obviously the stable integration of sequences encoding ribozymes is one approach, however this method can produce transgenic organisms in which the expression of either the transgene or endogenous mRNAs are altered as a result of insertional inactivation. In plants this approach is still suitable as many individual transgenic lines can be produced and screened. At this stage, there is only one published report describing transgenic plants expressing specific ribozyme sequences (Wegener *et al.*, 1994). Although the study reported a reduction in target gene expression, no control antisense or inactive ribozyme sequences were included. As part of the research for this thesis, several independent tRNA-ribozyme and tRNA-antisense expressing transgenic plants have been analysed.

In animal systems, where most ribozyme target sequences are ultimately aimed towad human applications, the production of a transgenic organism is not appropriate. In some studies however, aspects of cellular function and development are being analysed by producing transgenic laboratory organisms expressing hammerhead ribozymes designed to reduce the expression of specific gene products. Two reports have produced transgenic *Drosophila melanogaster* expressing ribozymes against the *white* eye phenotype (Heinrich *et al.*, 1993 - Fig.1.13 (14)) and a developmental gene, *ftz*, (Zhao and Pick, 1993 - Fig.1.13 (20)). Additionally, two other studies have produced transgenic mice expressing ribozymes against a glucokinase involved in mature onset diabetes (Efrat *et al.*, 1994 - Fig.1.13 (8)) and an mRNA encoding β2M, a protein thought to play an important role in the immune system (Larsson *et al.*, 1994 - Fig.1.13 (21)). Unfortunately, while all studies did observe an altered phenotype, only the work of Zhao and Pick (1993 - Fig.1.13 (20)) included antisense and inactivated ribozyme controls.

As an alternative, several methods have been tested for the exogenous delivery of hammerhead ribozymes to cultured cell-lines. While some of these provide transient expression of the ribozyme, others can be manipulated so that stable expression can be obtained. As well as analysing transgenic plants expressing the tRNA-ribozyme, this thesis describes a new mode of delivering hammerhead ribozymes to plant cells. This method is analogous to the many viral-based vectors available in animal systems.

Retroviral vectors containing the ribozyme sequence are the most widely used for high level expression of hammerhead ribozymes in mammalian cells. Upon infection of the cell, the single stranded RNA genome of the retrovirus is reverse transcribed and integrated into the genome. Once integrated, the sequence is transcribed by host-cell polymerases, infectious RNAs are produced, encapsidated and bud from the infected cells. Retroviral vectors have been engineered so that they are defective in their replication function. This means that once they are integrated, the retroviral sequences will actively transcribe but are unable to form infectious viral particles. In this way stably transformed cell-lines expressing the ribozyme sequences can be produced. Using this approach several independent cell-lines can be screened until the desired phenotype is observed. This transfected cell-line can then be re-implanted into an organism where the hope is that it will replace the defective cell-types with the ribozyme expressing ones. Retroviral vectors encoding ribozymes against HIV-1 (Weerasinghe *et al.*, 1991 - Fig.1.13 (22); Crisell *et al.*, 1993 - Fig.1.13 (23)), *BCRABL* oncogene (Shore *et al.*, 1993 - Fig.1.13 (18)), bovine leukemia virus (Cantor *et al.*, 1993 - Fig.1.13 (7)) and the c-fos proto-oncogene (Scanlon *et al.*, 1991 - Fig.1.13 (5)) have been effectively delivered to cultured cell-lines. The work of Shore *et al.* (1993 - Fig.1.13 (18)) and Baier *et al.* (1994) which were discussed in section 1.9.1.2(ii) have incorporated both the tRNA delivery mechanism and the retroviral vector. At this stage there is no published data on the re-introduction of these transfected cell-lines into whole organisms.

The research carried out in this thesis has also taken advantage of a replicating viral system to deliver ribozymes to plant cells. The plant geminivirus, African cassava mosaic virus (ACMV- see Stanley, 1993) has been adapted to deliver ribozyme or antisense sequences. ACMV is a single stranded DNA plant virus which relies on host components for replication, is localised within the nucleus and can replicate to high levels (see Davies *et al.*, 1987 for review). In this way, it is similar to the retroviral vectors used in the mammalian systems. However, as distinct from the retrovirus, ACMV autonomously replicates to produce extremely high levels of viral DNA which is maintained as an episome in the nucleus of plant cells. Chimeric viral sequences containing either the antisense-ribozyme or tRNA-ribozyme sequences have been constructed. In this way, both the high level expression obtained from the self-replicating ACMV and the stability conferred by either the antisense or tRNA sequences can be utilised. The ACMV vector will be discussed in more detail in the following chapters.

1.10. Conclusions and aims of this thesis

The discovery of RNA molecules such as the hammerhead ribozyme has provided a powerful tool for the potential manipulation of gene expression in living organisms. The initial excitement regarding the application of ribozymes has now developed into a wide area of study, as researchers have recognised that in order to successfully apply ribozymes to living cells, several areas need to be addressed. These include the determination of the structural and chemical basis of the cleavage reaction, and techniques aimed at optimising intracellular expression.

The main objective of this thesis has been to optimise the expression and stability of hammerhead ribozyme transcripts in plants. While the research in this thesis has been carried out in plant cells, many of the results obtained can be applied to future ribozyme design in both animal and plant systems.

CHAPTER 2

MATERIALS & METHODS

All oligonucleotides were synthesised on an Applied Biosystems model 392 DNA synthesiser by Lynda Graf (CSIRO Division of Plant Industry) or John Gardner (University of California, Davis). Molecular cloning and related techniques were carried out essentially as described by Sambrook *et al.* (1989). Plasmid constructions outlined below are all depicted on figures contained in an envelope at the back of this thesis. These figures are detachable and show all constructions used in the data presented in Chapters 3, 4 and 5.

PLASMID CONSTRUCTIONS

2.1. pApoly (Fig 2.1a)

A clone of the A component of the geminivirus African cassava mosaic virus (ACMV), pET012 was obtained from John Stanley (John Innes Institute, Norwich, UK). This plasmid contains a 727bp deletion within the coat protein open reading frame (nucleotides 467-1194, Ward *et al.*, 1988) and a unique *Eco*RV site at the site of this deletion. The DNA A was cloned as a *Bam*HI insert in M13. Modifications to this vector were carried out by Paul Feldstein and Cathy Chay (University of California, Davis). These included the insertion of a pUC19-derived plasmid, p129C, carrying the *colE1* bacterial origin of replication and chloramphenicol resistance gene and the removal of the M13 vector. p129C was inserted at the *Cla*I site to make pACMV and allowed for amplification in *E.coli.* A 946bp *BamHI/Cla*I fragment of the ACMV A genome containing the putative origin of replication (2124 - 2779 and 1 - 291) was isolated and re-inserted in a head-to-tail orientation to produce a 1.3 copy of the ACMV genome (minus the coat protein ORF). In addition, T7 and SP6 RNA polymerase promoter sequences were inserted to flank a 549bp insert. This insert was placed between the coat protein promoter and polyadenylation

Figure 2.1

a: pApoly vector used for expression of CAT target, ribozyme and antisense sequences in plant cells. p129C, (blue box), is the bacterial plasmid containing *colE1* bacterial origin of replication and chloramphenicol resistance gene (**Cm^r**). This plasmid was inserted at the *Cla*I site as indicated. Red boxes are 2 copies of the region containing the viral origin of replication with the internal arrows indicating the direction of replication of "sense" viral sequence. The endogenous coat protein promoter region is indicated with sites of **"TATA"**, transcription start **(t start)**, initiation codon **(AUG)**, transcription termination **(t stop)** and polyadenylation signals **(polyA)**. Δ **CP** represents the region of the coat protein open reading frame which has been deleted and replaced with polylinker sequence as indicated. Numbers in bold are nucleotides on the viral sequence while italicised numbers are the polylinker sequence.

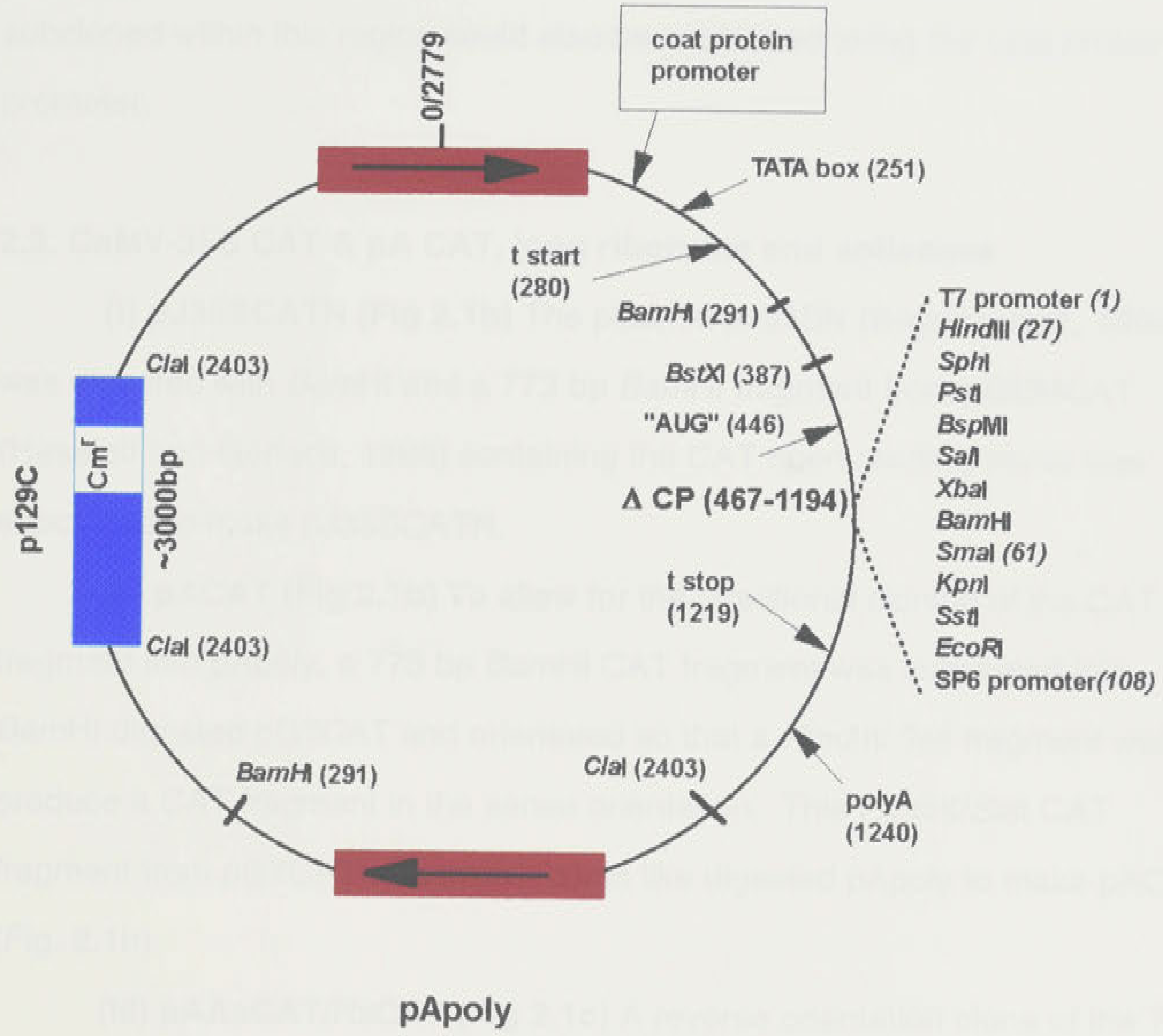
coat protein promoter
0/2779
TATA box (251)
t start (280)
BamHI (291)
BstXI (387)
"AUG" (446)
Δ CP (467-1194)
t stop (1219)
T7 promoter (1)
HindIII (27)
SphI
PstI
BspMI
SalI
XbaI
BamHI
SmaI (61)
KpnI
SstI
EcoRI
SP6 promoter(108)
ClaI (2403)
ClaI (2403)
Cm^r
p129C
~3000bp
polyA (1240)
ClaI (2403)
BamHI (291)
pApoly

Figure 2.1a

signals so that expression was obtained from these sequences. Subsequently, I removed the 549 base insert as a *Hind*III/*Sst*I fragment and replaced it with a *Hind*III/*Sst*I fragment of the polylinker derived from pUC19. This made the construct pApoly (Fig. 2.1a - nos. in italics, 1-108, represent insert flanked by T7 and SP6 RNA polymerase promoter sequences). Any sequences subcloned within this region could also be expressed using the coat protein promoter.

2.2. CaMV-35S CAT & pA CAT, long ribozyme and antisense

(i) pJ35SCATN (Fig 2.1b) The plasmid pJ35SN (Bogusz *et al.*, 1990) was digested with *Bam*HI and a 773 bp *Bam*HI fragment from pGEMCAT (Haseloff and Gerlach, 1988) containing the CAT open reading frame was subcloned to make pJ35SCATN.

(ii) pACAT (Fig 2.1b) To allow for the directional cloning of the CAT fragment into pApoly, a 773 bp *Bam*HI CAT fragment was subcloned into *Bam*HI digested pG7CAT and orientated so that a *Hind*III/*Sst*I fragment would produce a CAT fragment in the sense orientation. This *Hind*III/*Sst*I CAT fragment from pG7CAT was inserted into like digested pApoly to make pACAT (Fig. 2.1b).

(iii) pAAsCAT/RzCAT (Fig 2.1c) A reverse orientation clone of the 773 bp CAT insert in pGEM7zf+ (pG7AsCAT) was digested with *Hind*III/*Sst*I and the fragment subcloned into like digested pApoly to make the clone pAAsCAT (Fig. 2.1c).

To incorporate the four hammerhead ribozyme domains into the antisense sequence, site-directed mutagenesis was carried out (Kunkel *et al.*, 1987) using pGEMAsCAT as the template. Single stranded plasmid DNA isolated from an *ung- dut-* strain of *E.coli* was annealed with four oligonucleotides each containing hammerhead ribozyme domains and specific flanking sequence. Replication of the plasmid was completed with dNTPs, T4 DNA polymerase and T4 DNA ligase and introduced into *E.coli* strain DH5α.

Figure 2.1

b: Subcloning of CAT into pJ35SN and pApoly expression vectors for analysis in *N.tabacum* plant cells. pJ35SN contains a 430-bp segment of the 35S promoter from cauliflower mosaic virus (35S - shown in green), *BamH*I, *Sma*I and *EcoR*I restriction sites followed by termination signals from nopaline synthase (NOS-t - shown in red). Expression from pApoly is obtained from the ACMV coat protein promoter (ACMV-CP-dark blue) and termination signals (ACMV-t-yellow). The vertical arrows indicate the sites of the four GUC triplets in the CAT RNA that are targeted by ribozyme sequences contained in the long ribozyme RNA. The horizontal arrows indicate the direction of transcription *in vivo.*

c: Subcloning of CAT antisense (AsCAT) and long ribozyme (RzCAT) into pApoly expression vector. As in **b** expression of AsCAT and RzCAT are obtained from the ACMV coat protein promoter (dark blue) and termination signals (yellow) with the direction of transcription indicated by horizontal arrows. The four ribozyme sequences on RzCAT are indicated (1-4) with numbers corresponding to the target sites on the CAT RNA.

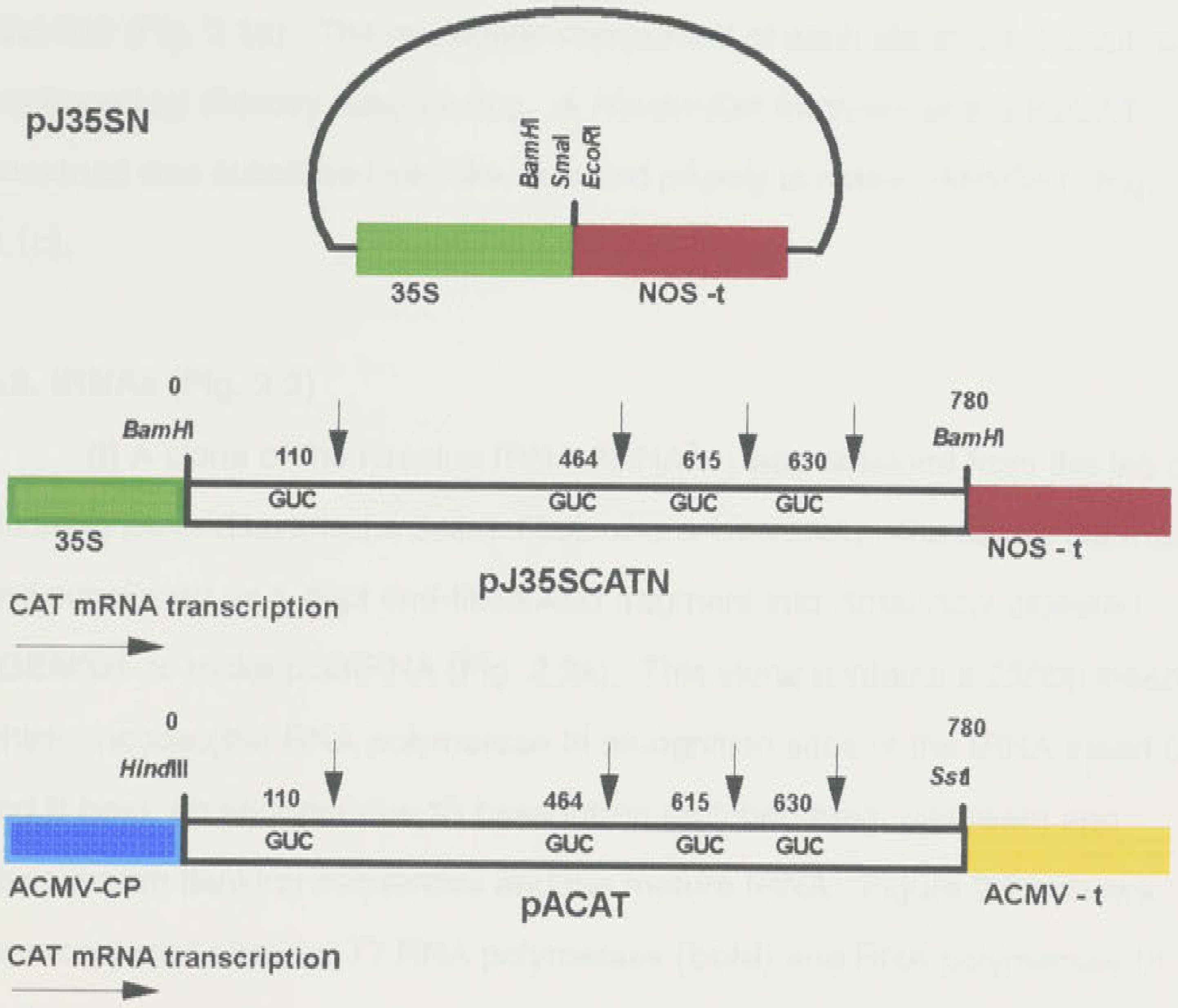
pJ35SN
BamHI
SmaI
EcoRI
35S
NOS -t
0
BamHI
110
464
615
630
780
BamHI
GUC
GUC
GUC
GUC
35S
NOS - t
pJ35SCATN
CAT mRNA transcription
0
HindIII
110
464
615
630
780
SstI
GUC
GUC
GUC
GUC
ACMV-CP
pACAT
ACMV - t
CAT mRNA transcription

Figure 2.1b

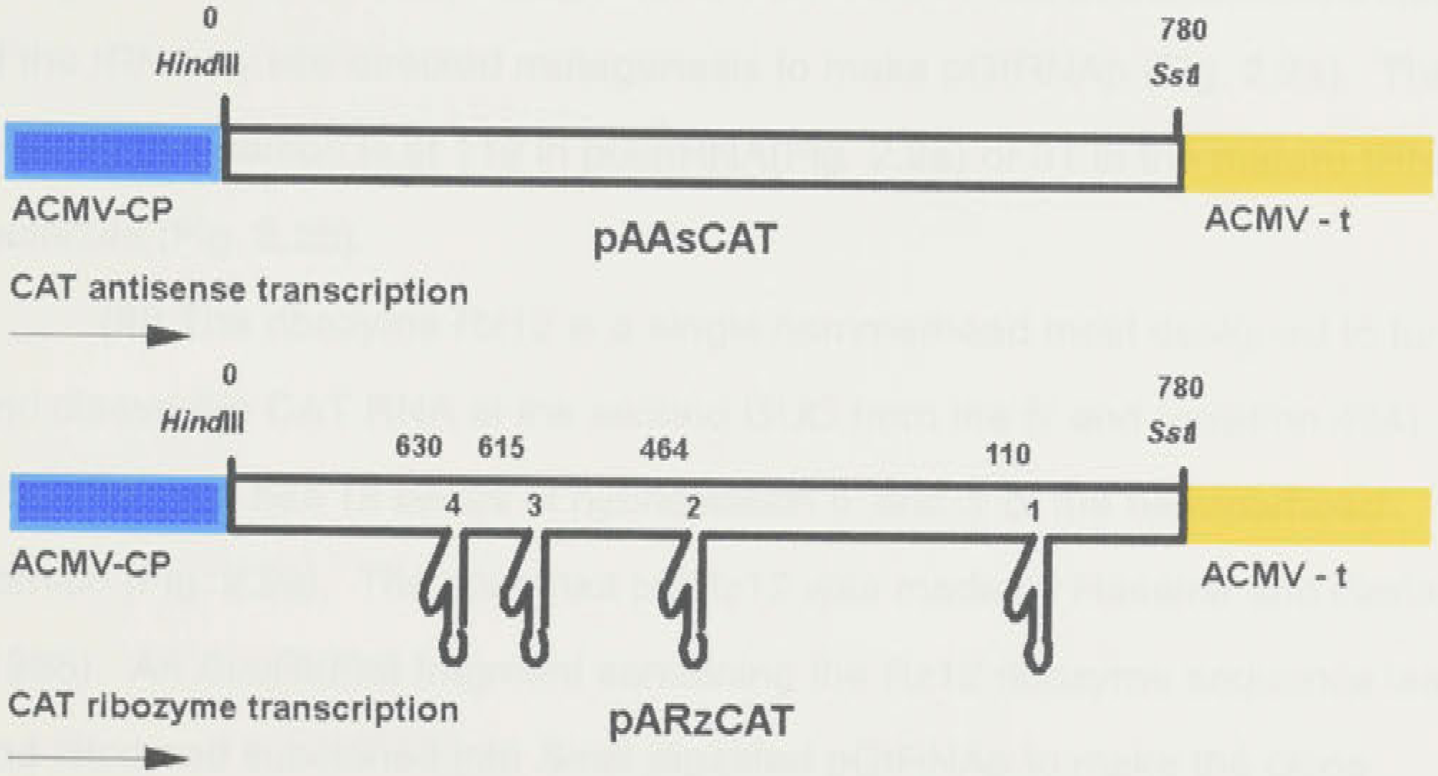
0
HindIII
780
SstI
ACMV-CP
pAAsCAT
ACMV - t
CAT antisense transcription
0
HindIII
630
615
464
110
780
SstI
4
3
2
1
ACMV-CP
ACMV - t
CAT ribozyme transcription
pARzCAT

Figure 2.1c

The resultant plasmid, pGRzCAT, encoded a ribozyme capable of cleaving the target CAT RNA sequence 3' of "GUC" trinucleotides at positions 110, 464, 615 and 630 (Fig. 2.1c). The nucleotide component of each ribozyme domain was confirmed by dideoxy -sequencing. A *Hind*III/*Sst*I fragment of the RzCAT construct was subcloned into like digested pApoly to make pARzCAT (Fig. 2.1c).

2.3. tRNAs (Fig. 2.2)

(i) A clone of the tyrosine tRNA ($tRNA^{Tyr}$) was obtained from the lab of Hildberg Beier (Bayerische Julius-Maximilians University, Wurzburg, Germany) and subcloned as a *Ssp*I end-filled/*Acc*I fragment into *Sma*I/*Acc*I digested pGEM3zf- to make pG3tRNA (Fig. 2.2a). This clone contains a 256bp insert which encodes the RNA polymerase III recognition sites of the tRNA insert (A and B box), an endogenous 13 base intron (hatched box), upstream and downstream flanking sequences and the mature tRNA. Figure 2.2a shows transcript start sites for T7 RNA polymerase (**bold**) and RNA polymerase III (*italics*).

(ii) A short oligodeoxyribonucleotide, containing three restriction enzyme recognition sites, *Bam*HI, *Sma*I, *Eco*RI, was inserted within the anticodon loop of the tRNA by site directed mutagenesis to make pGtRNAp (Fig. 2.2a). The position of insertion is at 112 in pG3tRNA(Fig. 2.2a) or 31 in the mature tRNA molecule (Fig. 2.2b).

(iii) The ribozyme Rz12 is a single hammerhead motif designed to target and cleave the CAT RNA at the second GUC from the 5' end (position 464). This ribozyme has 12 bases of hybridisation 5' and 3' of the hammerhead domain (Fig. 2.2c). The construct pGRz12 was made by Haseloff and Gerlach (1988). An *Eco*RI/*Pst*I fragment containing the Rz12 ribozyme sequence was end-filled and subcloned into *Sma*I digested pGtRNAp to make the clone pGtRNARz12.

Figure 2.2

a: Subcloning of 256 bp tRNA^{Tyr} sequence into pGEM3zf-. Boxes labelled A in green and B in red are RNA polymerase III promoter recognition sites; the yellow region represents a 13 base intron within the tRNA sequence. The transcription start site for T7 RNA polymerase is shown by numbers in bold; the internal arrow and numbers in italics represent RNA polymerase III transcript start. The arrow at position **112**/*31* on pGtRNAp indicates the site of insertion of *BamH*I, *Sma*I and *EcoR*I restriction sites (hatched black box). This is within the anticodon loop as shown in figure 2.2b.

b: Clover leaf motif of tRNA^{Tyr} sequence. Nucleotides comprising the A and B boxes, and the 13 base intron are color coded as in (**a**). The arrow shows the site of insertion of *BamH*I, *Sma*I and *EcoR*I restriction sites. The red circled C56 nucleotide was mutated to a G for mutagenesis of the RNA polymerase III promoter (see section 2.7). Nucleotide numbering is depicted for the mature tRNA^{Tyr} sequence. ψ at positions 35 and 55 are pseudouridines.

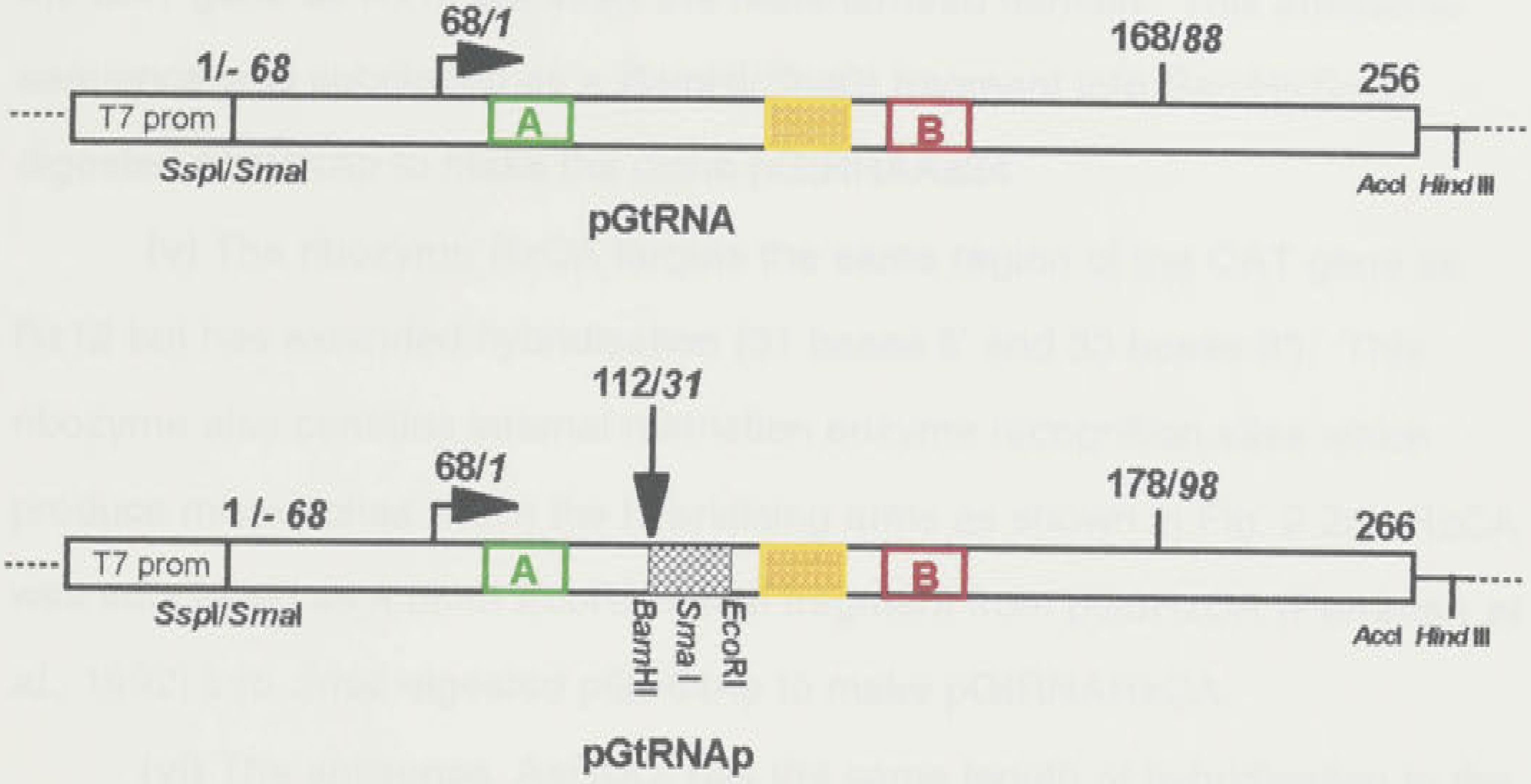
68/1
1/- 68
168/88
256
T7 prom
A
B
SspI/SmaI
AccI HindIII
pGtRNA
112/31
68/1
1 /- 68
178/98
266
T7 prom
A
B
BamHI
Sma I
EcoRI
SspI/SmaI
AccI HindIII
pGtRNAp

Figure 2.2a

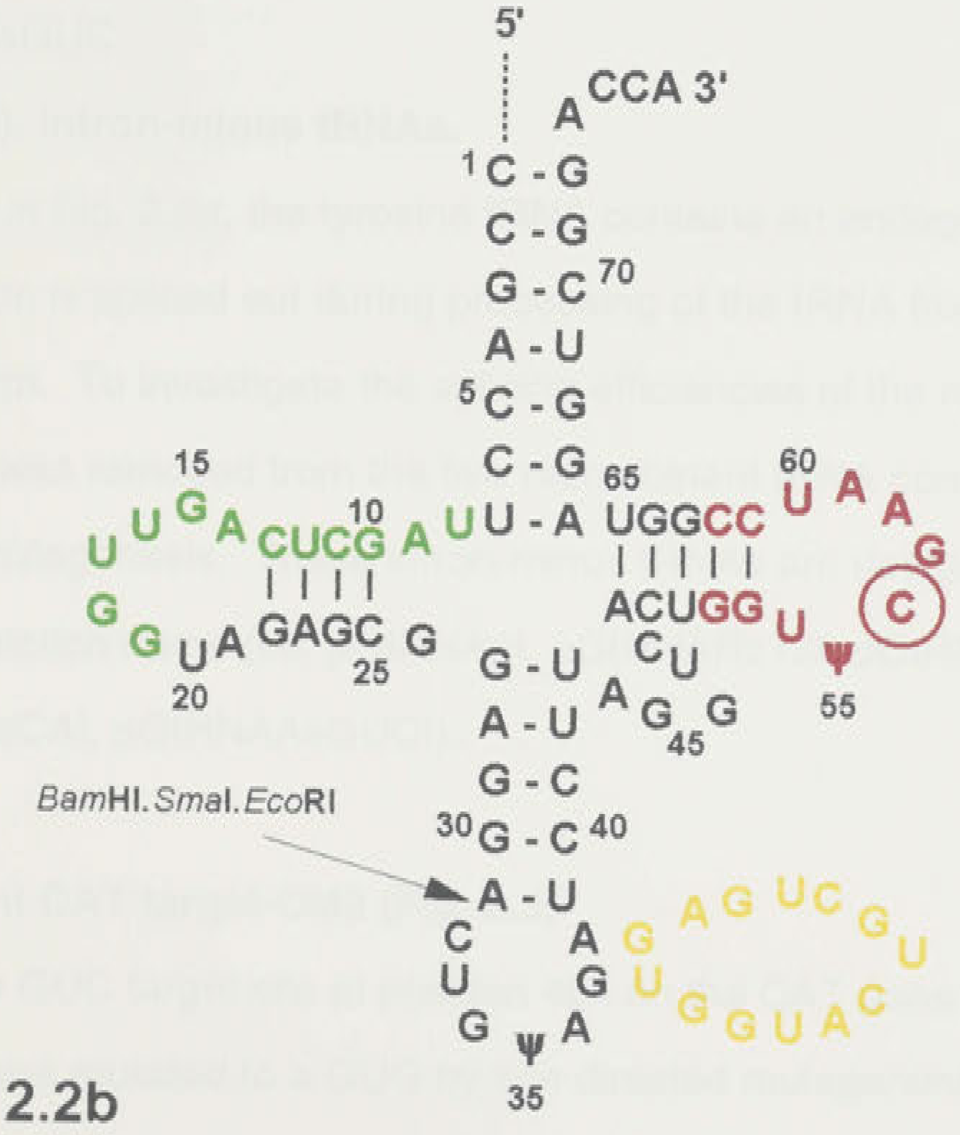
5'
CCA 3'
A
1C - G
C - G
G - C 70
A - U
5C - G
C - G 65
U - A
15
10
60
UUGACUCGAU
UGGCCUAAG
||||
|||||
G
G U A GAGC G
ACUGG U C
Ψ
25
20
55
G - U
A - U
G - C
30 G - C 40
A - U
C U G Ψ A G A
35
CU A G G 45
BamHI.SmaI.EcoRI
G A G U C G U C A U G G U G

Figure 2.2b

(iv) The antisense sequence, As24 was made by Cameron and Jennings (1989). This sequence contains the same extent of hybridisation to the CAT gene as Rz12 but lacks the hammerhead domain. This antisense sequence was subcloned as a *Bam*HI/*Sna*BI fragment into *Bam*HI/*Sma*I digested pGtRNAp to make the clone pGtRNAAs24.

(v) The ribozyme RzCA targets the same region of the CAT gene as Rz12 but has extended hybridisation (31 bases 5' and 33 bases 3'). This ribozyme also contains internal restriction enzyme recognition sites which produce mismatches within the hybridising arms as shown in Fig. 2.2d. RzCA was subcloned as a blunt *Eco*RI/*Hind*III fragment from pG3RzCA (Perriman *et al.*, 1992) into *Sma*I digested pGtRNAp to make pGtRNARzCA.

(vi) The antisense, AsGUC, has the same length of hybridisation to the CAT gene as the long ribozyme. It also contains the same mismatches so that the effect of the addition of the hammerhead domain could be accurately measured. AsGUC was subcloned from pGAsGUC (Perriman *et al.*, 1992) as a blunt *Eco*RI/*Hind*III fragment into *Sma*I digested pGtRNAp to make pGtRNAAsGUC.

(vii). intron-minus tRNAs.

As shown in Fig. 2.2a, the tyrosine tRNA contains an endogenous 13 base intron which is spliced out during processing of the tRNA from the pre to the mature form. To investigate the splicing efficiencies of the recombinant tRNAs, the intron was removed from the five recombinant tRNA constructs by site directed mutagenesis. These intron-minus tRNAs are designated "I" following the construction name (i.e. pGtRNApI, pGtRNARz12I, pGtRNAAs24I, pGtRNARzCAI, pGtRNAAsGUCI).

2.4. Mutant CAT target-CM2 (Fig. 2.3)

The GUC target site at position 464 on the CAT gene in the clone pG7CAT was mutated to a GUG by site directed mutagenesis. A GUG target triplet has been previously shown to be a noncleavable target under *in vitro*

Figure 2.2

c: Sequence of Rz12 ribozyme which is designed to anneal and cleave at position 464 on the CAT mRNA. The ribozyme confers complementarity of 12 bases 5' and 12 bases 3' of the target site.

d: Sequence of RzCA ribozyme which targets the same region on the CAT mRNA as **c** but has extended 5' and 3' hybridisation (31 bases 5' and 32 bases 3'). The internal nucleotides in blue are restriction sites (*Sma*I and *Eco*RV) which produce mismatches in the hybridising arms. *Hind*III and *EcoR*I restriction sites were used for subcloning into pGEM3zf+ (Perriman *et al.*, 1992) and pACMV vectors.

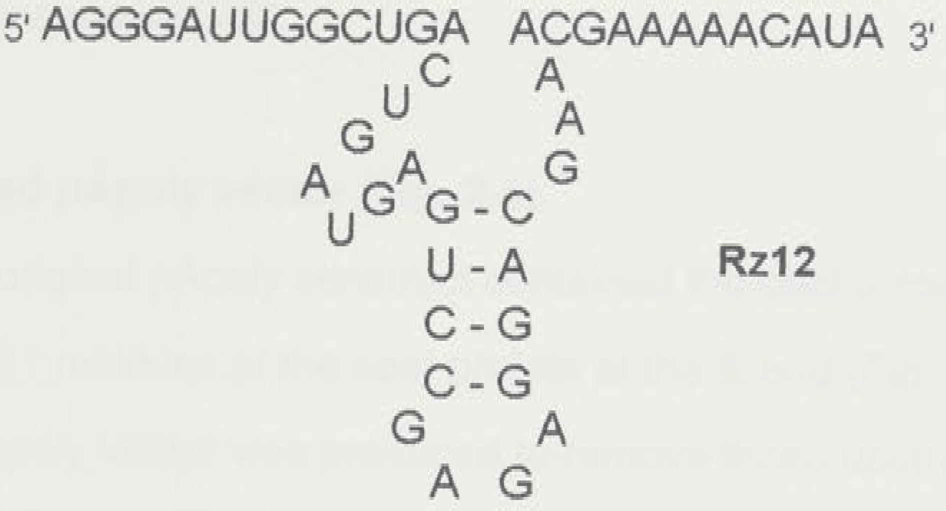
5' AGGGAUUGGCUGA ACGAAAAACAUA 3'
Rz12

Figure 2.2c

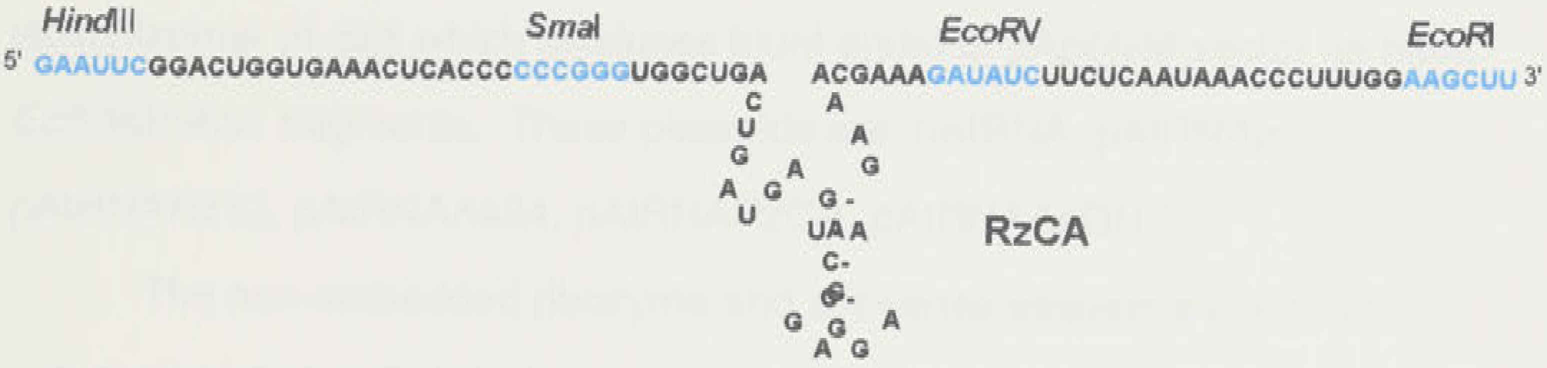
HindIII
SmaI
EcoRV
EcoRI
5' GAAUUCGGACUGGUGAAACUCACCCCCCGGGUGGCUGA ACGAAAGAUAUCUUCUCAAUAAACCCUUUGGAAGCUU 3'
RzCA

Figure 2.2d

conditions (Koizumi *et al.*, 1988a; Ruffner *et al.*, 1990a; Perriman *et al.*, 1992). This mutation maintains codon usage within the CAT open reading frame. The plasmid bearing the mutated CAT sequence is called pGCM2. A *Hind*III/*Sst*I fragment containing the CM2 insert was subcloned into like digested pApoly to make the plasmid pACM2.

2.5. Modified pApoly vector (Fig. 2.4).

The original pApoly construct contained the coat protein AUG start codon and 21 residues of the coat protein at the 5' end (Fig. 2.1a). The modified pApoly vector was produced to remove these upstream bases and used to express all tRNA and non-embedded antisense and ribozyme sequences. *BstX*I digested pApoly was treated with T4 DNA polymerase to form a blunt end. This was digested with *Sma*I and the plasmid religated to produce pApolyM (Fig. 2.4).

2.6. pApolyM expressing tRNA and non-embedded ribozyme/antisense sequences.

The six tRNA constructs were all subcloned into the *Ecl*136II site (an isoschizomer of *Sst*I which produces blunt ends) of pApolyM vector as blunt *Ecl*136II/*Acc*I fragments. These plasmids are: pAtRNA, pAtRNAp, pAtRNARz12, pAtRNAAs24, pAtRNARzCA, pAtRNAAsGUC.

The non-embedded ribozyme and antisense sequences were also subcloned into the *Ecl136*II site of pApolyM. Rz12 was subcloned as a blunt *EcoR*I/*Pst*I fragment, As24 was a blunt *BamH*I/*SnaB*I fragment and RzCA and AsGUC were both end-filled *Hind*III/*EcoR*I fragments.

2.7. Mutant RNA polymerase II and III pAtRNARz12 constructs (Fig. 2.5).

Mutations designed to inactivate either the RNA polymerase II or RNA polymerase III promoter of the pAtRNARz12 construct were made by site directed mutagenesis (Kunkel *et al.*, 1987). Mutagenesis of the RNA

Figure 2.3: Mutagenesis of the GUC target site at position 464 (arrowed) on the CAT RNA. Boxed region shows sequence alteration from GUC to GUG to create CM2 target construct with mutated nucleotides highlighted in red. CAT initiation codon [24(AUG)], ACMV coat protein promoter (ACMV-CP [dark blue]) and termination signals (ACMV-t [yellow]) are indicated.

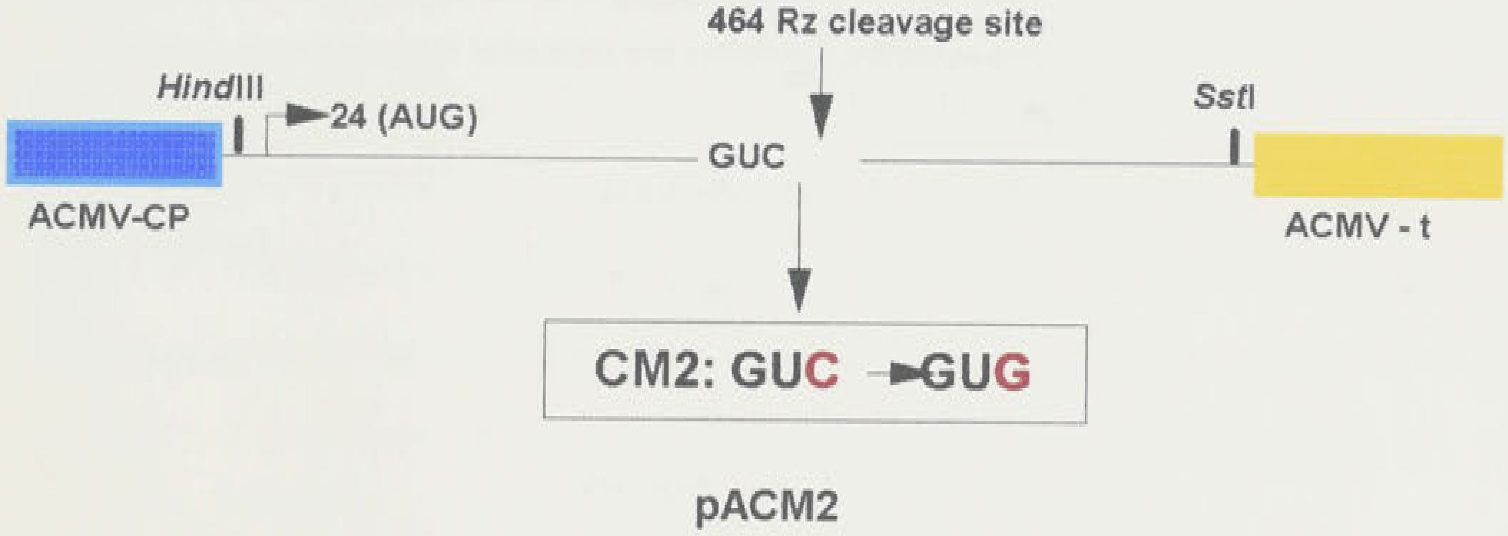
464 Rz cleavage site
*Hind*III
24 (AUG)
GUC
*Ssf*I
ACMV-CP
ACMV - t
CM2: GUC → GUG
pACM2

Figure 2.3

Figure 2.4: Construction of modified pApoly vector (pApolyM). The features of pApolyM are as for pApoly (figure 2.1a) except for the deleted 152bp region between *BstX*I - *Sma*I shown in the boxed region labelled Δ *BstX*I - *Sma*I. Within this box, the nucleotides in bold italics green represent the 5' and 3' ends of the deleted 152bp sequence. The nucleotide sequence after deletion of the 152 bp is shown to the right of the arrow within the Δ *BstX*I - *Sma*I boxed region. Restriction sites remaining within the inserted polylinker are indicated beneath the Δ *BstX*I - *Sma*I box.

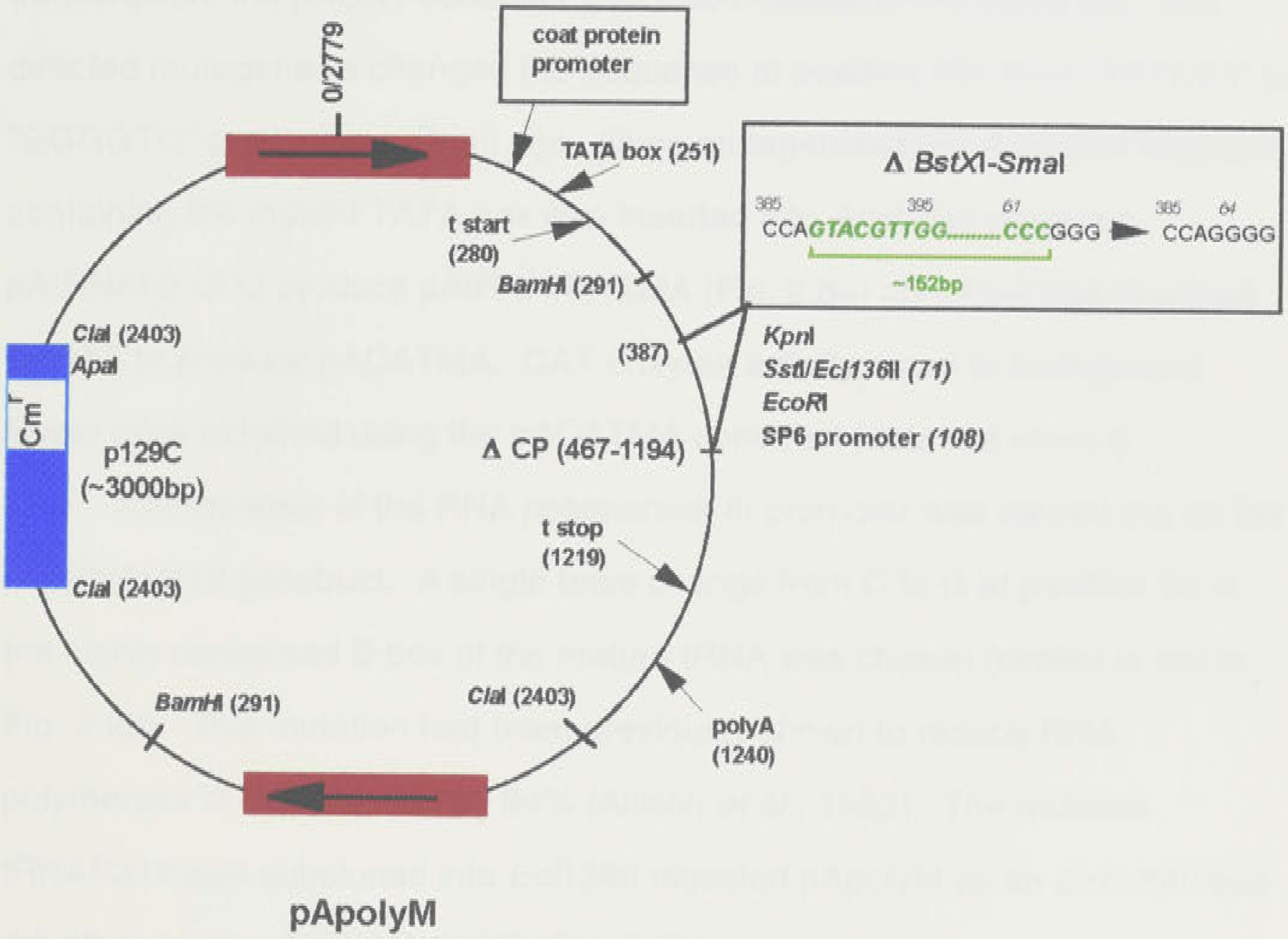
0/2779
coat protein promoter
TATA box (251)
t start (280)
BamHI (291)
(387)
Δ BstXI-SmaI
385
395
61
CCAGTACGTTGG.........CCCGGG
385
64
CCAGGGG
~152bp
KpnI
SstI/Ecl136II (71)
EcoRI
SP6 promoter (108)
ClaI (2403)
ApaI
Cm^r
p129C (~3000bp)
Δ CP (467-1194)
t stop (1219)
ClaI (2403)
BamHI (291)
ClaI (2403)
polyA (1240)
pApolyM

Figure 2.4

polymerase II promoter for the pAtRNARz12 constructs was obtained by first subcloning an *ApaI*/*SstI* fragment from pAtRNARz12 (see Fig. 2.4) into pGEM7zf+ which contains the f1 ori for single-stranded DNA production using an M13 (RK07) helper phage. This fragment contains the "TATA" box of the coat protein RNA polymerase II promoter (situated at position 251 on pApoly as shown in Fig. 2.4). To monitor the extent of the reduction in RNA polymerase II transcription, the pACAT construct was also mutated at the same site. Site directed mutagenesis changed the sequence at position 251 from "TATATA" to "GGGGTG" producing a *Dra*III site. Once mutagenised the *ApaI*/*SstI* fragment containing the mutant TATA box was inserted into *ApaI*/*SstI* digested pAtRNARz12 to produce pAtRNARz12MA (Fig. 2.5a) and *ApaI*/*SstI* digested pACAT to produce pACATMA. CAT enzyme activity equal to background levels were obtained using the pACATMA construct (data not shown).

Mutagenesis of the RNA polymerase III promoter was carried out on the pGtRNARz12 construct. A single base change from C to G at position 56 in the highly conserved B box of the mature tRNA was chosen (circled in red in Fig. 2.2b). This mutation had been previously shown to reduce RNA polymerase III transcription by 94% (Allison *et al.*, 1983). The mutated tRNARz12 was subcloned into *Ecl*136II digested pApolyM as an *Ecl*136II/*Acc*I (blunt) to make pAtRNARz12MB (Fig. 2.5b).

The double mutant, in which both promoter sequences have been inactivated was made by subcloning the *ApaI*/*SstI* fragment containing the mutant RNA polymerase II promoter into pAtRNARz12MB to produce pAtRNARz12MAB .

IN VITRO ANALYSIS

2.8 *In vitro* RNA transcription

CAT, ribozyme and antisense RNAs for the *in vitro* cleavage and splicing reactions were prepared by *in vitro* transcription using linearised plasmid DNAs. 1µg of linearised plasmid DNA was incubated with the following: 40mM Tris-

Figure 2.5

a: Mutagenesis of coat protein promoter on pAtRNARz12 construct. The tRNARz12 insert is the boxed region between *SstI*(*Ecl136*II) and *Eco*RI restriction sites. The Rz12 ribozyme insert is depicted by the triangle. A (green) and B (red) are RNA polymerase III promoter regions and the yellow box is 13 base intron. The coat protein start (pol II start) and termination (pol II termination) signals are shown as strike-through lettering to indicate their loss of function. The arrow pointing to the boxed region above the figure shows the approximate site of the sequence mutated to produce the mutant coat protein promoter (MA): TATATA at position 251-256 (shown in red italics) was changed to GGGTG creating a *Dra*III restriction site. The RNA polymerase III start (pol III start) and termination (pol III termination) signals are also shown. The distance (in bp) between the RNA polymerase II and III transcription start and termination sites are shown beneath the figure.

b: Mutagenesis of the RNA polymerase III promoter on pAtRNARz12 construct. Construct features are as outlined in **(a)** except that RNA polymerase III transcription start (pol III start) and termination (pol III termination) signals are now shown as strike-through lettering to indicate their loss of function. As for **(a)**, the arrow pointing to the boxed region above the figure shows the site of the mutation to produce the mutant RNA polymerase III promoter (MB): the C at position 56 (shown in red italics) was changed to a G as shown on the right side of the boxed nucleotides. The ψ at position 55 is a pseudouridine.

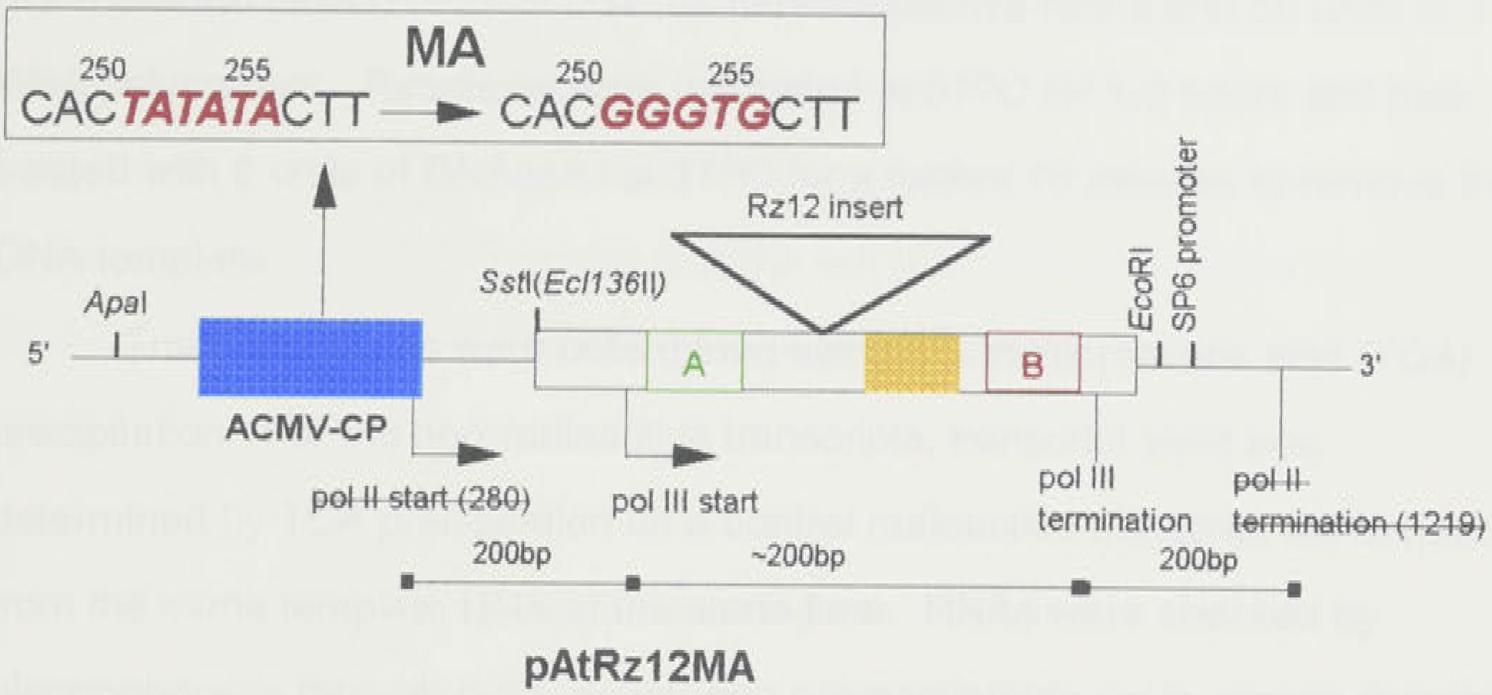
MA
250
255
CACTATATACTT
250
255
CACGGGTGCTT
Rz12 insert
Apal
SstI(Ecl136II)
EcoRI
SP6 promoter
5'
3'
A
B
ACMV-CP
pol II start (280)
pol III start
pol III termination
pol II termination (1219)
200bp
~200bp
200bp
pAtRz12MA

Figure 2.5a

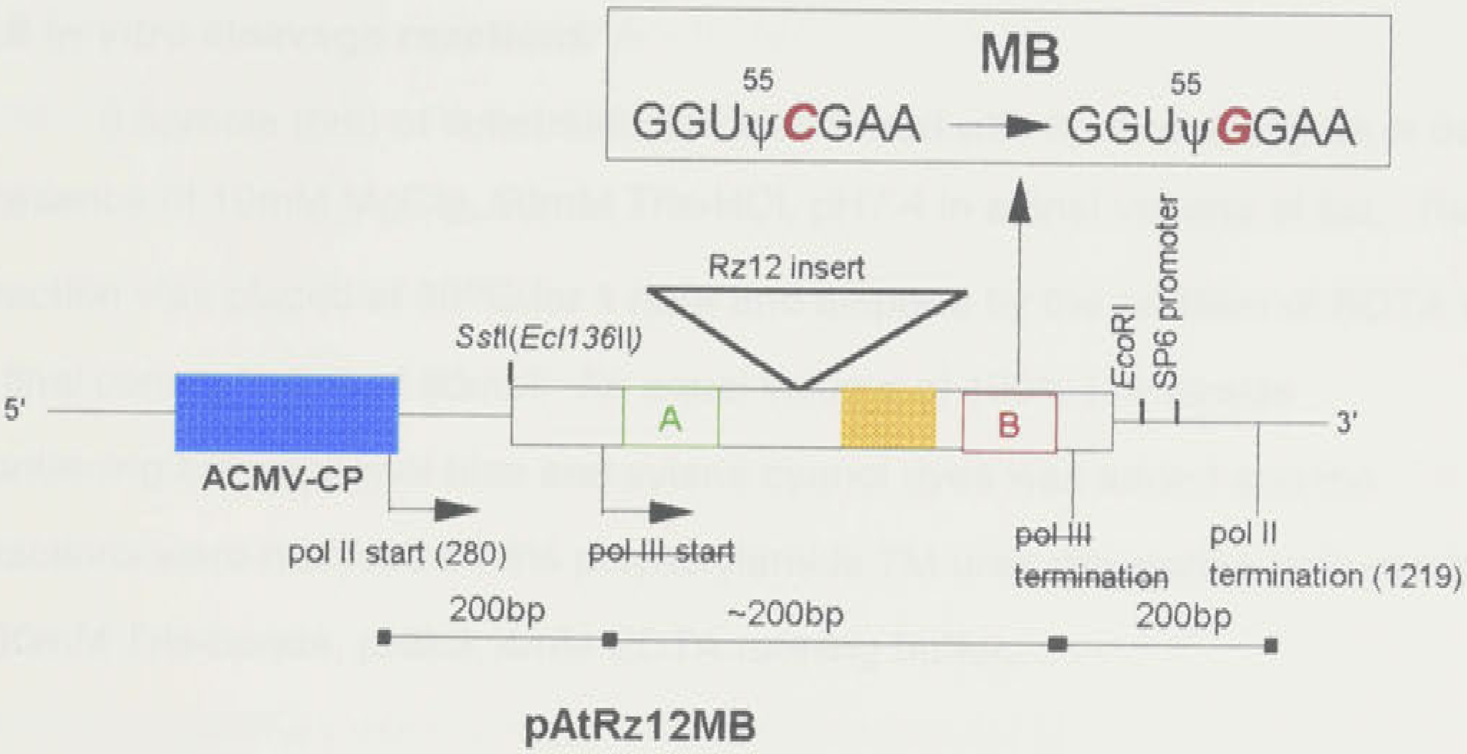
MB
55
GGUψCGAA
55
GGUψGGAA
Rz12 insert
SstI(Ecl136II)
EcoRI
SP6 promoter
5'
3'
A
B
ACMV-CP
pol II start (280)
pol III start
pol III termination
pol II termination (1219)
200bp
~200bp
200bp
pAtRz12MB

Figure 2.5b

HCl (pH 7.5), 6mM $MgCl_2$, 2mM spermidine, 10mM NaCl, 10mM DTT, 80 units RNasin, 1mM ATP, CTP and GTP and 0.25mM UTP + 60pmoles of α-^{32}P-UTP (for substrate RNAs) or 1mM UTP for non-radioactive RNAs and 50 units of T7 RNA polymerase. Reactions were incubated at 37°C for 1-2 hours and then treated with 2 units of DNAase I at 37°C for a further 15 minutes to remove the DNA template.

Transcript yields were determined using 5% trichloroacetic acid (TCA) precipitation. For the non-radioactive transcripts, transcript yield was determined by TCA precipitation on a control radioactive transcript transcribed from the same template DNA at the same time. RNAs were checked by electrophoresis through 6-8% denaturing polyacrylamide gel to ensure that the transcripts were the correct size and that yields were as determined by the TCA precipitation.

2.9 *In vitro* cleavage reactions

0.5pmole (pm) of substrate RNA was mixed with 3pm of ribozyme in the presence of 10mM $MgCl_2$, 50mM Tris-HCl, pH7.4 in a final volume of 5µl. The reaction was placed at 30°C for 1 hour and stopped by the addition of EDTA to a final concentration of 50mM. An equal volume of 100% formamide containing bromophenol blue and xylene cyanol dyes was added and the reactions were resolved on 6% polyacrylamide 7M urea denaturing gels using 180mM Tris-borate, pH8.3, 4mM EDTA running buffer.

2.10 Wheatgerm S100 extraction.

S100 wheatgerm extracts for cell free processing of the tRNA constructs (Stange & Beier, 1987) was obtained by floating 20g of crude wheatgerm in a mixture of 110ml cyclohexane + 500ml chloroform three times. The wheatgerm was dried overnight at room temperature and 5g was ground with an equal weight of acid-washed sand to a fine powder. 25ml extraction buffer (10mM Tris-acetate, pH7.6; 3mM Mg acetate; 50mM K acetate; 1mM DTT) was added and the mixture was centrifuged at 23,000 x g for 10mins. This centrifugation was repeated (after taking off supernatant and respinning) and then the resulting supernatant was spun at 100,000 x g for 2 hours. The supernatant was dialysed on ice in extraction buffer for 24 hours and then spun at 23,000 x g for 10 mins. The protein concentration was determined using a Bradford protein determination kit (Bio-rad) and the extracts were snap-frozen in liquid nitrogen and stored at -70°C. The protein concentration was approximately 24mg/ml.

2.11 tRNA^{Tyr} processing in S100 wheatgerm extracts.

Cell free processing was carried out based on the protocol described in Stange & Beier (1987). *In vitro* transcribed recombinant tRNAs were resuspended at 1µM. 2µl of the tRNA was mixed with 2µl of S100 wheatgerm extract and splicing buffer (6mM Mg acetate; 80mM spermine; 100mM K acetate; 20mM Tris-acetate, pH7.5; 15mM DTT; 0.8% Triton-X 100; 100µM CTP; 1mM ATP) in a volume of 10µl. The reactions were incubated at 30°C for 90 mins. Following this, the reaction was phenol extracted and the phenol phase back-extracted to ensure that maximum recovery of the tRNAs was obtained. The tRNAs were ethanol precipitated and resuspended in 100% formamide containing bromophenol blue and xylene cyanol loading dye. The tRNAs were analysed by electrophoresis through 8% denaturing polyacrylamide gel. Radioactive products were detected by autoradiography and then quantified using a Phosphoimager (Molecular Dynamics).

IN VIVO EXPRESSION

2.12 (i) Protoplast isolation:

A cell culture of *Nicotiana tabacum* (*c.v. Xanthi*) was used for protoplast isolation. The cell culture was maintained by subculturing every three days. 5ml was subcultured into 50ml of supplemented liquid KCMS media (MS organics; 0.1mg kinetin/ml; 0.2mg 2-4-D/ml, 1.5mM KH_2PO_4; 0.5mg/ml each of nicotinic acid, pyroxidine and thiamine; 100μg cefotaxime/ml; 2.5μg amphotericin/ml). Protoplast isolation was always carried out three days after subculture. 10-20ml of the 3 day old culture was spun down at 100 x g for 10 mins and resuspended in enzyme mix (1% cellulysin (Calbiochem); 1% Driselase (Sigma); 1% macerozyme (Yakult-Onzaka) in an equal ratio of ASW (311mM NaCl; 6.9mM KCl; 18.8mM $MgSO_4$; 16.7mM $MgCl_2$; 6.8mM $CaCl_2$; 1.75mM $NaHCO_3$; 10mM MES, pH 6.0) and 0.6mM mannitol (i.e. ASWM). The suspension was transferred to deep Petri dishes and rocked gently at 30°C for three hours (dark) with protoplast release assayed by analysis under an inverted microscope. Usually >80% cells were present as single protoplasts after a three hour incubation. Protoplasts were filtered through 150 micron mesh to isolate single cells, an equal volume of ASW was added and the cells were spun down at 100 x g for 10 mins. Cells were washed twice in 20ml of ASWM and spun at 100 x g for 10 minutes between each wash. After the second wash cells were resuspended in 20ml of ASWM and 50μl spotted on a haemocytometer for counting. Cell concentration was determined and the cells were spun down at 100 x g and resuspended in Zap media (10mM HEPES; 10mM NaCl; 120mM KCl; 4mM $CaCl_2$; 200mM mannitol, pH 7.2) at a concentration of 1.2×10^6 cells/ml.

(ii) Transfection

700μl aliquots of protoplasts were used per transfection. Transfection was obtained by electroporation using a Hoefer PG200 progenitor II. Each electroporation involved the co-electroporation of 5μg of the target construct with 15μg of either a control, antisense or ribozyme construct so that each event involved the same amount of input DNA. Each construct pairing was repeated a minimum of three times for each protoplast isolation. The conditions used for electroporation were 490μF capacitance, 330volts, single 8msec pulse with the electrodes in the electroporation chamber separated by 0.4mm. Following electroporation, cells were transferred to culture dishes and incubated in 3ml growth media (5% coconut water, 95% KCMS, 265mM mannitol; 100µg cefotaxime/ml; 2.5µg amphotericin/ml) at 26°C for 1-8 days. Cells were harvested and assayed for CAT activity, ACMV DNA replication and mRNA/tRNA^{Tyr} levels.

Cells were harvested by transferring to sterile 15ml Corex^{Tm} tubes and spinning down at 100 x g for 10 mins. Generally 200µl of the growing culture were snap-frozen for CAT assays and the remainder was used to isolate DNA and/or RNA. DNA and RNA were always isolated from fresh unfrozen cells.

(iii) CAT assays on transiently expressing cells

After pelleting, the cells were resuspended in 200µl of 0.25M Tris-HCl (pH 7.4) before being transferred into 1.5ml Eppendorf tubes. The cells were sonicated and extracts centrifuged at 14,000 x g for 10 mins at 4°C to remove cell debris. Protein concentrations were determined using a Bradford assay kit (Bio-rad). Equivalent amounts of protein for each extract were incubated at 37°C for 1.5 hours in the presence of 5µl of 10mM acetyl-coenzyme A and 18pmol of ^{14}C chloramphenicol. Reactions were stopped by the addition of 700µl of ethyl acetate. The ethyl acetate phase was extracted, dried and resuspended in 10µl of ethyl acetate for separation on silica gel thin-layer chromatography in 5% methanol and 95% chloroform. Radioactive products were detected by autoradiography and then quantified using an AMBIS Image Acquisition analyser to determine the proportion of ^{14}C chloramphenicol that had been acetylated. The average rates of acetylation were plotted using Lotus Freelance graphics.

(iv) DNA isolation from transiently expressing cells

Cells were collected as for the CAT assays and resuspended in 200µl TE. An equal volume of 2 x SDS extraction buffer (0.1mM Tris, pH 7.4; 2mM EDTA; 2% SDS) was added and the solution mixed. Proteinase K was added to 100µg/ml and the solution incubated at 37°C for 30 minutes. Following this, samples were extracted with equal volumes of phenol/chloroform and then nucleic acids precipitated in ethanol/sodium acetate. Nucleic acid samples were treated with 10µg of RNaseA to remove contaminating RNA prior to restriction enzyme digestion. DNAs were suspended at a concentration of 0.5mg/ml. 1-2µg of total DNA was digested with either *Dpn*I or *Mbo*I and analysed by Southern hybridisation.

(v) Southern blotting

Following digestion, DNAs were electrophoresed through 1-2% agarose (depending on the size of the fragment being analysed) containing 0.5µg/ml ethidium bromide. DNA bands were visualised under UV light and photographed. DNA was denatured in 1.5M NaCl; 0.5M NaOH for 40 mins, rinsed in H_20 and neutralised in 1.5M NaCl;1M Tris-HCl, pH 8.3. Transfer of the digested DNAs to Hybond N+ membrane was obtained in 10 x SSC (1 x SSC - 150 mM NaCl; 15mM Na_3 citrate, pH 7.0) and the wick method of transfer (Sambrook *et al.*, 1989). Following transfer the DNAs were fixed to the membrane by UV crosslinking at 1200 mjoules for 100 secs and briefly rinsed in 2 x SSC prior to prehybridisation. Prehybridisation and hybridisation was carried out at 42°C in hybridisation buffer (7% SDS; 0.25mM NaH_2PO_4; 50% formamide; 1mM EDTA; 0.25M NaCl). Radioactive DNA probes were made using an Amersham multiprime kit by incorporating α-^{32}P-dCTP and using agarose gel-isolated DNA fragments of the desired sequence as templates. Following overnight hybridisation the blots were rinsed in 2 x SSC;0.1% SDS and then washed in 25mM NaH_2PO_4; 1mM EDTA; 1% SDS at 60°C for 2 x 20 minutes. Bands were visualised by autoradiography and aligned with the photographed gel for interpretation.

(vi) RNA isolation from transiently expressing cells

Cells used for RNA isolation were pelleted as for DNA isolation. Total RNA was isolated from cells using 1ml of Trizol solution (Gibco, BRL) per 5-10 x 10^6 cells. Cells were lysed by repeated pipetting and the homogenised samples were incubated at room temperature for 5 mins. 200µl of chloroform was added and the samples mixed then incubated at room temperature for 2-3 mins. Samples were centrifuged at 12,000 x g for 15 mins at 4°C. The upper aqueous phase containing the RNA was transferred to a fresh tube and the

RNA precipitated by the addition of 0.5ml isopropanol. RNA was suspended at a final concentration of 1mg/ml and analysed by electrophoresis through non-denaturing 1% agarose.

(vii) Ribonuclease protection assays

RNase protection assays were performed according to the protocol RPAII (Ambion). 7-20μg (depending on the fragment to be protected - see results) of total RNA were used for the protection assays. A radiolabelled probe was produced by *in vitro* transcription of the antisense sequence of tRNARz12, tRNAAs24 or CAT using linearised plasmid templates as follows: 200ng linearised DNA (i.e. pAtRNARz12 or pAtRNAAs24/*Dra*I or pACAT/*Pvu*II); 1mM ATP,GTP,UTP; 50μM CTP; 5mM DTT; 1 unit RNasin (Promega); 5 x Buffer (40mM Tris-HCl, pH 8; 25mM NaCl; 8mM $MgCl_2$; 2mM spermidine); 30μCi α-^{32}P-CTP (800 Ci/mmol); 20 units SP6 RNA polymerase in a volume of 10μl. Approximately 2 x 10^5 cpm of radiolabelled probe was mixed with total RNA and incubated at 45°C overnight in hybridisation buffer (80% formamide; 100mM Na_3 citrate, pH 6.4; 300mM Na acetate, pH 6.4 and 1mM EDTA). An equal volume of digestion buffer containing RNaseT1 (100 units/ml) and RNaseA (5μg/ml) was added and the samples incubated for 30 mins at 37°C. Reactions were precipitated and resuspended in 100% formamide loading dye. Protected RNAs were resolved on 6-10% polyacrylamide gel electrophoresis and visualised by autoradiography. Assays were quantified using a Phosphoimager (Molecular Dynamics).

(viii) Reverse transcriptase-PCR (RT-PCR) of *in vivo* CAT mRNA.

The sequence of all PCR primers is shown in Fig. 2.8. First strand cDNA synthesis was carried out as follows: 5 μg total RNA and 0.5mg of oligo dT-TAG primer were incubated at 65°C for five minutes and then transferred to ice. To this were added 1st strand buffer (250mM Tris-Cl, pH 7.5; 375mM KCl; 15mM $MgCl_2$; 50mM DTT; 500mg/ml BSA); 0.5mM dNTP's, 0.5 units RNasin and 200 units Superscript reverse transcriptase (Gibco-BRL). The reaction was incubated at 45°C to minimise any effect of secondary structure on the

RNA. After 1 hour at 45°C, the RT reaction was diluted to 200μl with H_2O and 20μl used for the PCR reactions. The first strand primer was oligo dT with an 18 base unique sequence ("TAG"-Lincoln and Karrer, unpublished - Fig. 2.6 & 2.8) at the 5' end of the primer. This TAG sequence was used to prime for subsequent PCR amplifications. Dual PCR reactions were carried out on reaction samples. Primer 1 which anneals at positions 198-216 on the CAT sequence was designed to amplify full length CAT sequence (Fig. 2.6 & 2.8). Primer 2 anneals at positions 470-488, 3' of the ribozyme cleavage site and acts as a positive control for the presence of CAT RNA, cleaved or uncleaved (Fig. 2.6 & 2.8). To ensure that any reduction in accumulation of CAT RT-PCR products was not due to ribozyme cleavage during RNA extraction or cDNA synthesis, parallel RT-PCR experiments were done on mock transfected total RNA to which *in vitro* transcribed CAT +/- ribozyme were added (data not shown). Conditions were verified to be within linear range of amplification and were as follows: 52°C 2 mins, 72°C 40 mins, 30 cycles of 94°C 40 secs, 52°C 2mins, 72°C 3 mins followed by 72°C for 15 mins. Amplification was carried out using either 1 + TAG or 2 + TAG primer pairs (Fig. 2.6). 1/6 of the PCR reactions were loaded on agarose gels and southern blotted to determine the extent of amplification of the CAT sequence by the two primer pairs. Filters were analysed by autoradiography and total counts were determined using an AMBIS image acquisition analyser.

TRANSGENIC PLANT ANALYSIS

The plasmids pGtRNAAs24 and pGtRNARz12 were linearised with *Hind*III (see Fig. 2.2a) and inserted into *Hind*III digested binary vector pGA470 (obtained from Danny Llewellyn, CSIRO Division of Plant Industry). Transformation of these constructs into tobacco line,*Nicotiana tabacum* TI68, was carried out by Judy Gaudron and Rob de Feyter (CSIRO Division of Plant Industry). A homozygous TI68 plant expressing 35S promoter driven CAT, line 7-41, was obtained from Danny Llewellyn.

Figure 2.6: Method for PCR amplifying cleaved and/or uncleaved CAT mRNA isolated from *N.tabacum* plant cells and *N.tabacum* transgenic plants. For plant cells, first strand cDNA synthesis was carried out using the oligo dT-TAG primer (red). The "TAG" sequence is an 18 base unique sequence at the 5' end of the oligo dT-TAG primer which was used to prime off in subsequent PCR amplifications. Dual PCR reactions were carried out on each reaction pair. Primer 1 + TAG amplifies only uncleaved CAT mRNA. In contrast Primer 2 + TAG amplifies from both cleaved and/or uncleaved CAT mRNA. In the analysis of CAT mRNA from transgenic plants, primer 3 was used for first strand cDNA synthesis instead of the oligo-dT-TAG primer. Subsequent PCR amplifications for these reactions used primers 1 + 3 or 2 + 3. The numbers beneath primers 1, 2 and 3 indicate the priming sites on the CAT mRNA.

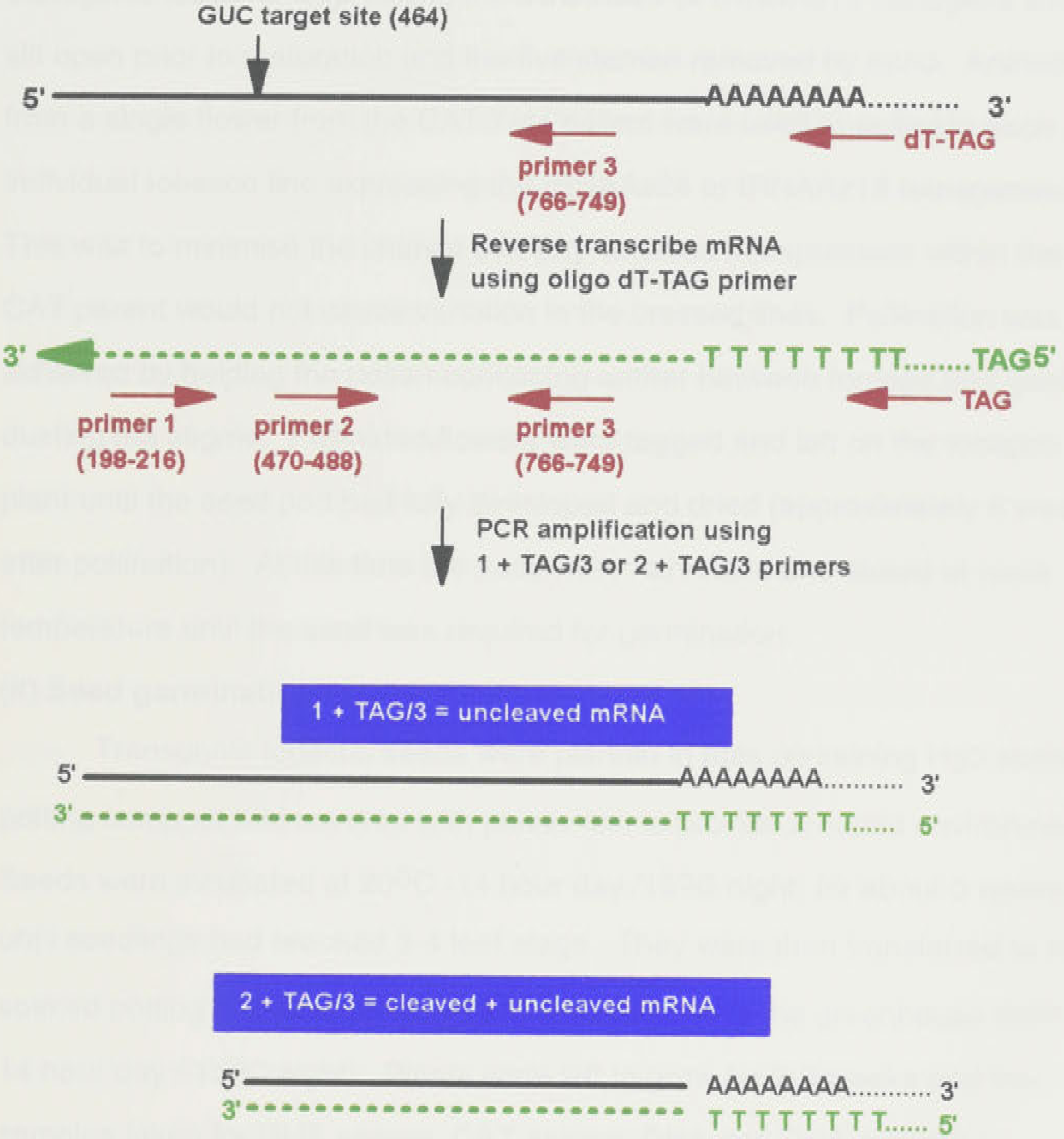
GUC target site (464)
5'
AAAAAAAA........... 3'
primer 3
(766-749)
dT-TAG
Reverse transcribe mRNA
using oligo dT-TAG primer
3'
T T T T T T TT........TAG5'
primer 1
(198-216)
primer 2
(470-488)
primer 3
(766-749)
TAG
PCR amplification using
1 + TAG/3 or 2 + TAG/3 primers
1 + TAG/3 = uncleaved mRNA
5'
AAAAAAAA........... 3'
3'
T T T T T T T T...... 5'
2 + TAG/3 = cleaved + uncleaved mRNA
5'
AAAAAAAA........... 3'
3'
T T T T T T T T...... 5'

Figure 2.6

2.13 (i) Crossing CAT and tRNAAs24 or tRNARz12 transgenic tobacco lines.

Pollen from the CAT parent line, 7-41, was used to pollinate the stigma of emasculated tobaccos containing either the tRNAAs24 or tRNARz12 transgenes. Emasculation was carried out as follows. Flowers on the transgenic tobaccos expressing the tRNAAs24 or tRNARz12 transgene were slit open prior to maturation and the five stamen removed by hand. Anthers from a single flower from the CAT 7-41 parent were used to pollinate each individual tobacco line expressing the tRNAAs24 or tRNARz12 transgenes. This was to minimise the chance that any variation in expression within the CAT parent would not cause variation in the crossed lines. Pollination was achieved by holding the pollen-containing anther between forceps and gently dusting the stigma. Pollinated flowers were tagged and left on the tobacco plant until the seed pod had fully developed and dried (approximately 6 weeks after pollination). At this time the pods were harvested and stored at room temperature until the seed was required for germination.

(ii) Seed germination

Transgenic tobacco seeds were planted in pots containing H_2O soaked potting compost and covered with plastic film to provide a humid environment. Seeds were incubated at 20°C -14 hour day /15°C night for about 3 weeks until seedlings had reached 3-4 leaf stage. They were then transferred to H_2O soaked potting compost (4 per pot) and transferred to the greenhouse (23°C - 14 hour day / 15°C night). Plants were left to grow for 2-3 weeks and then leaf samples taken for GUS assays, CAT assays, DNA and RNA extraction.

(iii) Histochemical GUS assays

GUS assays were carried out on single leaf samples from transgenic tobacco lines as follows. A leaf weighing approximately 100mg was homogenised using a Dynamax homogeniser in 200µl extraction buffer (100mM Tris-HCl, pH 6.8; 10% glycerol; 5% β-mercaptoethanol). Samples were ground by adding acid washed sand (a few grains) until homogenous. Samples were centrifuged at 14,000 rpm for 10 minutes at 4°C. 20µl of the supernate was transferred to an ELISA plate and mixed with 20µl of X-Glu solution (5mM ferricyanide; 5mM ferrocyanide; 0.3% Triton X-100; 0.1M Phosphate buffer, pH 7.0; 0.3% X-Glucuronidase). The reaction was covered and incubated at 37°C overnight.

(iv) CAT assays

A leaf piece weighing approximately 100mg was collected from each plant assayed. Every attempt was made to collect leaf samples of similar age and size to reduce any internal variation in CAT activities. 300µl of extraction buffer (0.5M sucrose; 0.25M Tris; 0.1% ascorbic acid; 0.1% cysteine-HCl) and a few grains of acid washed sand was added to each 100mg leaf sample. The samples were ground until homogenised and then centrifuged at 14,000 rpm for 10 mins at 4°C. Protein concentrations were determined using Bradford protein reagent (Bio-rad). Each CAT assay contained 60µg total protein extract. This amount of extract was determined to be within the linear range for the CAT assay. Assays were carried out as described for the transient system (see section 2.12 (iii)) except that the reactions were incubated at 37°C for 15 mins.

(v) DNA extraction

Approximately 1 gm of leaf tissue was frozen in liquid nitrogen and ground, with sand, to a fine powder in a mortar and pestle. 15ml of extraction buffer was added (100mM Tris, pH 8.0; 50mM EDTA, pH 8.0; 100mM NaCl; 1% SDS;10mM β-mercaptoethanol) and the samples incubated at 65°C for 10 mins. 5ml of K acetate was added and the extract incubated on ice for 20 mins. The samples were spun at 25,000 x g for 20 mins and the supernatant poured through Miracloth into 30 ml tubes. 10ml isopropanol and 1ml 5M NH_4 acetate was added and the DNAs precipitated at -20°C for 20 mins. The DNA was pelleted at 20,000 x g for 20 mins and the pellets washed in 70% ethanol. DNAs were dried and resuspended in 4ml H_2O. DNAs were further purified by

CsCl -ethidium bromide gradient centrifugation as follows: 3.9g CsCl and 240μl of 10mg/ml ethidium bromide was added to 4 ml of DNA solution. The samples were transferred to quick seal tubes and spun at 55,000 rpm in VTI65.2 rotor (Beckman) for 16 hours. DNAs were removed from the gradient and dialysed against three changes of H_20. Absorbance at 260nm was measured and the DNAs ethanol-precipitated and resuspended at 0.5mg/ml.

(vi) PCR analysis

10ng of total DNA from each tRNAAs24 and tRNARz12 transgenic line was analysed for the presence of tRNAAs24 and tRNARz12 transgenes by PCR. Primers t5 and t6 (Fig. 2.7a and 2.8) were specific for the amplification of the tRNAAs24 transgene. Primers t7 and t6 (Fig. 2.7b and 2.8) amplified the tRNARz12 transgene. Conditions of the PCR reactions were: (94°C 1'; 52°C 2'; 72°C 3') x 25 cycles. PCR reactions were electrophoresed through 2% agarose containing 0.5μg/ml ethidium bromide in 1xTBE buffer. DNAs were transferred to Hybond N+ and southern blotted to ensure the amplified sequence was the tRNA transgene. Transfer and southern hybridisation techniques were as described in 2.12 (v).

(vii) RNA extraction

Total RNA extractions were carried out as described for the transient system (see section 2.12(vi)) except for the following: 100mg of leaf tissue was ground in 1ml of Trizol reagent. Due to the high concentration of polysaccharides in the leaf tissue, it was necessary to centrifuge the samples at 14,000 rpm for 10 mins prior to the addition of chloroform. The supernatant was transferred to a new tube and the chloroform added to the clarified sample. RNAs were treated with 4 units of DNAase I by incubating at 37°C for 30 mins in the presence of 5mM Tris.HCl, pH 8.0; 5mM NaCl; 1mM $MgCl_2$; 10mM DTT; 50 units RNasin. This was followed by phenol:chloroform-isoamyl alcohol (24:24:1) extraction and 2.7M LiCl precipitation. Finally, the RNAs were precipitated with ethanol/sodium acetate and resuspended at a concentration of 1mg/ml.

Figure 2.7

a: Primers t6 and t5 positions for PCR analysis of tRNAAs24 transgene and transcript in *N.tabacum* transgenic plants. The horizontal arrows show 5' to 3' direction for each primer; the left hand arrow shows start of RNA polymerase III $tRNA^{Tyr}$ transcript. Numbers in bold are sites on the complete tRNA sequence (i.e including 5' and 3' flanking sequences) derived from the T7 promoter, while numbers in italics represent the same sites on the $tRNA^{Tyr}$ transcript derived from the RNA polymerase III promoter (see also Fig. 2.2b). A (green), B (red) and yellow box are as described in Fig. 2.2a and 2.5. The vertical arrow shows position of As24 insertion (see also Fig. 2.2a).

b: Primers t7 and t5 positions for PCR analysis of tRNARz12 transgene and transcript in *N.tabacum* transgenic plants. Numbers and arrows are as for $tRNA^{Tyr}$ and tRNAAs24; note that primer t5 is situated 21 bp further 3' than on tRNAAs24 although this primes off the same region of the tRNA. This is because the Rz12 insert is 21bp larger than the As24 insert.

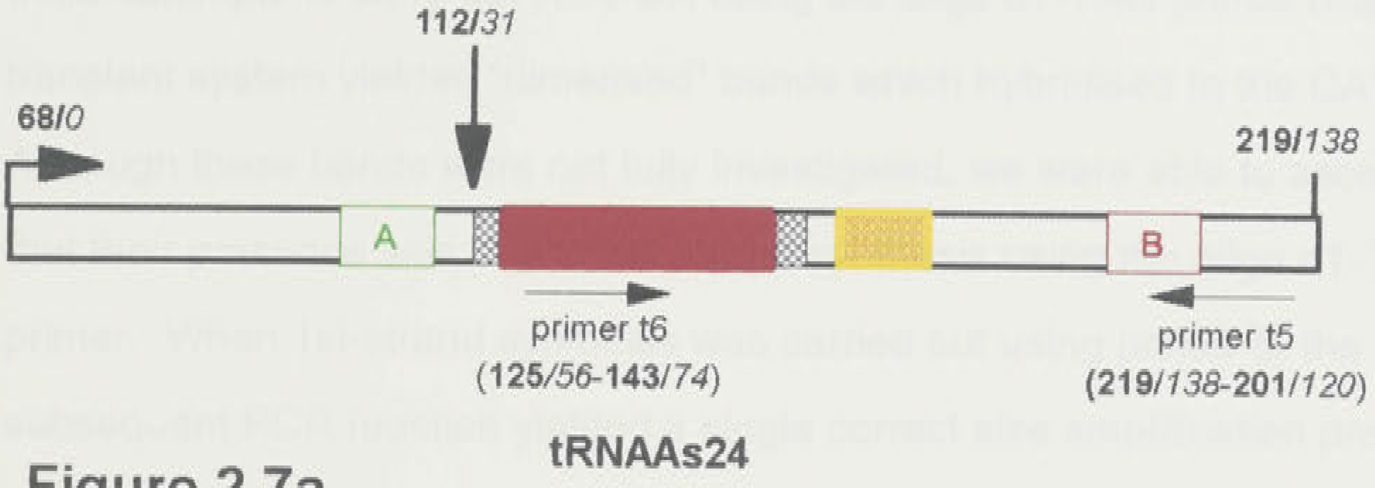
112/31
68/0
219/138
A
B
primer t6
(125/56-143/74)
primer t5
(219/138-201/120)
tRNAAs24

Figure 2.7a

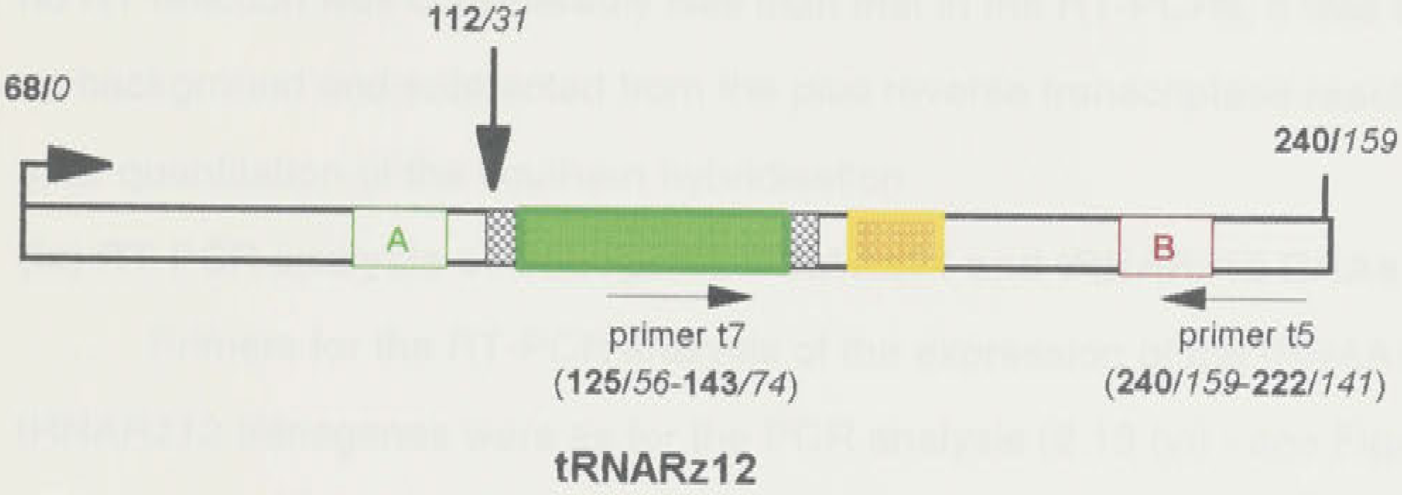
112/31
68/0
240/159
A
B
primer t7
(125/56-143/74)
primer t5
(240/159-222/141)
tRNARz12

Figure 2.7b

(viii) RT-PCR analysis of transgenic CAT mRNA

RT-PCR analysis of CAT mRNA was carried out as for the transient system except for the following: 1µg of total RNA was used for 1st strand cDNA reactions. 1st strand cDNA reactions were carried out using primer 3 (Fig. 2.6 & 2.8). This primer annealed at positions 766 - 749 on the CAT sequence. Initial attempts to carry out RT-PCR using the oligo dT-TAG primer used in the transient system yielded "dimerised" bands which hybridised to the CAT probe. Although these bands were not fully investigated, we were able to ascertain that their presence was due to 1st strand synthesis using the oligo dT-TAG primer. When 1st-strand synthesis was carried out using primer 3, the subsequent PCR reaction yielded a single correct size amplification product. As primer 3 was an internal primer (and therefore could also anneal to any contaminating DNA) "no reverse transcriptase" (no RT) controls were carried out for each RT-PCR reaction. Although the RNA samples had been DNAase I treated (see RNA extraction), we still observed a small amount of amplification in the no RT reactions suggesting that contaminating DNA was still present in our total RNA samples. Since the amplification product corresponding to the no RT reaction was considerably less than that in the RT-PCRs, it was treated as background and subtracted from the plus reverse transcriptase reactions after quantitation of the southern hybridisation.

(ix) RT-PCR analysis of transgenic tRNAAs24 and tRNARz12 RNAs

Primers for the RT-PCR analysis of the expression of the tRNAAs24 and tRNARz12 transgenes were as for the PCR analysis (2.13 (vi) - see Figs. 2.7 & 2.8). To enable the specific amplification of the tRNAAs24 and tRNARz12 RNAs, in the presence of the endogenous $tRNA^{Tyr}$, primers t6 (As24 see Fig. 2.7a) and t7 (Rz12 - see Fig. 2.7b) were used. RT-PCR for the tRNA transgenes was carried out as for the CAT mRNA (2.13 (viii)). The sequence of all tRNA primers is shown in Fig. 2.8. The priming position for t5 includes the 13 base intron since this sequence is not removed from the tRNAAs24 and tRNARz12 transcripts during processing.

Figure 2.8: Sequence of all primers used for CAT and tRNA PCR and RT-PCR analysis. See sections 2.12 (viii), 2.13 (vi), (viii) and (ix) and Figures 2.6 and 2.7 for specific details of use.

Primers for CAT and tRNA PCR & RT-PCR analysis

Primer 1
5' CCGGCCTTTATTCACATT 3'

Primer 2
5' CCAATCCCTGGGTGAGTTTC 3'

Primer 3
5' GCCATTCATCCGCTTATT 3'

oligo dT-TAG
5' GGGCGAATTCTAGGGATCCTT
TTTTTTTTTTTTTTTTTTTTTTGG 3'

TAG
5' GGGCGAATTCTAGGGATCC 3'

Primer t4
5' CAGTTGGTAGAGCGGAGG 3'

Primer t5
5' ATCCGACCTACCGGATTCG 3'

Primer t6
5' GGGATTGGCTGAACGAA 3'

Primer t7
5' GGGATTGGCTGACTGATG 3'

Figure 2.8

CHAPTER 3

ENHANCED *IN VIVO* EXPRESSION OF LONG RIBOZYME, ANTISENSE AND CAT TARGET SEQUENCES USING A SELF-REPLICATING VIRAL-BASED VECTOR.

INTRODUCTION

Three aspects of intracellular expression are important in the design of hammerhead ribozymes for their successful delivery to cells. These include the stability, concentration and intracellular location of both the ribozyme and substrate RNAs. One method for increasing the stability of the ribozyme transcript is to incorporate it within a long antisense sequence (Heinrich *et al.*, 1993; Homann *et al.*, 1993; Perriman *et al.*, 1993; Cameron and Jennings, 1994). We have previously shown that a long antisense with four hammerhead domains targeting CAT mRNA, can reduce CAT activity in plant cells by up to 54%. The analogous antisense sequence reduced CAT activity by 24%. To obtain this level of suppression, the ribozyme containing plasmid was delivered in 360 fold excess over the target expressing plasmid, indicating the need for high concentrations of the ribozyme molecule (Perriman *et al.*, 1993). A similar level of CAT gene reduction has been obtained in animal cells using the same ribozyme sequence (Cameron and Jennings, 1994).

The aim of the present study was to establish a system in which ribozyme-antisense gene expression could be increased without increasing the amount of ribozyme containing plasmid delivered to the cell. The approach chosen was a transient system in which the ribozyme-antisense (RzCAT), chloramphenicol acetyl transferase (CAT) target and control antisense (AsCAT) sequences were expressed from a self-replicating vector based on the plant virus, African cassava mosaic virus (ACMV).

ACMV (Stanley, 1983) is a bipartite ssDNA virus which is a member of the geminivirus group (see Stanley, 1993 for review). Of these two DNA components, DNA A can replicate autonomously and assemble virus particles in the absence of DNA B which is required for both cell-to-cell spread and symptom production. Thus, in a protoplast system, DNA A can be maintained without the presence of DNA B, and has been effectively developed as an independent, self-replicating vector (Ward *et al.*, 1988).

Geminiviruses have been shown to replicate to high levels within the nucleus of dividing plant cells (Harrison, 1985; Timmermans *et al.*, 1992). Replication of ACMV is tightly linked to the cells replication cycle (Accotto *et al.*, 1993), therefore the advantages of using geminivirus-based vectors over a non-replicating approach include high level and prolonged expression of incorporated sequences. A 60-fold increase in expression level obtained from geminiviruses has been reported by Brough *et al.* (1992a) who assayed gene expression from replicating and non-replicating derivatives of another bipartite geminivirus, tomato golden mosaic virus (TGMV). This suggests that ribozyme or antisense sequences expressed in a geminivirus vector could be enhanced several fold over that obtained from the non-replicating vectors.

The development of the ACMV viral vectors was dependent on the characterisation of a coat protein deficient mutant of ACMV A which did not affect replication or viral spread in plants (Stanley and Townsend, 1986). A 727bp deletion, which removed most of the coat protein gene, was infectious when replaced with the CAT gene (Ward *et al.*, 1988). In addition, high levels of CAT expression were detected, thus displaying the efficacy of ACMV A as an autonomously replicating vector for expressing foreign gene sequences in plant cells.

The experiments outlined in this chapter were designed to evaluate the efficacy of expressing the RzCAT construct from an ACMV A self-replicating vector. This was done by replacing the coat protein sequence of ACMV A with a pUC19-derived polylinker (see materials and methods; Fig. 2.1a). CAT target, RzCAT and AsCAT sequences were then sub-cloned into this region and expressed using the endogenous RNA polymerase II coat protein promoter and polyadenylation signals (see Fig. 2.1b & c).

RESULTS

In vitro cleavage assays of the RzCAT ribozyme used in this study were published in Perriman *et al.* (1993). These results showed that, when this ribozyme was present in a 6-fold molar excess over the CAT target, the $t_{1/2}$ (i.e. the time required for half of the available substrate to be cleaved) was 18 minutes at 37°C. When expressed in a 360-fold excess in the transient system, CaMV35S driven RzCAT (35SRzCAT) was able to reduce CAT activity by up to 52%; 30% more than that observed for the analogous AsCAT (35SAsCAT) construct.

To determine if the self-replicating ACMV vector could increase and prolong gene expression, CAT activity was compared from either non-replicating 35SCAT or replicating ACMVCAT constructs (see Fig. 2.1b).

3.1 Comparison of CAT activities from pJ35SCATN and pACAT vectors

Nicotiana tabacum protoplasts were electroporated with 5μg of either pACAT or pJ35SCATN constructs. Aliquots were removed at 1, 3, 5 and 8 days post transfection and assayed for relative CAT activities. Across three independent experiments pACAT expression increased 30 fold from 1 to 3 days and maintained this level of expression to the final time point of 8 days. In contrast, pJ35SCATN expression was maximum at 1 day, halved by three days and equivalent to background levels at 5 and 8 days (Fig. 3.1). A comparison of CAT activities when both constructs were showing maximum expression, i.e. pJ35SCATN at 1 day and pACAT at 5 days, showed that expression from the pACAT vector was approximately 19-fold greater than that from the pJ35SCATN construct. Thus, the pACAT vector was able to confer a 19-fold increase in CAT expression levels, and to maintain this level of expression for up to 8 days post transfection.

Figure 3.1: Time course of CAT activities from pJ35SCAT and pACAT constructs. Relative % acetylations (y) are plotted against days post transfection (x). The table shows mean and standard errors for the two constructs at 1 (red), 3 (yellow), 5 (white) and 8 (blue) days after transfection into *N.tabacum* plant cells.

Figure 3.2: Example of replication of ACMVCAT constructs *in vivo.* Southern blot analysis of pACAT DNA isolated from *N.tabacum* plant cells 0, 1, 3, 5 and 8 days post transfection. The blot, probed with radiolabelled CAT sequence, shows *Dpn*I and *Mbo*I digestion for each time point. The lanes labelled 1-10 represent the following for pACAT analysis: lane **1**, 1 day *Dpn*I; lane **2**, as for lane 1 but *Mbo*I; lane **3**, 3 day *Dpn*I; lane **4**, as for lane 3 but *Mbo*I; lane **5**, 5 day *Dpn*I; lane **6**, as for lane 5 but *Mbo*I; lane **7**, 8 day *Dpn*I; lane **8**, as for lane 7 but *Mbo*I; lane **9**, plasmid pACAT *Dpn*I; lane **10**, as for lane 9 but *Mbo*I. The DNA products of digestion by restriction endonucleases are: **CAT 1**, bacterial gene for chloramphenicol resistance from pACAT construct, this fragment is lost as ACMVCAT replicates and accumulates (see Fig. 2.1a and section 2.1 for further details); **CAT 2**, CAT target sequence insert; **HMW**, undigested pACAT sequence.

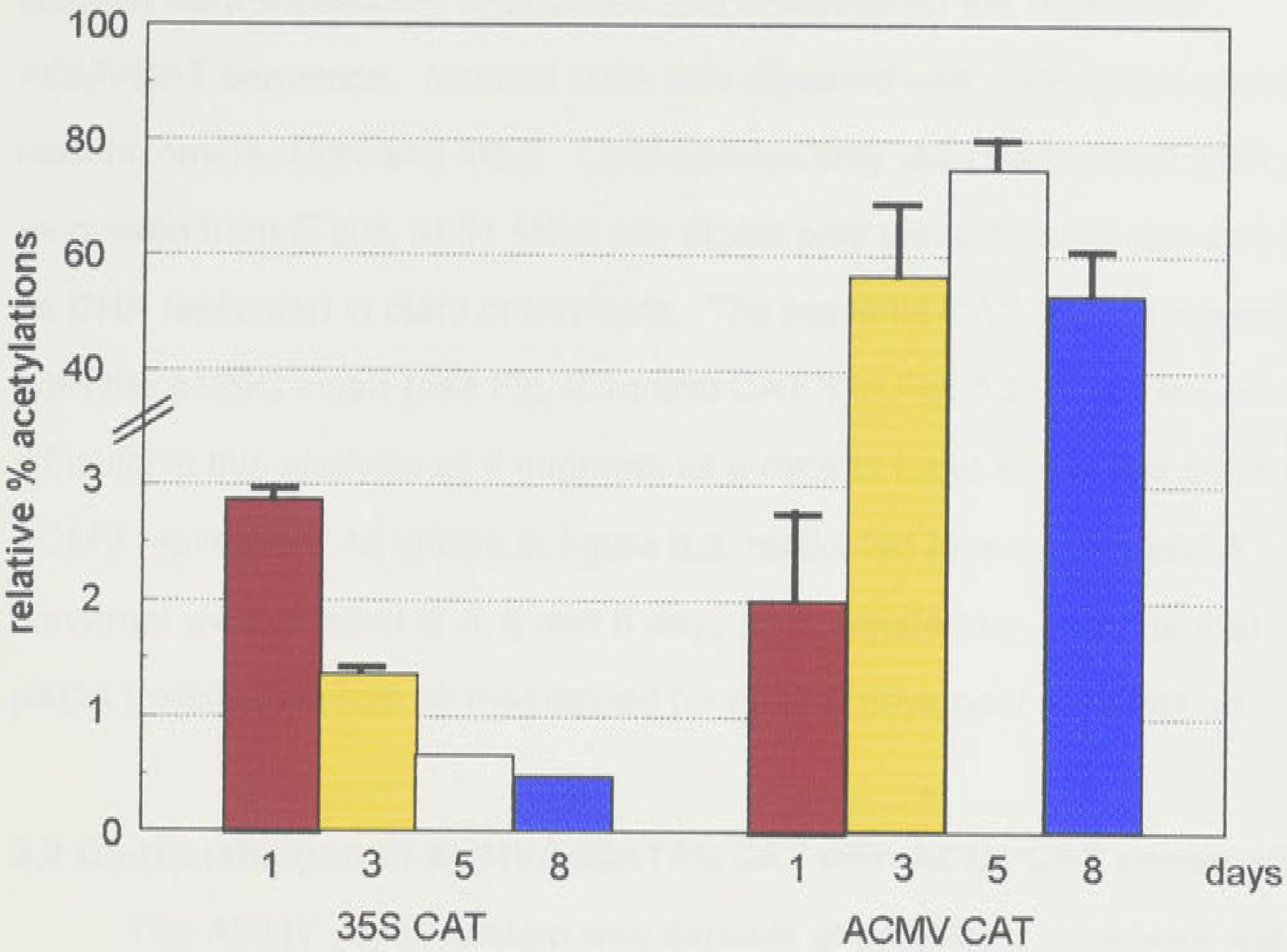

Figure 3.1

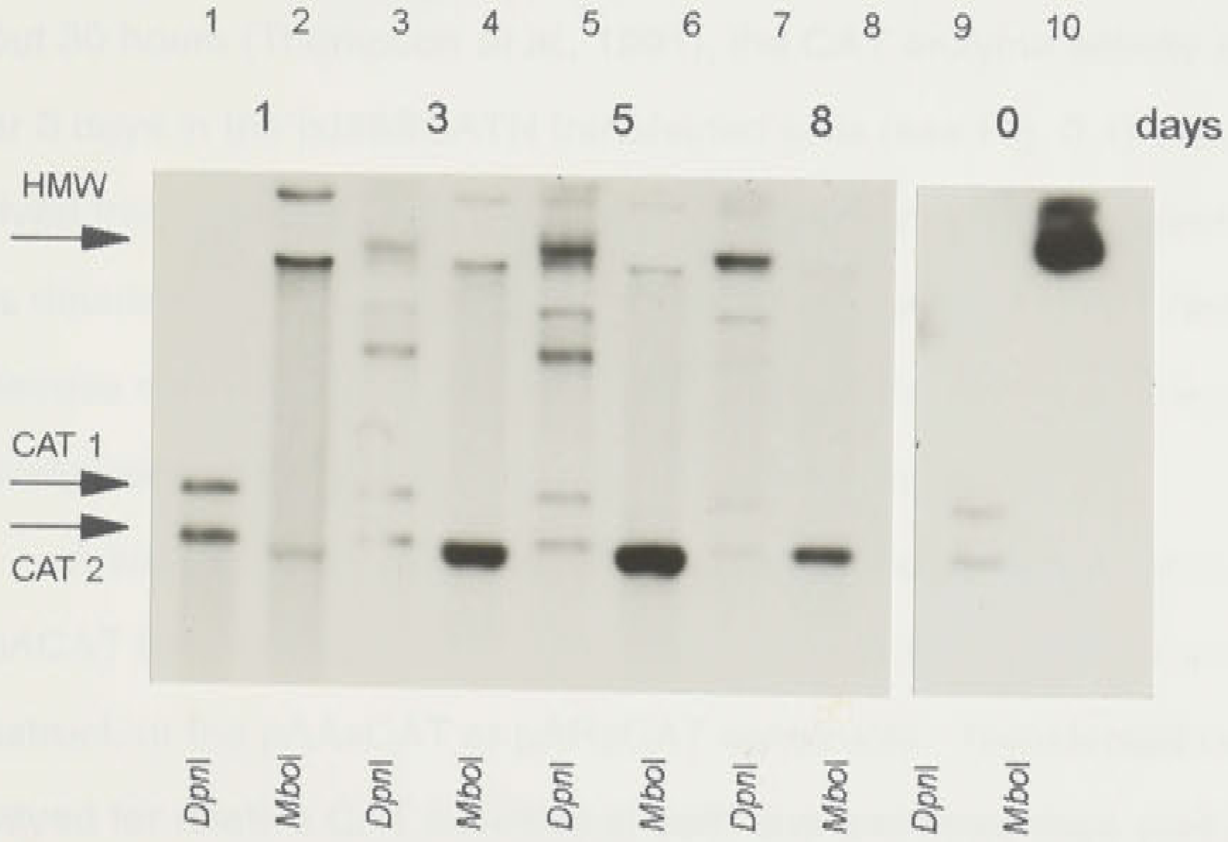
1
2
3
4
5
6
7
8
9
10
1
3
5
8
0
days
HMW
CAT 1
CAT 2
DpnI
MboI
DpnI
MboI
DpnI
MboI
DpnI
MboI
DpnI
MboI

Figure 3.2

As further evidence of autonomous replication of pACAT, DNA was isolated from transfected protoplasts and analysed for the replicated ACMVCAT sequence. Isolated DNA was digested with methylation sensitive isoschizomers, *Dpn*I and *Mbo*I. *Dpn*I cleaves only *dam* methylated DNA, as recovered from *E.coli*, while *Mbo*I can digest only unmethylated sequence such as DNA replicated in plant protoplasts. The bacterial CAT gene, expressed from the p129C insert (see Fig. 2.1a and CAT 1 in Fig. 3.2), does not present difficulty in this analysis as it migrates as a distinct band and is lost during ACMV replication. As shown in figure 3.2, replicated forms of the pACAT construct were evident at 3, 5 and 8 days post transfection showing that pACAT replication can be maintained for up to 8 days post transfection.

3.2 Co-transfection of ACMVAsCAT/RzCAT with ACMVCAT constructs.

The ACMV vector system was capable of producing increased and extended levels of expression over that obtained with the non-replicating vector. However, the pACAT construct did not increase its expression until three days post transfection, at which point CAT activity from the pJ35SCATN construct was reduced by 50%. As CAT protein has an intracellular half-life of about 30 hours (Thompson *et al.*, 1991), the CAT enzyme activity observed after 3 days in the pJ35SCATN transfected cells (see Fig. 3.1) was probably derived from residual protein rather then newly translated CAT protein. It was thus decided to use the ACMV vector to deliver both target and ribozyme or antisense sequences. In this way the co-transfected molecules would be actively transcribing and expressing at the same time.

A series of five independent experiments were carried out in which 5μg of pACAT target was co-transfected together with 15μg of either a control construct, or the pAAsCAT or pARzCAT constructs. Transfected cells were assayed for relative CAT activities at both one and three days post transfection. There was no significant difference in the inhibition of CAT activity in the presence of the pAAsCAT or the pARzCAT constructs at either time point. At

Figure 3.3: Relative expression of CAT gene in the presence of pApoly (control - red), pAAsCAT (antisense - yellow), or pARzCAT (long ribozyme - green) in *N.tabacum* plant cells. Shown are the averaged results from 5 independent experiments assayed either 1 or 3 days post transfection. Each bar represents the mean relative % acetylation observed from 5μg of pACAT, on addition of 15 μg of either pAAsCAT antisense or pARzCAT long ribozyme, when control CAT expression is normalised at 100%. Standard errors are shown for each construct pairing at both time points. Each experiment involved at least triplicate samples of each of the three construct combinations: CAT + control, CAT + antisense, and CAT + long ribozyme.

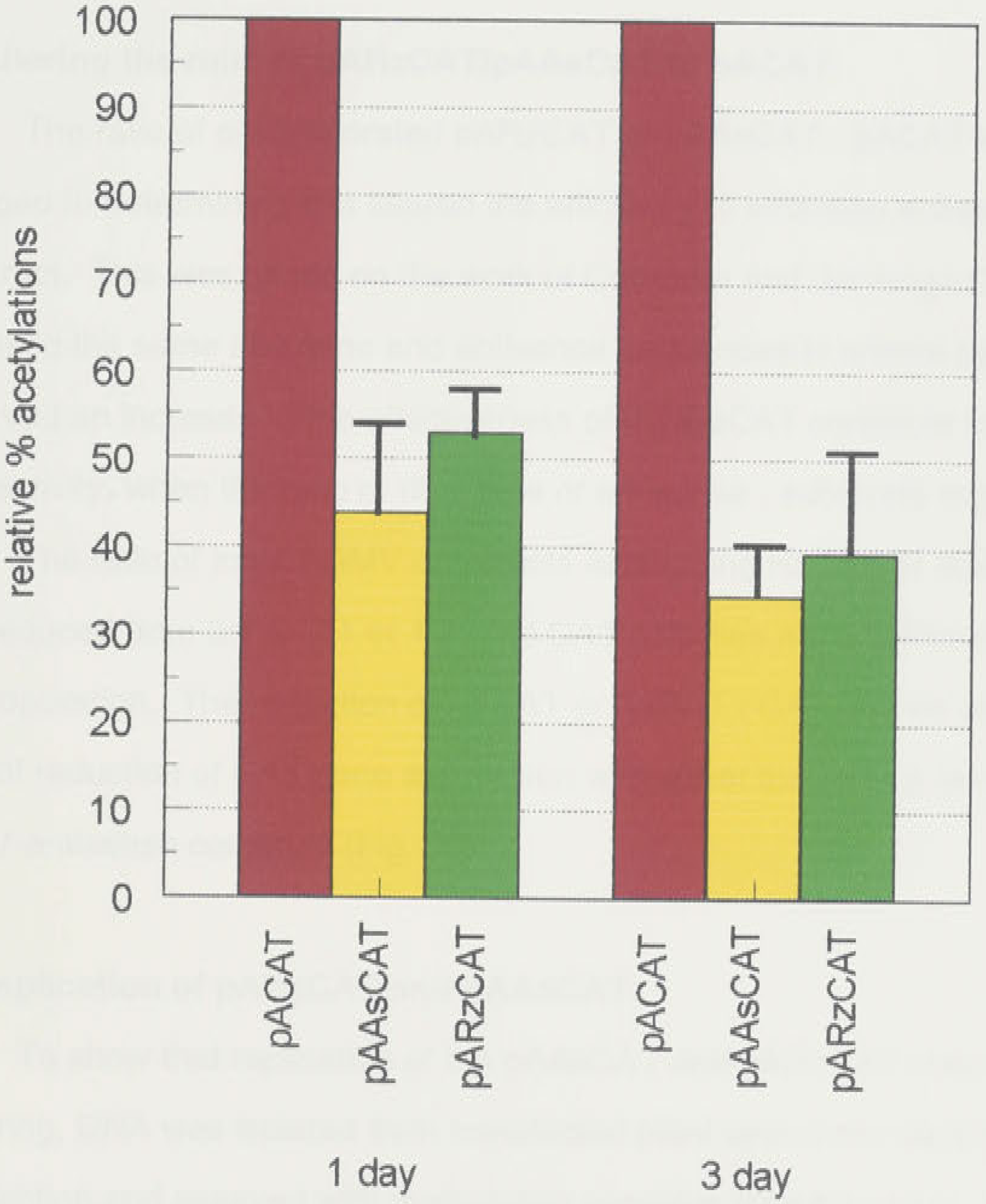
relative % acetylations
100
90
80
70
60
50
40
30
20
10
0
pACAT
pAAsCAT
pARzCAT
pACAT
pAAsCAT
pARzCAT
1 day
3 day

Figure 3.3

one day post transfection, both constructs reduced CAT activity to around 50% of control values while by three days CAT activity had further decreased to 35% of control values (Fig. 3.3). Analysis of co-transfected protoplasts at five days post transfection showed that the 35% level of reduction was maintained (data not shown).

3.3 Altering the ratio of pARzCAT/pAAsCAT to pACAT.

The ratio of electroporated pARzCAT or pAAsCAT : pACAT was changed to determine if this altered the efficiency of inhibition induced by either construct. This was based on the work of Cameron and Jennings (1994) who had used the same ribozyme and antisense sequences in animal cells. They observed an increase in the effectiveness of the RzCAT construct in reducing CAT activity, when the ratio of ribozyme or antisense : substrate was reduced.

The ratio of input ACMV constructs expressing RzCAT or AsCAT : CAT was reduced from 3:1 to 2:1 or 1:1, and CAT activities assayed three days post electroporation. The reduction of RzCAT or AsCAT : CAT had no effect on the level of reduction of CAT gene expression with either the ACMV-ribozyme or ACMV-antisense construct (Fig. 3.4).

3.4 Replication of pARzCAT and pAAsCAT.

To show that replication of the pAAsCAT and pARzCAT constructs was occurring, DNA was isolated from transfected plant cells three days post transfection and assayed with methylation sensitive isoschizomers, in an identical manner to that used to monitor pACAT replication in section 3.1. Both constructs showed *Mbo*I digestible molecules indicating that replication was occurring in both instances (Fig. 3.5). Hence, the lack of enhanced inhibition by the pARzCAT construct did not appear to be due to a lower replication level of this sequence.

Figure 3.4: Altering the ratio of pACAT : pAAsCAT antisense or pARzCAT ribozyme plasmid transfected into *N.tabacum* plant cells. As for Fig. 3.3, the relative expression of pACAT is shown in the presence of control (red), antisense (yellow) and long ribozyme (green) constructs. The amount of pACAT construct was fixed at 5 µg while the pAAsCAT and pARzCAT were reduced to either 10µg (i.e. 2 : 1) or 5 µg (i.e. 1 : 1). CAT activities were measured 3 days post transfection.

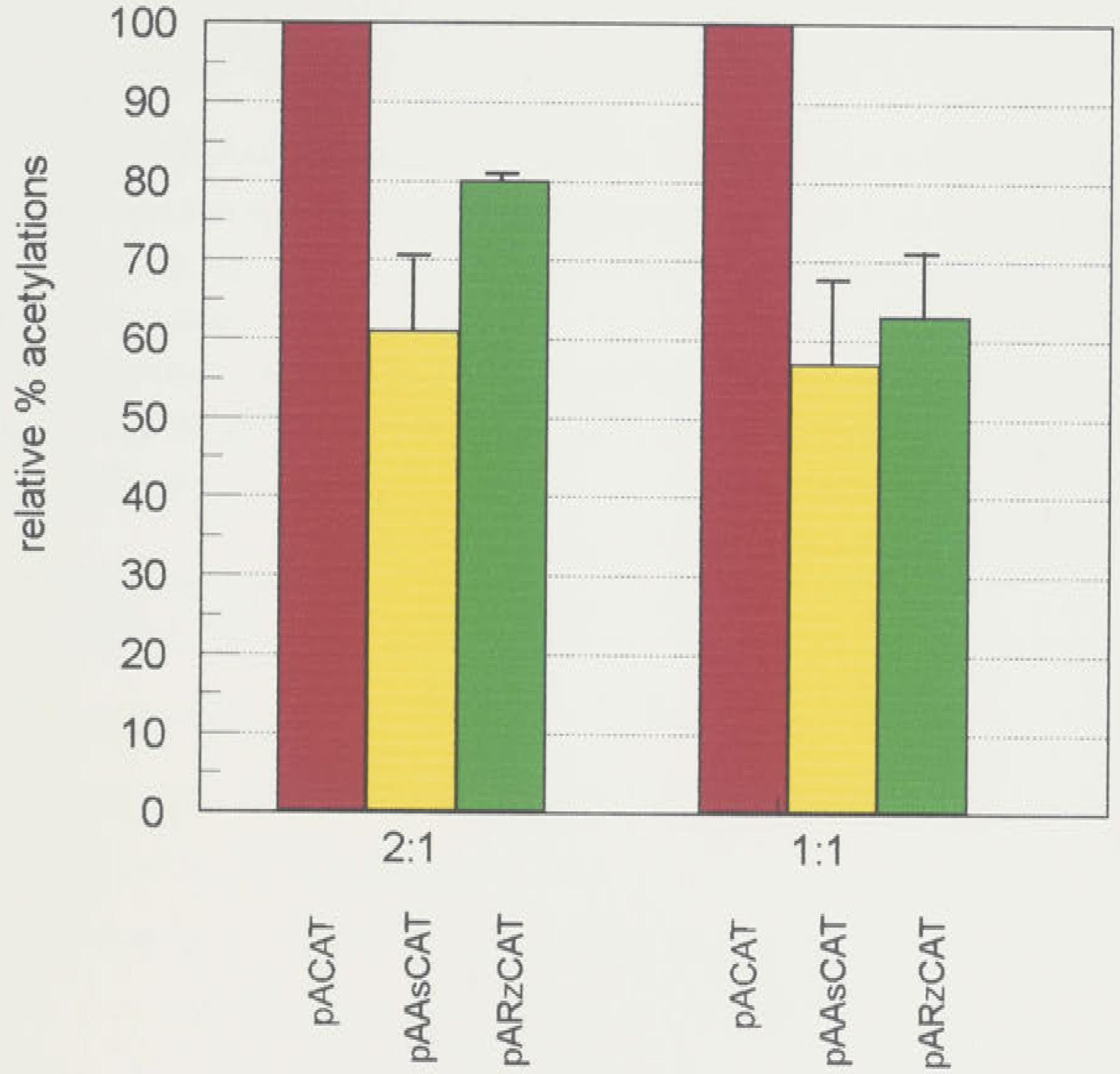
relative % acetylations
100
90
80
70
60
50
40
30
20
10
0
2:1
1:1
pACAT
pAAsCAT
pARzCAT
pACAT
pAAsCAT
pARzCAT

Figure 3.4

Figure 3.5: Examples of the replication of pAAsCAT (antisense) and pARzCAT (long ribozyme) constructs. Southern blot analysis of DNAs isolated three days post transfection. As for figure 3.2, the blots, probed with radiolabelled CAT sequence, show *Dpn*I and *Mbo*I digestion for pAAsCAT or pARzCAT transfected *N.tabacum* plant cells. The lanes labelled 1-5 represent the following: lane **1**, plasmid pAAsCAT *Dpn*I; lane **2**, pAAsCAT *Dpn*I; lane **3**, as for lane 2 but *Mbo*I; lane **4**, pARzCAT *Dpn*I; lane **5**, as for lane 4 but *Mbo*I. The DNA products are: **CAT 1**, as in figure 3.2; **RzCAT**, pARzCAT long ribozyme insert; **AsCAT**, pAAsCAT antisense insert; **HMW**, undigested pAAsCAT or pARzCAT sequence.

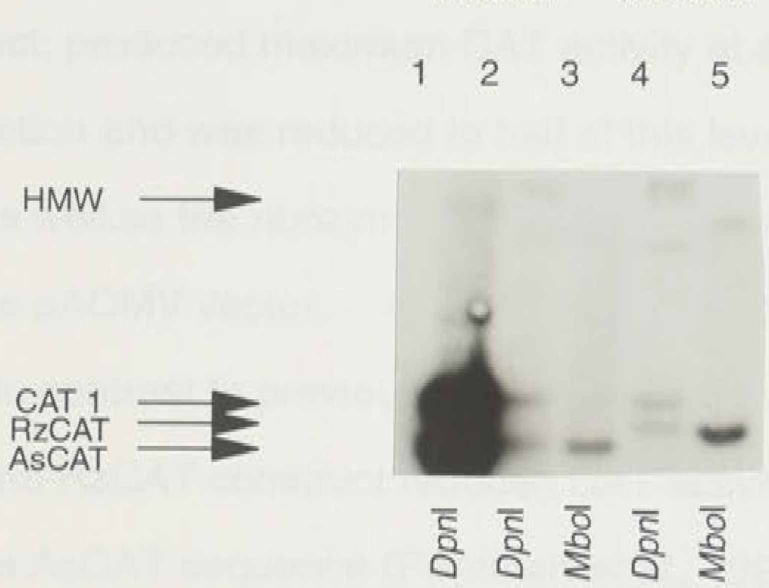
pAAsCAT
pARzCAT
1
2
3
4
5
HMW
CAT 1
RzCAT
AsCAT
DpnI
DpnI
MboI
DpnI
MboI

Figure 3.5

DISCUSSION

The results show that sequences delivered within the replicating vector, pACMV, have increased and prolonged expression in dividing plant cells. Analysis of CAT activity expressed from the coat protein promoter of the pACMV vector showed that expression was increased up to 19-fold over that obtained from a non-replicating 35S driven construct. Additionally, this high level expression was maintained for the 8 day duration of the experiment. Autonomous replication of the recombinant pACMV vector, containing the CAT open reading frame, was also observed with replicative forms of the ACMVCAT construct maintained to 8 days. In contrast, the non-replicating 35SCAT construct, produced maximum CAT activity at around 24 hours post transfection and was reduced to half of this level by three days. Consequently, CAT, as well as the ribozyme and antisense constructs, were all expressed from the pACMV vector.

In contrast to previous work using the non-replicating 35S vector, in which the RzCAT construct reduced CAT activity to a significantly greater level than the AsCAT sequence (Perriman *et al.*, 1993), the co-transfection of pARzCAT or pAAsCAT sequences with pACAT, resulted in equivalent levels of CAT gene reduction. This suggested that an antisense mechanism and not ribozyme cleavage was the primary mode of gene inactivation in the present study.

One possible explanation, which could account for the difference between the data presented here and our previous results, is the greater effectiveness of the CAT antisense to reduce CAT activity when expressed from pACMV, rather than the 35S vector. The action of the antisense RNA in the present study may have masked any apparent cleavage by the ribozyme construct.

Alternatively, the increased level of RNA transcripts from the ACMV vectors (i.e. both CAT and AsCAT or RzCAT) could affect the interactions between these mRNAs. For example, it is possible that, instead of enhancing *in vivo* ribozyme-cleavage rates, higher levels of both CAT and RzCAT transcripts within the cell could increase the probability that the two RNAs interact in various "inactive" conformations (i.e. either inter- or intramolecular) thus diminishing the chances of forming the active CAT/RzCAT hybrid (Fedor and Uhlenbeck, 1990; Heus *et al.*, 1990; van der Vlugt *et al.*, 1993). Such interactions, although not able to enhance the reduction of CAT gene expression by ribozyme mediated cleavage, could still reduce expression by blocking translation in the same way as an antisense mechanism.

Another possible explanation may lie in the different ratios of ribozyme: substrate plasmid used in each study. Using the 35S vector, a 360-fold excess of ribozyme to substrate plasmid provided conditions in which ribozyme-mediated CAT gene inhibition was greater than control antisense delivered at the same molar excess (Perriman *et al.*, 1993). In the present study, using the pACMV vector, this plasmid ratio was lowered to 3:1, 2:1 or 1:1. Under these conditions, the antisense increased in effectiveness, and both the antisense and ribozyme constructs reduced CAT activity to equivalent levels. These results are in contrast with the data of Cameron and Jennings (1994). Using the same ribozyme, antisense and target sequences in animal cells, they found that a > 10^3 excess of the RzCAT or AsCAT RNA reduced CAT activity to the same level, whereas decreasing this ribozyme/antisense : substrate ratio to ~ 4 : 1, led to an increased level of suppression by the RzCAT, compared with the AsCAT construct.

Although all three studies used the same ribozyme, antisense and target sequences, several differences do exist. The different promoter and termination signals used within each study means that the constructions contain different 5' and 3' untranslated sequences. These sequences may alter the relative transcript stabilities within each system. In addition, the different promoters probably produce different transcript levels, leading to varied RNA concentrations. These variations between systems could produce the contrasting results obtained. It is possible that to obtain ribozyme-mediated

CAT inhibition using a ribozyme of this type, specific RNA concentrations of the substrate and/or ribozyme RNAs are required. The determination of RNA levels in both animal and plant systems would help to address this. In addition, determining the RNA levels would make the comparison between the ACMV and 35S delivery mechanisms easier to interpret, since it would indicate how critical the overall transcript levels are in obtaining CAT mRNA inhibition.

To minimise the influence of antisense effects in reducing CAT activity, the following chapters describe experiments in which the pACMV vector was used to express ribozyme sequences containing much shorter helices I and III. To enhance the stability of these molecules, ribozyme and antisense sequences were embedded within a plant tyrosine-tRNA.

CHAPTER 4

IN VITRO ANALYSIS OF tRNA-EMBEDDED RIBOZYME & ANTISENSE RNAs

INTRODUCTION

The inability of the long ribozyme to enhance antisense reduction of CAT gene expression, prompted us to investigate other means of obtaining ribozyme mediated inhibition in plant cells. Two single hammerhead ribozymes, both targeting GUC-464 (see Fig. 2.1b) and containing either 24 (Rz12) or 60 (RzCA) bases of hybridisation to this region of the CAT RNA, were developed. These were designed to reduce the influence of antisense effects and possible inactive conformations of the ribozyme and target RNAs.

One potential disadvantage of short ribozyme transcripts such as these, is their intracellular instability (Cameron and Jennings, 1989). To address this aspect, the ribozymes were embedded within the anticodon loop of a tobacco tyrosine tRNA (tRNA^{Tyr}-Stange and Beier, 1986). These chimeric constructs may also provide a further means of enhancing ribozyme expression through the use of the endogenous tRNA promoter. This chapter will describe the *in vitro* analysis of these tRNA^{Tyr}-ribozymes, as well as the control tRNA-antisense sequences.

Unlike mRNAs which are transcribed by RNA polymerase II, tRNAs, as well as 5s rRNA, U6 snRNA and several other small RNAs, are transcribed by RNA polymerase III (for review see Geiduschek, 1988). RNA polymerase III transcripts contain two highly conserved sequence blocks, A and B, downstream of the transcription start site, both of which are essential for active transcription. A and B are separated by a region ranging from 31 to 93 bases for different tRNAs. Engineered A-B box separations have extended this range to 21-365 bases (Baker *et al.*, 1986; Fabrizio *et al.*, 1987), however, this separation may vary for different tRNA sequences. Thus, the ribozymes were inserted between the A and B boxes and correspond to the anticodon loop of the tobacco tRNA^{Tyr} molecule. This region of a methionine tRNA (tRNA^{Met}) had been previously adapted to successfully deliver a ribozyme to *Xenopus* oocytes (Cotten and Birnsteil, 1989) (Fig. 4.1).

As the main objective of this study was to express these recombinant tRNAs *in vivo*, one aspect of the *in vitro* assays involved the analysis of maturation of both the wildtype (i.e. the tRNA without any inserts) and recombinant tRNAs. The steps involved in the maturation of tRNAs follow a sequential series of events (Fig. 4.2). Initially, the primary tRNA transcript is processed at its 5' and 3' ends. Following this, a 5'CCA 3' triplet is ligated to the mature 3' end. In most eukaryotic tRNAs, these two steps are all that is required for the formation of a mature tRNA. However tRNA^{Tyr}, such as the tobacco tRNA^{Tyr} used in this study, contain an endogenous intron which requires an additional processing step. In these tRNAs, the intron is spliced and the two tRNA halves are religated to form a mature tRNA^{Tyr} molecule (Fig. 4.2 - van Tol *et al.*, 1987).

Complete maturation of the tRNA transcript is probably essential for export from the nucleus to the cytoplasm (Tobian *et al.,* 1985). Therefore, the loss of any one of the processing steps may be critical in determining the intracellular location of that tRNA. This could determine the types of substrate RNAs a chimeric tRNA-ribozyme could successfully target and inactivate. For example, the genome of RNA viruses, which are exclusively cytoplasmic, may not be accessible to a tRNA-ribozyme which is maintained in the nucleus. For this reason, the efficiency of each of the processing steps was analysed for both recombinant and wildtype tRNA^{Tyr} sequences. This work involved the use of a wheatgerm extract, which can accurately process and splice tobacco tRNA^{Tyr} into the mature form (Stange and Beier, 1987).

The second aspect of the *in vitro* analysis involved only the ribozyme sequences. These experiments were designed to analyse the effect that the additional tRNA^{Tyr} sequences had on the *in vitro* cleavage rates catalysed by Rz12 and RzCA ribozymes. In addition, the effect that processing of the

Figure 4.1: Sequence of tobacco tyrosine-tRNA (tRNA^{Tyr}) used to express ribozyme and antisense sequences. Nucleotides in green are the A box, red are the B box, and yellow are a 13 base intron. Nucleotides ψ at positions 35 and 55 are modified nucleotides; pseudouridines. The arrow indicates the site of insertion of ribozyme or antisense sequences within the anticodon loop. Nucleotide numbering is for the mature tRNA sequence. The boxed region labelled "D stem" indicates one of the critical regions implicated in complete maturation of pre-tRNA^{Tyr} sequences (see discussion).

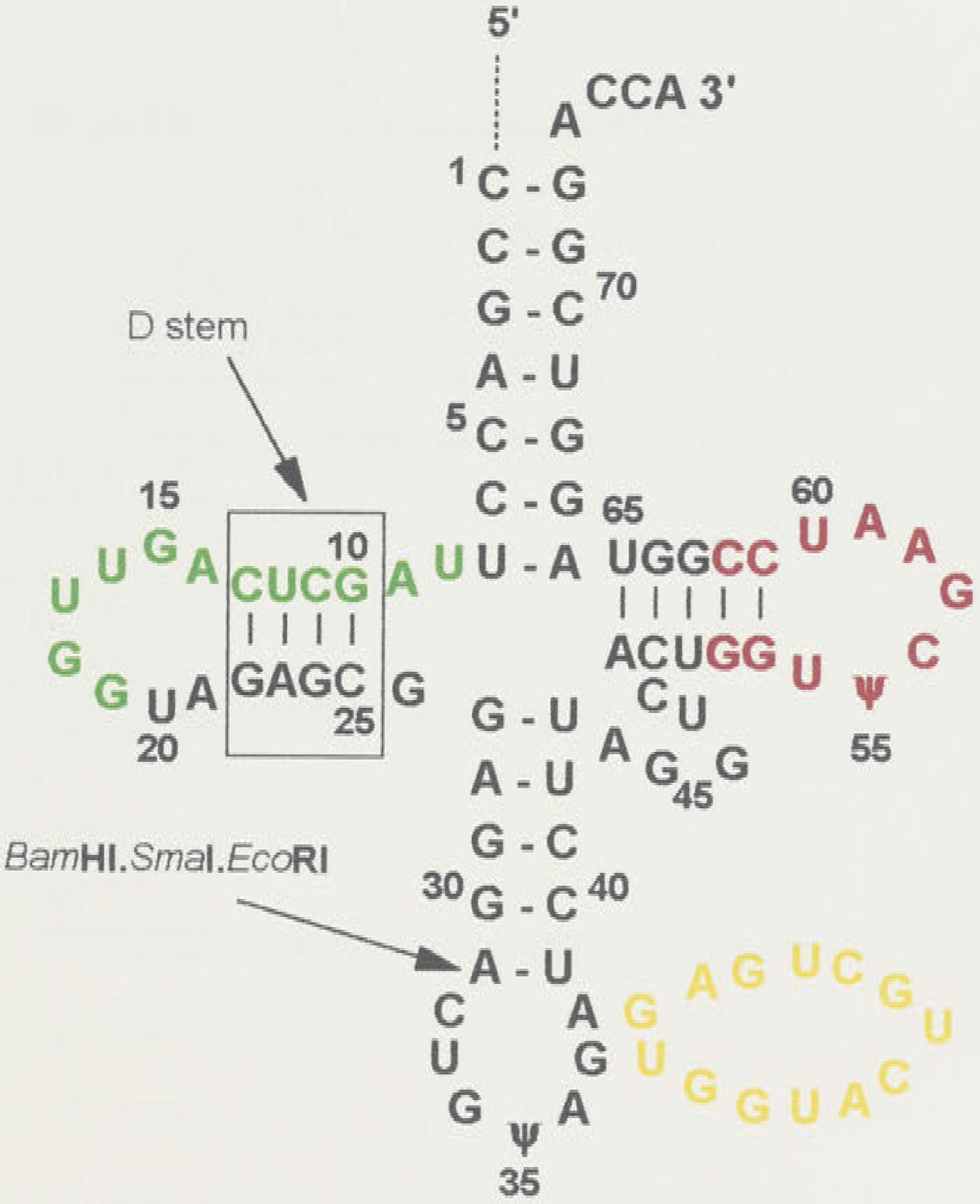
5'
ACCA 3'
1
C - G
C - G
G - C 70
A - U
5
C - G
C - G 65
D stem
15
10
60
UUGA CUCG A U U - A UGGCC UAAG
GAGC
G
ACUGG U Ψ C
GGUA
20
25
55
G - U
A - U
CU
A
G 45 G
BamHI.SmaI.EcoRI
G - C
30 G - C 40
A - U
C A G AGUCGU
U G U GGUAC
G Ψ A
35

Figure 4.1

Figure 4.2: The steps involved in the processing of intron-containing tRNA^{Tyr} transcripts to form mature tRNA^{Tyr}. The 3 sequential steps of processing are shown with tRNA sequence in red and intron in black. The numbers next to the vertical arrows refer to steps in the maturation process listed above the figure.

Steps toward the formation of a mature tRNA

1. removal of the 5' and 3' flanking sequences.
2. addition of CCA to the mature 3' end.
3. cleavage of the intron and ligation of the 2 tRNA halves to form mature tRNA.

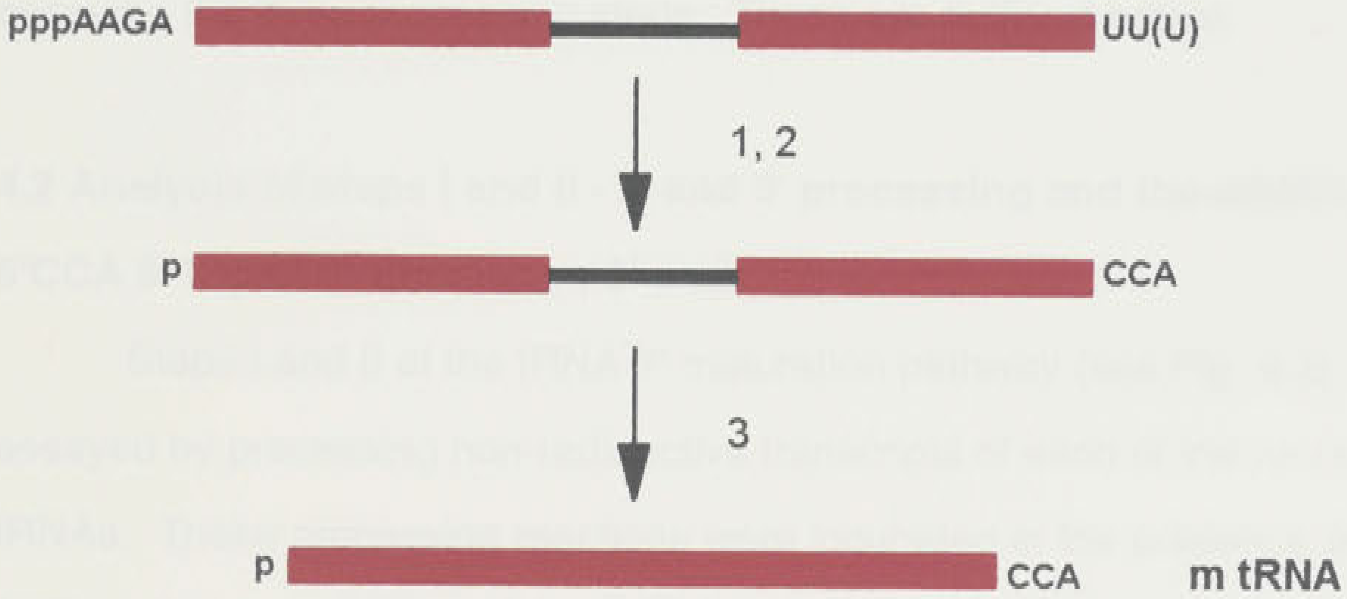
pppAAGA
UU(U)
1, 2
p
CCA
3
p
CCA
m tRNA

Figure 4.2

tRNA^{Tyr}-ribozymes had on cleavage rates was also determined. The results of these *in vitro* analyses were used as a guide to the potential effectiveness of the Rz12 and RzCA ribozymes for subsequent *in vivo* applications.

RESULTS

4.1 Maturation of recombinant and wildtype tRNA^{Tyr} transcripts in wheatgerm extracts.

The maturation of the recombinant tRNA^{Tyr} transcripts was determined by measuring the conversion of the recombinant pre-tRNA^{Tyr} into putative mature products. This analysis established that the accumulation of putative mature tRNA^{Tyr} products took place for all constructs and that these products were dependent upon the addition of wheatgerm extract (Fig. 4.3).

The extent of processing of the recombinant tRNAs was determined by assaying the three processing steps. These are outlined below.

4.2 Analysis of steps I and II - 5' and 3' processing and the addition of the 5'CCA 3' triplet to the mature 3' end.

Steps I and II of the tRNA^{Tyr} maturation pathway (see Fig. 4.2) were assayed by processing non-radioactive transcripts of each of the recombinant tRNAs. These processing reactions were incubated in the presence of P^{32}-CTP so that the addition of the 5'CCA 3' triplet to the mature 3' end could be monitored. To ensure that the accumulated product band was equivalent to that observed in the original processing assays, radiolabelled recombinant tRNA^{Tyr} transcripts were also processed and analysed alongside the non-radioactive transcripts. As shown in figure 4.4 all the recombinant tRNA constructs processed to step II of the maturation pathway.

4.3 Analysis of step III - splicing the endogenous 13 base intron.

Complete processing of the recombinant tRNAs was assayed by first removing the 13 base intron from the wildtype and each of the five recombinant

Figure 4.3: Analysis of the *in vitro* maturation of recombinant and wildtype tRNA^{Tyr} transcripts using a wheatgerm extract. Radiolabelled *in vitro* transcripts of each of the 6 tRNA^{Tyr} constructs (i.e. tRNA, tRNAp, tRNAAs24, tRNARz12, tRNAAsGUC, tRNARzCA) were incubated at 30°C for 1.5 hours in the presence (**+** ; lanes 2, 4, 6, 8 and 10) or absence (lanes 1, 3, 5, 7 and 9) of the wheatgerm extract. Products were analysed on 8% polyacrylamide/7M urea gels as outlined in materials and methods (section 2.11). Arrowed bands represent the following: **P1**, putative mature tRNA (wildtype); **P2**, putative mature tRNAp (+ polylinker); **P3**, putative mature tRNAAs24 (+ antisense, As24); **P4**, putative mature tRNARz12 (+ ribozyme, Rz12); **P5**, putative mature tRNAAsGUC (+ antisense, AsGUC); **P6**, putative mature tRNARzCA (+ ribozyme, RzCA); **P7**, processed 5' and 3' flanking sequences.

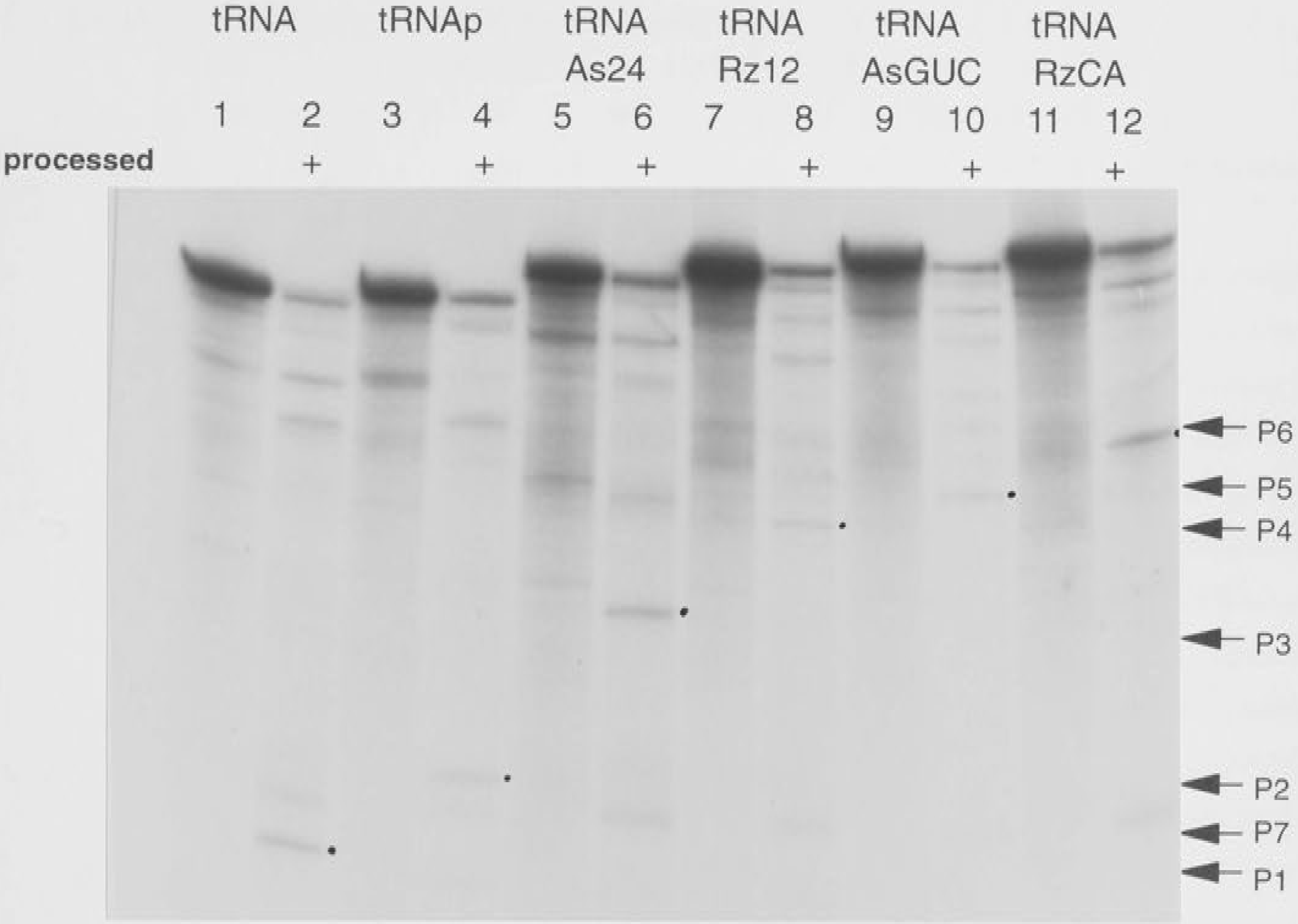
tRNA
tRNAp
tRNA As24
tRNA Rz12
tRNA AsGUC
tRNA RzCA
1 2 3 4 5 6 7 8 9 10 11 12
processed
+ + + + + +
P6
P5
P4
P3
P2
P7
P1

Figure 4.3

Figure 4.4: Analysis of the processing of recombinant and wildtype $tRNA^{Tyr}$ to step 2 of the maturation pathway (see Fig. 4.2). Lanes 1 -18 are as follows: lane **1**, radiolabelled tRNA; lane **2**, radiolabelled tRNA + wheatgerm extract; lane **3**, tRNA + wheatgerm extract + radiolabelled CTP; lane **4**, radiolabelled tRNAp; lane **5**, radiolabelled tRNAp + wheatgerm extract; lane **6**, tRNAp + wheatgerm extract + radiolabelled CTP; lane **7**, radiolabelled tRNAAs24; lane **8**, radiolabelled tRNAAs24 + wheatgerm extract; lane **9**, tRNAAs24 + wheatgerm extract + radiolabelled CTP; lane **10**, radiolabelled tRNARz12; lane **11**, radiolabelled tRNARz12 + wheatgerm extract; lane **12**, tRNARz12 + wheatgerm extract + radiolabelled CTP; lane **13**, radiolabelled tRNAAsGUC; lane **14**, radiolabelled tRNAAsGUC + wheatgerm extract; lane **15**, tRNAAsGUC + wheatgerm extract + radiolabelled CTP; lane **16**, radiolabelled tRNARzCA; lane **17**, radiolabelled tRNARzCA + wheatgerm extract; lane **18**, tRNARzCA + wheatgerm extract + radiolabelled CTP. Arrowed bands are as in figure 4.3 and represent the following: **P1**, putative mature tRNA (wildtype); **P2**, putative mature tRNAp (+ polylinker); **P3**, putative mature tRNAAs24 (+ antisense, As24); **P4**, putative mature tRNARz12 (+ ribozyme, Rz12); **P5**, putative mature tRNAAsGUC (+ antisense, AsGUC); **P6**, putative mature tRNARzCA (+ ribozyme, RzCA); **P7**, processed 5' and 3' flanking sequences.

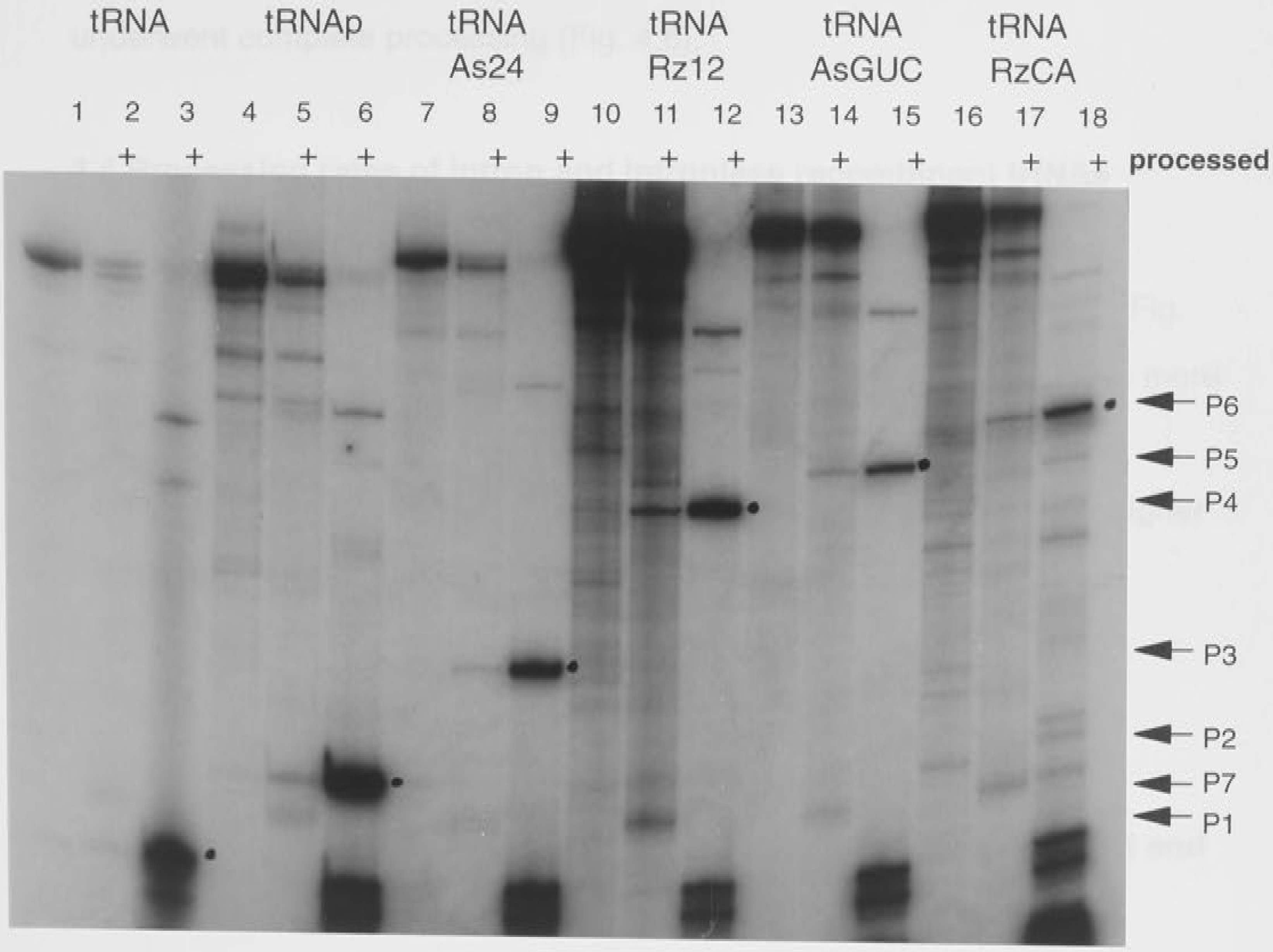
tRNA
tRNAp
tRNA As24
tRNA Rz12
tRNA AsGUC
tRNA RzCA
1 2 3 4 5 6 7 8 9 10 11 12 13 14 15 16 17 18
+ + + + + + + + + + + +
processed
P6
P5
P4
P3
P2
P7
P1

Figure 4.4

constructs. These constructs are differentiated from the original tRNA sequences by an "I" following the construct name. A comparison of the processing of intron-plus (i+) and intron-minus (i-) forms of each construct showed that none of the recombinant tRNAs were able to splice out the 13 base intron (Fig. 4.5). In contrast, 8% of the wildtype tRNA^{Tyr} sequence underwent complete processing (Fig. 4.6).

4.4 Processing rates of intron and intronless recombinant tRNAs

Although none of the recombinant tRNA^{Tyr} underwent complete maturation, processing rates for all of the constructs were determined (Fig. 4.6). For each recombinant tRNA^{Tyr}, processing of the i- construct was more efficient than that of the corresponding i+ construct. Furthermore, the processing rates for the tRNAp construct (i+ and i-) were consistently higher than any of the other tRNAs (including the wildtype tRNA^{Tyr}).

As the insert size increased, the extent of processing for the recombinant tRNAs was reduced (Fig. 4.6).

4.5 Analysis of *in vitro* cleavage efficiencies by tRNA^{Tyr}-embedded and non-embedded Rz12 and RzCA ribozymes

The *in vitro* cleavage efficiencies of the tRNA^{Tyr}-embedded (i+ and i-) and non-embedded Rz12 and RzCA ribozymes were measured by the conversion of full length CAT transcript into the predicted 5' and 3' cleavage products. The analysis established that cleavage was dependent upon the addition of either the non-embedded or tRNA^{Tyr}-embedded ribozyme sequences and that all six constructs cleaved the CAT RNA at the expected site (Fig. 4.7).

In three independent experiments, in which ribozyme was present in a six-fold molar excess, 72% and 38% of the CAT RNA was cleaved by the non-embedded Rz12 and i+ tRNARz12 ribozymes respectively. In the same series of experiments, the RzCA ribozyme in the non-embedded and i+ tRNA^{Tyr}-

Figure 4.5: Examples of *in vitro* analysis of processing of the intron-plus (i+) and intron-minus (i-) recombinant tRNA^{Tyr} constructs to step III (i.e. splicing of the 13 base intron) using wheatgerm extract. The lanes 1-16 show the following radiolabelled recombinant tRNA^{Tyr} transcripts: lane **1**, tRNAAs24I (i-) + wheatgerm extract; lane **2**, tRNAAs24I(i-) ; lane **3**, tRNAAs24 (i+) + wheatgerm extract; lane **4** tRNAAs24 (i+); lane **5**, tRNApI (i-) + wheatgerm extract; lane **6**, tRNApI (i-); lane **7**, tRNAp (i+) + wheatgerm extract; lane **8**, tRNAp (i+); lane **9**, tRNARz12 (i+) ; lane **10**, tRNARz12 (i+) + wheatgerm extract; lane **11**, tRNARz12I (i-); lane **12**, tRNARz12I (i-) + wheatgerm extract; lane **13**, tRNAAsGUC (i+); lane **14**, tRNAAsGUC (i+) + wheatgerm extract; lane **15**, tRNAAsGUCI (i-); lane **16**, tRNAAsGUCI (i-) + wheatgerm extract. The processed products are: **P2**, "mature" tRNAp (+ intron); **P2A**, "mature tRNApI (- intron); **P3**, "mature" tRNAAs24 (+ intron); **P3A**, "mature" tRNAAs24I (- intron); **P4**, "mature" tRNARz12 (+ intron); **P4A**, "mature" tRNARz12I (-intron); **P5**, "mature" tRNAAsGUC (+ intron); **P5A**, "mature" tRNAAsGUCI (- intron); **P7**, processed 5' and 3' flanking sequences.

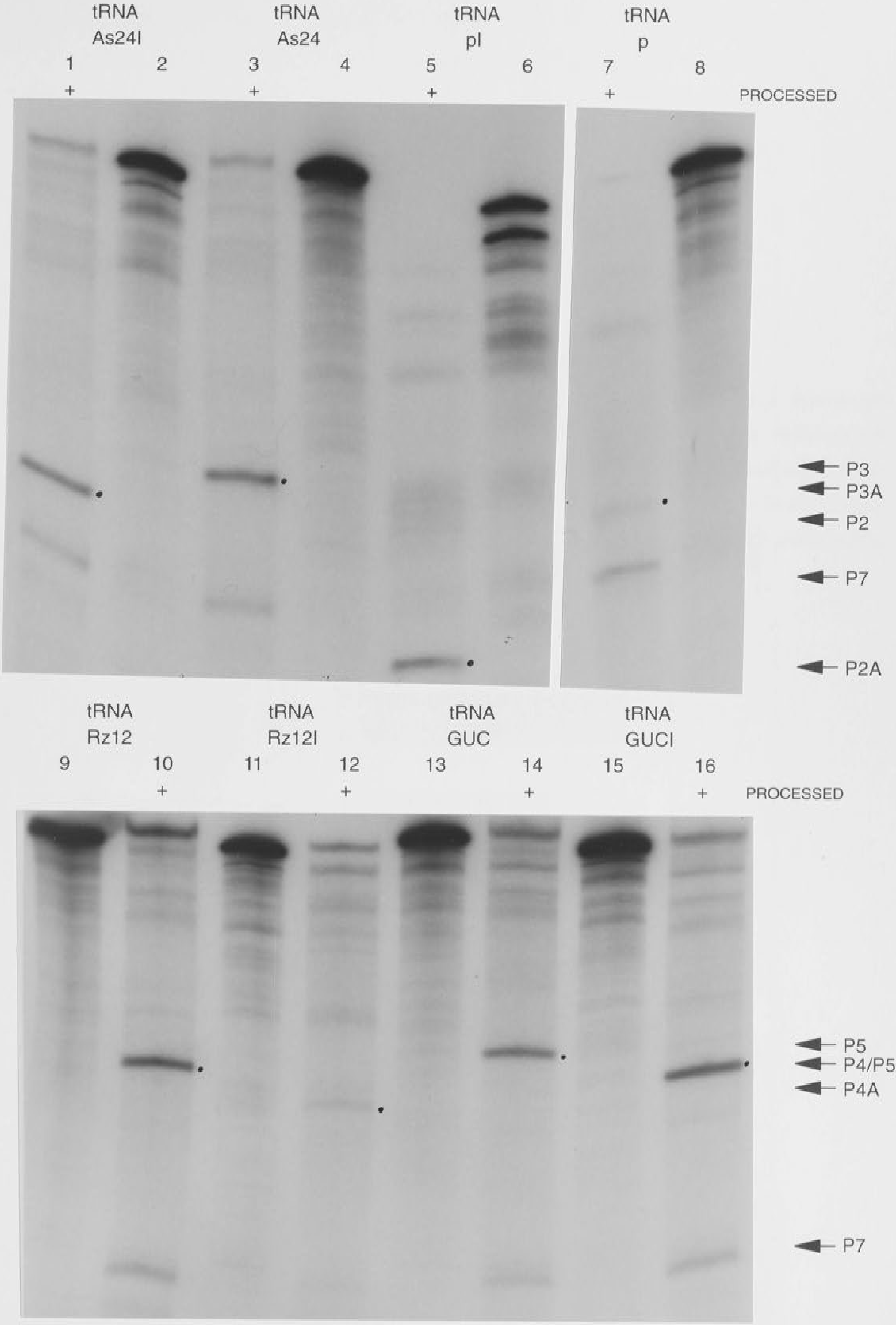
tRNA
As24I
tRNA
As24
tRNA
pI
tRNA
p
1
2
3
4
5
6
7
8
+
+
+
+
PROCESSED
P3
P3A
P2
P7
P2A
tRNA
Rz12
tRNA
Rz12I
tRNA
GUC
tRNA
GUCI
9
10
11
12
13
14
15
16
+
+
+
+
PROCESSED
P5
P4/P5A
P4A
P7

Figure 4.5

Figure 4.6: Average *in vitro* processing rates after 90 minutes incubation for recombinant intron-plus (i+) and intron-minus (i-) tRNA^{Tyr} transcripts. % processing (y axis) is plotted for each construction listed along the x axis with average % processing (% proc) shown beneath the graph. +* indicates the % complete processing of the wildtype tRNA^{Tyr} sequence under the same *in vitro* conditions.

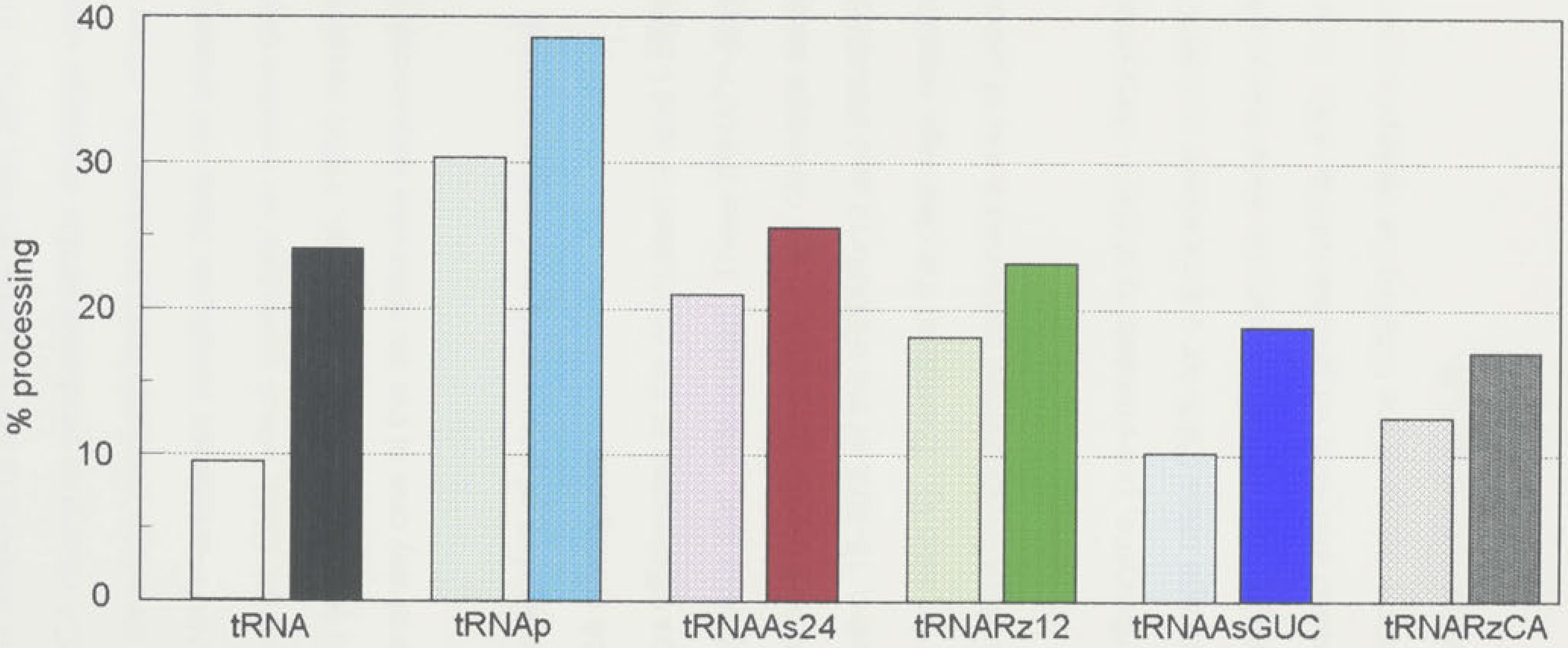

intron:	+*	+	+	-	+	-	+	-	+	-	+	-
% proc:	8	24	30	39	21	26	18	23	10	18	13	17

+* complete processing

Figure 4.6

embedded forms, induced 32% and 26% cleavage respectively (Fig. 4.8). In addition, the cleavage rates induced by the i- tRNA-ribozymes were also determined. The i- tRNARz12 ribozyme had a slightly increased rate of cleavage over that of the i+ tRNARz12 (48% compared with 38%). In contrast, both the i+ and i- tRNARzCA ribozyme produced similar cleavage rates (32% for i- and 27% for i+). No cleavage products were produced by either of the non-embedded, i+ or i- tRNA^{Tyr}-antisense constructs (data not shown).

A mutant CAT transcript, CM2, which contained an inactive cleavage site (GUG instead of GUC; see Fig. 2.3; Perriman *et al.*, 1992) remained uncleaved in the presence of any one of the six ribozyme sequences (Fig. 4.7).

4.6 *In vitro* cleavage efficiencies of processed and unprocessed tRNARz12 and tRNARzCA ribozymes

The *in vitro* cleavage efficiencies of the processed i+ and i- tRNARz12 and tRNARzCA ribozymes were also determined. These tRNA^{Tyr}-ribozyme constructs were processed and precipitated prior to the cleavage assays. Figure 4.6 shows that, *in vitro*, 15-20% of the tRNARz12 and tRNARzCA sequences are processed (to step II). Therefore, the cleavage reactions involving these processed tRNA^{Tyr}-ribozymes contained a mix of processed and unprocessed tRNA^{Tyr} sequences.

For the tRNARz12 ribozyme, pre-processing of the i+ ribozymes significantly increased cleavage rates (38% for unprocessed and 58% for processed) while the cleavage rates for the i- ribozyme were marginally reduced (48% for unprocessed and 40% for processed-Fig. 4.9). In contrast, processing of both the i+ and i- forms of the tRNARzCA ribozyme produced significantly reduced cleavage rates (Fig. 4.9).

DISCUSSION

This chapter has investigated the *in vitro* efficiencies of a series of short ribozyme and antisense constructs which have been embedded within a

Figure 4.7: *In vitro* hammerhead-ribozyme mediated cleavage of CAT and CM2 (mutant CAT) targets by non-embedded and tRNA-embedded ribozymes. An autoradiograph of a dried electrophoresis gel containing products of *in vitro* cleavage reactions. The *in vitro* transcripts of the CAT and CM2 substrates, but not the ribozymes were radioactively labelled. Reaction conditions were 1 hour at 30°C. The lanes labelled 1-7 for both CAT and CM2 represent: **1**, 0.5 pmole CAT/CM2 RNA incubated alone; **2**, 0.5 pmole CAT/CM2 RNA + 3 pmole Rz12 (non-embedded); **3**, 0.5 pmole CAT/CM2 RNA + 3 pmole tRNARz12 (tRNA-embedded [i+]); **4**, 0.5 pmole CAT/CM2 RNA + 3 pmole tRNARz12I (tRNA-embedded [i-]); **5**, 0.5 pmole CAT/CM2 RNA + 3 pmole RzCA (non-embedded); **6**, 0.5 pmole CAT/CM2 RNA + 3 pmole tRNARzCA (tRNA-embedded [i+]); **7**, 0.5 pmole CAT/CM2 RNA + 3 pmole tRNARzCAI (tRNA-embedded [i-]). The RNA species are as follows: **Sub**, CAT/CM2 target; **5'P**, cleavage product 5' of the target site; **3'P**, cleavage product 3' of the target site.

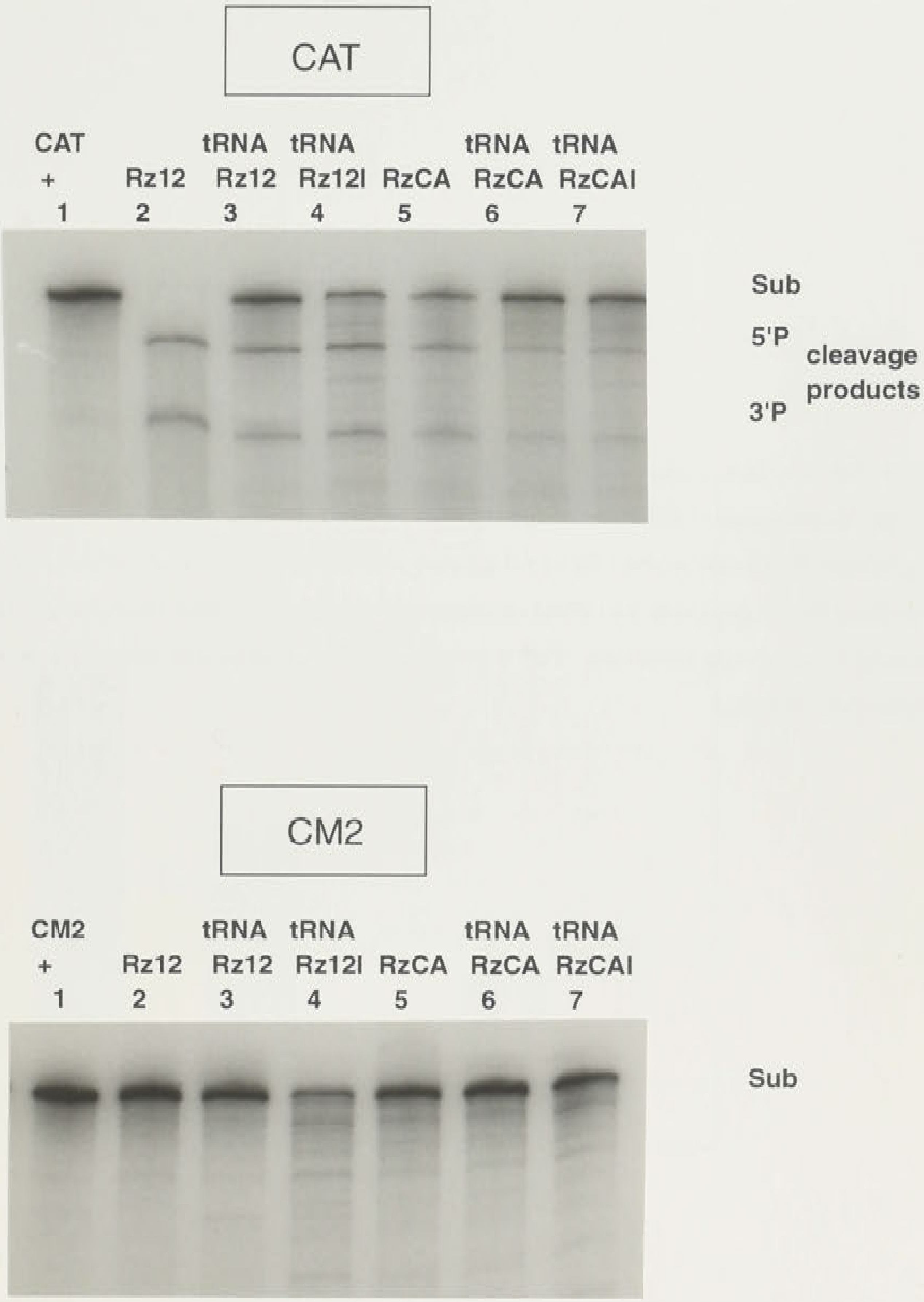

30°C, 60 mins; 0.5pm CAT: 3pm Rz

Figure 4.7

Figure 4.8: Bar graph of *in vitro* cleavage reactions involving CAT substrate RNA and showing average % cleavage of CAT transcript by non-embedded Rz12 (blue), tRNA-embedded Rz12 [i+] (yellow), tRNA-embedded Rz12 [i-] (green), non-embedded RzCA (white), tRNA-embedded RzCA [i+] (red) and tRNA-embedded RzCA [i-] (orange) ribozymes in three independent cleavage reactions. The Y axis shows % cleavage and error bars represent 2 standard deviations.

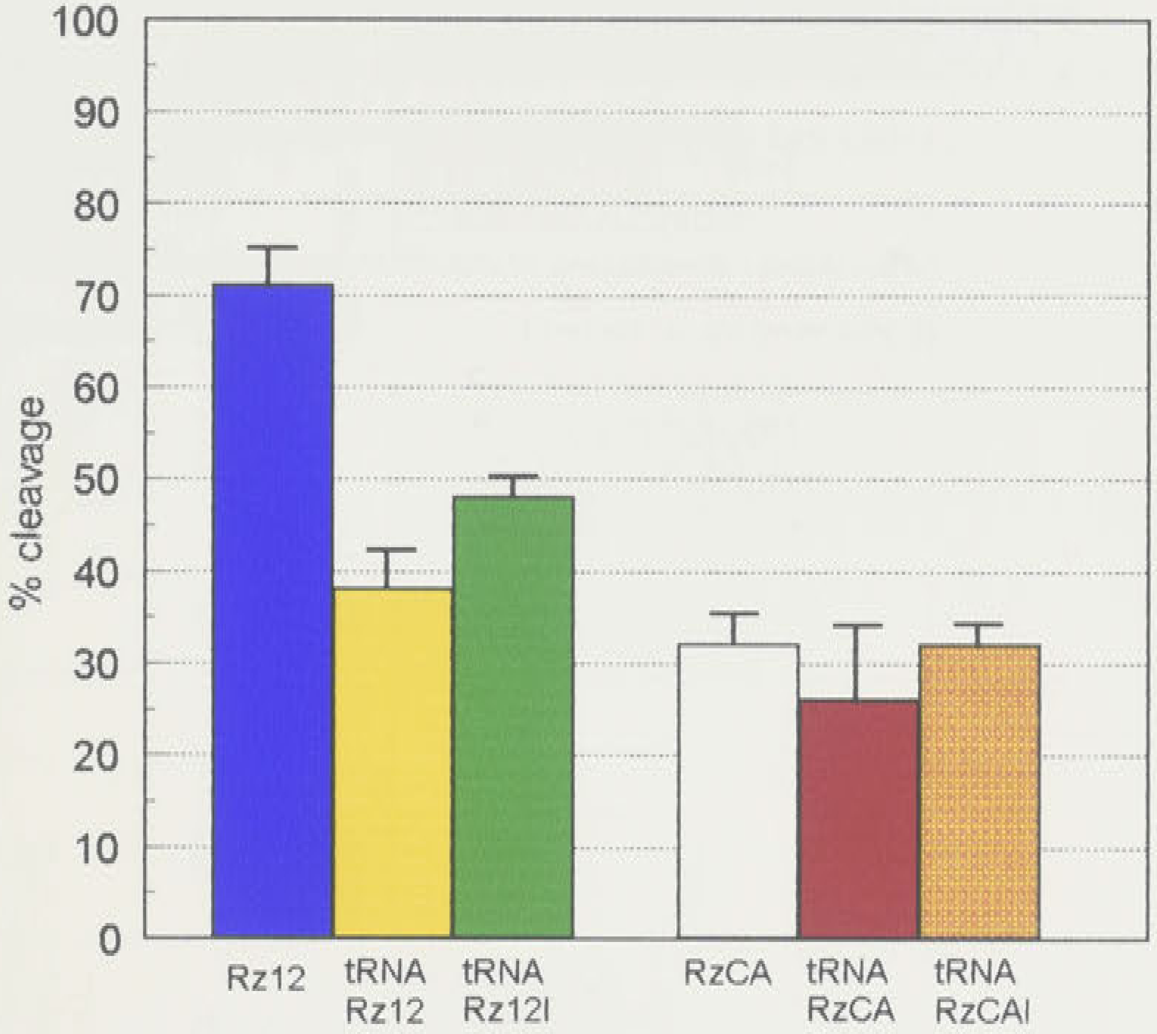

100
90
80
70
60
50
40
30
20
10
0
% cleavage
Rz12
tRNA Rz12
tRNA Rz12I
RzCA
tRNA RzCA
tRNA RzCAI

Figure 4.8

Figure 4.9: Bar graph of *in vitro* cleavage reactions showing average % cleavage of the CAT transcript by non-embedded, processed and unprocessed tRNA-embedded Rz12 and RzCA ribozymes. % cleavage (y axis) is plotted in the presence of each ribozyme construct (x axis) with error bars showing 2 standard deviations. Processing of the tRNA-embedded Rz12 or RzCA transcripts prior to cleavage is indicated by "+" beneath the graph. Average % cleavage for each ribozyme construct is also shown beneath the graph.

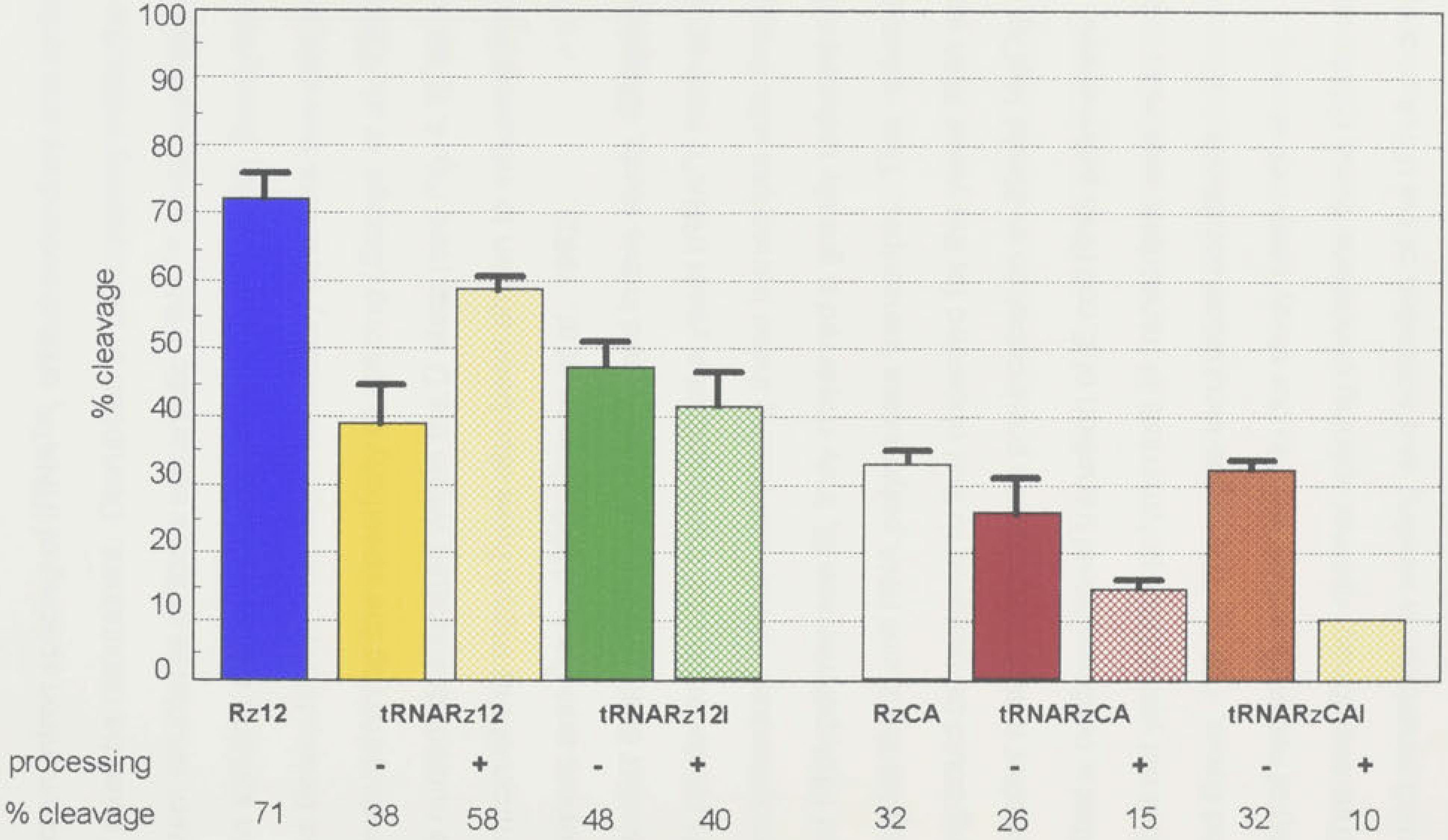
% cleavage
100
90
80
70
60
50
40
30
20
10
0
Rz12
tRNARz12
tRNARz12I
RzCA
tRNARzCA
tRNARzCAI
processing
- + - + - + - +
% cleavage
71 38 58 48 40 32 26 15 32 10

Figure 4.9

tobacco-tRNA^{Tyr}. The analyses showed that all the recombinant tRNAs could successfully process the 5' and 3'ends, and add the 5' CCA 3' triplet sequence to the 3' end (Fig. 4.4). However, in all cases, the 13-base intron contained within the recombinant tRNA^{Tyr} was not spliced from the tRNA intermediates (Fig. 4.5).

To obtain intron splicing of tRNA^{Tyr}, critical secondary and tertiary interactions must be maintained. Disruption of base-pairing within the anticodon stem structures of three eucaryotic tRNA^{Tyr} have been shown to reduce intron splicing efficiency (Shapero and Greer, 1992; Szweykowska-Kulinska and Beier, 1991). The intron secondary structure has also been implicated in determining the specificity of splicing (Stange *et al.*, 1992). In addition, the nucleotides located within the D stem (see Fig. 4.1), as well as the correct formation of this region have also been shown to influence intron splicing (Shapero and Greer, 1992; Stange *et al.*, 1992).

In a similar design to the constructs used in this study, Shapero and Greer (1991) produced *in vitro* transcripts of a yeast tRNA^{Tyr} from an upstream *E.coli* RNA polymerase. When comparing these transcripts with those made *in vitro* by yeast RNA polymerase III, they observed a greatly reduced rate of intron splicing for the *E.coli* RNA polymerase transcripts. This reduced level of intron splicing could be restored to that observed for the yeast RNA polymerase III transcripts after a high temperature pre-incubation in 20mM $MgCl_2$, suggesting that a conformational transition of *E.coli* RNA polymerase transcripts, but not yeast RNA polymerase III transcripts, was required (Shapero and Greer, 1991). These pre-incubation conditions had no effect on intron splicing of recombinant tRNA^{Tyr} in our study (data not shown), suggesting that even under optimal splicing conditions these tRNAs cannot form the correct structure for binding and activation of the tRNA endonuclease.

The lack of splicing, and therefore complete maturation, of the recombinant tRNAs is likely to also influence the transport of these chimeric sequences from the nucleus to the cytoplasm. Recent work analysing a tRNA^{Met} sequence in *Xenopus* oocytes found that mutations which affected tRNA processing also affected transport. It was concluded that tRNA transport, like maturation must see the correct tRNA shape (Tobian *et al.*, 1985). This is further supported by the results of Cotten and Birnsteil (1989) who embedded a ribozyme within the anticodon loop of the same *Xenopus* tRNA^{Met}. While tRNA^{Met}-ribozyme transcripts were readily found within the nucleus, no transcript was detected in cytoplasmic extracts. These results suggest that the tRNA^{Tyr}-ribozyme and tRNA^{Tyr}-antisense constructs used in this study are also likely to be maintained in the nucleus.

All recombinant tRNA^{Tyr} constructs demonstrated processing to step II of the maturation pathway (see Fig. 4.4). A slight decrease in processing efficiencies to this step were observed when the insert size was 85 bases or larger. The processing rates for the i- constructs when compared to the i+ sequences were uniformly increased. In addition, the construct containing the 10bp polylinker, tRNAp, consistently produced a greater percentage of processed forms than any of the other constructs, including the wildtype tRNA^{Tyr} sequence (Fig. 4.6).

The analysis of the cleavage rates catalysed by the non-embedded and tRNA^{Tyr}-embedded ribozymes suggested that the secondary and tertiary interactions involving these molecules can also have an effect on the cleavage rates. Embedding the Rz12 ribozyme in the tRNA^{Tyr} sequence reduced cleavage rates from 72% to 38% (Fig. 4.8). In contrast, cleavage rates in the presence of the RzCA ribozymes were only marginally reduced from 32% to 27%, upon embedding within the tRNA^{Tyr} sequence (Fig. 4.8). The extended length of the hybridisation sequences conferred by the RzCA ribozyme probably means that this sequence is able to form the active hybrid at the same rate, in the presence or absence of the tRNA^{Tyr} sequences.

This is supported by the data for the i- and, in part, by the processed tRNA^{Tyr}-ribozymes. The removal of the intron from the tRNARz12 ribozyme increased the rates of cleavage, suggesting that the presence of this additional sequence in the original construct was inhibiting the formation of the active substrate-ribozyme hybrid. The cleavage rates of the i+ tRNARz12 ribozyme were further increased by processing the transcript, thus removing 5' and 3' nucleotides and further reducing the surrounding sequence which could interfere with hybrid formation. For the tRNARzCA ribozyme, the removal of the intron had little effect on the rate of cleavage, again suggesting that the substrate-ribozyme hybrid for the RzCA ribozyme was unaffected by the $tRNA^{Tyr}$ sequence (Fig. 4.8).

One unexpected result was the small decrease in cleavage rates observed when the processed form of the i- tRNARz12 ribozyme was the active molecule. Previous results had suggested that cleavage by the Rz12 ribozyme was increased when the surrounding 5' and/or 3' nucleotides decrease. The processed i- tRNARz12 ribozyme has the least number of nucleotides surrounding the ribozyme sequence and therefore was expected to induce higher rates of cleavage than the other tRNARz12 constructs. In addition, processing of both the i+ and i- tRNARzCA ribozymes dramatically reduced cleavage rates induced by both these molecules. As was the case with the tRNARz12 ribozyme, the cleavage rates for the processed i- tRNARzCA ribozyme were lower than the i+ form (Fig. 4.9).

Although only a small percentage of the $tRNA^{Tyr}$-ribozymes were observed to undergo processing, these results suggest that this action can have a significant effect on the cleavage rates. It is possible that during processing of some of the $tRNA^{Tyr}$-ribozymes, modified nucleotides were introduced at sites within the hammerhead sequence thereby reducing its activity. It is known that approximately 10% of the nucleotides within eucaryotic tRNA molecules are post-transcriptionally modified. This modification generally involves specific nucleotides and does not appear to be a random process (McClain, 1993), however, it is unknown what the effect of additional nucleotides such as the ribozyme sequences in this study would have on the position and extent of the nucleotide modification process within tRNAs. This explanation is possible for the tRNARzCA ribozymes as the processed forms of both the i+ and i- constructs showed greatly reduced cleavage rates. For the tRNARz12 ribozyme, however, only the processed i- construct showed reduced cleavage rates. It is unlikely that nucleotide modifications affecting cleavage rates would occur in the i- but not the i+ forms of this ribozyme.

Processing of the i- forms of both tRNA-ribozymes reduced cleavage rates. This suggests that the synthetic removal of the intron and the subsequent processing of these tRNA-ribozymes has affected the ability of the ribozyme to induce cleavage. For the tRNARzCA ribozymes, the additive effect of the modified nucleotides and removing the intron could explain the further reduction observed when the i- tRNARzCA ribozyme was processed. Extensive further analysis would be required to determine exactly what aspect of the maturation pathway of these tRNA^{Tyr}-ribozymes is affecting their subsequent rates of cleavage.

These *in vitro* assays have provided valuable information regarding the potential effectiveness of the Rz12 and RzCA ribozymes expressed as non-embedded or tRNA^{Tyr}-embedded ribozymes. The cleavage assays involving the tRNA^{Tyr}-ribozymes and non-embedded ribozymes have suggested that the tRNA^{Tyr} sequence can reduce the rate of cleavage of a short (Rz12) ribozyme but have little effect on a longer (RzCA) ribozyme. Additional information for the tRNA^{Tyr}-ribozymes was obtained by processing the molecules prior to cleavage analyses. The tRNARz12 i+ ribozyme showed increased rates of cleavage upon processing, while the tRNARz12 i- showed a small decrease. In contrast, cleavage rates for the tRNARzCA i+ and i- constructs were significantly reduced following processing. On the basis of these *in vitro* results, the tRNARzCA and i- tRNARz12 ribozymes may not provide the most effective means of reducing target gene expression *in vivo.* For this reason, only the Rz12 and tRNARz12 ribozymes, and their corresponding antisense constructs, As24 and tRNAAs24, were tested in subsequent *in vivo* assays.

CHAPTER 5

EXPRESSION OF tRNA^{Tyr}-EMBEDDED AND NON-EMBEDDED RIBOZYME AND ANTISENSE SEQUENCES IN PLANT CELLS

INTRODUCTION

While hammerhead ribozymes have been used to cleave many target RNAs *in vitro* (e.g. Haseloff and Gerlach, 1988; Saxena & Ackerman, 1990; Lamb and Hay, 1990; Evans *et al.*, 1992; Mazzolini *et al.*, 1992), there has been much less success in ribozyme mediated gene inactivation *in vivo* (see Fig. 1.13 for examples). This is particularly the case for plant systems with only four reports of ribozyme-induced gene reduction (Steinecke *et al.*, 1992, 1994; Perriman *et al.*, 1993; Wegener *et al.*, 1994).

As outlined in chapter 1, several animal-based studies have now developed actively transcribing tRNA sequences for *in vivo* ribozyme expression (Cotten and Birnsteil, 1989; Yuyama *et al.*, 1992; Shore *et al.*, 1993; Bouvet *et al.*, 1994; Kandolf, 1994; Baier *et al.*, 1994). While these studies have been successful in achieving target gene reduction and high level RNA polymerase III expression of tRNA-ribozymes, the lack of antisense or inactive ribozyme controls has meant that the source of target gene reduction has not been clearly established. The aim of this research was to investigate the effectiveness of a tRNA-ribozyme or control tRNA-antisense sequence for reducing target gene expression in plant cells.

An additional control, in which the GUC-464 triplet on the CAT target was mutated to a non-cleavable GUG (CM2; Perriman *et al.,* 1992; see Fig. 2.3), provided a further means of differentiating ribozyme and antisense mediated inhibition in this system. *In vitro* cleavage assays (see Fig. 4.7) established that this target could not be cleaved by the ribozymes used in this study. To further increase the levels of ribozyme and antisense transcripts, the sequences were delivered to plant cells using the self-replicating ACMV vector described in previous chapters.

In chapter 4, *in vitro* cleavage assays involving both the tRNA-embedded and non-embedded ribozymes showed that site-specific cleavage of the CAT RNA transcript occurred. The Rz12, ribozyme was the most active, and, although this ribozyme showed reduced cleavage rates when embedded within the $tRNA^{Tyr}$, this rate could be significantly increased, to approach that of the non-embedded ribozyme, following tRNA processing. Cleavage rates with the RzCA ribozyme, were lower, but were not affected by the presence of the unprocessed $tRNA^{Tyr}$ sequence. In contrast to the tRNARz12 ribozyme however, cleavage rates for the tRNARzCA ribozyme were significantly decreased when these transcripts were processed. Therefore, only the Rz12 and tRNARz12 ribozymes were analysed *in vivo* .

An additional aspect of the *in vivo* tRNARz12 design was the presence of two potentially active promoters: the RNA polymerase II promoter derived from the coat protein of the ACMV sequence and the endogenous RNA polymerase III promoter (see Fig. 5.5a). The results also detail the effectiveness of ribozyme transcripts in reducing CAT gene expression when derived from either or both of these promoters.

RESULTS

5.1 CAT activities from the mutant and normal CAT targets.

To establish the CM2 construct as a valid control to monitor ribozyme-mediated inhibition of CAT mRNA, CAT activities for either the GUG-containing CM2 target or the GUC-containing CAT target were determined. This was to ensure that equivalent levels of CAT activity were expressed from either target, making their direct comparison in the presence of ribozyme and antisense constructs valid. A series of independent transfections, in which either pACAT or pACM2 constructs were electroporated into protoplasts, showed similar CAT activities for both target sequences (Fig. 5.1).

Figure 5.1: *In vivo* CAT activities for GUC-containing CAT, and GUG-containing CM2 constructs assayed 3 days post transfection. The CAT assays labelled 1-7 are: **1**, mock inoculated *N.tabacum* cells; **2 - 4**, three independent transfections of 5μg pACAT + 15μg pAtRNA; **5-7**, three independent transfections of 5μg pACM2 + 15μg pAtRNA. The assay species are: **A**, unacetylated ^{14}C-chloramphenicol; **B**, **C**, acetylated ^{14}C-chloramphenicol.

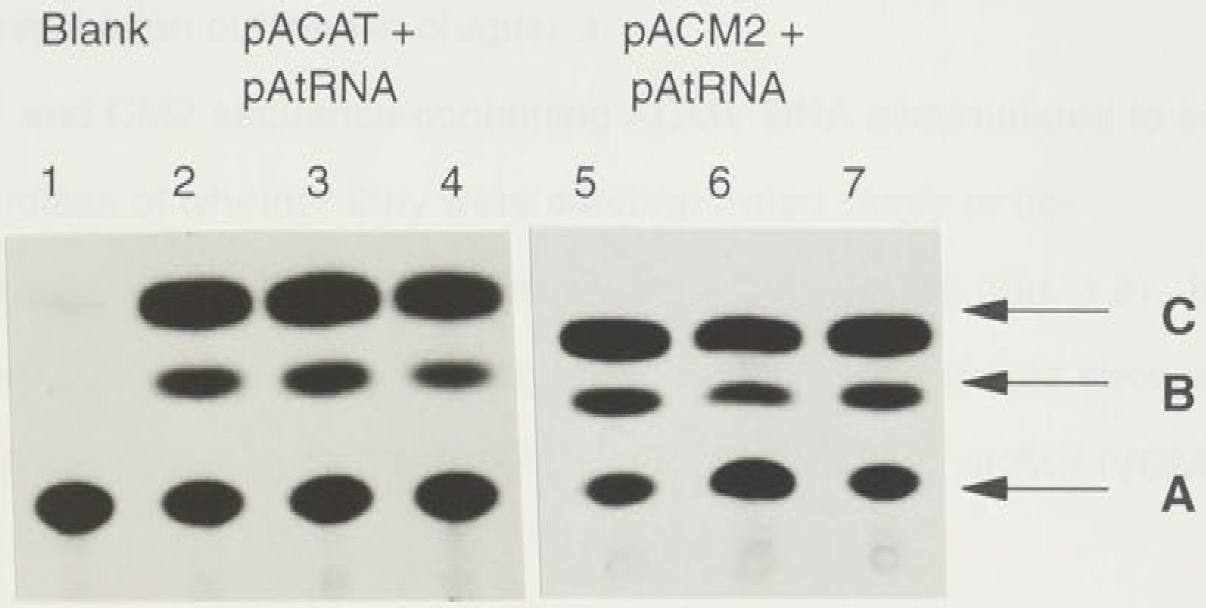
Blank
pACAT +
pAtRNA
pACM2 +
pAtRNA
1
2
3
4
5
6
7
C
B
A

Figure 5.1

5.2 Analysis of replication of ACMV constructs *in vivo.*

To determine the effectiveness of the non-embedded and tRNA-embedded ribozymes *in vivo*, CAT target together with antisense or ribozyme constructs were delivered to plant cells in the ACMV vectors. To ensure that any reduction in CAT activity observed in this system was not due to inhibition of replication of the target ACMV constructs, DNA was isolated from transfected protoplasts and digested using methylation sensitive isoschizomers, *Dpn*I and *Mbo*I as for the analysis of pACAT, pARzCAT and pAAsCAT replication outlined in chapter 3.

CAT and CM2 sequence-containing ACMV DNA accumulated to similar levels regardless of whether they were electroporated singly or co-electroporated with a ribozyme or antisense ACMV construct (Fig. 5.2). In addition, the ribozyme and antisense-containing ACMV constructs showed replication products in the presence of either the ACMVCAT or ACMVCM2 sequences (Fig. 5.3).

5.3 *In vivo* efficiencies of non-embedded and tRNA-embedded ribozymes.

Having shown that all pACMV constructs were replicating, the relative effects of the two ribozymes on CAT and CM2 gene expression were examined. The presence of the tRNARz12 ribozyme reduced CAT activity to less than 20% of the control. The non-embedded ribozyme reduced activity to 40% of the control. The two antisense constructs were less effective, reducing CAT activity to 60%-70% of the control (Fig. 5.4a). These results contrast with the *in vitro* assays presented in chapter 4 (Fig. 4.7 & 4.8), in which Rz12 was more effective than the tRNARz12 ribozyme.

When the CM2 target was assayed, all the antisense and ribozyme constructs reduced CAT activity to about 60% of the control (Fig. 5.4b). This reduction is likely to be due entirely to an antisense mechanism.

In the presence of the non-embedded ribozyme, the CAT target showed a slightly reduced level relative to the mutant CM2 target suggesting some

Figure 5.2: Example of replication of ACMVCAT constructs *in vivo*. Southern blot analysis of pACAT DNA isolated from *N.tabacum* cells three days post transfection. The blots, probed with radiolabelled CAT sequence, show *Dpn*I and *Mbo*I digestion for each construct pairing. The lanes labelled 1-7 represent the following: **1**, plasmid pACAT *Dpn*I; **2**, pACAT + pAtRNA *Dpn*I; **3**, as for 2 but *Mbo*I; **4**, pACAT + pAtRNARz12 *Dpn*I; **5**, as for 4 but *Mbo*I; **6**, pACAT + pAtRNAAs24 *Dpn*I; **7**, as for 6 but *Mbo*I. The DNA products are: **CAT 1**, bacterial gene for chloramphenicol resistance from pACMV constructs (see chapter 2, Fig. 2.1a), this fragment is lost as ACMV replicates and accumulates; **CAT 2**, CAT target sequence insert; **HMW**, undigested pACAT sequence.

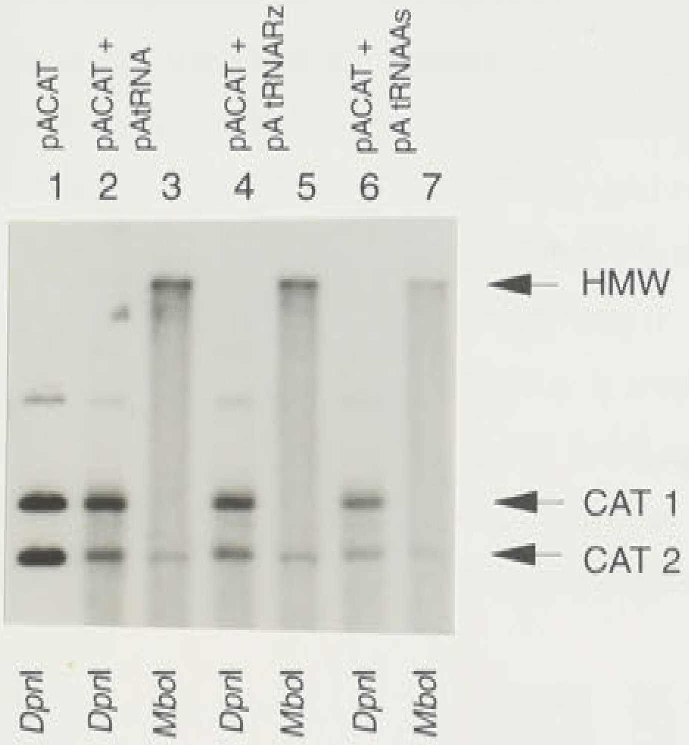
pACAT
pACAT + pAtRNA
pACAT + pA tRNARz
pACAT + pA tRNAAs
1
2
3
4
5
6
7
HMW
CAT 1
CAT 2
DpnI
DpnI
MboI
DpnI
MboI
DpnI
MboI

Figure 5.2

Figure 5.3: Examples of the *in vivo* replication of ACMV-derived tRNA-embedded and non-embedded ribozyme and antisense constructs. As for figure 5.2, southern blot analysis of pAtRNARz12, pAtRNAAs24, pARz12 and pAAs24 DNAs isolated from *N.tabacum* cells three days post transfection. The blots, probed with tRNARz12 (1-3), tRNAAs24 (4-6), Rz12 (7-9) and As24 (10-12) show *Dpn*I and *Mbo*I digestion for each construct co-transfected with pACAT DNA. The lanes 1-12 show: **1**, pAtRNARz12 *Dpn*I; **2**, pACAT + pAtRNARz12 *Dpn*I; **3**, as for 2 but *Mbo*I; **4**, pAtRNAAs24 *Dpn*I; **5**, pACAT + pAtRNAAs24 *Dpn*I; **6**, as for 5 but *Mbo*I; **7**, pARz12 *Dpn*I; **8**, pACAT + pARz12 *Dpn*I; **9**, as for 8 but *Mbo*I; **10**, pAAs24 *Dpn*I; **11**, pACAT + pAAs24 *Dpn*I; **12**, pACAT + pAAs24 *Mbo*I. The products of digestion for each ribozyme/antisense construct are arrowed.

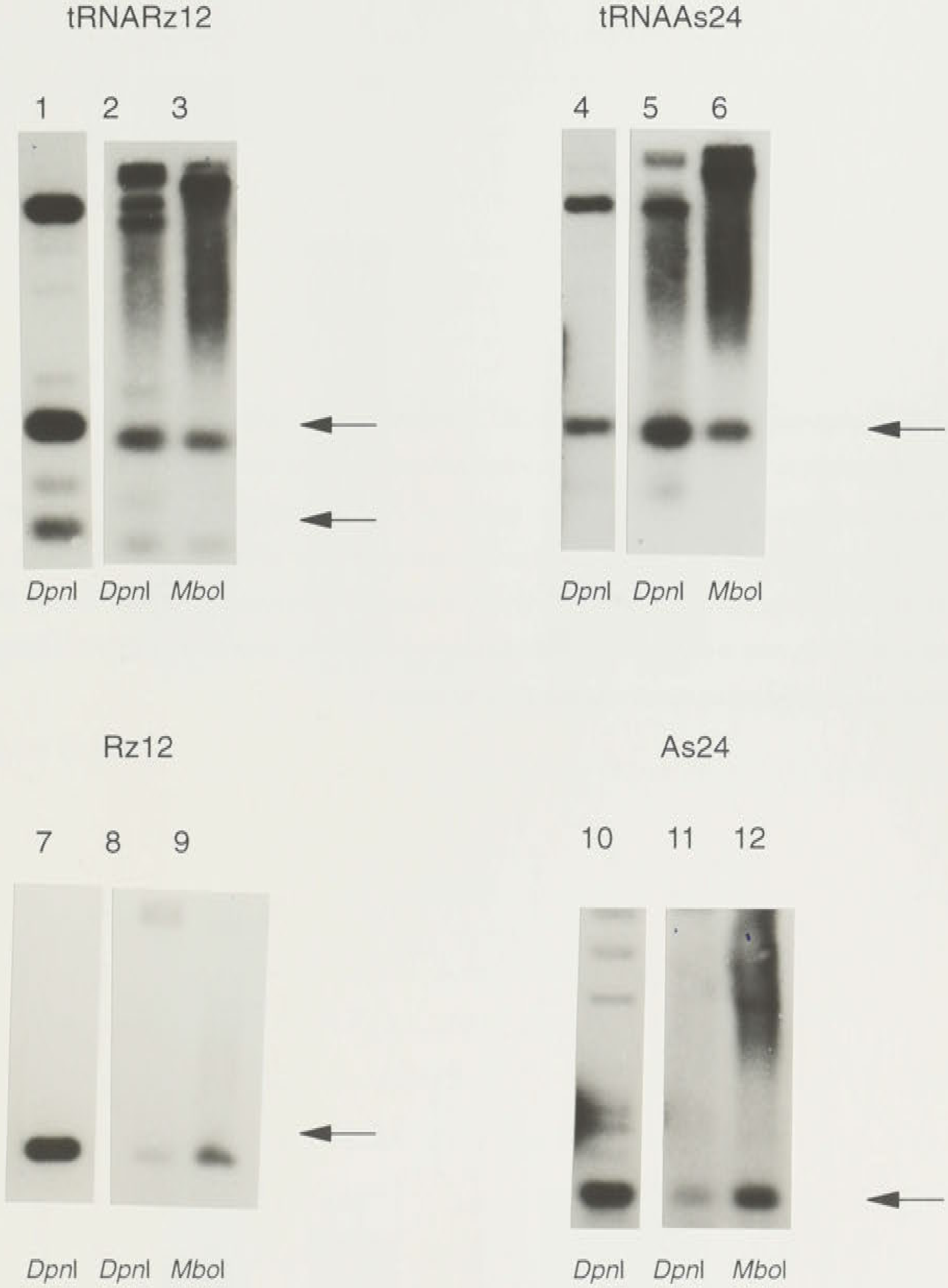
tRNARz12
tRNAAs24
1
2
3
4
5
6
DpnI
DpnI
MboI
DpnI
DpnI
MboI
Rz12
As24
7
8
9
10
11
12
DpnI
DpnI
MboI
DpnI
DpnI
MboI

Figure 5.3

Figure 5.4: Expression of the **(a)** wildtype CAT and **(b)** mutant CM2 targets from the ACMV vector in the presence of control (grey), non-embedded ribozyme (yellow), non-embedded antisense (red), tRNA-embedded ribozyme (green) or tRNA-embedded antisense (blue) ACMV vectors 3 days post transfection. Chloramphenicol acetylation for co-transfected ribozyme and antisense constructions were expressed as a percentage of acetylation of co-transfected tRNA plasmid (i.e. control), and results of seven protoplast preparations were averaged. The tables present the mean and standard error for each combination.

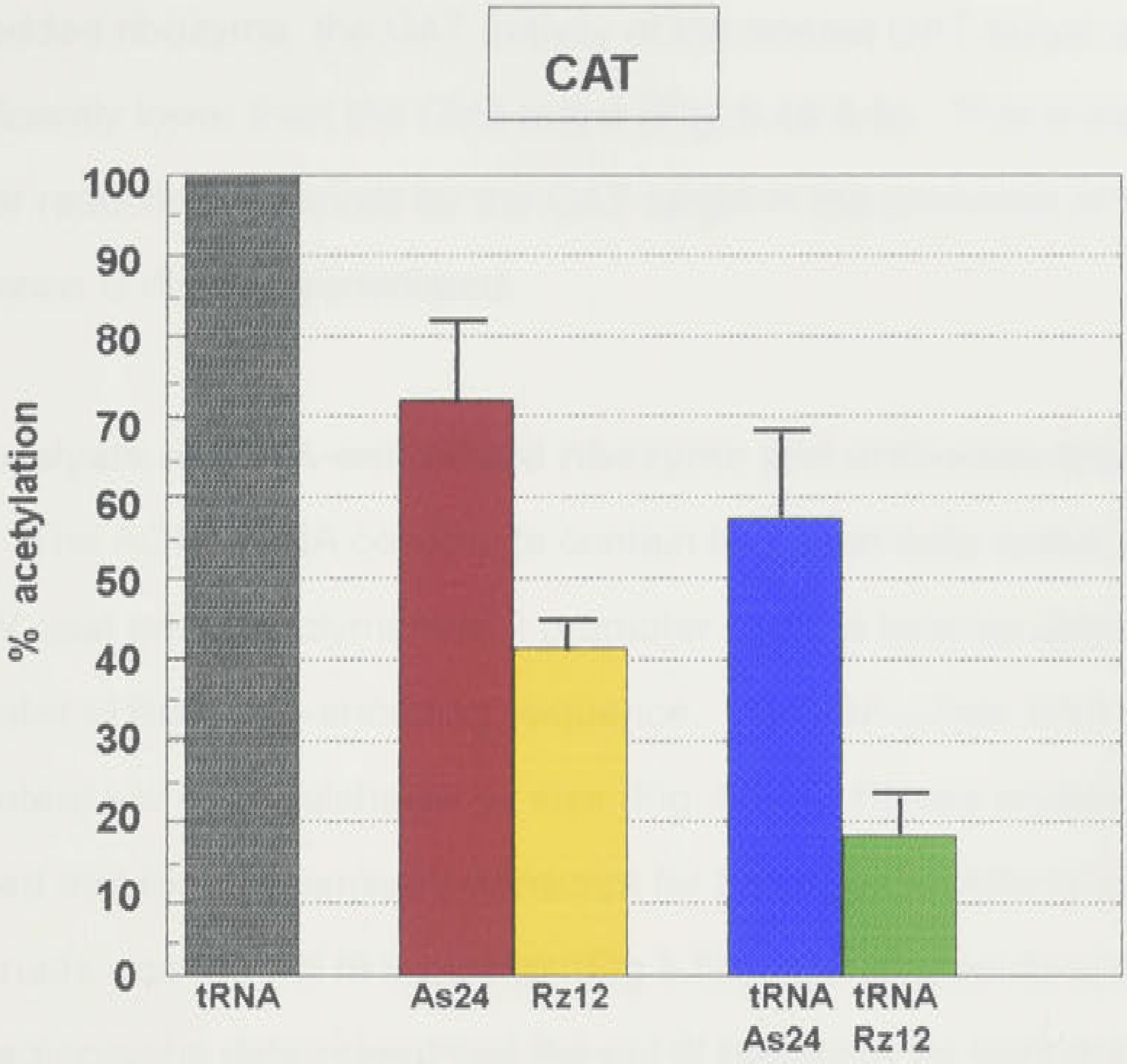

Figure 5.4a

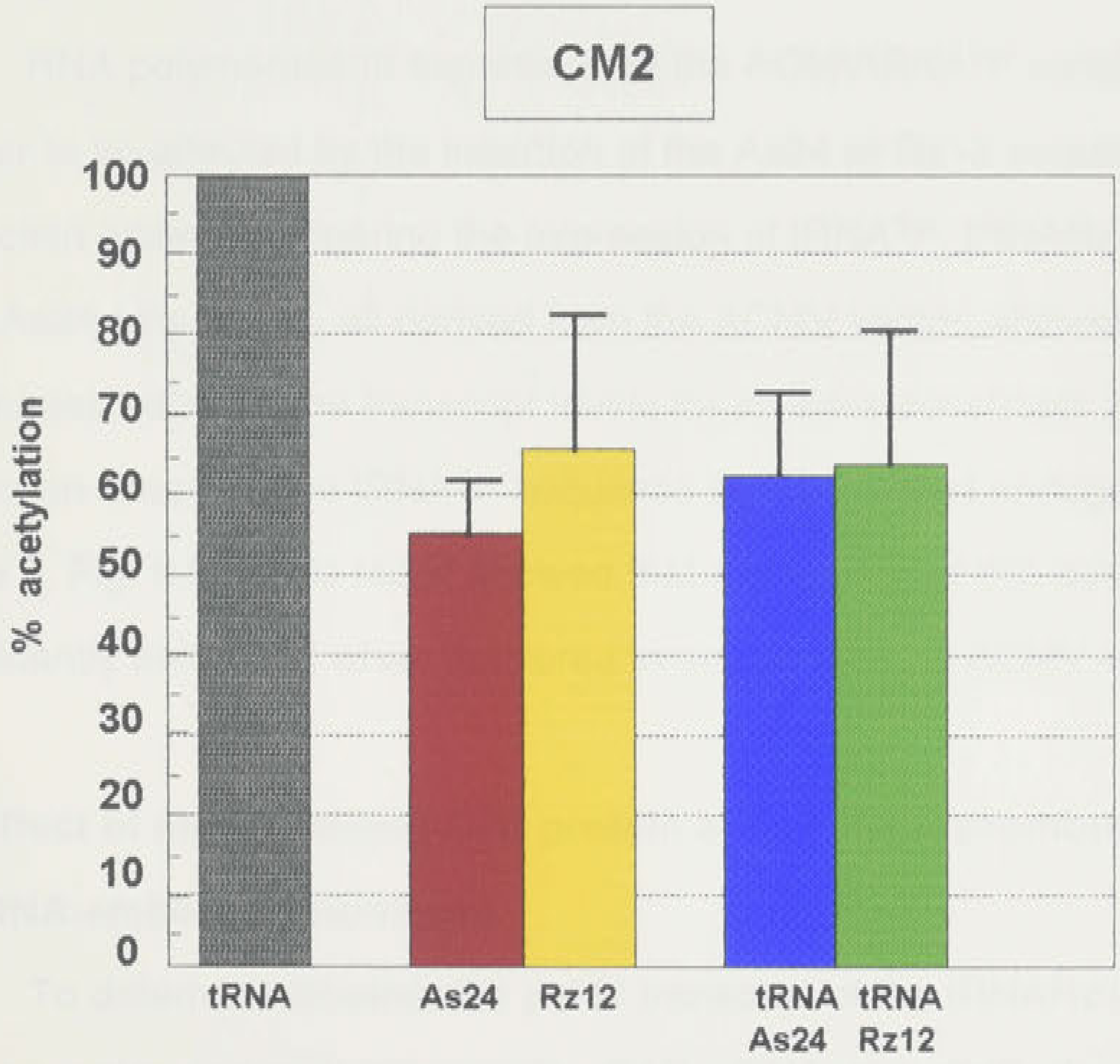

Figure 5.4b

ribozyme contribution (Fig. 5.4a & b). In the presence of the tRNA-embedded ribozyme, the CAT activity of the normal CAT target was significantly lower than the CM2 target (Fig. 5.4a & b). This shows that the further reduction observed for the CAT target in the presence of the tRNARz12 sequence is ribozyme-mediated.

5.4 Analysis of tRNA-embedded ribozyme and antisense transcripts

The ACMVtRNA constructs contain two potentially active promoters: the ACMV coat protein polymerase II promoter and the internal polymerase III promoter of the tRNA-encoding sequence. The transcripts from these promoters are distinguishable by size (Fig. 5.5a). RNase protection assays showed that the predominant transcript for both the tRNARz12 and tRNAAs24 constructs was the pol III transcript (Fig 5.5b). Densitometric scanning of the autoradiographs determined that the pol III transcript for both the tRNARz12 and tRNAAs24 transcripts was at least 150 fold more abundant than the pol II transcript.

RNA polymerase III expression of the ACMVtRNA^{Tyr} constructs did not appear to be affected by the insertion of the As24 or Rz12 sequences. RNase protection assays comparing the expression of tRNA^{Tyr}, tRNARz12 and tRNAAs24 sequences, all derived from the ACMV vector, showed no significant differences between the transcript levels for all three constructs (Fig. 5.6). The protection assay on the tRNA^{Tyr} sequence also protected endogenous tRNA^{Tyr} (Lane 3, Fig. 5.6). This result showed that expression of this sequence was significantly enhanced when delivered to cells within the ACMV vector.

5.5 Effect of mutagenising coat protein and/or tRNA promoter sequences on tRNA-embedded ribozyme

To determine whether the pol III transcript of the tRNARz12 construct was the active molecule cleaving the CAT mRNA, the effect of mutagenising and inactivating one or both of the promoter sequences was examined (Fig.

Figure 5.5:

a: Map of pAtRNARz12 or pAtRNAAs24 constructions showing transcription start and stop sites for RNA polymerase II (i.e. pol II start and pol II termination) and RNA polymerase III (i.e. pol III start and pol III termination) derived transcripts. The distance in bp between pol II and pol III start and stop sites is indicated beneath the figure. The approximate length of the riboprobe transcript used for RNase protection assays in figures 5.5b, 5.6 and 5.7b is also shown as a hatched line.

b: RNase protection assay for the relative abundance of pol II and pol III transcripts of tRNARz12 (1-4) and tRNAAs24 (5-8). Lanes 1-8 are: **1**, undigested tRNARz12 riboprobe; **2**, RNase A/T1 digested tRNARz12 riboprobe; **3**, tRNARz12 probe + 10μg RNA from mock transfected *N.tabacum*; **4**, tRNARz12 probe + 10μg RNA from pACAT + pAtRNARz12 transfected *N.tabacum*; **5**, undigested tRNAAs24 riboprobe; **6**, RNase A/T1 digested tRNAAs24 riboprobe; **7**, tRNAAs24 probe + 10μg RNA from mock transfected *N.tabacum*; **8**, tRNAAs24 probe + 10μg RNA from pACAT + pAtRNAAs24 transfected *N.tabacum*. RNA species are: **pol II**, RNA polymerase II derived tRNARz12 or tRNAAs24 transcripts; **pol III**, RNA polymerase III derived tRNARz12 or tRNAAs24 transcripts; **undig**, undigested tRNARz12 or tRNAAs24 riboprobe. RNA molecular weight markers are indicated.

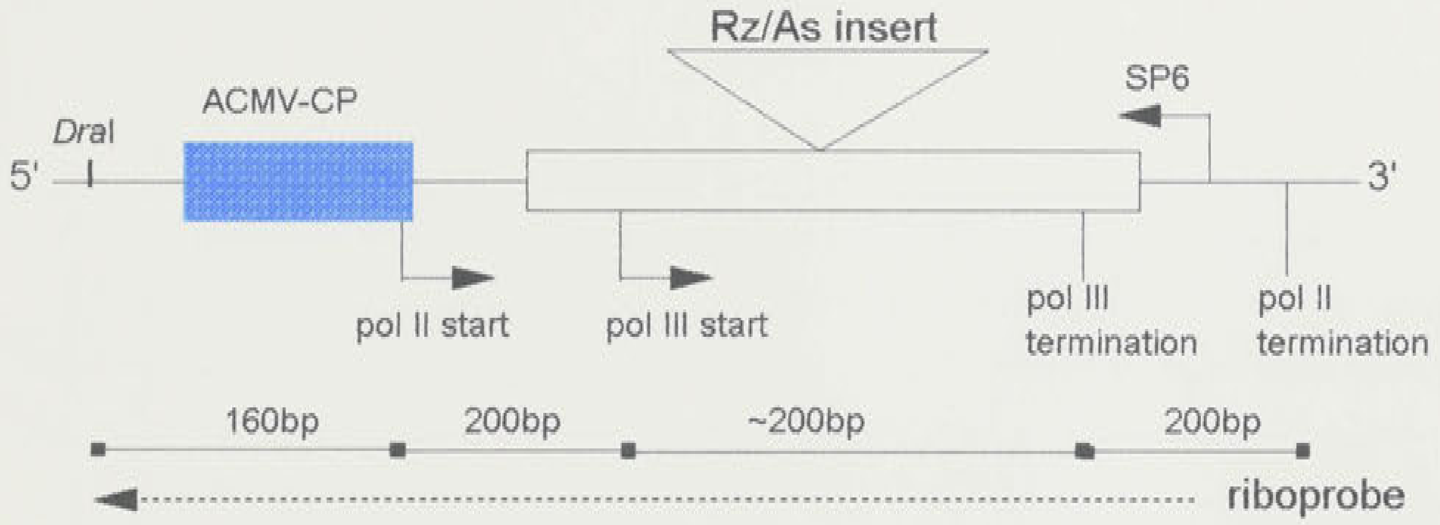
Rz/As insert
ACMV-CP
SP6
DraI
5'
3'
pol II start
pol III start
pol III termination
pol II termination
160bp
200bp
~200bp
200bp
riboprobe

Figure 5.5a

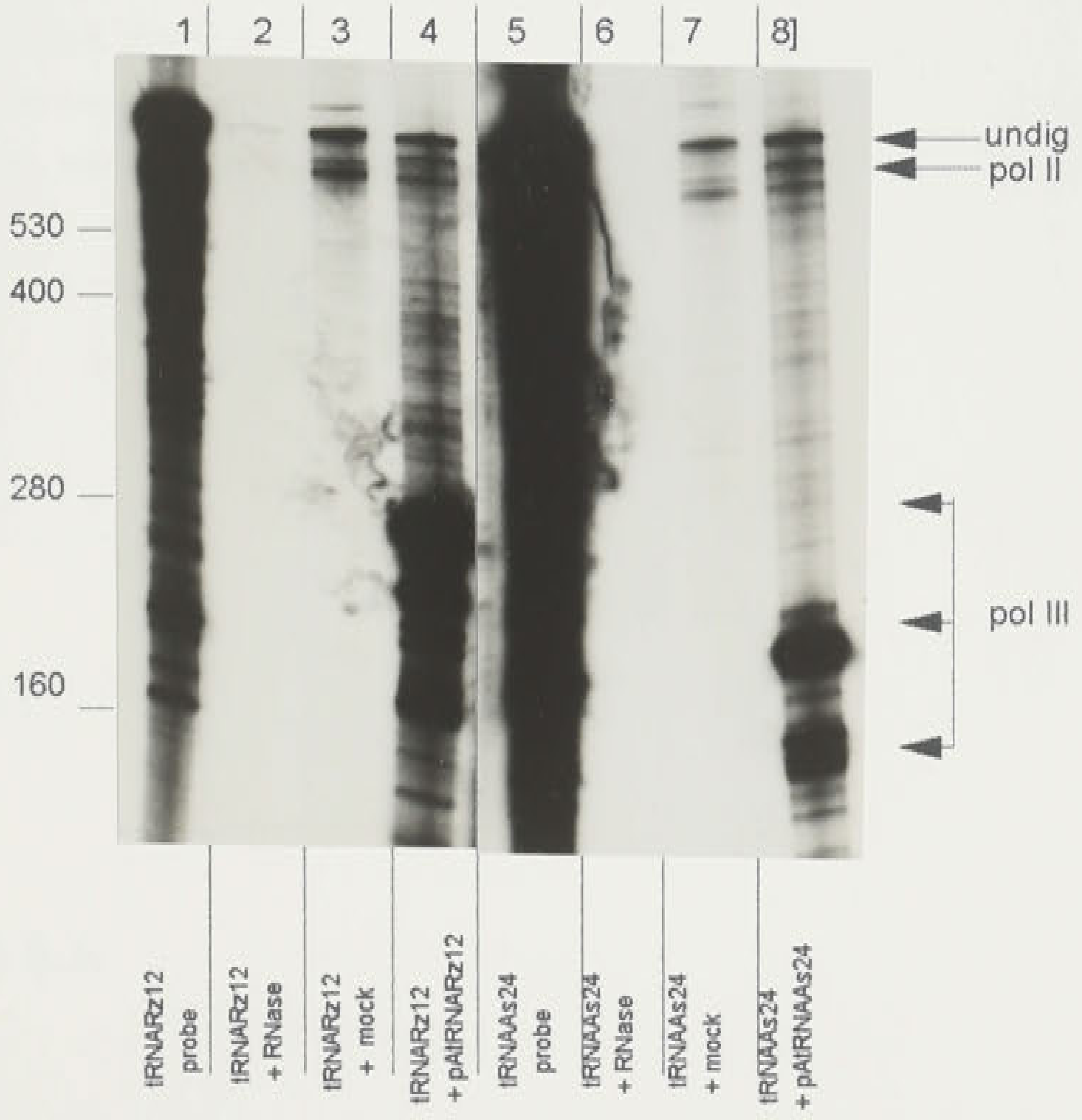
1
2
3
4
5
6
7
8]
530
400
280
160
undig
pol II
pol III
tRNARz12 probe
tRNARz12 + RNase
tRNARz12 + mock
tRNARz12 + pAtRNARz12
tRNAAs24 probe
tRNAAs24 + RNase
tRNAAs24 + mock
tRNAAs24 + pAtRNAAs24

Figure 5.5b

Figure 5.6: RNase protection assay for the relative abundance of RNA polymerase III transcripts from ACMV vectors expressing tRNA (lanes 1-4), tRNAAs24 (lanes 5-8) or tRNARz12 (lanes 9-12) sequences. Lanes 1-12 are: **1**, undigested tRNA riboprobe; **2**, RNase A/T1 digested tRNA riboprobe; **3**, tRNA probe + 10μg RNA from mock transfected *N.tabacum*; **4**, tRNA probe + 10μg RNA from pACAT + pAtRNA transfected *N.tabacum*; **5**, undigested tRNAAs24 riboprobe; **6**, RNase A/T1 digested tRNAAs24 riboprobe; **7**, tRNAAs24 probe + 10μg RNA from mock transfected *N.tabacum*; **8**, tRNAAs24 probe + 10μg RNA from pACAT + pAtRNAAs24 transfected *N.tabacum*; **9**, undigested tRNARz12 riboprobe; **10**, RNase A/T1 digested tRNARz12 riboprobe; **11**, tRNARz12 probe + 10μg RNA from mock transfected *N.tabacum*; **12**, tRNARz12 probe + 10μg RNA from pACAT + pAtRNARz12 transfected *N.tabacum*. RNA species are: **pol II**, RNA polymerase II derived tRNARz12, tRNAAs24 and tRNA transcripts; **pol III**, RNA polymerase III derived tRNARz12, tRNAAs24 and tRNA transcripts; **undig**, undigested tRNARz12, tRNAAs24 or tRNA riboprobe. RNA molecular weight markers are indicated.

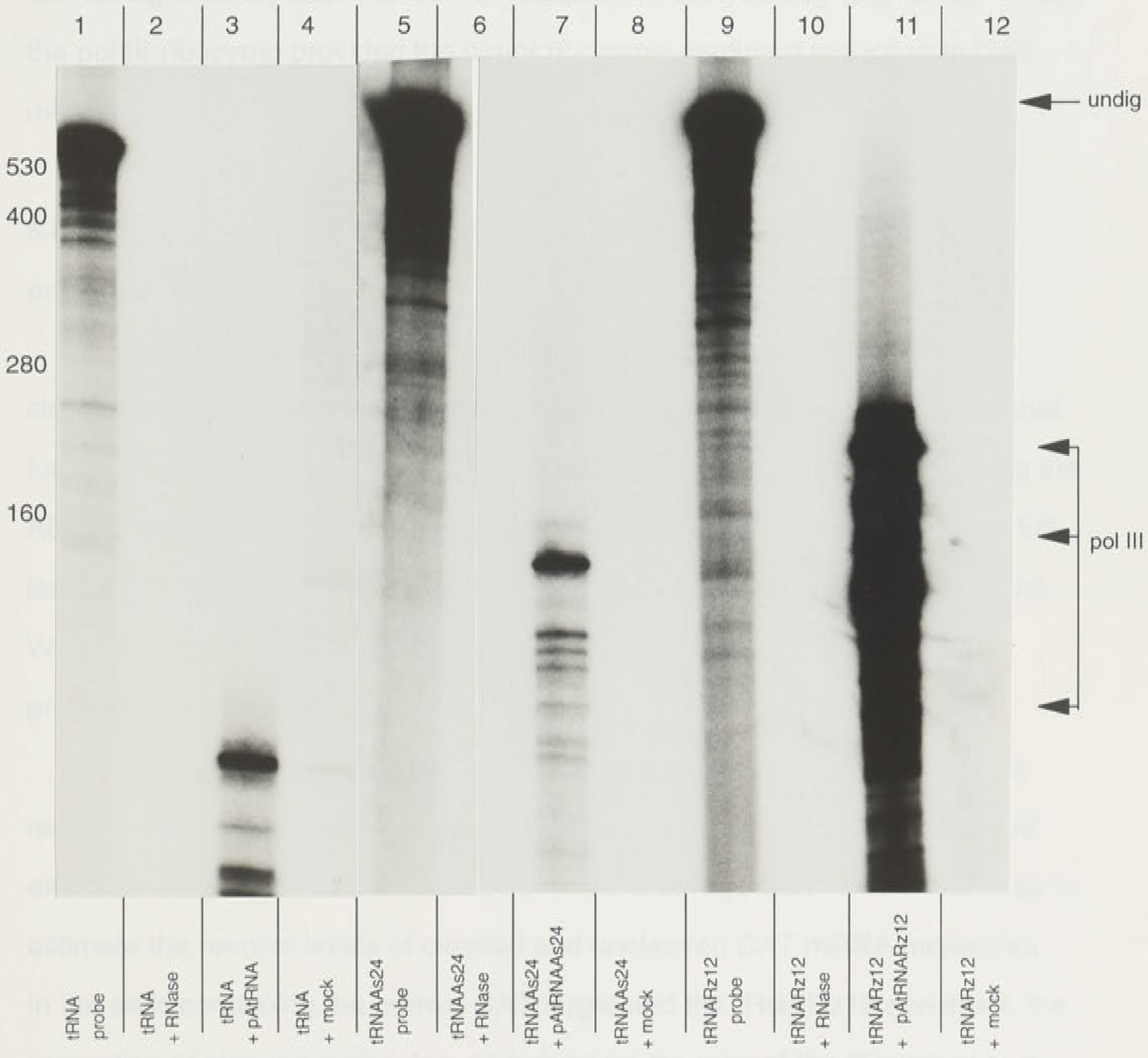
1
2
3
4
5
6
7
8
9
10
11
12
530
400
280
160
undig
pol III
tRNA probe
tRNA + RNase
tRNA + pAtRNA
tRNA + mock
tRNAAs24 probe
tRNAAs24 + RNase
tRNAAs24 + pAtRNAAs24
tRNAAs24 + mock
tRNARz12 probe
tRNARz12 + RNase
tRNARz12 + pAtRNARz12
tRNARz12 + mock

Figure 5.6

5.7a). RNase protection assays showed that transcripts derived from either the pol III (MB), pol II (MA) or both promoters (MAB) were significantly decreased after mutagenising (Fig. 5.7b).

Mutagenesis of the pol III promoter of the tRNARz12 construct restored CAT activity to control levels. In contrast, mutagenesis of the pol II promoter did not significantly alter the level of reduction in CAT activity (Fig. 5.7c). Thus, the pol III-ribozyme provided the major ribozyme-mediated reduction in CAT mRNA.

5.6 Analysis of accumulation of CAT mRNA and ribozyme cleavage products *in vivo.*

RNase protection assays were used to try to visualise ribozyme cleavage products from the transfected plant cells. These assays showed that full length CAT mRNA could be protected in control transfections containing the ACMV constructs expressing CAT and the empty tRNA vector, but that no full length CAT mRNA was protected in the presence of the tRNARz12 construct. We were not able to detect RNA sequences representing the cleavage products (Fig. 5.8).

Ribozyme cleavage products were assayed in the plant cells using a reverse transcriptase-PCR (RT-PCR) approach with primers which amplified either full length CAT mRNA or RNA 3' of the cleavage site. This enabled us to estimate the relative levels of cleaved and uncleaved CAT mRNA molecules. In the cells containing the normal CAT target and the tRNARz12 construct, the proportion of cleaved molecules, as judged by the ratio of the 3' product to the full length CAT product, was 3.3 (Fig. 5.9). This was significantly higher than any of the other ribozyme or antisense-target combinations. This increased proportion of amplification products representing the 3' cleavage product, in the presence of the tRNARz12 construct, demonstrates that *in vivo* cleavage of CAT mRNA was occurring.

Figure 5.7:

a: Map of pAtRNARz12 construction indicating base substitutions carried out to produce defective RNA polymerase II (MA) and/or RNA polymerase III (MB) promoter sequences (see chapter 2, Fig. 2.5). For the construction of pAtRz12MA plasmid, the TATATA sequence at position 251-256 was altered to GGGTG (see MA box above plasmid map). For the construction of pAtRz12MB plasmid, the C at position 56 was altered to a G (see MB box). A (green) and B (red) are RNA polymerase III recognition signals and the light blue box is 13 base intron. Pol II and III start sites are indicated as in previous figures except that lettering is strike through indicating loss of function. ψ at position 55 in the transcript of pAtRNARz12MB is a pseudouridine. The plasmid pAtRNARz12MAB (not shown) contains both promoter mutations.

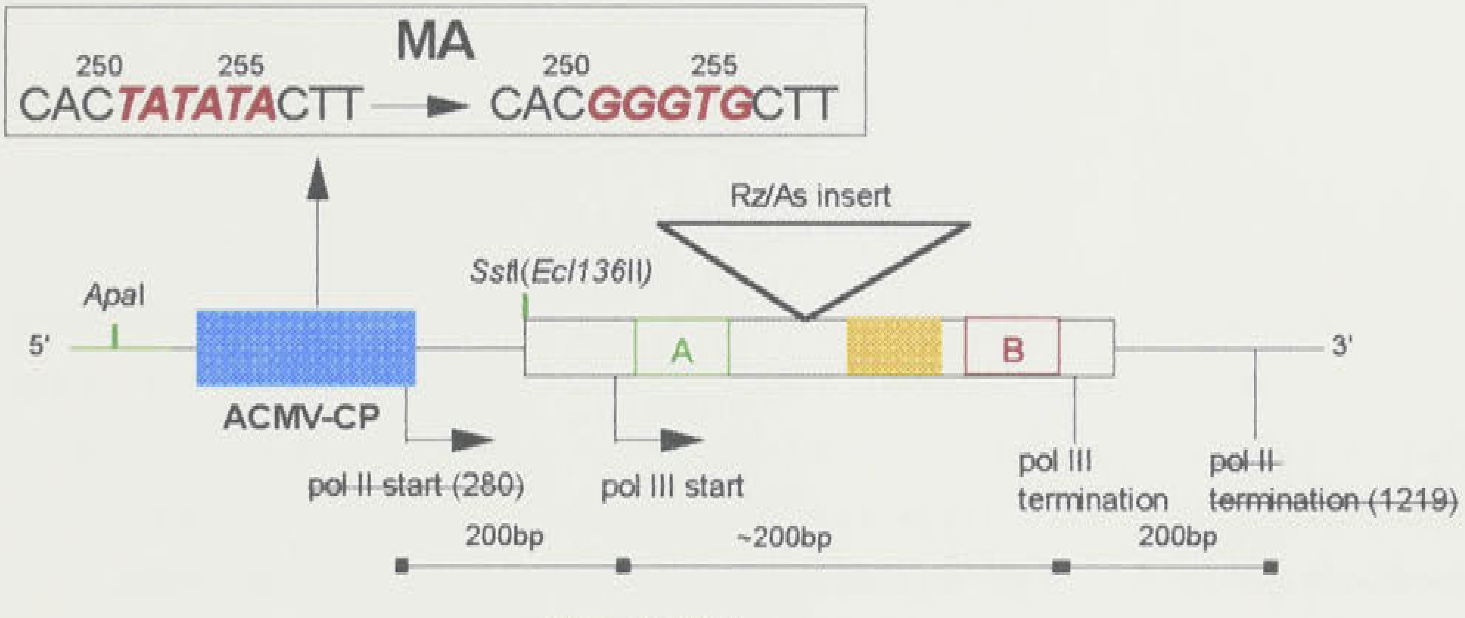
MA
250
255
CACTATATACTT
250
255
CACGGGTGCTT
Rz/As insert
ApaI
SsfI(Ecl136II)
5'
A
B
3'
ACMV-CP
~~pol II start (280)~~
pol III start
pol III termination
~~pol II termination (1219)~~
200bp
~200bp
200bp

pAtRz12MA

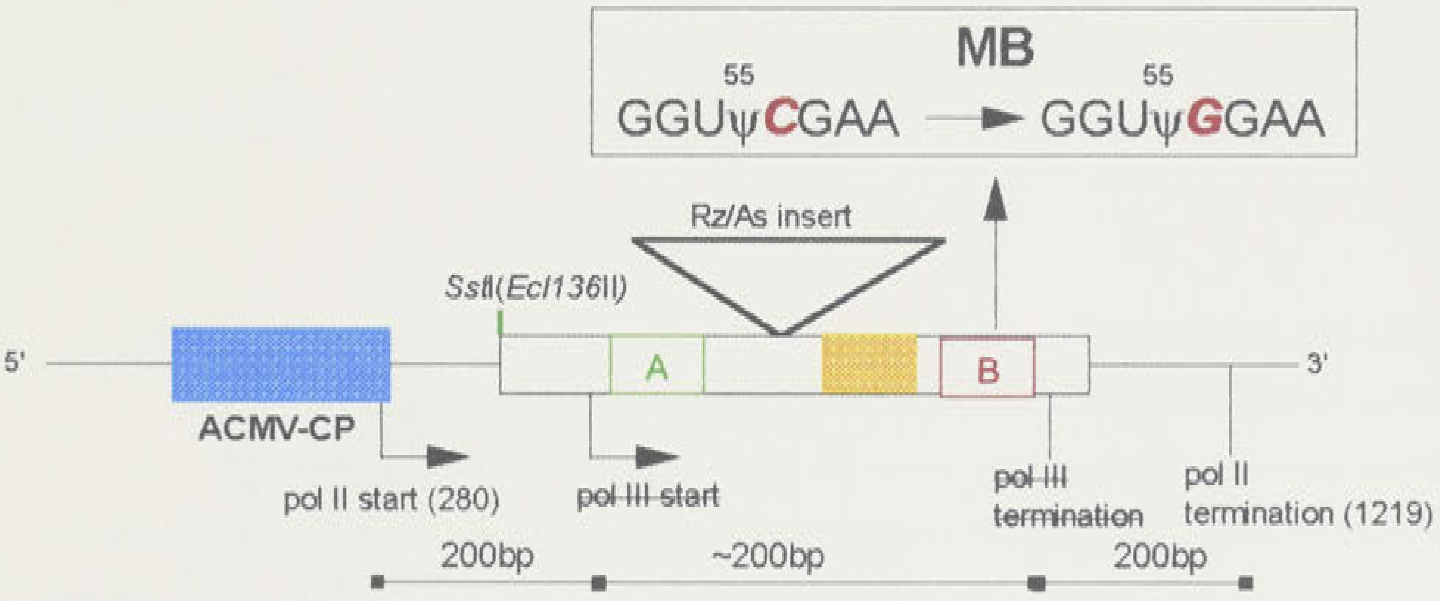
MB
55
GGUψCGAA
55
GGUψGGAA
Rz/As insert
SsfI(Ecl136II)
5'
A
B
3'
ACMV-CP
pol II start (280)
~~pol III start~~
~~pol III termination~~
pol II termination (1219)
200bp
~200bp
200bp

pAtRz12MB

Figure 5.7a

Figure 5.7

b: RNase protection assay showing relative abundance of pol II and/or pol III derived tRNARz12 transcripts for mutant promoter constructs. Lanes 1-7 are: **1**, undigested tRNARz12 riboprobe; **2**, RNase A/T1 digested tRNARz12 riboprobe; **3**, tRNARz12 probe + 10µg RNA from mock transfected *N.tabacum*; **4**, tRNARz12 probe + 10µg RNA from pACAT + pAtRNARz12 transfected *N.tabacum*; **5**, tRNARz12 probe + 10µg RNA from pACAT + pAtRNARz12MA transfected *N.tabacum*; **6**, tRNARz12 probe + 10µg RNA from pACAT + pAtRNARz12MB transfected *N.tabacum*; **7**, tRNARz12 probe + 10µg RNA from pACAT + pAtRNARz12MAB transfected *N.tabacum*. RNA species are as for 5.5b and 5.6: **pol II**, RNA polymerase II transcripts; **pol III**, RNA polymerase III transcripts; **undig**, undigested tRNARz12 riboprobe.

c: Expression of CAT from the ACMV vector in the presence of tRNARz12 constructs containing mutant RNA polymerase II and/or III promoter sequences. As for Fig. 5.4, chloramphenicol acetylation in the presence of control (grey), tRNARz12 (green), tRNARz12MA (red), tRNARz12MB (yellow) and tRNARz12MAB (white) was expressed as a percentage of the acetylation of co-transfected ACMVtRNA plasmid, and the results of three independent preparations averaged. The table presents the mean and standard error for each combination.

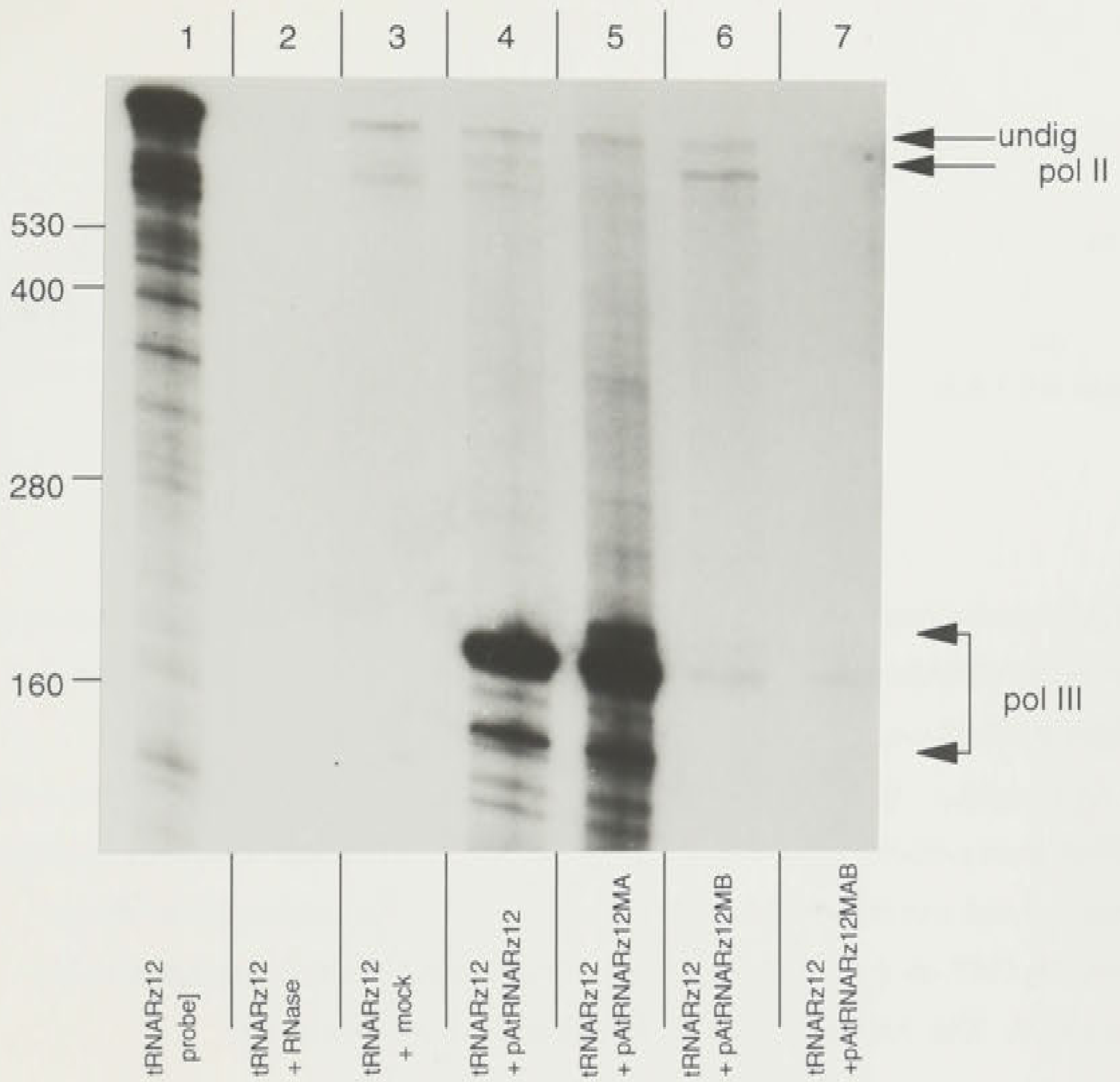
1
2
3
4
5
6
7
530
400
280
160
undig
pol II
pol III
tRNARz12 probe]
tRNARz12 + RNase
tRNARz12 + mock
tRNARz12 + pAtRNARz12
tRNARz12 + pAtRNARz12MA
tRNARz12 + pAtRNARz12MB
tRNARz12 +pAtRNARz12MAB

Figure 5.7b

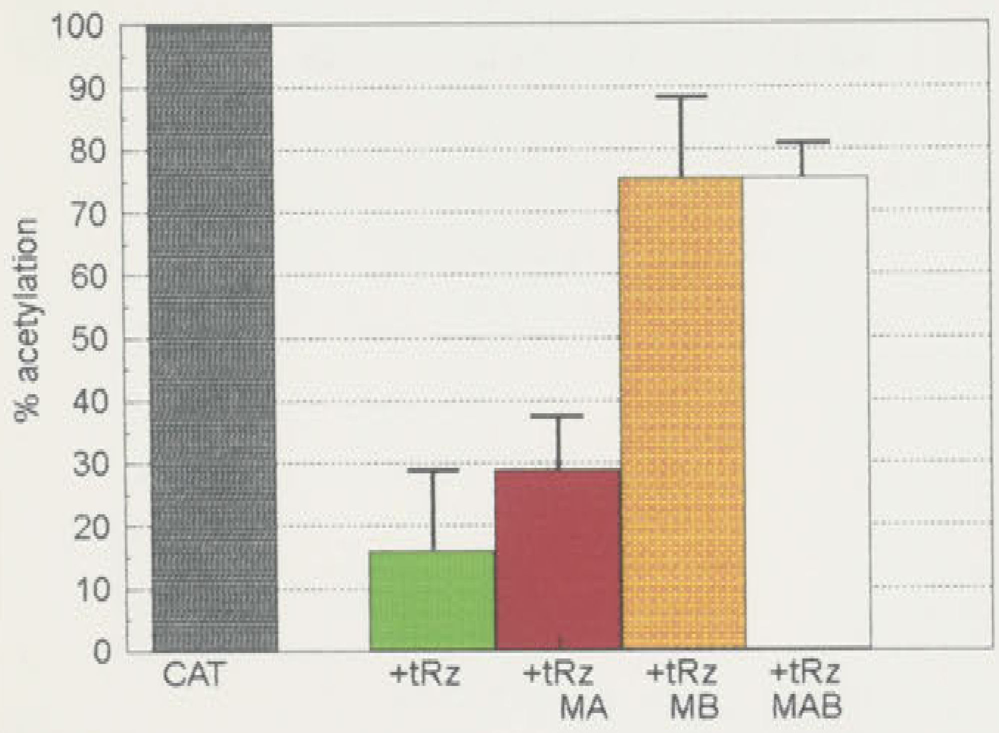

Figure 5.7c

Figure 5.8: RNase protection for the relative abundance of CAT mRNA in the presence or absence of the ACMVtRNARz12 construct. Lanes 1-5 are: **1**, undigested CAT probe; **2**, RNase A/T1 digested CAT probe; **3**, CAT probe + 20µg RNA from mock transfected *N.tabacum*; **4**, CAT probe + 20µg RNA from pACAT + pAtRNA transfected *N.tabacum*; **5**, CAT probe + 20µg RNA from pACAT + pAtRNARz12 transfected *N.tabacum*. The RNA species is: **CAT**, CAT riboprobe and protected CAT mRNA fragment. The figure above the RNase protection shows the CAT riboprobe derived from SP6 RNA polymerase transcription of pACAT/*Pvu*II plasmid. The dotted line shows the approximate probe length.

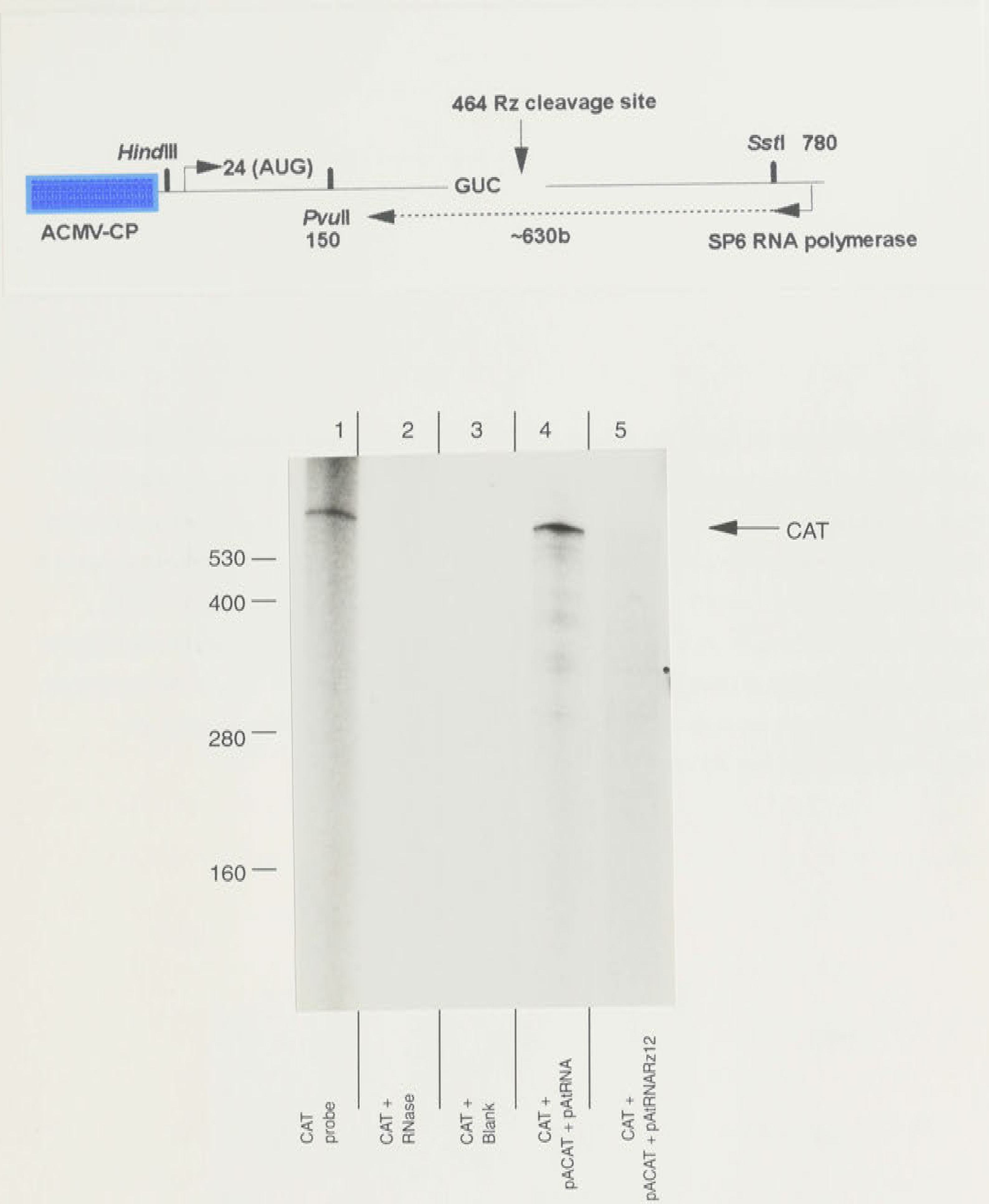
464 Rz cleavage site
HindIII
24 (AUG)
GUC
SstI 780
ACMV-CP
PvuII
150
~630b
SP6 RNA polymerase
1
2
3
4
5
530
400
280
160
CAT
CAT probe
CAT + RNase
CAT + Blank
CAT + pACAT + pAtRNA
CAT + pACAT + pAtRNARz12

Figure 5.8

Figure 5.9: Analysis by RT-PCR of accumulation of uncleaved and cleaved CAT mRNA. Southern hybridisation blot of reverse transcriptase- and PCR-generated products with total RNA extracted from transfected *N.tabacum* cells as template, for CAT or CM2 target constructs. Co-transfected constructs were: lanes **1** and **2**, pAtRNA; lanes **3** and **4**, pAtRNARz12; lanes **5** and **6**, pAtRNAAs24; lanes **7** and **8**, pARz12; lanes **9** and **10**, pAAs24. **Band 1** is the product corresponding to uncleaved CAT mRNA (primers 1 + TAG; odd numbered lanes), and **band 2** is the product of cleaved or uncleaved CAT mRNA (primers 2 + TAG; even numbered lanes). The numbers beneath each pair of 1 + TAG and 2 + TAG amplification products represent the ratio of band 2 : band 1 for each construct pairing.

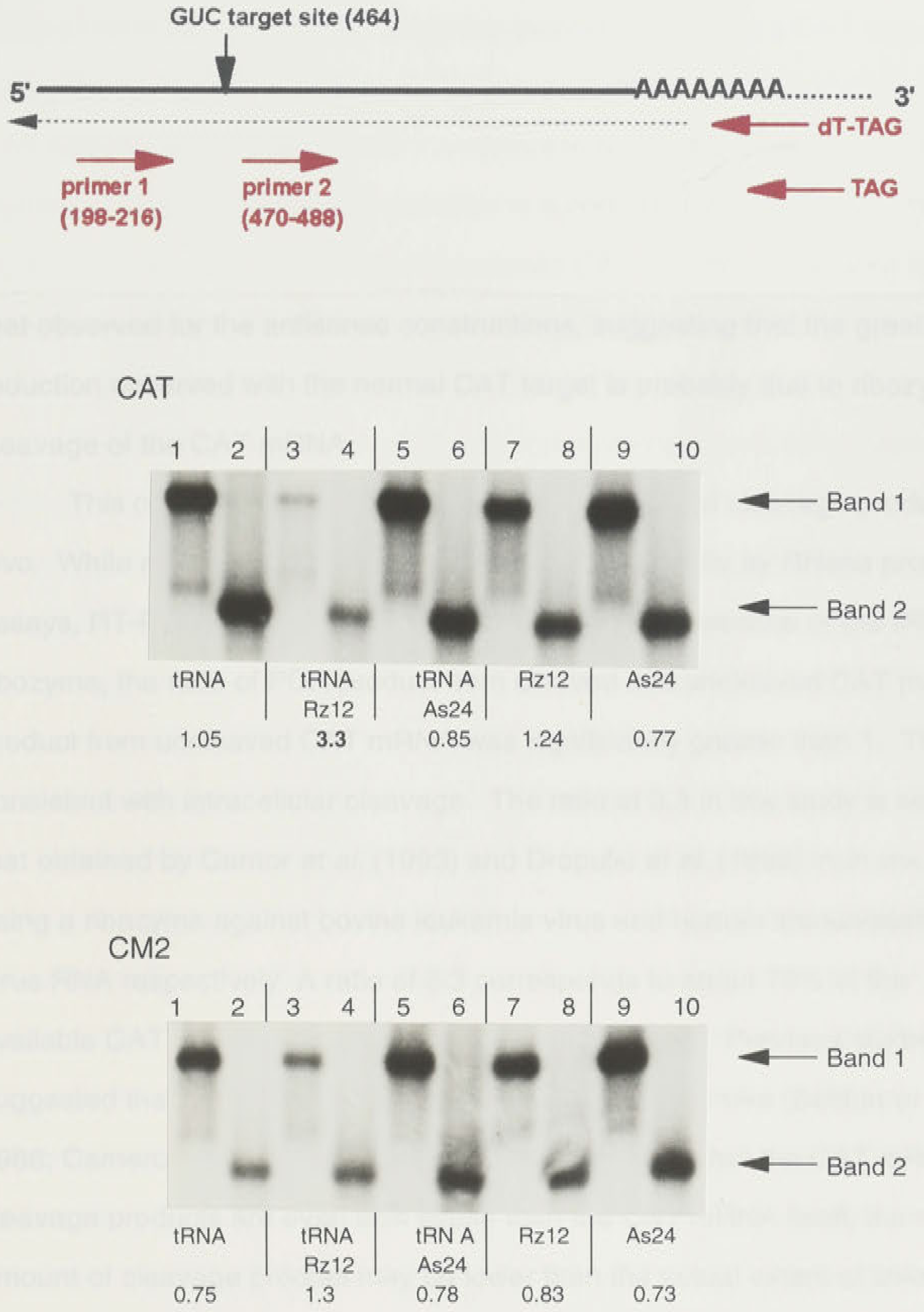
GUC target site (464)
5'
AAAAAAAA..........
3'
dT-TAG
primer 1
(198-216)
primer 2
(470-488)
TAG
CAT
1 2 3 4 5 6 7 8 9 10
Band 1
Band 2
tRNA
tRNA Rz12
tRN A As24
Rz12
As24
1.05
3.3
0.85
1.24
0.77
CM2
1 2 3 4 5 6 7 8 9 10
Band 1
Band 2
tRNA
tRNA Rz12
tRN A As24
Rz12
As24
0.75
1.3
0.78
0.83
0.73

Figure 5.9

DISCUSSION

These results have demonstrated that transfection of tobacco protoplasts with self-replicating vectors expressing a CAT target sequence and a tRNA-embedded ribozyme resulted in an 80% reduction in CAT activity. In the presence of the mutant target, CM2, in which a known cleavable GUC target site was mutated to a non-cleavable GUG (Perriman *et al.*, 1992), the tRNARz12 sequence reduced CAT activity to the same level as that observed for the antisense constructions, suggesting that the greater reduction observed with the normal CAT target is probably due to ribozyme cleavage of the CAT mRNA.

This conclusion is also supported by the assay of cleavage products *in vivo*. While no cleavage products were observed directly by RNase protection assays, RT-PCR on CAT mRNA showed that, in the presence of the tRNA-ribozyme, the ratio of PCR product from cleaved and uncleaved CAT mRNA to product from uncleaved CAT mRNA was significantly greater than 1. This is consistent with intracellular cleavage. The ratio of 3.3 in this study is similar to that obtained by Cantor *et al.* (1993) and Dropulic *et al.* (1992) in *in vivo* assays using a ribozyme against bovine leukemia virus and human immunodeficiency virus RNA respectively A ratio of 3.3 corresponds to about 70% of the available CAT mRNA sequences being cleaved *in vivo*. Previous studies have suggested that the CAT mRNA is inherently unstable *in vivo* (Seldon *et al.*, 1986; Cameron and Jennings, 1989). Since it is likely that the CAT mRNA cleavage products are even less stable than the CAT mRNA itself, the detected amount of cleavage product may be lower than the actual extent of cleavage of CAT mRNA by the tRNA-ribozyme. This would also explain why the RNase protection assays did not detect *in vivo* derived ribozyme cleavage products.

As shown in chapter 4, the tRNARz12 ribozyme was less effective than the non-embedded Rz12 ribozyme *in vitro*, but in the *in vivo* experiments presented in this chapter, the tRNA-ribozyme was more effective. The three likely ways in which a tRNA molecule could enhance a ribozymes effectiveness *in vivo*, are increased transcription, increased stabilisation and/or optimal intracellular localisation of the transcript. No direct evidence has been obtained for the increased stability of the tRNA-ribozyme in this system. In addition, there is no evidence regarding the intracellular location of the tRNA-ribozyme transcripts. Based on previous studies (Tobian *et al.*, 1985; Cotten and Birnstiel, 1989), the modifications to the tertiary structure of the tRNA used in this study are likely to diminish transport to the cytoplasm. Therefore, it is probable that the tRNA-embedded ribozyme is nuclear, perhaps giving it greater target accessibility.

The steady state levels of this ribozyme derived from the polymerase III promoter, are in large excess (~150 times) over the RNA polymerase II transcript levels. A similar chimeric pol II/pol III tRNA construction in yeast cells, also showed a high ratio of pol III to pol II transcripts (Kinsey and Sandemeyer, 1991). Inactivation of the RNA polymerase III promoter in our system decreased ribozyme activity confirming that a high level of the tRNARz12 transcript was necessary for ribozyme effectiveness (Fig. 5.7). The Rz12 and tRNARz12 transcripts expressed from the same RNA polymerase II promoter produced different levels of reduction in CAT activity. While the non-embedded ribozyme did reduce CAT activity (Fig. 5.4a- CAT + Rz12), the RNA polymerase II derived tRNA-embedded ribozyme had only minimal effect (Fig. 5.7c - CAT + tRNARz12MB). These results suggest that the increased effectiveness of the tRNARz12 construct is due primarily to the high level transcription of this molecule from the RNA polymerase III promoter. They also demonstrate that, when both the non-embedded and tRNA-embedded ribozyme are expressed at equivalent levels *in vivo*, the non-embedded ribozyme is the more efficient molecule. In this respect, the *in vitro* and *in vivo* cleavage assays for the two ribozyme constructs are in agreement.

A comparison of the relative levels of transcription of the wildtype and recombinant $tRNA^{Tyr}$ constructs revealed no significant difference in expression between the three sequences. Interestingly, the transcript levels of the normal tRNA^{Tyr} were considerably higher when expressed from the ACMV vector than the endogenous tRNA^{Tyr} levels. The possible implications of this will be discussed in more detail in chapter 6.

By combining RNA polymerase III transcription of a chimeric tRNA sequence and an autonomously replicating vector, we have obtained high levels of ribozyme RNAs in plant cells. These high levels of ribozyme RNAs showed enhanced reduction of CAT activity that is consistent with ribozyme-mediated cleavage. Similar results for tRNA delivery systems have also been achieved in *Xenopus* oocytes (Cotten and Birnstiel, 1989; Bouvet *et al.*, 1994; Kandolf, 1994) and a human cell culture (Shore *et al.*, 1993; Baier *et al.*, 1994). Based on the results presented here, chapter 6 will detail experiments which assay the effectiveness of the tRNARz12 construct in reducing target gene activity in transgenic plants.

CHAPTER 6

ANALYSIS OF tRNARz12 AND tRNAAs24 CONSTRUCTS IN TRANSGENIC TOBACCO.

INTRODUCTION

The results presented in chapter 5 established the effectiveness of delivering the hammerhead ribozymes using the $tRNA^{Tyr}$ sequence in a transient system. The aim of the present study was to extend this work so as to use the tRNA-ribozyme constructs to produce target gene inactivation in stably transformed plants. The tRNARz12 and tRNAAs24 constructs were integrated into the genome of tobacco *Nicotiana tabacum*, Ti68, and analysed for their effectiveness in reducing CAT gene activity in whole plants.

A number of independent tobacco lines expressing either the tRNARz12 or tRNAAs24 transgenes were established. These ribozyme and antisense constructs used the endogenous RNA polymerase III promoter of the $tRNA^{Tyr}$ sequence. These constructs also co-expressed the β-glucuronidase (GUS) reporter gene, which was used to monitor whether the plants were transformed.

The target CAT sequence was expressed in an independently transformed Ti68 tobacco line, using the CaMV35S promoter (Guilley *et al.*, 1982). One CAT expressing line, which segregated as a single insertion event, was self-pollinated for four generations and homozygous F4 seed used to cross with F1 tRNARz12 or tRNAAs24 transformants (depicted as tRNARz12 x 35SCAT and tRNAAs24 x 35SCAT in the text). The sibling progeny of each of these crosses contained a mix of $tRNA^{Tyr}$ transgene + and - individuals, while all plants contained the 35SCAT gene. This allowed us to assay for the effect on CAT activity of the presence and absence of the $tRNA^{Tyr}$ constructs in the families derived from each independent transformant. Data is presented for 16 independent tRNARz12 lines and 14 independent tRNAAs24 lines.

RESULTS

6.1. The tRNA-ribozyme or tRNA-antisense co-segregates with GUS activity

To ensure that GUS+ plants contained either of the tRNA^{Tyr}-transgenes, and that GUS- did not, PCR analysis was carried out on randomly selected individual GUS+ and GUS- plants from each independent transformant. PCR reactions showed that all GUS+ plants contained the corresponding tRNA-transgene while none of the GUS- plants tested positive (Fig. 6.1). This meant that our primary GUS screen for the presence or absence of the tRNARz12 or tRNAAs24 transgene was valid.

6.2 Analysis of CAT expression in transgenic plants

8 sibling progeny from each of the 16 tRNARz12 x 35SCAT and 14 tRNAAs24 x 35SCAT crosses were initially assayed for GUS activity. CAT activities were subsequently determined and the mean % acetylation was plotted for GUS+ and GUS- plants within each cross (Fig. 6.2). The results showed that none of the 16 independent transformants containing the tRNARz12 or 14 containing the tRNAAs24 sequences had significantly reduced CAT activity compared to that in sibling plants lacking the corresponding transgene.

6.3 CAT mRNA levels in transgenic plants: a comparison with pACAT transfected plant cells

It was possible that a small reduction in CAT mRNA levels might not have been detected by assaying for CAT enzyme activity. GUS+ and GUS- progeny from 5 independent tRNARz12 x 35SCAT (i.e. lines 15, 20, 35, 43 and 49; see Fig. 6.2) transformants and 3 independent tRNAAs24 x 35SCAT lines (i.e. 27, 28 and 30; see Fig. 6.2) were selected for the analysis of CAT mRNA levels. These lines were chosen because they showed a slight reduction in CAT enzyme activity in the presence of either transgene. The ratio of amplified

Figure 6.1: Example of co-segregation of tRNA^{Tyr} transgene with GUS activity. PCR analysis of GUS + and GUS - individuals from 9 independent tRNARz12 and 9 independent tRNAAs24 Ti68 lines. Lanes represent tRNARz12 lines 1, 3, 15, 16, 19, 20, 21, 35 and 43 and tRNAAs24 lines 3, 4, 8, 15, 16, 24, 27, 28 and 30. GUS + and GUS - individuals are indicated above the gel. Molecular weight markers are pUC19/*Hpa*II (Bresatec). The arrows indicate the tRNARz12 or tRNAAs24 amplification products (see chapter 2; section 2.13 (vi) for details of primers and PCR protocol).

tRNARz12

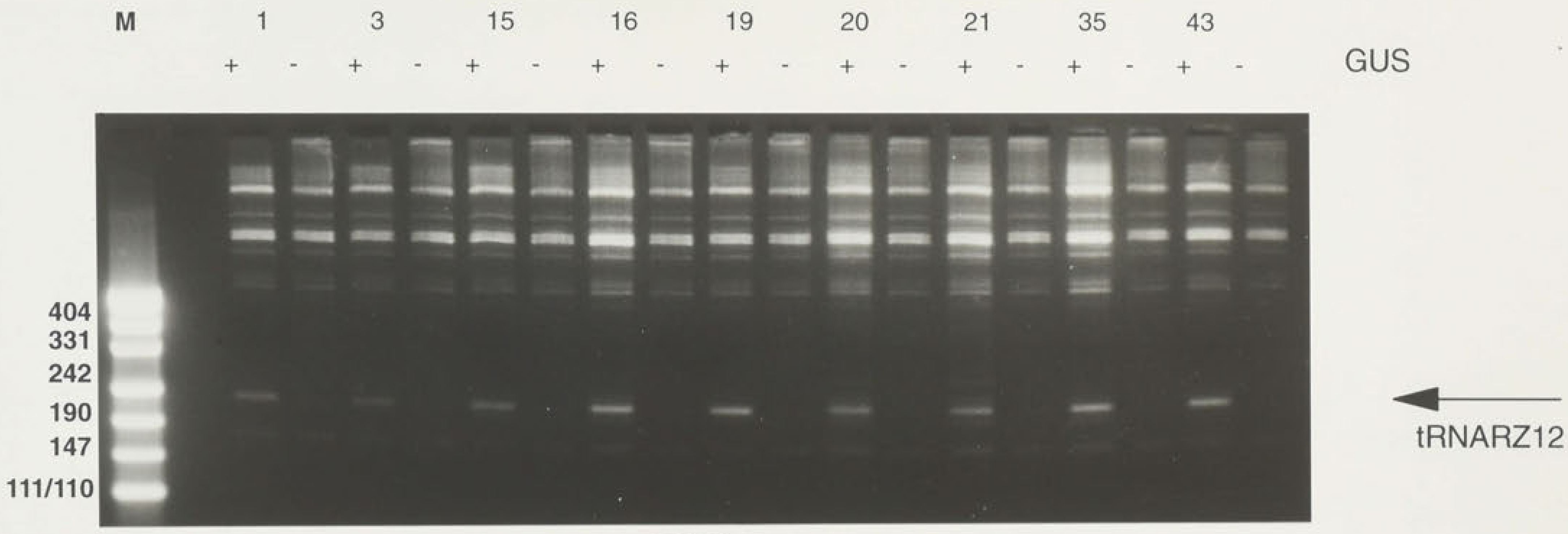
M
1
3
15
16
19
20
21
35
43
GUS
+ - + - + - + - + - + - + - + - + -
404
331
242
190
147
111/110
tRNARZ12

tRNAAs24

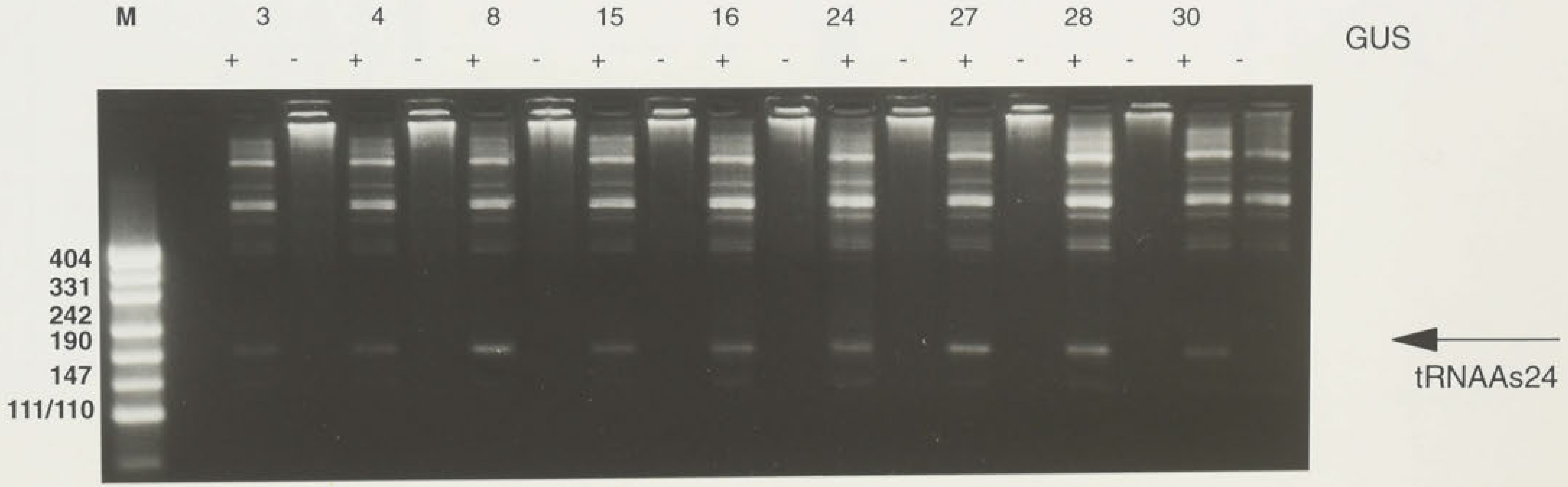
M
3
4
8
15
16
24
27
28
30
GUS
+ - + - + - + - + - + - + - + - + -
404
331
242
190
147
111/110
tRNAAs24

Figure 6.1

Figure 6.2: Analysis of CAT enzyme activity in 16 (tRNARz12 x 35SCAT) and 14 (tRNAAs24 x 35SCAT) lines. The mean % acetylation (y axis) is plotted for GUS + and GUS - sibling progeny from each cross (x axis). This represents the % acetylation from 8 individuals within each cross. Bars in red are GUS + (tRNARz12) plants, bars in blue are GUS + (tRNAAs24) plants and bars in yellow are GUS - . Error bars represent 2 standard deviations.

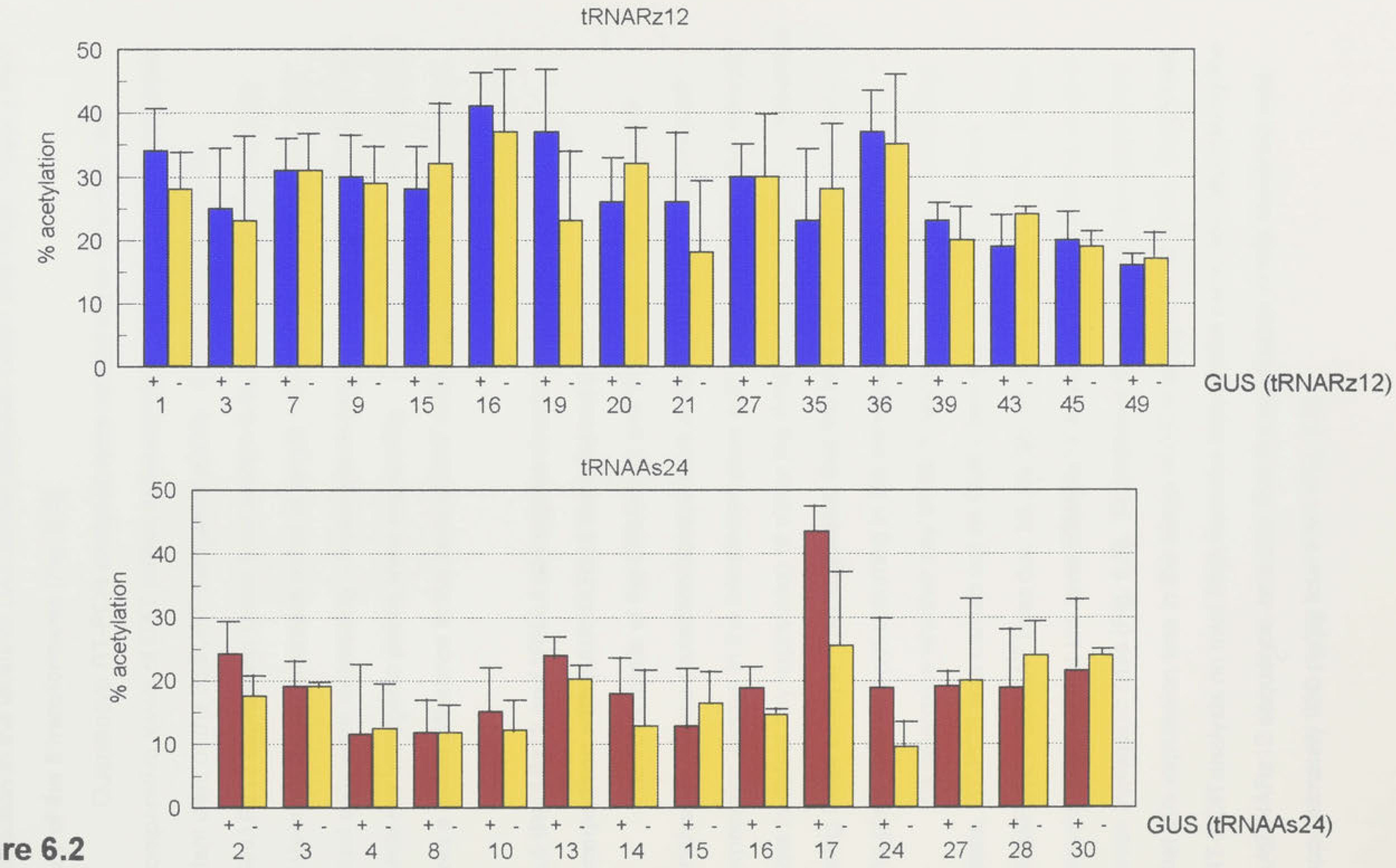
tRNARz12
50
40
30
20
10
0
% acetylation
+ -
1
3
7
9
15
16
19
20
21
27
35
36
39
43
45
49
GUS (tRNARz12)
tRNAAs24
50
40
30
20
10
0
% acetylation
+ -
2
3
4
8
10
13
14
15
16
17
24
27
28
30
GUS (tRNAAs24)

Figure 6.2

CAT product from GUS- : GUS + plants within each transformed line approximated 1 (Fig. 6.3). This suggests that there was no significant reduction in the levels of CAT mRNA between GUS+ and GUS- progeny from any of the 8 transformants (Fig. 6.3).

Quantitative RT-PCR analyses were carried out to determine the comparative levels of CAT mRNA expressed in either the pACAT-transfected plant cells or the 35SCAT-transgenic plants. In combination with the tRNARz12 expression levels (see section 6.4), these results were used to determine the approximate ratios of target : ribozyme in each system. The plant cells were expressing ~ 8 picograms (pg) of CAT mRNA/μg of total RNA while the transgenic plants were expressing ~ 4 pg/μg (Fig. 6.4). Hence there was a 2-fold difference in the level of CAT mRNA between the two systems.

6.4 tRNARz12 and tRNAAs24 expression in transgenic plants: a comparison with pAtRNARz12 transfected plant cells.

The RNA levels of the tRNARz12 and tRNAAs24 constructs were analysed. RNase protection assays were carried out as for the equivalent expression assays in the transfected plant cells (see chapter 5). We were not able to detect any expression of either the tRNARz12 or tRNAAs24 transgenes using these assays. This suggested that the high level expression obtained in the plant cells was not occurring in the transgenic plants.

To determine whether any tRNA^{Tyr} transgene expression was taking place, RT-PCR was carried out on GUS+ progeny from 5 independent tRNARz12 x 35SCAT lines (i.e. 15, 20, 35, 43 and 49; see Fig. 6.2). These assays revealed that low level tRNARz12 expression was present in most of these transgenic lines (Fig. 6.5). Quantitative RT-PCR analysis determined that this expression was in the range of 0-0.5 pg/μg of total RNA. In contrast, RT-PCR analysis on total RNA from the transfected plant cells expressing the pAtRNARz12 sequence, revealed that the expression of this construct was approximately 930 pg/μg total RNA (Fig. 6.5).

Figure 6.3: RT-PCR and southern hybridisation analysis of CAT mRNA levels from GUS + and GUS - progeny in 5 (tRNARz12 x 35SCAT: i.e; 15, 20, 35, 43 and 49) and 3 (tRNAAs24 x 35SCAT: i.e; 27, 28 and 30) lines. GUS + plants are in odd numbered lanes, GUS - are in even numbered lanes. Lanes 1-10 are tRNARz12 x 35SCAT lines and lanes 11-16 are tRNAAs24 x 35SCAT lines. The arrow indicates the PCR amplified CAT product. Values beneath lane numbering are the ratio of CAT amplification products from GUS- : GUS + plants within each line.

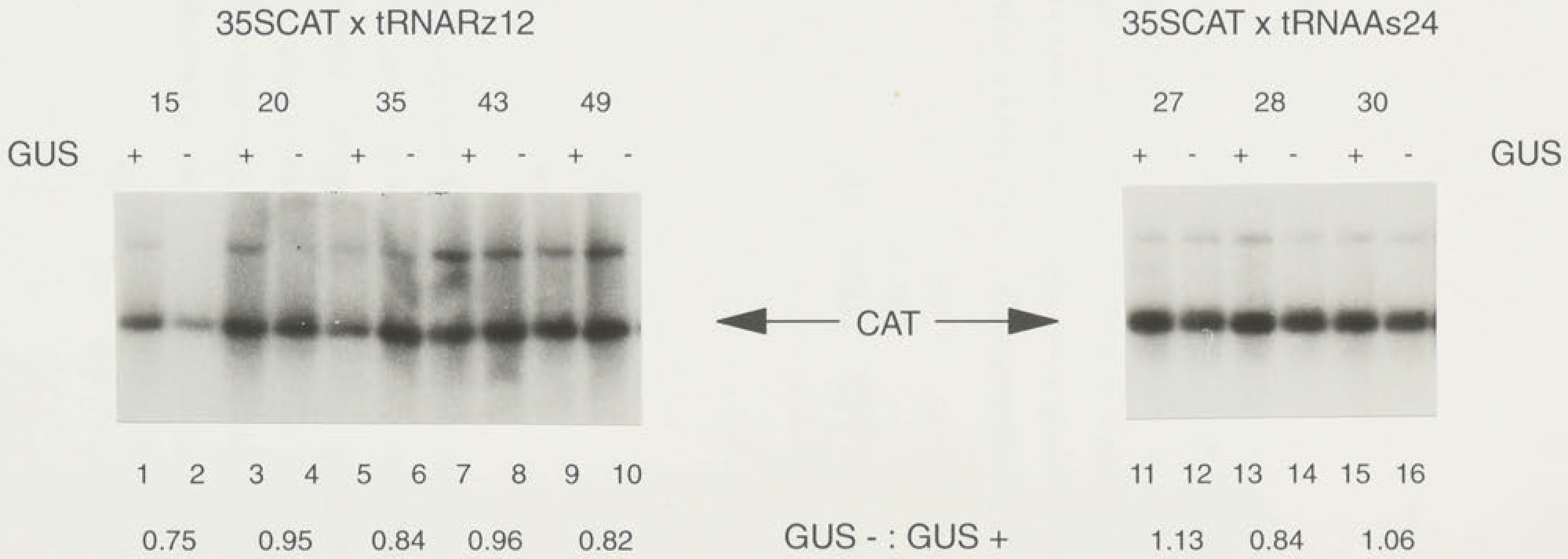
35SCAT x tRNARz12
15 20 35 43 49
GUS + - + - + - + - + -
1 2 3 4 5 6 7 8 9 10
0.75 0.95 0.84 0.96 0.82
CAT
GUS - : GUS +
35SCAT x tRNAAs24
27 28 30
+ - + - + - GUS
11 12 13 14 15 16
1.13 0.84 1.06

Figure 6.3

Figure 6.4: Comparison of CAT mRNA levels from pACAT + pAtRNA transfected plant cells and 35SCAT transgenic plants by RT-PCR analysis and southern hybridisation. Lanes 1-3 are: 1, RNA from pACAT + pAtRNA transfected plant cells; 2, RNA from GUS- tRNARz12 x 35SCAT (line 20); 3, RNA from GUS - tRNARz12 x 35SCAT (line 35). The arrow indicates the PCR amplified CAT product. The numbers beneath the gel are picograms (pg) of CAT mRNA per microgram (µg) of total RNA (see chapter 2; section 2.13(viii) for further details of quantitation of PCR products).

Figure 6.5: Comparison of tRNARz12 RNA levels from pACAT + pAtRNARz12MA (i.e. mutant coat protein promoter construct; see chapter 5) transfected plant cells and 5 (tRNARz12 x 35SCAT) lines using RT-PCR and southern hybridisation analysis. Lanes 1-6 are: **1**, RNA from tRNARz12 x 35SCAT (line 15); **2**, as for 1 but line 20; **3**, as for 1 but line 3; **4**, as for 1 but line 43; **5**, RNA from pACAT + pAtRNARz12MA; **6**, as for 1 but line 49. The tRNARz12 PCR amplified product is indicated. As for Fig. 6.4, the numbers beneath the figure are pg of tRNARz12 RNA per µg of total RNA.

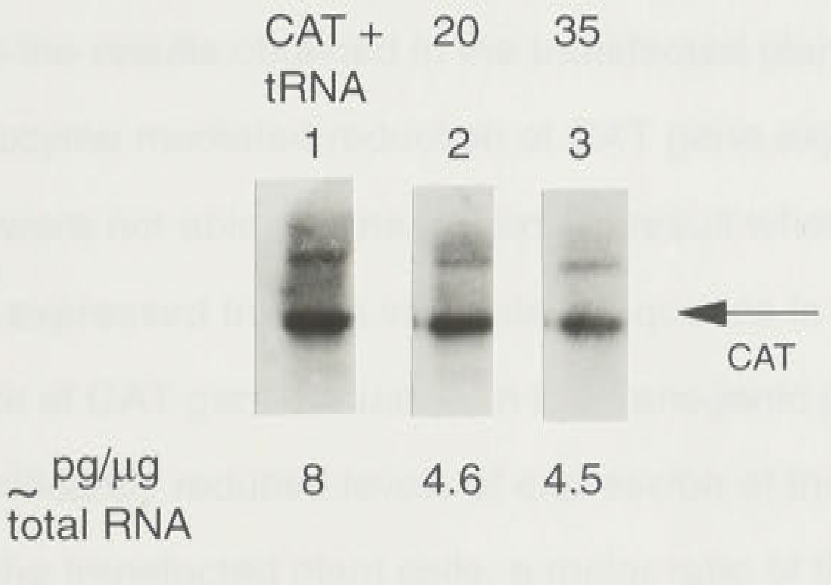
CAT +
tRNA
20
35
1
2
3
CAT
~ pg/µg
total RNA
8
4.6
4.5

Figure 6.4

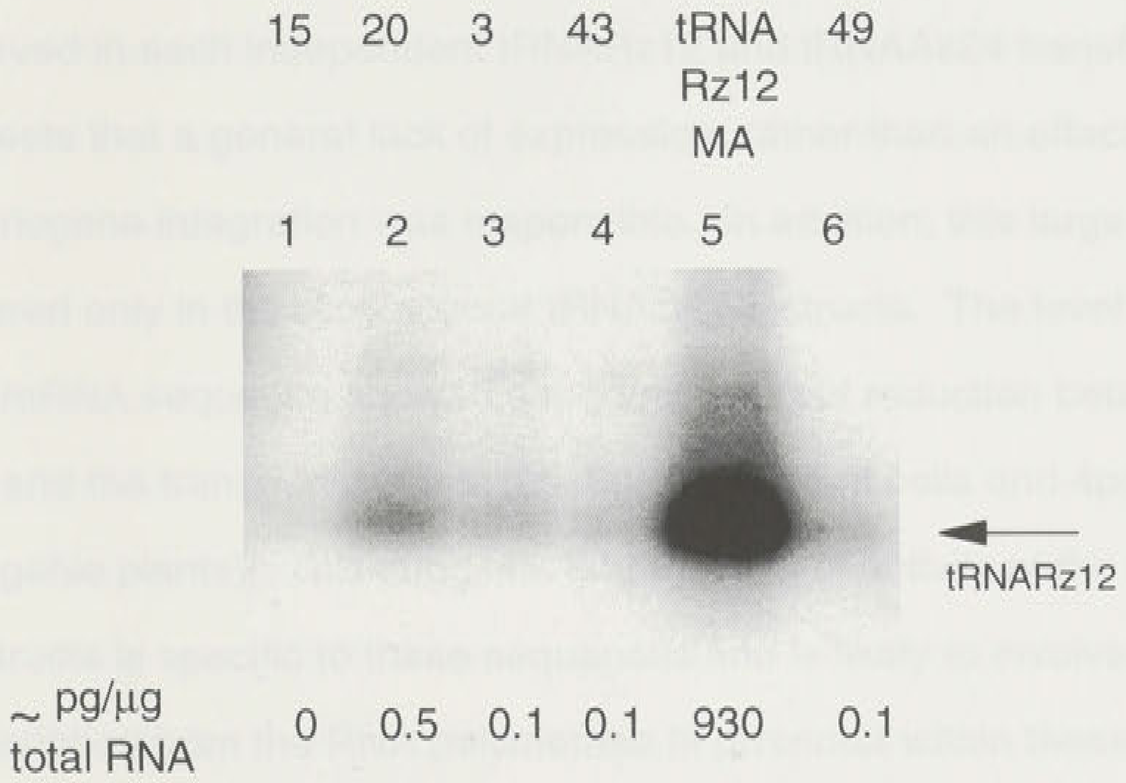
15
20
3
43
tRNA
Rz12
MA
49
1
2
3
4
5
6
tRNARz12
~ pg/µg
total RNA
0
0.5
0.1
0.1
930
0.1

Figure 6.5

In molar terms, the tRNA-ribozyme : substrate ratio in the plant cells was approximately 620:1, whereas in the transgenic plants this ratio was in the range of 0-0.7:1.

DISCUSSION

Despite the results obtained in the transfected plant cells, in which tRNARz12 ribozyme mediated reduction of CAT gene expression was observed, we were not able to obtain a similar result when the tRNARz12 construct was expressed from an integrated sequence in transgenic tobacco lines. This lack of CAT gene reduction in the transgenic plants was most likely due to the significantly reduced levels of expression of the tRNARz12 construct. In the transfected plant cells, a molar ratio of tRNARz12 ribozyme : CAT substrate of approximately 620 : 1 was sufficient to obtain > 80% reduction in CAT gene expression. In contrast, the corresponding ratio in the transgenic plants was in the range of 0-0.7 : 1.

The large reduction in recombinant $tRNA^{Tyr}$ transcript levels was observed in each independent tRNARz12 and tRNAAs24 transformant. This suggests that a general lack of expression, rather than an effect due to the site of transgene integration was responsible. In addition, this large reduction occurred only in the recombinant $tRNA^{Tyr}$ constructs. The level of the target CAT mRNA sequence showed a modest two-fold reduction between the plant cells and the transgenic plants (i.e. 8pg/µg in plant cells and 4pg/µg in transgenic plants). This suggests that the lack of activity of the $tRNA^{Tyr}$ constructs is specific to these sequences and is likely to involve the level of transcription from the RNA polymerase III promoter within these recombinant $tRNA^{Tyr}$ sequences.

One mechanism which may explain the differences in tRNARz12 and tRNAAs24 RNA levels between the two systems maybe that the use of the ACMV vector causes elevated expression of the $tRNA^{Tyr}$-constructs in the plant cells due to the . In mammalian systems, viruses and their associated viral gene products can sometimes increase the level of RNA polymerase III expression by increasing the activity of one of the transcription factors, transcription factor IIIC (TFIIIC). Specific examples of this effect include the adenovirus E1A protein (e.g. Datta *et al.,* 1991), SV40 (White *et al.*, 1990), hepatitis B virus X-gene protein (Aufiero and Schnieder, 1990), herpes simplex virus protein "ICP27" (Jang and Latchtein, 1992) and the human immunodeficiency virus Tat protein (Jang *et al.*, 1992). Two of these studies also observed a simultaneous increase in tRNA transcription upon viral infection (Datta *et al.*, 1991; White *et al.*, 1990).

It is possible that African cassava mosaic virus, on which the ACMV vector is based, influences the expression of RNA polymerase III based transcripts by increasing TFIIIC expression. Such an increase could lead to high levels of RNA polymerase III encoded sequences such as was observed for the recombinant tRNA^{Tyr} used in the studies detailed in chapter 5.

Furthermore, RNase protections (see chapter 5, Fig. 5.6) comparing wildtype tRNA^{Tyr} expression in mock inoculated plant cells, with that of the pAtRNA^{Tyr} inoculated cells, showed that expression from the pAtRNA^{Tyr} construct was significantly higher than that observed for the endogenous tRNA^{Tyr}. This could simply be due to the increased number of templates (i.e. due to the replication of the ACMV vector) from which transcription of this sequence can occur. Alternatively the virus and/or its gene products could be affecting tRNA^{Tyr} gene expression.

Future studies in which the endogenous tRNA transcript levels (i.e. as distinct from those derived from the ACMV vector) are monitored, in response to ACMV infection, will establish if increased steady state levels of tRNA transcripts are evident. Should this be the case, the manipulation of the ACMV-tRNA vector to provide a delivery system for whole plants may provide an ideal means of obtaining high level RNA polymerase III-based expression of incorporated sequences.

A second mechanism for the differential tRNA^{Tyr} gene expression could involve a specific reduction in RNA polymerase III transcription of the recombinant tRNAs in the transgenic plants. This could result from methylation of the cytosine residues on the integrated tRNARz12 and tRNAAs24 sequences. Methylation of plant genomes occurs at the carbon-5 of cytosine residues in the sequences CG and CNG (Gruenbaum *et al.*, 1981), whereas mammalian genomes are only methylated in the sequence CG. This means that, in general, plant genomes are methylated to a much greater degree than mammalian genomes (reviewed in Finnegan *et al.*, 1993).

There are several examples of gene silencing correlating with DNA methylation of RNA polymerase II transcribed transgenes in both plants (e.g. Matzke *et al.*, 1989; Meyer *et al.*, 1993; Ingelbrecht *et al.*, 1994) and animals (e.g. Doerfler, 1990). However, relatively few reports exist on the effects of methylation on transcription of RNA polymerase III-based transgenes in either system (Besser *et al.*, 1990; Jutterman *et al.*, 1991; Doerfler, 1993).

One study in which *in vitro* methylated tRNA-lysine (tRNA^{Lys}) genes were microinjected into*Xenopus* oocytes, showed that transcription of the tRNA^{Lys} gene was inhibited 80% when compared with the non-methylated sequence (Besser *et al.*, 1990). Methylation sensitive restriction enzyme analysis established that, of the five CG sites contained within the tRNA^{Lys} coding region, two sites were not methylated and therefore not responsible for the down-regulation. However, of the three remaining CG sites, one was contained within one of the promoter regions (B box) and two others immediately adjacent, therefore making them good candidates for methylation-based transcriptional inactivation. In another study, Juttermann *et al.* (1991) showed that the transcription of a related RNA polymerase III transcribed gene (i.e. VA1 gene of adenovirus type 2 DNA) was also reduced by *in vitro* methylation when it was subsequently transfected into HeLa cells. The methylation of three CG sequences within the A box was shown to be responsible for the down-regulation of the VA1 transcription (Doerfler, 1993).

These reports show that cytosine-methylation of RNA polymerase III based sequences can have an effect on the subsequent transcription rates of these genes. If cytosine-methylation is the cause of transcriptional down-regulation of the tRNA^{Tyr} transgenes in our system, the universal nature of this reduction suggests that these sequences display an elevated susceptibility to being methylated.

Transcriptional regulation due to cytosine-methylation of the ACMV-tRNA^{Tyr} sequences in the transfected plant cells is unlikely. Previous studies on geminivirus replication have shown that ACMV (Ermak *et al.*, 1993) and the related virus, tomato golden mosaic virus (TGMV-Brough *et al.*, 1992b) can both replicate their genomes, and maintain them, free of cytosine-methylation. This indicates that if methylation is causing the down-regulation of the tRNARz12 and tRNAAs24 sequences in the transgenic plants, then their delivery to the plant cells using the methylation-resistant ACMV vector was fortunate.

Although the RNA levels of the tRNARz12 transgene were low, we did observe a range in expression levels between independent transformants (0-0.5 pg/μg RNA). This range could be explained by differential methylation of the independent transgenes. Should this be the case, however, we would have expected to observe some transgenic lines expressing the recombinant tRNA^{Tyr} at equivalent, or close to endogenous tRNA^{Tyr} levels. Since most tRNAs are multigene families, it is difficult to elucidate the exact concentration of tRNA transcripts from an individual tRNA gene. The tRNA^{Tyr} gene used in this study belongs to a family of at least 11 members (Fuchs *et al.*, 1992).

The molar ratio of ribozyme : substrate RNAs in the transgenic plants was significantly diminished compared with that obtained in the plant cells. If this contrasting ribozyme : target ratio is the primary cause of the lack of ribozyme effectiveness in the transgenic plants, methods aimed toward increasing tRNA-ribozyme transgene expression should also result in successful target gene reduction. These will be discussed in more detail in chapter 7.

CHAPTER 7

THE APPLICATION OF HAMMERHEAD RIBOZYMES FOR TARGETED *IN VIVO* GENE INACTIVATION

7.1. Conclusions of this study

The aim of this project was to develop hammerhead ribozymes for targeted gene inactivation in plants. These ribozymes were designed so as to increase their expression and stability *in vivo*. The initial *in vivo* screening was done using transient expression in *N.tabacum* plant cells. The following sections summarise the results obtained.

(i). A long antisense containing 4 hammerhead domains (i.e. RzCAT) directed against CAT mRNA, was the first ribozyme tested. Previous results, using the 35S promoter and non-replicating vectors, had shown that, when delivered in 360-fold excess, the RzCAT ribozyme reduced CAT activity to 54% of control levels. This was 30% more than the equivalent antisense control (Perriman *et al.*, 1993).

To further enhance this level of CAT gene suppression without increasing the amount of ribozyme containing plasmid delivered to the cell, a self-replicating viral-based vector, pACMV, was developed. Increased expression from this ACMV vector was evidenced by the analysis of CAT activity, which was 19 times greater than that obtained from the non-replicating 35S-vector (Chapter 3; Fig. 3.1). Co-transfection of pACMV expressing CAT and either RzCAT, or control antisense RNAs (i.e. at a ratio of 1 CAT : 3 RzCAT or AsCAT plasmids) gave significant but equivalent reductions in CAT enzyme activity. This suggested an antisense mechanism rather than ribozyme cleavage was the primary mode of gene inactivation (Chapter 3; Fig. 3.3, 3.4).

(ii). To reduce the influence of antisense effects, and gain a measure of the extent of ribozyme-mediated gene inactivation, ribozyme sequences containing short hybridising arms were made. To enhance the stability of these sequences *in vivo*, ribozyme and control antisense were embedded within the anticodon loop of a tyrosine-tRNA from tobacco (i.e. tRNA^{Tyr}).

(iii). The potential of these ribozymes to cleave CAT mRNA when embedded in the tRNA^{Tyr} structure, was assayed *in vitro,* and compared to the non-tRNA^{Tyr} embedded ribozymes. These assays showed that, when the tRNA^{Tyr}-ribozymes and non-embedded ribozymes were expressed at equal concentrations, the most efficient ribozyme was the non-embedded ribozyme, Rz12, with the analogous tRNARz12-ribozyme 50% less efficient (Chapter 4; Fig. 4.7, 4.8 & 4.9).

These *in vitro* cleavage assays were analysed at a fixed time point (1.5 hours) with ribozyme in a 6-fold molar excess. The cleavage rates induced by these molecules could be further analysed by determining the enzymatic turnover and other kinetic parameters. The determination of these values could further explain the observed rates of *in vitro* cleavage. In addition, they may define the rate-limiting step for each ribozyme-substrate reaction therefore providing a more accurate means of predicting *in vivo* efficiencies.

(iv). The *in vivo* efficiency of the tRNARz12-ribozyme was analysed by co-transfection of pACMV expressing the tRNA^{Tyr}-ribozyme and CAT. CAT enzyme expression was reduced 85%, which was significantly more than the reduction in the presence of non-embedded ribozyme, or tRNA^{Tyr}-embedded and non-embedded antisense constructs (Chapter 5; Fig. 5.4a).

Cleavage activity by the tRNA^{Tyr}-ribozyme was further distinguished from an antisense effect by mutating the single non-base paired nucleotide in the target sequence (i.e. "C") to a guanosine. This rendered the substrate uncleavable (Chapter 4; Fig. 4.7) but did not affect CAT expression (Chapter 5; Fig. 5.1), or alter the effects induced by the antisense (Chapter 5; Fig. 5.4). When this mutant CAT target, CM2, was assayed for CAT activity, there was no difference between the antisense and ribozyme constructs. This suggested that the greater reduction seen for the tRNA^{Tyr}-ribozyme with the normal CAT target was ribozyme-mediated (Chapter 5; Fig. 5.4b). CAT mRNA analysis supported this view by showing, in the presence of the tRNA^{Tyr}-ribozyme, a reduction in full length message and a significant accumulation of RNA representing the 3' cleavage product (Chapter 5; Fig. 5.9).

(v). The tRNA^{Tyr}-ribozyme construct expressed from the pACMV vector, contained two active promoters. Mutagenesis of either or both of these promoters revealed that the predominant and active ribozyme transcript in reducing CAT expression in the plant cells, was derived from the RNA polymerase III promoter of the tRNA insert (Chapter 5; Fig. 5.7b & c). A molar ratio of ribozyme derived from RNA polymerase III transcription and CAT substrate from ACMV-coat protein transcription of 620 ribozyme : 1 substrate RNA was determined (Chapter 6; Fig. 6.4 & 6.5).

(vi). Following the transient studies, the tRNA^{Tyr}-ribozyme and tRNA^{Tyr}-antisense constructs were transformed into *N.tabacum* Ti68 plants. The CAT target was present in a separate Ti68 plant as a homozygous single insertion. CAT x tRNA^{Tyr}-ribozyme or tRNA^{Tyr}-antisense crosses were carried out and the progeny assayed for relative CAT activity. No reduction in CAT enzyme activity or CAT mRNA levels were observed in the presence of either tRNA^{Tyr} transgene (Chapter 6; Fig. 6.2 & 6.3). Analysis of the tRNA^{Tyr}-ribozyme transcripts revealed significantly diminished levels relative to the transient expression obtained from the replicating vectors in plant cells. This resulted in a reduced molar ratio of ribozyme RNA in the transgenic plants ranging from an undetectable level to 0.7 ribozyme : 1 substrate, and probably explains the lack of reduction in observed CAT expression (Chapter 6; Fig. 6.4 & 6.5).

7.2. The *in vivo* requirement for high molar concentrations of ribozymes.

The apparent requirement for a large ribozyme:substrate ratio shown in this study is not surprising. As outlined in chapter 1 (section 1.9), an important, yet poorly defined, aspect of the design of hammerhead ribozymes for *in vivo* applications, is the optimisation of their intracellular location. The co-localisation of the ribozyme and target used in the present study was not addressed. This means that many, or perhaps most, of the ribozyme transcripts may never interact with the target RNA.

Based on previous studies (Tobian *et al.*, 1985; Cotten and Birnstiel, 1989), and the *in vitro* analysis of the maturation process of the chimeric $tRNA^{Tyr}$ sequences in this study (Chapter 4), it is likely that these transcripts are largely confined to the nucleus. For the CAT target, and other nuclear target RNAs, this may be useful as it may provide optimal target accessibility. However, nuclear-entrapment could limit the types of substrate RNAs a chimeric tRNA-ribozyme could successfully target and inactivate (i.e. nuclear verses cytoplasmic). In addition, tRNAs which do not undergo the normal maturation and transport processes could be more susceptible to nuclease attack, thus rendering them less stable than normal tRNA sequences.

7.3. The delivery of tRNA-ribozymes.

If tRNA-ribozyme constructions are to be further developed, an important area of future research is the determination of their intracellular location. Other types of tRNA-ribozyme constructions, such as tRNA-ribozyme sequences in which the ribozyme has been inserted in positions other than the anticodon loop, could be tested. These types of chimeric tRNAs might behave more like their endogenous counterparts, and provide a means of delivering hammerhead ribozymes for targeted gene inactivation in either the nucleus or the cytoplasm. Chimeric tRNA-ribozyme sequences in which the ribozyme has been incorporated within the intron (Bouvet *et al.*, 1994; Kandolf, 1994) or the 3' end (Shore *et al.*, 1993; Baier *et al.*, 1994) of the tRNA molecule have been produced, although no data has been published regarding the intracellular location of these molecules. Another region for ribozyme insertion, not yet investigated but which could also be considered, is the variable region of the tRNA motif.

An alternative approach to developing chimeric tRNA-ribozyme constructs, might be to simply use the high level transcription of the tRNA promoter sequences, and have alternative stabilising sequences (i.e. other than the tRNA motif) at the 5' and 3' ends of the ribozyme. This may help to circumvent low tRNA-ribozyme expression, such as that observed in the transgenic plants analysed in this study. It is possible that the plant may recognise recombinant tRNAs as "misfunctioning" tRNAs, and respond by rapidly removing these transcripts. However, if the ribozyme construct was not behaving as a tRNA, the cell may "allow" higher levels of these transcripts to accumulate.

Several other ribozyme delivery systems could also be adapted to plant-based gene inactivation. It is possible that some of these might provide high steady-state levels of ribozyme transcripts when expressed in both plant cells and transgenic plants. These include the addition of stabilising stems and/or loops (e.g. Sioud and Drlica, 1991), or the delivery within small nuclear RNAs (i.e. snRNAs; DeYoung *et al.*, 1994), RNA polymerase I transcripts (Menke *et al.*, 1995) or self-circularising RNAs (Kisich *et al.,* 1995).

7.4. The ACMV-tRNA system as an *in vivo* screen.

The combination of the ACMV-based self-replicating vector and pol III expression provided the high levels of tRNA-ribozyme production required to induce ribozyme-mediated target gene reduction in plant cells. At present, however, the ACMV-tRNA system is limited to use in plant cells. Vector instability and variable levels of viral infection has led to only limited use of geminivirus-vectors as a means of delivering sequence to whole plants.

However, this system is ideal for the rapid assay of several aspects of ribozyme/substrate design in plant cells. Such assays can circumvent the necessity for the large scale production of transgenic plants by providing a rapid primary *in vivo* screen of a large number of ribozyme sequences. One application could be the *in vivo* analysis of substrate target-site accessibility. In addition, ribozymes containing base substitutions (i.e. such as some of those outlined in chapter 1, section 1.6) and which have demonstrated enhanced catalytic activities *in vitro,* could be tested for relative *in vivo* capabilities.

7.5. Prospects for *in vivo* gene inactivation using hammerhead ribozymes.

Although hammerhead ribozyme activity has been extensively studied *in vitro* (see chapter 1), the parameters for efficient *in vivo* use are poorly defined. In particular, there have been only three publications demonstrating ribozyme-mediated reduction of gene expression in plant cells (Steinecke *et al.*, 1992; Perriman *et al.*, 1993; Steinecke *et al.*, 1994) and one in transgenic plants (Wegener *et al.,* 1994), although the latter lacked appropriate controls to discount an antisense mediated inhibition. The studies presented here have extended the application of ribozymes *in vivo*, with the inhibition of CAT activity in plant cells by the delivery of a ribozyme as a tRNA-modified transcript expressed from the ACMV self-replicating vector.

The research presented in this thesis has demonstrated, that using the current ribozyme design, and techniques of intracellular expression and delivery, a high molar excess of ribozyme is required to obtain ribozyme-mediated target gene inactivation *in vivo*. The results showed that an abundantly expressed tRNA-embedded ribozyme increased CAT gene inhibition over that obtained in the presence of a less abundant non-embedded ribozyme. This finding was supported by mutagenesis of the tRNA promoter, which led to diminished levels of the tRNA-embedded ribozyme and no longer reduced CAT activity in the plant cells (Chapter 5; Fig. 5.7). Additionally, significantly reduced tRNA-ribozyme transcript levels failed to reduce CAT enzyme activity in the transgenic plants (Chapter 6). These results are consistent with the successful application of ribozymes in animal cells (e.g. Cotten and Birnstiel, 1989: 500-1000 ribozyme : substrate; Cameron and Jennings, 1989: 1000 ribozyme : substrate).

The current requirement for high molar concentrations of ribozyme limits the application of hammerhead ribozymes as gene therapy agents. Future optimisation of *in vivo* ribozyme activity will therefore require several areas of research. In addition to the *in vivo* aspects of intracellular location and enhanced stabilities, analyses aimed toward defining ribozymes with increased catalytic efficiencies (i.e. such as those outlined in chapter 1; section 1.6) are also important. Improving these aspects of ribozyme design should provide conditions in which lower ratios of ribozyme : substrate will be sufficient for ribozyme-mediated inactivation of gene expression *in vivo*.

References:

Accotto G.P., Mullineaux P.M., Brown S.B. & Marie D (1993) Digitaria Streak Geminivirus replicative forms are abundant in S-phase nuclei of infected cells. *Virology*, **195**: 257-259

Alberts B., Bray D., Lewis J., Raff M., Roberts K. & Watson J.D. (1989) *Molecular biology of the cell (2nd edition).* Garland Publishing Inc., New York, p. 62

Allison D.S., Goh S.H. & Hall B.D. (1983) The promoter sequence of a yeast $tRNA^{Tyr}$ gene. *Cell,* **34:** 655-664

Atkins D. & Gerlach W.L. (1994) Artificial ribozyme and antisense gene expression in *Saccharomyces cerevisiae. Ant. Res. Develop.*, **4:** 109-117

Aufiero B. & Schneider R.J. (1990) The hepatitis B virus x-gene product *trans*-activates both RNA polymerase II and III promoters. *EMBO J.*, **9:** 497-504

Baier G., Coggeshall K.M., Baier-Bitterlich G., Giampa L., Telford D., Herbert E., Shih W. & Altman A. (1994) Construction and characterisation of *lck-* and *fyn-* specific tRNA: ribozyme chimeras. *Mol. Immun.*, **31:** 923-932

Baker R.E., Hall B.D., Camier S. & Sentenac A (1987) Gene size differentially affects the binding of yeast transcription factor τ to two intragenic regions. *Proc. Natl. Acad. Sci. U.S.A.*, **84:** 8768-8772

Bertrand E.L. & Rossi J.J. (1994) Facilitation of hammerhead ribozyme catalysis by the nucleocapsid protein of HIV-1 and the heterogeneous nuclear ribonucleoprotein A1. *EMBO J.*, **13:** 2904-2912

Besser D., Gotz F., Schulze-Forster K., Wagner H., Kroger H. & Simon D. (1990) DNA methylation inhibits transcription by RNA polymerase III of a tRNA gene, but not of a 5s rRNA gene. *FEBS.*, **269:** 358-362

Bogusz D., Llewellyn D.J., Craig S., Dennis E.S., Appleby C.A. & Peacock W.J. (1990) Nonlegume hemoglobin genes retain organ-specific expression in heterologous transgenic plants. *Plant Cell,* **2:** 633-641

Bouvet P., Dimitrov S. & Wolffe A.P. (1994) Specific regulation of *Xenopus* chromosomal 5S rRNA gene transcription *in vivo* by histone H1. *Genes and Develop.*, **8**: 1147-1159

Brough C.B., Sunter G., Gardiner W.E. & Bisaro D.M. (1992a) Kinetics of tomato golden mosaic virus DNA replication and coat protein promoter activity in *Nicotiana tabacum* protoplasts. *Virology*, **187**: 1-9

Branch A.D. & Robertson H.D. (1991) Efficient *trans* cleavage and a common structural motif for the ribozymes of the human hepatitis δ agent. *Proc. Natl. Acad. Sci. U.S.A.*, **88:** 10163-10167

Brough C.B., Gardiner W.E., Inamder N.M., Zhang X.Y., Ehrlich M. & Bisaro D.M. (1992b) DNA methylation inhibits propagation of tomato golden mosaic virus DNA in transfected protoplasts. *Plant Mol. Biol.*, **18:** 703-712

Bruening G. (1990) Compilation of self-cleaving sequences from plant virus satellite RNAs and other sources. *Methods in Enzymology*, **180:** 546-558

Buvoli M., Cobianchi F., Biamonti G. & Riva S. (1990) Recombinant hnRNP protein A1 and its N-terminal domain show preferential affinity for oligodeoxynucleotides homologous to intron/exon acceptor sites. *Nuc. Acids Res.*, **18:** 6595-6600

Buzayan J.M., Gerlach W.L. & Bruening G. (1986) Non-enzymatic cleavage and ligation of RNAs complementary to a plant virus satellite RNA. *Nature*, **323**: 349-353

Buzayan J.M., Feldstein P.A., Segrelles C. & Bruening G. (1988) Autolytic processing of a phosphorothioate diester bond. *Nuc. Acids Res.*, **16**: 4009-4023

Cameron F.H. & Jenning P.A. (1989) Specific gene suppression by engineered ribozymes in monkey cells. *Proc. Natl. Acad. Sci. U.S.A.*, **86:** 9139-9143

Cameron F.H. & Jennings P.A. (1994) Multiple domains in a ribozyme construct confer increased suppressive activity in monkey cells. *Ant. Res. Develop.*, **4:** 87-94

Cantor G.H., McElwain T.F., Birkebak T.A. & Palmer G.H. (1993) Ribozyme cleaves rex/tax mRNA and inhibits bovine leukemia virus expression. *Proc. Natl. Acad. Sci. U.S.A.*, **90:** 10932-10936

Carter K.C., Taneja K.L. & Lawrence J.B. (1991) Discrete nuclear domains of poly(A) RNA and their relationship to the functional organisation of the nucleus. *J. Cell. Biol.*, **115:** 1191-1202

Carter K.C., Bowman D., Carrington W., Fogarty K., McNeil J.A., Fay F.S. & Lawrence J.B. (1993) A three-dimensional view of precursor messenger RNA metabolism within the mammalian nucleus. *Science*, **259:** 1330-1335

Casas-Finet J.R., Smith J.D., Kumar A., Kim J.G., Wilson S.H. & Karpel R.L. (1993) Mammalian heterogeneous ribonucleoprotein A1 and its constituent domains. *J. Mol. Biol.*, **229:** 879-889

Cech T.R. & Bass B.L. (1986) Biological catalysis by RNA. *Ann. Rev. Biochem.*, **55:** 599-629

Cech T.R. (1987) The chemistry of self-splicing RNA and RNA enzymes. *Science*, **236:** 1532-1539

Cech T.R. (1990) Self-splicing of group 1 introns. *Ann. Rev. Biochem.*, **59:** 543-568

Chen C.J., Banerjea A.C., Harmison G.G., Haglund K. & Schubert M. (1992) Multitarget ribozyme directed to cleave at up to nine highly conserved HIV-1 env RNA regions inhibits HIV-1 replication-potential effectiveness against most presently sequenced HIV-1 isolates. *Nuc. Acids Res.*, **20**: 4581-4589

Chuat J.C. & Galibert F. (1989) Can ribozymes be used to regulate procaryote gene expression? *Biochem. Biophys. Res. Comm.*, **162**: 1025-1029

Ciliberto G., Dathan N., Frank R., Philipson L. & Mattaj I.W. (1986) Formation of the 3' end on UsnRNAs requires at least three sequence elements. *EMBO J.*, **5:** 2931-2937

Crisell P., Thompson S. & James W. (1993) Inhibition of HIV-1 replication by ribozymes that show poor activity *in vitro*. *Nuc. Acids Res.*, **21**: 5251-5255

Coatzee T., Herschlag D. & Belfort M. (1994) *Escherichia coli* proteins, including ribosomal protein S12, facilitate *in vitro* splicing of phage T4 introns by acting as RNA chaperones. *Genes & Develop.*, **8:** 1575-1588

Cotten M. & Birnstiel M.L. (1989) Ribozyme mediated destruction of RNA *in vivo. EMBO J.*, **8:** 3861-3866

Dahm S.C. & Uhlenbeck O.C. (1990) Characterisation of deoxy- and ribo-containing oligonucleotide substrates in the hammerhead self-cleavage reaction. *Biochimie*, **72**: 819-823

Dahm S.C. & Uhlenbeck O.C. (1991) Role of divalent metal ions in the hammerhead RNA cleavage reaction. *Biochemistry,* **30**: 9464-9469

Darnell J. (1986) Macromolecules in procaryotic and eucaryotic cells. In Darnell J., Lodish H. & Baltimore D. (eds) *Molecular cell biology.* Scientific American Books Publishers, New York, pp261-267

Datta S., Soong C.J., Wang D.M. & Harter M.L. (1991) A purified adenovirus 289-amino acid E1A protein activates RNA polymerase III transcription *in vitro* and alters transcription factor TFIIIC. *J. Virol.*, **65**: 5297-5304

Davies J.W., Townsend R. & Stanley J. (1987) In Hohn T. & Shell J. (eds)*Plant DNA infectious agents.*, Springer-Verlag, New York, pp31-52

DeYoung M.B., Kincade-Decker J., Boehm C.A., Riek R.P., Mamone J.A., McSwiggen J.A. & Graham R.M. (1994) Functional characterization of ribozymes expressed using U1 and T7 vectors for the intracellular cleavage of ANF mRNA. *Biochemistry*, **33:** 12127-12138

Doerfler W. (1990) The significance of DNA methylation patterns: promoter inhibition by sequence-specific methylation is one functional consequence. *Phil. Trans. R. Soc. London B.*, **326:** 253-265

Doerfler W. (1993) Pattern of *de novo* methylation and promoter inhibition: studies on the adenovirus and the human genome. In Jost J.P. & Saluz H.P. (eds) *DNA methylation: Molecular biology and biological significance*, Birkhauser Verlag, Switzerland, pp262-299.

Dropulic B., Lin N.H., Martin M.A. & Jeang K.T. (1992) Functional characterisation of a U5 ribozyme: Intracellular suppression of human immunodeficiency virus type 1 expression. *J. Virol.*, **66:** 1432-1441

Eckner R., Ellmeier W. & Birnstiel M.L. (1991) Mature mRNA 3' end formation stimulates RNA export from the nucleus. *EMBO J.*, **10:** 3513-3522

Eckstein F. (1985) Nucleoside Phosphorothioates. *Ann Rev. Biochem.*, **54:** 367-402

Efrat S., Leiser M., Wu Y.J., Fusco-DeMane D., Emran O.A., Surana M., Jetten T.L., Magnuson M.A., Weir G. & Fleischer N. (1994) Ribozyme mediated attenuation of pancreatic β-cell glucokinase expression in transgenic mice results in impaired glucose-induced insulin secretion. *Proc. Natl. Acad. Sci. U.S.A.*, **91**: 2051-2055

Ermak G., Paszkowski U., Wohlmuth M., Scheid O.M. & Paszkowski J (1993) Cytosine methylation inhibits replication of African cassava mosaic virus by two distinct mechanisms. *Nuc. Acids Res.,* **21:** 3445-3450

Evans G.J., Brown J.W.S., Waugh R., Wilson T.M.A. & Turner P.C. (1992) The effects of ribozymes on gene expression in plants. *Biochem. Soc. Trans.*, **20**: 344S

Fabrizio P., Coppo A., Fruscotoni P., Benedetti P., Di Segni G. & Tocchini-Valentini G.P. (1987) Comparative mutational analysis of wild-type and stretched $tRNA^{Leu}$ gene promoters. *Proc. Natl. Acad. Sci. U.S.A.,* **84:** 8763-8767

Fedor M.J. & Uhlenbeck O.C. (1990) Substrate sequence effects on hammerhead RNA catalytic efficiency. *Proc. Natl. Acad. Sci. U.S.A.*, **87**: 1668-1672

Feldstein P.A., Buzayan J.M. & Bruening G. (1989) Two sequences participating in the autolytic processing of satellite tobacco ringspot virus complementary RNA. *Gene,* **82:** 53-61

Finnegan E.J., Brettell R.I.S. & Dennis E.S. (1993) The role of DNA methylation in the regulation of plant expression. In Jost J.P. & Saluz H.P. (eds) *DNA* *methylation: Molecular biology and biological significance*, Birkhauser Verlag, Switzerland, pp 218-261

Forster A.C. & Symons R.H. (1987a) Self-cleavage of plus and minus RNAs of a virusoid and a structural model for the active sites. *Cell*, **49:** 211-220

Forster A.C. & Symons R.H. (1987b) Self-cleavage of virusoid RNA is performed by the proposed 55-nucleotide active site. *Cell*, **50**: 9-16

Forster A.C. & Altman S. (1990) External guide sequences for an RNA enzyme. *Science*, **249**: 783-786

Fu D.J. & McLaughlin L.W. (1992a) Importance of specific purine amino and hydroxyl groups for efficient cleavage by a hammerhead ribozyme. *Proc. Natl. Acad. Sci. U.S.A.*, **89**: 3985-3989

Fu D.J. & McLaughlin L.W. (1992b) Importance of specific adenosine N7-nitrogens for efficient cleavage by a hammerhead ribozyme. A model for magnesium binding. *Biochemistry*, **31**: 10941-10949

Fuchs T., Beier D. & Beier D. (1992) The tRNA^{Tyr} multigene family of *Nicotiana rustica*: genome organization, sequence analysis and expression *in vitro. Plant Mol. Biol.*, **20:** 869-878

Geiduschek E.P. & Tocchini-Valentini G.P. (1988) Transcription by RNA polymerase III. *Ann. Rev. Biochem.,* **57:** 873-914

Gruenbaum Y., Naveh-Many T., Cedar H. & Razin R. (1981) Sequence specificity of methylation in higher plant DNA. *Nature,* **292:** 860-862

Guerrier-Takada C., Gardiner K.J., Marsh T., Pace N.R. & Altman S. (1983) The RNA moiety of Ribonuclease P is the catalytic subunit of the enzyme. *Cell*, **35**: 849-857

Guilley H., Dudley R.K., Jonard G., Balazs E. & Richards K.E. (1982) Transcriptions of cauliflower mosaic virus DNA: detection of promoter sequences and characterisation of transcripts. *Cell*, **30:** 763-773

Guo H.C.T. & Collins R.A. (1995) Efficient *trans*-cleavage of a stem-loop RNA substrate by a ribozyme derived from *Neurospora* VS RNA. *EMBO J.*, **14:** 368-376

Ha J. & Kim K.H. (1994) Inhibition of fatty acid synthesis by expression of an acetyl-CoA carboxylase-specific ribozyme gene. *Proc. Natl. Acad. Sci. U.S.A.*, **91:** 9951-9955

Hampel A. & Tritz R. (1989) RNA catalytic properties of the minimum (-) sTRSV sequence. *Biochemistry*, **28:** 4929-4933

Harrison B.D. (1985) Advances in geminivirus research. *Annual Rev. Phytopath.*, **23:** 55-82

Haseloff J. & Gerlach W.L. (1988) Simple RNA enzymes with new and highly specific endoribonuclease activities. *Nature,* **334:** 585-591

Haseloff J. & Gerlach W.L. (1989) Sequences required for the self-catalysed cleavage of tobacco ringspot virus. *Gene,* **82:** 43-52

Heidenreich O. & Eckstein F. (1992) Hammerhead ribozyme-mediated cleavage of the long terminal repeat RNA of human immunodeficiency virus type 1. *J. Biol. Chem.*, **267:** 1904-1909

Heidenreich O., Benseler F., Fahrenholz A. & Eckstein F. (1994) High activity and stability of hammerhead ribozymes containing 2'-modified pyrimidine nucleosides and phoshorothioates. *J. Biol. Chem.*, **269:** 2131-2138

Heinrich J.C., Tabler M. & Louis C. (1993) Attenuation of *white* gene expression in transgenic *Drosophila melanogaster*: Possible role of a catalytic antisense RNA. *Dev. genetics*, **14:** 258-265

Hendry P., McCall M.J., Santiago F.S. & Jennings P.A. (1992) A ribozyme with DNA in the hybridising arms displays enhanced cleavage ability. *Nuc. Acids Res.,* **20**: 5737-5741

Herschlag D., Khosla M., Tsuchihashi Z. & Karpel R.L. (1994) An RNA chaperone activity of non-specific RNA binding proteins in hammerhead ribozyme catalysis. *EMBO J.*, **13:** 2913-2924

Hertel K.J., Pardi A., Uhlenbeck O.C., Koizumi M., Ohtsuka E., Uesugi S., Cedergren R., Eckstein F., Gerlach W.L., Hodgson R. & Symons R.H. (1992) A numbering system for the hammerhead ribozyme. *Nuc. Acid. Res.,* **20:** 3252

Heus H.A., Uhlenbeck O.C. & Pardi A. (1990) Sequence-dependent structural variations of hammerhead RNA enzymes. *Nuc. Acids Res.,* **18**: 1103-1108

Holm P.S., Scanlon K.J. & Dietel M. (1994) reversion of multidrug resistance in the P-glycoprotein-postive human pancreatic cell line (EPP85-181RDB) by introduction of a hammerhead ribozyme. *Br. J. Cancer*, **70:** 239-243

Homann M., Tzortzakaki S., Rittner K., Sczakiel G. & Tabler M. (1993) Incorporation of the catalytic domain of a hammerhead ribozyme into antisense RNA enhances its inhibitory effect on the replication of human immunodeficiency virus type 1. *Nuc. Acids Res.,* **21:** 2809-2814

Hutchins C.J., Rathjen P.D., Forster A.C. & Symons R.H. (1986) Self-cleavage of plus and minus RNA transcripts of avocado sunblotch viroid. *Nuc. Acids Res.,* **14:** 3627-3640

Ingelbrecht I., Van Houdt H., Van Montagu M. & Depicker A. (1994) Posttranscriptional silencing of reporter transgenes in tobacco correlates with DNA methylation. *Proc. Natl. Acad. Sci. U.S.A.,* **91:** 10502-10506

Inokuchi Y., Yuyama N., Hirashima A., Nishikawa S., Ohkawa J. & Taira K. (1994) A hammerhead ribozyme inhibits the proliferation of an RNA coliphage SP in *Escherichia coli. J. Biol. Chem.,* **269:** 11361-11366

Izant J. (1992) in Erickson R.P. & Izant J.G. (eds) *Gene Regulation: Biology of Antisense RNA and DNA.* Raven Press, New York, pp 183-195

Jang K.L. & Latchman D.S. (1992) The herpes simplex virus immediate-early protein ICP27 stimulates the transcription of cellular Alu repeated sequences by increasing the activity of transcription factor TFIIIC. *Biochem. J.,* **284:** 667-673

Jang K.L., Collins M.K. & Latchman D.S. (1992) The human immunodeficiency virus Tat protein increases the transcription of human Alu repeated sequences by increasing the activity of the cellular transcription factor TFIIIC. *J. Acquir. Immun. Defic. Syndr.,* **5:** 1142-1147

Jaffe E.K. & Cohn M. (1979) Diasteromers of the nucleoside phosphorothiates as probes of the structure of the metal nucleotide substrates and of the nucleotide binding site of yeast hexokinase. *J. Biol. Chem.*, **254:** 10839-10845

Jutterman R., Hosokawa K., Kochanek S. & Doerfler W. (1991) Adenovirus Type 2 VA1 RNA transcription by polymerase III is blocked by sequence-specific methylation. *J Virol.*, **65:** 1735-1742

Kandolf H. (1994) The H1A histone variant is an *in vivo* represser of oocyte-type 5S gene transcription in *Xenopus laevis* embryos. *Proc. Natl. Acad. Sci. U.S.A.*, **91:** 7257-7261

Karpel R.L., Miller N.S. & Fresco J.R. (1982) Mechanistic studies of ribonucleic acid renaturation by a helix-destablizing protein. *Biochemistry,* **21:** 2102-2108

Karnahl U. & Wasternack C. (1992) Half-life of cytoplasmic rRNA and tRNA, of plastid rRNA and of uridine nucleotides in heterotrophically and photoorganotrophically grown cells of *Euglena Gracilis* and its apoplastic mutant W_3BUL. *Int. J. Biochem.*, **24:** 493-497

Kashani-Sabet K., Funato T., Tone T., Jiao L., Wang W., Yoshida E., Kashifinn B.I., Shitara T., Wu A.M., Moreno J.G., Traweek S.T., Ahlering T.E. & Scanlon K.J. (1992) Reversal of the malignant phenotype by an anti-*ras* ribozyme. *Ant. Res. Develop.*, **2**: 3-15

Kashani-Sabet M., Funato T., Florenes V.A., Fodstad O. & Scanlon K.J. (1994) Suppression of the neoplastic phenotype *in vivo* by an anti-*ras* ribozyme. *Cancer Research*, **54:** 900-902

Kiehntopf M., Brach M.A., Licht T., Petschauer S., Karawajew L., Kirschning C. & Herrmann F. (1994) Ribozyme mediated cleavage of the *MDR*-1 transcript restores chemosensitivity in previously resistant cancer cells. *EMBO J.*, **13**: 4645-4652

Kinsey P.T. & Sandmeyer S.B. (1991) Adjacent pol II and pol III promoters: transcription of the yeast retrotransposon Ty3 and a target tRNA gene. *Nuc. Acids Res.,* **19:** 1317-1324

Kisich K.O., Stecha P.F., Harter H.A. & Stinchcomb D.T. (1995) Inhibition of TNF-α secretion by murine macrophages following *in vivo* and *in vitro* ribozyme treatment. *J. Cell. Biochem.*, **19A**: 221

Kobayashi H., Dorai T., Holland J.F. & Ohnuma T. (1994) Reversal of drug sensitivity in multidrug-resistant tumor cells by an *MDR*1 (*PGY*1) ribozyme. *Cancer Research*, **54:** 1271-1275

Koizumi M., Iwai S. & Ohtsuka E. (1988a) Construction of a series of several self-cleaving RNA duplexes using synthetic 21-mers. *FEBS Lett.*., **228**: 228-230

Koizumi M., Iwai S. & Ohtsuka E. (1988b) Cleavage of specific sites of RNA by designed ribozymes. *FEBS Lett.*, **239**: 285-288

Koizumi M., Hayase Y., Iwai S., Kamiya H., Inoue H. & Ohtsuka E. (1989) Design of RNA enzymes distinguishing a single base mutation in RNA. *Nuc. Acids Res.,* **17:** 7059-7091

Koizumi M. & Ohtsuka E. (1991) Effects of phosphorothioate and 2-amino groups in hammerhead ribozymes on cleavage rates and Mg^{2+} binding. *Biochemistry*, **30**: 5145-5150

Koizumi M., Kamiya H. & Ohtsuka E. (1992) Ribozymes designed to inhibit transformation of NIH3T3 cells by the activated c-Ha-*ras* gene. *Gene*, **117**: 179-184

Koizumi M., Kamiya H. & Ohtsuka E. (1993) Inhibition of c-Ha-*ras* gene expression by hammerhead ribozymes containing a stable C(UUCG)G hairpin loop. *Biol. Pharm. Bull.*, **16:** 879-883

Kruger K., Grabowski P.J., Zaug A.J., Sands J., Gottschling D.E. & Cech T.R. (1982) Self-splicing RNA: Autoexcision and autocyclization of the ribosomal RNA intervening sequence of *Tetrahymena. Cell*, **31:** 147-157

Kumar A. & Wilson S.H. (1990) Studies of the strand-annealing activity of mammalian hnRNP complex protein A1. *Biochemistry,* **29:** 10717-10722

Kunkel T.A., Roberts J.D. & Zakour R.A. (1987) Rapid and efficient site specific mutagenesis without phenotypic selection. *Methods in Enzymology*, **154:** 367-382

Lamb J.W. & Hay R.J. (1990) Ribozymes that cleave potato leafroll virus RNA within the coat protein and polymerase genes. *J. Gen. Virol.*, **71**: 2257-2264

Lange W., Cantin E.M., Finke J. & Dolken G. (1993) *In vitro* and *in vivo* effects of synthetic ribozymes targeted against BCR/ABL mRNA. *Leukemia*, **7**: 1786-1794

Lange W., Daskalakis M., Finke J. & Dolken G. (1994) Comparison of different ribozymes for efficient and specific cleavage of BCR/ABL related mRNAs. *FEBS Lett.*, **338**: 175-178

Larsson S., Hotchkiss G., Andang M., Nyholm T. & Inzunza J. (1994) Reduced β2-microglobulin mRNA levels in transgenic mice expressing a designed hammerhead ribozyme. *Nuc. Acids Res.*, **22**: 2242-2248

Lee C.G., Zamore P.D., Green M.R. & Hurwitz J. (1993) RNA annealing activity is intrinsically associated with U2AF. *J. Biol. Chem.*, **268:** 13472-13478

L'Huillier P.J., Davis S.R. & Bellamy A.R. (1992) Cytoplasmic delivery of ribozymes leads to efficient reduction in α-lactalbumin mRNA levels in C1271 mouse cells. *EMBO J.*, **11**: 4411-4418

Li Y., Guerrier-Takada C. & Altman S. (1992) Targeted cleavage of mRNA *in vitro* by RNase P from *Escherichia coli*. *Proc. Natl. Acad. Sci. U.S.A.*, **89:** 3185-3189

Matzke M.A., Primig M., Trnovsky J. & Matzke A.J.M. (1989) Reversible methylation and inactivation of marker genes in sequentially transformed tobacco plants. *EMBO J.*, **8:** 643-649

Mazzolini L., Axelos M., Lescure N. & Yot P. (1992) Assaying synthetic ribozymes in plants: high-level expression of a functional hammerhead structure fails to inhibit target gene activity in transiently transformed protoplasts. *Plant Mol. Biol.*, **20:** 715-731

Mei H.Y., Kaaret T.W. & Bruice T.C. (1989) A computational approach to the mechanism of self-cleavage of hammerhead RNA. *Proc. Natl. Acad. Sci. U.S.A.*, **86:** 9727-9731

Menke A. & Hobom G. (1995) Double ribozyme mediated cleavage of influenza A NP-vRNA. *J. Cell. Biochem.*, **19A**: 223

Meyer P., Heidmann J. & Niederhof I. (1993) Differences in DNA-methylation are associated with a paramutation phenomenon in transgenic petunia. *Plant J.*, **4:** 89-100

McCall M.J., Hendry P. & Jennings P.A. (1992) Minimal sequence requirements for ribozyme activity. *Proc. Natl. Acad. Sci. U.S.A.*, **89**: 5710-5714

McClain W.H. (1993) Transfer RNA identity. *The FASEB J.*, **7:** 72-78

Michel F. & Dujon B. (1983) Conservation of RNA secondary structures in two intron families including mitochondrial-, chloroplast- and nuclear-encoded members. *EMBO J.*, **2:** 33-38

Muller G., Strack B., Dannull J., Sproat B.S., Surovoy A., Jung G. & Moelling K. (1994) Amino acid requirements of the nucleocapsid protein of HIV-1 for increasing catalytic activity of a Ki-ras ribozyme *in vitro. J. Mol. Biol.*, **242:** 422-429

Munroe S. & Dong X. (1992) Heterogeneous nuclear ribonucleoprotein A1 catalyzes RNA:RNA annealing. *Proc. Natl. Acad. Sci. U.S.A.,* **89:** 895-899

Murphy F.L. & Cech T.R. (1989) Alteration of substrate specificity for the endoribonucleolytic cleavage of RNA by the *Tetrahymena* ribozyme. *Proc. Natl. Acad. Sci. U.S.A.*, **86:** 9218-9222

Odai O., Hiroaki H., Sakata T., Tanaka T. & Uesugi S. (1990) The role of a conserved guanosine residue in the hammerhead-type RNA enzyme. *FEBS.*, **267**:150-152

Ohkawa J., Yuyama N., Takebe Y., Nishikawa S. & Taira K. (1993) Importance of independence in ribozyme reactions: Kinetic behaviour of trimmed and of simply connected multiple ribozymes with potential activity against human immunodeficiency virus. *Proc. Natl. Acad. Sci. U.S.A.*, **90**: 11302-11306

Olsen D.B., Benseler F., Aurup H., Pieken W.A. & Eckstein F. (1991) Study of a hammerhead ribozyme containing 2'-modified adenosine residues. *Biochemistry*, **30**: 9735-9741

Paolella G., Sproat B.S. & Lamond A.I.(1992) Nuclease resistant ribozymes with high catalytic activity. *EMBO J.*, **11**: 1913-1919

Pecoraro V.L., Hermes J.D. & Cleland W.W. (1984) Stability constants of Mg^{2+} and Cd^{2+} complexes of adenine nucleotides and thionucleotides and rate constants for formation and dissociation of MgATP and MgADP. Biochemistry, **23:** 5262-5271

Perreault J.P., Wu T., Cousineau B., Ogilvie K.K. & Cedergren R. (1990) Mixed deoxyribo- and ribo-oligonucleotides with catalytic activity. *Nature,* **344**: 565-567

Perrault J.P., Labuda D., Usman N., Yang J.H. & Cedergren R. (1991) Relationship between 2'-hydroxyls and magnesium binding in the hammerhead RNA domain: A model for ribozyme catalysis. *Biochemistry*, **30**: 4020-4025

Perriman R., Delves A. & Gerlach W.L. (1992) Extended target-site specificity for a hammerhead ribozyme. *Gene*, **113**: 157-163

Perriman R., Graf L. & Gerlach W.L. (1993) A ribozyme that enhances gene suppression in tobacco protoplasts. *Ant. Res. Develop.*, **3**: 253-263

Pieken W., Olsen D.B., Benseler F., Aurup H. & Eckstein F. (1991) Kinetic characterisation of ribonuclease resistant 2'-modified hammerhead ribozymes. *Science*, **253:** 314-317

Pley H.W., Flaherty K.M. & McKay D.B. (1994) Three dimensional structure of a hammerhead ribozyme. *Nature,* **372:** 68-74

Pontius B.W. & Berg P. (1990) Renaturation of complementary DNA strands mediated by purified mammalian heterogeneous nuclear ribonucleoprotein A1 protein: Implications for a mechanism for rapid molecular assembly. *Proc. Natl. Acad. Sci. U.S.A.*, **87**: 8403-8407

Pontius B.W. & Berg P. (1992) Rapid assembly and disassembly of complementary DNA strands through an equilibrium intermediate state mediated by A1 hnRNP protein. *J. Biol. Chem.*, **267:** 13815-13818

Portman D.S. & Dreyfuss G. (1994) RNA annealing activities in HeLa nuclei. *EMBO J.*, **13:** 213-221

Potter P.M., Harris L.C., Remack J.S., Edwards C.C. & Brent T.P. (1993) Ribozyme mediated modulation of human O^6-methylguanine-DNA methyltransferase expression. *Cancer Research*, **53**: 1731-1734

Prody G.A., Bakos J.T., Buzayan J.M. Schneider I.R. & Bruening G. (1986) Autolytic processing of dimeric plant virus satellite RNA. *Science,* **231**: 1577-1580

Pyle A.M. (1993) Ribozymes: A distinct class of metalloenzymes. *Science*, **261:** 709-714

Rossi J.J., Cantin E.M., Sarver N. & Chang P.F. (1991) The potential use of catalytic RNAs in therapy of HIV infection and other diseases. *Pharmac. Ther.*, **50:** 245-254

Rozen F., Edery I., Meerovitch K., Dever T.E., Merrick W.C. & Sonenberg N. (1990) Bidirectional RNA helicase activity of eucaryotic translation initiation factors 4A and 4F. *Mol. Cell. Biol.*, **10:** 1134-1144

Ruffner D.E., Stormo G.D. & Uhlenbeck O.C. (1990a) Sequence requirements of the hammerhead RNA self-cleavage reaction. *Biochemistry*, **29**: 10695-10702

Ruffner D.E. & Uhlenbeck O.C. (1990b) Thiophosphate interference experiments locate phosphates important for the hammerhead RNA self-cleavage reaction. *Nuc. Acids Res.,* **18**: 6025-6029

Saenger W. (1984) *Principles of Nucleic Acid Structure.* Springer-Verlag, New York, pp 17-21

Sambrook J., Fritsch E.F. & Maniatis T. (1989) *Molecular cloning: a laboratory manual.* 2nd ed., Cold Spring Harbor, New York

Sarver N., Cantin E.M., Chang P.S., Zaia J.A., Ladne P.A., Stephens D.A. & Rossi J.J. (1990) Ribozymes as potential anti-HIV-1 therapeutic agents. *Science,* **247**: 1222-1225

Saxena S.K. & Ackerman E.J. (1990) Ribozymes correctly cleave a model substrate and endogenous RNA *in vivo*. *J. Biol. Chem.*, **265:** 17106-17109

Scanlon K.J. Jiao L., Funato T., Wang W., Tone T., Rossi J.J. & Kashani-Sabet M. (1991) Ribozyme mediated cleavage of c-*fos* mRNA reduces gene expression of DNA synthesis enzymes and metallothionein. *Proc. Natl. Acad. Sci. U.S.A.*, **88**: 10591-10595

Scanlon K.J., Ishida H. & Kashani-Sabet M. (1994) Ribozyme-mediated reversal of the multidrug-resistant phenotype. *Proc. Natl. Acad. Sci. U.S.A.*, **91:** 11123-11127

Selden R.F., Howie K.B., Rowe M.E., Goodman H.M. & Moore D.D. (1986) Human growth hormone as a reporter gene in regulation studies employing transient gene expression. *Mol. Cell. Biol.*, **6:** 3173-3179

Shapero M.H. & Greer C.L. (1991) Conformational transition required for efficient splicing of transcripts from hybrid I promoter yeast tRNA gene fusion. *Biochemistry,* **30:** 6465-6475

Shapero M.H. & Greer C.L. (1992) Exon sequence and structure requirements for tRNA splicing in *Saccharomyces cerevisiae. Biochemistry,* **31:** 2359-2367

Sheldon C.C. & Symons R.H. (1989) Mutagenesis analysis of a self-cleaving RNA. *Nuc. Acids Res.,* **17**: 5556-5562

Shimayama T., Sawata S., Komiyama M., Takagi Y., Tanaka Y., Wada N., Sugimoto N., Rossi J.J., Nishikawa F., Nishikawa S. & Taira K. (1992) Substitution of non-catalytic stem and loop regions of hammerhead ribozyme with DNA counterparts only increases K_m without sacrificing the catalytic step (K_{cat}): a way to improve substrate specificity. *Nuc. Acids Res. Symp. Ser.*, **27:** 17-18

Shimayama T., Nishikawa F., Nishikawa S. & Taira K. (1993) Nuclease-resistant chimeric ribozymes containing deoxyribonucleotides and phosphorothioate linkages. *Nuc. Acid Res.,* **21:** 2605-2611

Shore S.K., Nabissa P.M. & Reddy E.P. (1993) Ribozyme mediated cleavage of the *BCRABL* oncogene transcript: *in vitro* cleavage of RNA and *in vivo* loss of P210 protein-kinase activity. *Oncogene*, **8:** 3183-3188

Sioud M. & Drlica K. (1991) Prevention of human immunodeficiency virus type 1 integrase expression in *Escherichia coli* by a ribozyme. *Proc. Natl. Acad. Sci. U.S.A.*, **88:** 7303-7307

Sioud M., Natvig J.B., Forre O. (1992) Preformed ribozyme destroys tumor necrosis factor mRNA in human cells. *J. Mol. Biol.*, **223**: 831-835

Sioud M. (1994) Interaction between Tumour necrosis factor a ribozyme and cellular proteins. *J. Mol. Biol.*, **242:** 619-629

Slim G. & Gait M.J. (1991) Configurationally defined phosphorothioate-containing oligoribonucleotides in the study of the mechanism of cleavage of hammerhead ribozymes. *Nuc. Acids Res.*, **19**: 1183-1188

Slim G. & Gait M.J. (1992) The role of the exocyclic amino groups of conserved purines in hammerhead ribozyme cleavage. *Biochem. & Biophys. Res. Comm.*, **183**: 605-609

Snyder D.S., Wu Y., Wang J.L., Rossi J.J., Swiderski P., Kaplan B.E. & Forman S.J. (1993) Ribozyme-mediated inhibition of *bcr-abl* gene expression in a philadelphia chromosome positive cell line. *Blood,* **82**: 600-605

Stange N. & Beier H. (1986) A gene for the major cytoplasmic tRNA^{Tyr} from *Nicotiana rustica* contains a 13 nucleotides long intron. *Nuc. Acids Res.*, **14:** 8691

Stange N. & Beier H. (1987) A cell-free plant extract for accurate pre-tRNA processing, splicing and modification. *EMBO J.*, **6**: 2811-2818

Stange N., Beier D. & Beier H. (1992) Intron excision from tRNA precursors by plant splicing endonuclease requires unique features of the mature tRNA domain. *Eur. J., Biochem.*, **210:** 193-200

Stanley J. (1983) Infectivity of the cloned geminivirus genome requires sequences from both DNAs. *Nature,* **305:** 643-645

Stanley J. (1993) Geminiviruses: plant viral vectors. *Current Opinions in Genetics & Development,* **3**: 91-96

Stanley J. & Townsend R. (1986) Infectious mutants of cassava latent virus generated *in vivo* from intact recombinant DNA clones containing single copies of the genome. *Nuc. Acids Res.*, **14**: 5981-5988

Steinecke P., Herget T. & Schreier P.H. (1992) Expression of a chimeric ribozyme gene results in endonucleolytic cleavage of target mRNA and a concomitant reduction of gene expression *in vivo. EMBO J.*, **11**: 1515-1530

Steinecke P., Steger G. & Schreier P.H. (1994) A stable hammerhead structure is not required for endonucleolytic activity of a ribozyme *in vivo. Gene,* **149:** 47-54

Sullenger B.A. & Cech T.R. (1993) Tethering ribozymes to a retroviral packaging signal for destruction of viral RNA. *Science,* **262:** 1566-1569

Sullenger B.A. & Cech T.R. (1994) Ribozyme-mediated repair of defective mRNA by targeted trans-splicing. *Nature,* **371:** 619-622

Sun L.Q., Warrilow D., Wang L., Witherington C., Mcpherson J. & Symonds G. (1994) Ribozyme mediated suppression of Moloney Murine leukemia virus and human imunodeficiency virus type I replication in permissive cell lines. *Proc. Natl. Acad. Sci. U.S.A.,* **91:** 9715-9719

Swanson M.S. & Dreyfuss G. (1988) RNA binding specificity of hnRNP proteins: a subset bind to the 3' end of introns. *EMBO J.,* **7:** 3519-3529

Symons R.H. (1992) Small catalytic RNAs. *Annu. Rev. Biochem.*, **61:** 641-71

Symons R.H. (1994) Ribozymes. *Curr. Op. Struct. Biol.*, **4:** 322-330

Szweykowska-Kulinska Z. & Beier H. (1991) Plant nonsense suppressor tRNA^{Tyr} genes are expressed at very low levels *in vitro* due to inefficient splicing of the intron-containing pre-tRNAs. *Nuc. Acids Res.*, **19:** 707-712

Tang X.B., Hobom G. & Luo D. (1994) Ribozyme mediated destruction of influenza A virus *in vitro* and *in vivo. J. Med. Virol.*, **42**: 385-395

Taylor N.R., Kaplan B.E., Swiderski P., Li H. & Rossi J.J. (1992) Chimeric DNA-RNA hammerhead ribozymes have enhanced *in vitro* catalytic efficiency and increased stability *in vivo. Nuc. Acids Res.*, **20**: 4559-4565

Thompson J.F., Hayes L.S. & Lloyd D.B. (1991) Modulation of firefly luciferase stability and impact on studies of gene regulation. *Gene,* **103**: 171-177

Timmermans M.C.P., Das O.P. & Messing J. (1992) Trans replication and high copy numbers of wheat dwarf virus vectors in maize cells. *Nuc. Acids Res.*, **20:** 4047-4054

Tobian J.A., Drinkard L. & Zasloff M. (1985) tRNA nuclear transport: Defining the critical regions of human $tRNA^{Met}$ by point mutagenesis. *Cell,* **43:** 415-422

Tone T., Kasheni-Sabet M., Funato T., Shitara T., Yoshida E., Kashfian B.I., Horng M., Fodstadt O. & Scanlon K.J. (1993) Suppression of EJ cells tumorigenicity. *In vivo,* **7:** 471-476

Tsuchihashi Z., Khosla M. & Herschlag D. (1993) Protein enhancement of hammerhead ribozyme catalysis. *Science*, **262:** 99-102

Tuschl T. & Eckstein F. (1993) Hammerhead ribozymes: importance of stem-loop II for activity. *Proc. Natl Acad. Sci. U.S.A.*, **90**: 6991-6994

Uhlenbeck O.C. (1987) A small catalytic oligoribonucleotide. *Nature*, **328:** 596-599

van der Vlugt R.A.A., Prins M. & Goldbach R. (1993) Complex formation determines the activity of ribozymes directed against potato virus Yn genomic RNA sequences. *Virus Research*, **27**: 185-200

van Tol H., Stange N., Gross H.J. & Beier H (1987) A human and plant intron-containing $tRNA^{Tyr}$ gene are both transcribed in a HeLa cell extract but spliced along different pathways. *EMBO J.*, **6:** 35-41

Ventura M., Wang P., Franck N. & Saragosti S. (1994) Ribozyme targeting of HIV-1 LTR. *Biochem. Biophys. Res. Comm.*, **203:** 889-898

Ward A., Etessami P. & Stanley J. (1988) Expression of a bacterial gene in plants mediated by infectious geminivirus DNA. *EMBO J.*, **7**: 1583-1587

Wassarman D.A. & Steitz J.A. (1991) Alive with DEAD proteins. *Nature* , **349:** 463-464

Weerasinghe M., Liem S.E., Asad S., Read S.E. & Joshi S. (1991) Resistance to human immunodeficiency virus type 1 (HIV-1) infection in human CD4+ lymphocyte-derived cell lines conferred by using retroviral vectors expressing an HIV-1 RNA specific ribozyme. *J. Virol.*, **65:** 5531-5534

Wegener D., Steinecke P., Herget T., Petereit I., Philipp C. & Schreier P.H. (1994) Expression of a reporter gene is reduced by a ribozyme in transgenic plants. *Mol. Gen. Genet.*, **245:** 465-470

White R.J., Stott D. & Rigby P.W. (1990) Regulation of RNA polymerase III transcription in response to Simian virus 40 transformation. *EMBO J.*, **9:** 3713-3721

Williams D.M., Pieken W.A. & Eckstein F. (1992) Function of specific 2'-hydroxyl groups of guanosines in a hammerhead ribozyme probed by 2' modifications. *Proc. Natl. Acad. Sci. U.S.A.,* **89**: 918-922

Woese C.R., Winker S. & Gutell R.R. (1990) Architecture of ribosomal RNA constraints on the sequence of "tetraloops". *Proc. Natl. Acad. Sci. U.S.A.,* **87:** 8467-8471

Xing Y., Johnson C.V., Dobner P.R. & Lawrence J.B. (1993) Higher level organization of individual gene transcription and RNA splicing. *Science,* **259:** 1326-1330

Yang J., Perrault J.P., Labuda D., Usman N. & Cedergren R. (1990) Mixed DNA/RNA polymerase are cleaved by the hammerhead ribozyme. *Biochemistry*, **29**: 11156-11160

Yu M., Ojwang J., Yamada O., Hampel A., Rapapport J., Looney D. & Wong-Staal F. (1993) A hairpin ribozyme inhibits expression of diverse strains of human immunodeficiency virus type 1. *Proc. Natl. Acad. Sci. U.S.A.*, **90:** 6340-6344

Yuan Y., Hwang E.S. & Altman S. (1992) Targeted cleavage of mRNA by human RNase P. *Proc. Natl. Acad. Sci. U.S.A.*, **89:** 8006-8010

Yuan Y. & Altman S. (1994) Selection of guide sequences that direct efficient cleavage of mRNA by Human Ribonuclease P. *Science,* **263:** 1269-1273

Yuan Y. & Altman S. (1995) Substrate recognition by human RNase P: identification of small, model substrates for the enzyme. *EMBO J.*, **14:** 159-168

Yuyama N., Ohkawa J., Inokuchi Y., Shirai M., Sato A., Nishikawa S. & Taira K. (1992) Construction of a tRNA-embedded-ribozyme trimming plasmid. *Biochem. Biophys. Res. Comm.*, **186:** 1271-1279

Zaug A.J. & Cech T.R. (1986) The intervening sequence RNA of *Tetrahymena* is an enzyme. *Science*, **231:** 470-475

Zhao J.J. & Pick L. (1993) Generating loss of function phenotypes of the *fushi tarazu* gene with a targeted ribozyme in *Drosophila*. *Nature*, **365**: 448-451

Zhou C., Bahner I.C., Larson G.P., Zaia J.A., Rossi J.J. & Kohn D.B. (1994) Inhibition of HIV-1 in human T-lymphocytes by retrovirally transduced anti-*tat* and *rev* hammerhead ribozyme. *Gene,* **149:** 33-39

Zon G. & Stec W.J. (1991) Phosphorothioate oligonucleotides. In Eckstein F. (ed), *Oligonucleotides and Analogues - A practical approach,* Oxford University Press, Oxford, pp 87-103

8mz
QP623.5
.C36
P47
1995

Chapter 3 - constructions

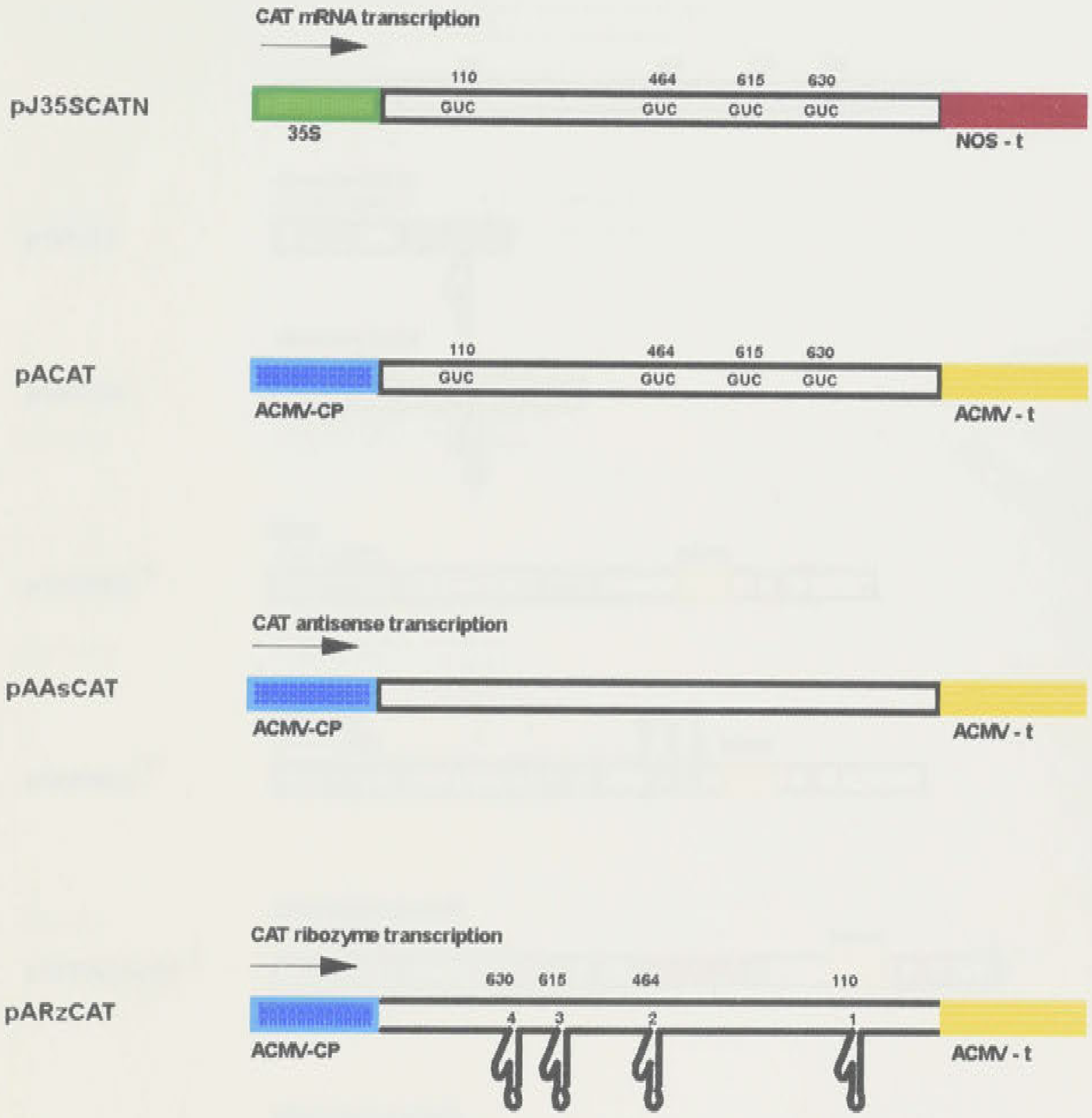
CAT mRNA transcription
pJ35SCATN
110
464
615
630
GUC
GUC
GUC
GUC
35S
NOS - t
pACAT
110
464
615
630
GUC
GUC
GUC
GUC
ACMV-CP
ACMV - t
CAT antisense transcription
pAAsCAT
ACMV-CP
ACMV - t
CAT ribozyme transcription
pARzCAT
630
615
464
110
4
3
2
1
ACMV-CP
ACMV - t

8m2
QP623.5
.C3C
P47
1995

Chapter 4 - constructions

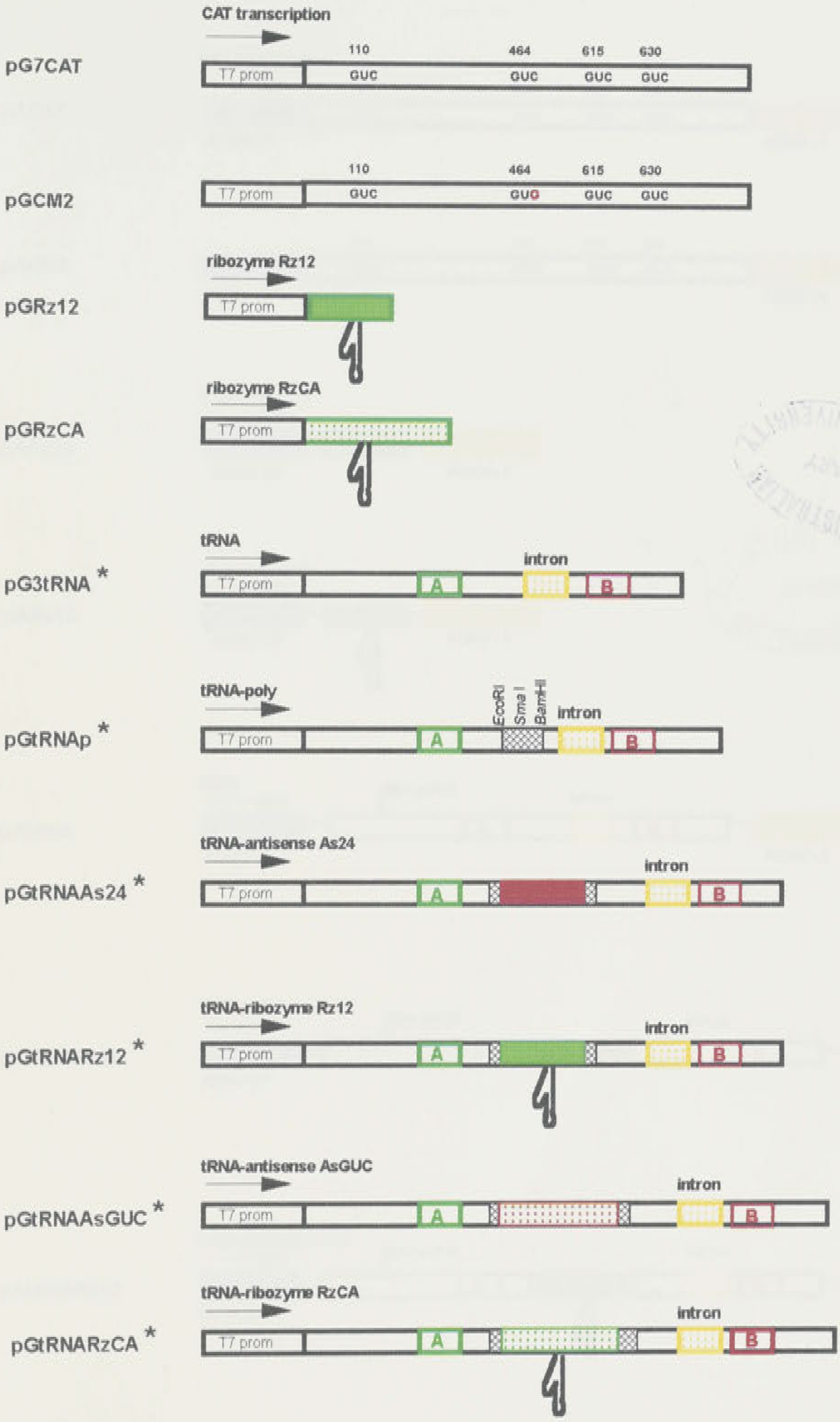
CAT transcription
pG7CAT
T7 prom
110 GUC
464 GUC
615 GUC
630 GUC
pGCM2
T7 prom
110 GUC
464 GUG
615 GUC
630 GUC
ribozyme Rz12
pGRz12
T7 prom
ribozyme RzCA
pGRzCA
T7 prom
tRNA
pG3tRNA *
T7 prom
A
intron
B
tRNA-poly
pGtRNAp *
T7 prom
A
EcoRI
Sma I
BamHI
intron
B
tRNA-antisense As24
pGtRNAAs24 *
T7 prom
A
intron
B
tRNA-ribozyme Rz12
pGtRNARz12 *
T7 prom
A
intron
B
tRNA-antisense AsGUC
pGtRNAAsGUC *
T7 prom
A
intron
B
tRNA-ribozyme RzCA
pGtRNARzCA *
T7 prom
A
intron
B

* intron minus (i-) constructs lack 13 base intron (yellow hatched box)

THE AUSTRALIAN NATIONAL UNIVERSITY LIBRARY

8m2
QP623.5
.C36
P47
1995

Chapter 5 - constructions

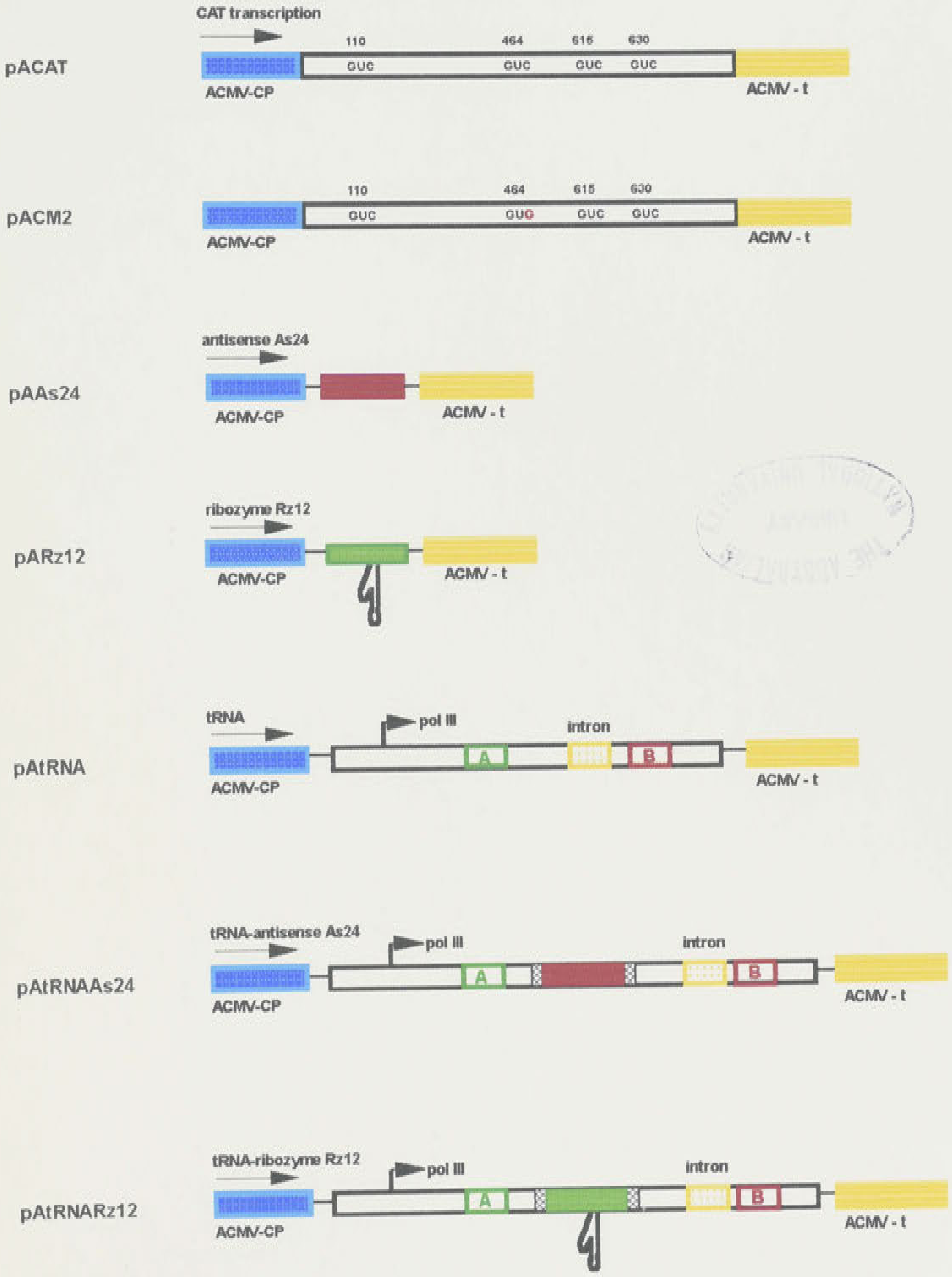
pACAT
CAT transcription
110
464
615
630
GUC
GUC
GUC
GUC
ACMV-CP
ACMV - t
pACM2
110
464
615
630
GUC
GUG
GUC
GUC
ACMV-CP
ACMV - t
pAAs24
antisense As24
ACMV-CP
ACMV - t
pARz12
ribozyme Rz12
ACMV-CP
ACMV - t
pAtRNA
tRNA
pol III
intron
A
B
ACMV-CP
ACMV - t
pAtRNAAs24
tRNA-antisense As24
pol III
intron
A
B
ACMV-CP
ACMV - t
pAtRNARz12
tRNA-ribozyme Rz12
pol III
intron
A
B
ACMV-CP
ACMV - t